STUDIES ON CATIONIC HYDROPHOBIC DENDRONS AND HYDROPHILIC DENDRIMERS

A thesis presented by

Khuloud T Al-Jamal, BSc (Pharmacy)

in partial fulfillment of the requirements for the degree of

Doctor of Philosophy

of the

University of London

This thesis describes research conducted in the School Of Pharmacy, University of London between 2000 and 2004 under the supervision of Professor A. T. Florence. I certify that the research described is original and that any parts of the work that have been conducted by collaboration are clearly indicated. I also certify that I have written all text herein and have clearly indicated by suitable citation any part of this dissertation that has already appeared in publication.

Signature **Date 01/02/2005**

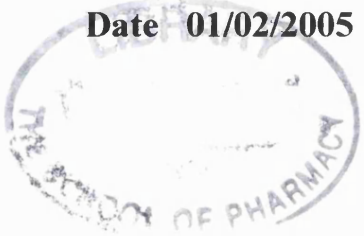

ProQuest Number: 10104692

All rights reserved

INFORMATION TO ALL USERS
The quality of this reproduction is dependent upon the quality of the copy submitted.

In the unlikely event that the author did not send a complete manuscript
and there are missing pages, these will be noted. Also, if material had to be removed,
a note will indicate the deletion.

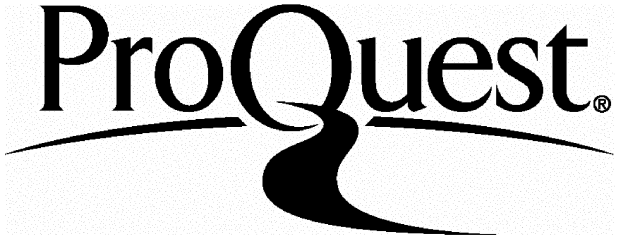

ProQuest 10104692

Published by ProQuest LLC(2016). Copyright of the Dissertation is held by the Author.

All rights reserved.
This work is protected against unauthorized copying under Title 17, United States Code.
Microform Edition © ProQuest LLC.

ProQuest LLC
789 East Eisenhower Parkway
P.O. Box 1346
Ann Arbor, MI 48106-1346

To Mum and Dad

Thank you for everything

"....the whole becomes not only more than, but very different from the sum of its parts."

P.W. Anderson
Science 1972

ACKNOWLEDGEMENTS

First and foremost, I would like to express my deep gratitude to my supervisor, Professor Alexander T. Florence for his guidance and advice over the past years. I especially thank him for his fatherly support and thoughtfulness.

I would like to thank Dr T. Sakthivel for his excellent lab guidance throughout my first year and Dr V. Jaitley for his useful discussions and sharing his computer skills with everyone.

I wish to thank Dr F. Florence for her friendship and encouragement with her warm smile. My heartfelt thanks to Professor T. Arafat and Professor Z. El-Deen in Jordan for inspiring me at the beginning of this journey.

It is impossible to mention everyone who has made a difference to my work, but I would especially like to thank Dr J. Turton for his help and great input into the *in vivo* studies, Dr R. Falconer and Dr. J. Malkinson in the chemistry department for their expertise, Mr D. McCarthy for his great microscopy work, Dr M. Zloh for the NMR data and Dr C. James for the wonderful molecular modelling. I also cannot forget Ruth for making my cell culture studies an enjoyable experience, and Bridget for her helpfulness and fabulous efficiency.

I would like to thank my friends for their constant encouragement, namely: Sumia, , Alia, Asma, Suha, Hanan and Raya. Last but not least Hala and her family for their warmness.

For being great colleagues and friends, especially during the difficult times, I wish to thank Naseem, Gaurang, Suzie, Chandra, Behrooz, Baljit, Pla, Orawan, Safura, Andrew, Pav and Parajit.

I can't express my gratitude to my parents, brothers and sisters, especially Wafa for putting up with me during the writing up stage.

The financial support from Petra University, The Overseas Research Scholarship, and GlaxoSmithKline is gratefully acknowledged.

ABSTRACT

A group of cationic amphiphilic polylysine dendrons and dendrimers of various geometries and lipophilicity were synthesised and characterised to investigate their potential uses in drug delivery.

An interesting intrinsic fluorescence was discovered in these molecules without a fluorophore, a property which can be used as a tool in their visualisation and quantification of cellular uptake. The complexation between dendrimers and a small dye molecule carboxyfluorescein was also studied to prove the ability of the dendrimer to act as nanocarrier devices.

Engineering dendrimers and dendrons (partial dendrimers) is by controlling their generation number, number of branching units and surface functionalities. Dendrons of the appropriate hydrophile-lipophile balance (HLB), size and topology can self-assemble into higher order structures, broadening their potential for use as drug and gene carriers. Novel supramolecular vesicular structures comprised of a cationic lipidic dendron were developed and named "dendrisomes". Dendrisomes were tested for their potential as drug delivery carriers for benzyl penicillin (penicillin G), used as a model of a negatively charged water soluble drug. Their interaction with cholesterol was also studied using techniques such as photon correlation spectroscopy, transmission electron microscopy and differential scanning calorimetry. The gradual transformation of dendrisomes into isotropic surfactant/dendron mixed micelles was achieved via the interaction with the non-ionic surfactant, Triton X-100.Thestoichiometry of the dendron-surfactant interaction was determined.

Heparin is a negatively charged polysaccharide which is known for its anticoagulant activity, pro-angiogenic character and poor oral absorption. A hydrophilic dendrimer with 64 amino groups was complexed with heparin via electrostatic interactions to form heparin dendriplexes. An effect on heparin anticoagulant activity, angiogenic properties as well as its absorption profile is anticipated upon complexation, depending on the physicochemical properties and stability of the dendriplexes *in vitro* and *in vivo*. The modulation of heparin anticoagulant activity *in vitro* and *in vivo* was studied: complete association occurs at 1:1 mass ratio at which ratio the anticoagulant activity of heparin is abolished. A change in heparin pharmacodynamic and pharmacokinetic properties occurred when complexed with the dendrimer, demonstrated by uptake measurements across Caco-2 monolayers and biodistribution (in rats) of [^{3}H] labelled dendrimer, [^{3}H] labelled heparin and the dendriplexes. However, the use of dendrimers as an approach to enhance heparin absorption *in vitro* and *in vivo* was not much successful due to the low uptake enhancement ratio and heparin deactivation.

It is concluded that dendrimers and dendrons are potential tools in drug delivery as discrete nanodevices (uni-micellar dendrimers), supramolecular assemblies (dendrisomes) and active moieties themselves (as heparin antidote and in angiogenesis therapy).

TABLE OF CONTENTS

ACKNOWLEDGEMENTS..... iv

ABSTRACT..... v

LIST OF FIGURES.....xiii

LIST OF TABLES.....xix

ABBREVIATIONS.....xx

CHAPTER I.....1

INTRODUCTION.....1

1.1. SUPRAMOLECULAR ASSEMBLY.....3

1.2. DENDRIMER-SURFACTANT ASSEMBLIES.....9

1.3. POLYLYSINE DENDRONS AND DENDRIMERS.....12

1.3.1. Surface monolayer formulation.....13

1.3.2. Formulation of dendrimer-derived nanoparticles.....15

1.3.3. Polyanionic-cationic dendron/dendrimer complexes.....17

1.3.3.1. Dendron - DNA complexes.....17

1.3.4. Micellar aggregates.....20

1.4. CONCLUSION AND CORRELATION TO WORK IN THE THESIS.....22

CHAPTER II.....23

DESIGN AND SYNTHESIS OF CATIONIC LIPIDIC AND NON-LIPIDIC LYSINE-BASED DENDRON AND DENDRIMER DELIVERY SYSTEM.....23

2.1. DENDRIMER SYNTHESIS.....23

2.1.1. Solid phase peptide synthesis.....23

2.1.1.1. Resin as solid support.....26

2.1.1.2. Protection/deprotection of functional groups.....28

2.1.1.3. Activation and coupling.....29

2.1.1.4. Cleavage from the solid support.....33

2.1.1.5. Problems associated with peptide synthesis and some useful measures undertaken.....35

2.1.2. Dendrimer and dendron design and construction.....36

2.1.2.1. Synthesis of α-amino tetradecanoic acid.....36

2.1.2.2. Synthesis of *N*-Boc- α-amino tetradecanoic acid.....38

2.1.2.3. Types of dendrimers synthesised.....39

2.1.2.4. Purification of dendrimers.....40

2.1.2.5. Solubility of the compounds synthesised.....44

2.1.2.6. Spectrophotometry.....44

2.1.2.7. NMR.....45

***CHAPTER III*.....49**

***INTRINSIC FLUORESCENCE OF AMINO TERMINATED POLYAMIDE POLYLYSINE DENDRIMERS AND STUDYING THEIR INTERACTIONS WITH CARBOXYFLUORESCEIN USING SPECTROPHOTOMETRY AND SPECTROFLUORIMETRY*.....49**

3.1. EXPERIMENTAL.....50

3.1.1. Materials.....50

3.1.2. Synthesis of Gly-$Lys_{31}(NH_2)_{32}$ and Gly-$Lys_{63}(NH_2)_{64}$ dendrimers.....50

3.1.3. UV-Vis and fluorescence spectroscopy.....50

3.1.4. Molecular modelling of the dendrimer and the dye molecule.....51

3.1.5. Separation of free CF from the entrapped CF..... 51

3.2. RESULTS AND DISCUSSION.....52

3.2.1. Intrinsic dendrimer fluorescence..... 52

3.2.2. Dendrimer-CF complexation..... 55

3.2.3. Molecular

modelling.....58

3.2.4. Factors affecting dendrimer-dye complexation.....58

3.2.4.1. pH.....58

3.2.4.2. Ionic strength.....60

3.2.4.3. CF/dendrimer molar ratio..... 60

3.2.5. The reversibility and the stability of the complex..... 60

3.3. CONCLUSION.....62

***CHAPTER IV*.....63**

***DENDRISOMES: VESICULAR STRUCTURES DERIVED FROM A CATIONIC LIPIDIC DENDRON*.....63**

4.1. EXPERIMENTAL.....64

4.1.1. Materials.....64

4.1.2. Synthesis of the amphipathic dendron.....64

4.1.3. Surface pressure study..... 64

4.1.4. Molecular modelling of the dendron.....64

4.1.5. Dendron self-assembly and dendrisome formation.....66

4.1.6. Transmission electron microscopy.....66

4.1.7. Measurement of dendrisome diameter and zeta potential.....66

4.1.8. Phase transition behaviour of the supramolecular aggregates..... 67

4.1.9. Dendrisome encapsulation efficiency.....67

4.1.10. *In vitro* drug release..... 67

4.2. RESULTS AND DISCUSSION.....68

4.2.1. Design of the amphipathic dendron and molecular modelling.....68

4.2.2. Dendron self-assembly and dendrisome formation.....69

4.2.3. Encapsulation efficiency and *in vitro* release.....73

4.3. CONCLUSION.....81

***CHAPTER V*.....82**

***SOLUBILISATION AND TRANSFORMATION OF DENDRISOMES INTO MIXED MICELLES*.....82**

5.1. EXPERIMENTAL.....82

5.1.1. Materials.....82

5.1.2. Synthesis of the amphipathic dendron..... 82

5.1.3. Preparation of dendrisome -Triton X-100 mixtures.....83

5.1.4. Observation and size measurement of the supramolecular aggregates..... 83

5.1.5. Turbidimetry.....83

5.1.6. Quantification of the solubilised lipidic peptide dendron..... 83

5.2. RESULTS AND DISCUSSION.....85

5.2.1. Dendrisomes and Triton X-100.....85

5.2.2. Turbidity measurement.....85

5.2.3. Size measurement and TEM of the aggregates.....86

5.2.4. BCA assay of the supernatants.....90

5.3. CONCLUSION.....91

CHAPTER VI.....93

TRANSEPITHELIAL TRANSPORT OF A POLYLYSINE DENDRIMER ACROSS CACO-2 MONOLAYERS.....93

6.1. Experimental.....94

6.1.1. Materials.....94

6.1.2. Synthesis of Gly-$Lys_{63}(NH_2)_{64}$ dendrimer.....94

6.1.3. Caco-2 cell culture.....94

6.1.4. Cell viability (MTT assay).....95

6.1.5. Permeability of [^{3}H] labelled dendrimer across Caco-2 monolayer.....97

6.1.6. TEER and PEG 4000 permeability.....98

6.2. Results and discussion.....101

6.2.1. MTT toxicity assay.....101

6.2.2. TEER, dendrimer and PEG 4000 permeability.....103

6.3. Conclusion.....113

CHAPTER VII.....114

DENDRIPLEXES: HEPARIN-DENDRIMER COMPLEXES.....114

7.1. EXPERIMENTAL.....115

7.1.1. Materials.....115

7.1.2. Synthesis of Gly-$Lys_{63}(NH_2)_{64}$ dendrimer.....115

7.1.3. Preparation of heparin dendriplexes.....115

7.1.4. TEM, size and zeta potential measurement.....115

7.1.5. MB spectroscopy.....116

7.1.6. Antifactor Xa assay.....116

7.1.7. Association of heparin dendriplexes with Caco-2 monolayers.....117

7.1.8. Transport of heparin dendriplexes across Caco-2 monolayers.....118

7.2. RESULTS AND DISCUSSION.....118

7.2.1. Shape, size and zeta potential measurement of the dendriplexes.....118

7.2.2. MB/heparin assay.....122

7.2.3. *In vitro* anticoagulant activity of heparin dendriplexes.....123

7.2.4. Association of heparin dendriplexes with Caco-2 monolayers.....127

7.2.5. Transport of heparin dendriplexes across Caco-2 monolayers.....129

7.3. CONCLUSION.....133

***CHAPTER VIII*.....134**

***BIODISTRIBUTION OF HEPARIN DENDRIPLEXES AND DENDRIMER IN RATS*.....134**

8.1. EXPERIMENTAL.....135

8.1.1. Materials.....135

8.1.2. Synthesis of Gly-$Lys_{63}(NH_2)_{64}$ dendrimer.....135

8.1.3. Preparation of heparin dendriplexes.....135

8.1.4. Animals.....135

8.1.5. Experimental design and dosing.....135

8.1.6. Blood collection and radioactivity in organs.....136

8.1.7. Anti-factor Xa assay.....137

8.2. RESULTS AND DISCUSSION.....138

8.2.1. *In vivo* anticoagulant activity of heparin and heparin dendriplexes after oral and subcutaneous administration.....138

8.2.2. Oral uptake of heparin, the cationic dendrimer and heparin dendriplexes.....144

8.3. CONCLUSION..... 153

CHAPTER IX**.....154**

REFLECTIONS**.....154**

APPENDIX I**.....158**

BIBLIOGRAPHY**.....174**

LIST OF PUBLICATIONS**.....207**

LIST OF FIGURES

Chapter I

Figure 1.1: Schematic representation of the dendritic structure.....2

Figure 1.2: Schematic representation of supramolecular dendrimer with individual dendrons assembled around a molecular template.....3

Figure 1.3: Two-component supramolecular dendritic gels.....5

Figure 1.4: Schematic representation of the self-assembly of flat tapered monodendrons and conical monodendrons.....7

Figure 1.5: Schematic representation of the proposed self-assembly of the host-guest complex of monodendrons and guest molecules.....8

Figure 1.6: A schematic of the relationships between the primary dendron and dendrimer structures and the aggregated states.....12

Figure 1.7: Possible models of association of a lipophilic dendrimer in aqueous dispersions.....13

Figure 1.8: A schematic of the adsorption of a lipidic dendrimer spread at the air-water interface.....14

Figure 1.9: Surface pressure-isotherms of lipidic peptide dendrimers.....15

Figure 1.10: Nanoparticles made of lipophilic dendrimers..... 17

Figure 1.11: Computer generated model of DNA dendriplexes.....19

Figure 1.12: Transmission electron micrographs of dendriplexes.....19

Figure 1.13: TEM photomicrographs of the micellar aggregates of $(C_{14})_3Lys_2(NH_2)_8$ dendron in 0.1% sodium chloride and in water.....20

Figure 1.14: Delineation of the general structure of an amphipathic dendrons.....21

Chapter II

Figure 2.1: General principle of peptide bond formation.....24

Figure 2.2: Overview of a peptide chain assembly using SPPS.....25

Figure 2.3: Various processes to be considered prior to and after coupling.....26

Figure 2.4: Common *N*-protecting groups.....28

Figure 2.5: Chemical structure of some active aryl and *O*-acyl-hydroxylamine esters.....30

Figure 2.6: Pathways of DCC mediated coupling.....32

Figure 2.7: HBTU mediated coupling pathways.....33

Figure 2.8: Generic chemical structure of a α-lipoamino acid.....37

Figure 2.9: Steps involved in the synthesis of α-amino tetradecanoic acid.....38

Figure 2.10: Boc-protection of α-amino tetradecanoic acid.....39

Figure 2.11: Solid phase peptide synthesis of compound 2a.....41

Figure 2.12: Chemical structures of the lipidic and non-lipidic dendrimers.....42

Figure 2.13: RP-HPLC chromatograms of some dendrimers.....43

Figure 2.14: SEC chromatograms of some dendrimers.....43

Figure 2.15: UV spectra of compound 2c.....44

Figure 2.16: ^{1}H NMR spectrum extract for compound 2b in D_2O.....46

Figure 2.17: ^{1}H NMR spectrum extract for compound 2c in D_2O.....47

Figure 2.18: 2D NMR TOCSY spectrum for compound 2b in D_2O.....47

Figure 2.19: 2D NMR TOCSY spectrum for compound 2c in D_2O.....48

Chapter III

Figure 3.1: Calibration plot of the dendrimer in water by fluorescence spectroscopy 53

Figure 3.2: Emission spectra of various dendrimer concentrations in water.....53

Figure 3.3: Photographs of a range of macromolecules concentrations exposed to visible light and to a UV transilluminator.....54

Figure 3.4: UV/Vis spectra of free CF and complexed CF and a plot of A_{450}/A_{498} versus dye/dendrimer molar ratio.....56

Figure 3.5: Effect of dendrimer concentration on CF fluorescence.....57

Figure 3.6: Molecular modelling of the dendrimer and CF molecule.....59

Figure 3.7: Separation of free and complexed CF by gel filtration.....61

Chapter IV

Figure 4.1: The chemical structure of a lipid-lysine dendron synthesised.....68

Figure 4.2: Dynamics simulations of the dendron $(C_{14})_3Lys_7(C_{14})_8(NH_2)_8$ in vacuum and in a polar environment.....70

Figure 4.3: Transmission electron micrograph of the dendrisomes and a schematic representation of bilayer formation of the lipidic dendron.....72

Figure 4.4: A surface pressure-area isotherm of the lipidic dendron $(C_{14})_3Lys_7(C_{14})_8(NH_2)_8$ spread on water.....72

Figure 4.5: TEM of dendrisomes prepared by reverse-phase evaporation technique with increased cholesterol content.....74

Figure 4.6: DSC trace of dendrisomes.....75

Figure 4.7: Percentage penicillin G entrapment in dendrisomes of various cholesterol content.....77

Figure 4.8: The relationship between drug/dendron molar ratio and dendrisome size.....78

Figure 4.9: *In vitro* release of penicillin G from dendrisomes and liposomes.....80

Chapter V

Figure 5.1: The chemical structure of Triton X-100.....84

Figure 5.2: The turbidity of dendrisome-surfactant suspensions and the hydrodynamic Z-average diameter of the aggregates.....86

Figure 5.3: TEM of dendrisomes and dendrisome-surfactant aggregates.....87

Figure 5.4: A schematic illustration of the proposed stages of solubilisation.....89

Figure 5.5: The percentage relative dendron solubilised versus Triton X-100: dendron molar ratio.....91

Chapter VI

Figure 6.1: A summary of the MTT assay procedures.....96

Figure 6.2: Caco-2 monolayer assembly.....100

Figure 6.3: Percentage cell viability of Caco-2 cells versus dendrimer concentration.....102

Figure 6.4: Effect of dendrimer concentrations on TEER measurement of Caco-2 monolayer.....104

Figure 6.5: TEER recovery of Caco-2 monolayers after exposure to dendrimers.....105

Figure 6.6: Percentage cumulative [^{14}C]-PEG 4000 transport over filters with and without Caco-2 cells at various dendrimer concentrations.....106

Figure 6.7: Percentage cumulative transport of [^{14}C]PEG 4000 across Caco-2 monolayers in the presence of dendrimer versus time.....107

Figure 6.8: The correlation between the TEER and the percentage [^{14}C]-PEG 4000 transported.....107

Figure 6.9: Percentage cumulative [^{3}H]-dendrimer transport over filters with and without Caco-2 cells.....108

Figure 6.10: Percentage cumulative transport of [^{3}H]-dendrimer across Caco-2 monolayers.....109

Chapter VII

Figure 7.1: The chemical structure of sulphated heparin.....119

Figure 7.2: TEM of the heparin dendriplexes.....120

Figure 7.3: Heparin dendriplexes size (nm) versus time (day).....120

Figure 7.4: UV/Vis spectra of free MB and MB/heparin.....122

Figure 7.5: A_{664}/A_{568} ratio of MB versus +/- charge ratio.....123

Figure 7.6: Heparin anticoagulant activity versus heparin concentration at various heparin: dendrimer mass ratio.....124

Figure 7.7: Percentage of [^{3}H]-heparin associated with Caco-2 monolayers, with and without dendrimer, in DMEM or OptiMEM-1, for 4 and 24h.....128

Figure 7.8: Percentage cumulative transport of [^{3}H]-heparin dendriplexes (0.2 mg/ml) across Caco-2 monolayers as a function of time.....130

Figure 7.9: Effect of heparin (0.2 mg/ml):dendrimer complexation ratio on TEER of Caco-2 monolayers as a function of time 130

Figure 7.10: Percentage cumulative transport of [^{3}H]-heparin dendriplexes (1 mg/ml) across Caco-2 monolayers as a function of time.....131

Figure 7.11: Effect of heparin (1 mg/ml):dendrimer complexation ratio on TEER of Caco-2 monolayers as a function of time.....131

Figure 7.12: Uptake enhancement ratio as a function of heparin:dendrimer mass ratios after 4h and 24h incubation.....132

Chapter VIII

Figure 8.1: Heparin calibration curve using the anti-factor Xa assay.....139

Figure 8.2: Active heparin plasma concentration (IU/ml) versus time (h) in sprague-dawley rats.....140

Figure 8.3: The percent injected dose of heparin or the dendriplexes recovered per gram of tissue as a function of time.....142

Figure 8.4: The subcutaneous injection site after injection with heparin or the dendriplexes.....143

Figure 8.5: The percent oral dose of the dendriplexes recovered per gram of tissue as a function of time.....146

Figure 8.6: The percent oral dose of heparin recovered per gram of tissue as a function of time.....147

Figure 8.7: Ratio of the percent recovered of oral dendriplexes to heparin; oral dendriplexes to dendrimer and subcutaneous dendriplexes to heparin.....149

Figure 8.8: The percentage recovered into plasma and lungs of the all formulations studied as a function of time.....150

Figure 8.9: The percent oral dose of the dendrimer recovered per gram of tissue as a function of time.....152

LIST OF TABLES

Table 2.1: Examples of some resins used in SPPS.....27

Table 2.2: A list of the compounds synthesised.....40

Table 2.3: Chemical shifts δ of external and internal lysine protons as assigned by 2D TOCSY.....46

Table 4.1: Dendrisomes Z-average size and zeta-potential with different cholesterol ratios.....73

Table 6.1: The effect of dendrimer concentration on the P*app* of [^{3}H]-dendrimer and [^{14}C]PEG 4000.....112

Table 7.1: Z-average size and zeta-potential of dendriplexes of various dendrimer:heparin ratios.....121

Table 8.1: Organ biodistribution of free and complexed heparin as a function of time after subcutaneous administration.....141

Table 8.2: Organ biodistribution of free and complexed heparin as a function of time after oral administration.....141

LIST OF ABBREVIATIONS

AT-III	**antithrombine III**
BCA	bicinchoninic acid
Boc	tert-Butoxycarbonyl
$C_{12}E_6$	hexaoxyethylenedodecyl ether
CF	carboxyfluorescein
CHOL	cholesterol
CPK	Corey-Pauling-Koltun
DCC or DCCI	dicyclohexylcarbodiimide
DCM	dichloromethane
DCU	*N,N'*-dicyclohexylurea
DIEA	*N,N*-diisopropylethylamine
DMEM	Dulbecco's modified Eagle medium
DMF	*N,N*-dimethylformamide
DMS	dimethyl sulphide
DMSO	dimethylsulfoxide
DSC	differential scanning calorimetry
DSPC	distearoyl phosphatidylcholine
DTAB	dodecyltetrammonium bromide
DVB	divinylbenzene
ESI-MS	electro-spray ionisation mass spectrometry
FCS	foetal calf serum
Fmoc	9-fluorenylmethoxycarbonyl
GPC	gel permeation chromatography
HBSS	Hank's balanced salt solution
HBTU	O-benzotriazolyl-*N,N,N',N'*-tetramethyluronium hexafluorophosphate
HF	hydrogen fluoride
HLB	hydrophile-lipophile balance
HOBt	1-hydroxybenztriazole
HOSu	*N*-hydroxysuccinimide
HPLC	high pressure liquid chromatography
IP	intraperitoneal
KOH	potassium hydroxide
LI	large intestine
MALDI-TOF	matrix-assisted laser desorption ionisation time of flight mass spectrometry
MB	methylene blue
MBHA	4-methyl benzhydralamine
MTT	3-(4,5-dimethylthiazol-2-yl)-2,5-diphenyltetrazolium bromide
MWCO	molecular weight cut off

NEAA	non-essential amino-acids
NMP	*N*-methylpyrrolidone
O.D	optical density
PAMAM	poly(amidoamine) dendrimers
P*app*	apparent permeability
PBS	phosphate buffered saline
PCS	photon correlation spectroscopy
PEG	polyethylene glycol
PPI	poly(propylene imine)
PPV	poly(*p*-phenyl vinylene
PS	polystyrene
REV	reverse-phase evaporation
SDS	sodium dodecyl sulphate
SEC	size exclusion chromatography
SI	small intestine
SPPS	solid phase peptide synthesis
TEER	transepithelial electrical resistance
TEM	transmission electron microscopy
TFA	trifluoroacetic acid
TFMSA	trifluoromethanesulfonic acid
TLC	thin layer chromatography
TMC	*N*-trimethyl chitosan
UFH	unfractionated heparin

Chapter I

INTRODUCTION

The word dendrimer is derived from the Greek words 'dendron', meaning tree or branch, and 'meros' denoting for the smallest repeating structural unit. Dendrimers are defined as two or more dendrons that emanate from a common core- a central juncture which can be a single atom or an atomic group **(Figure 1.1)**. The dendritic structure is characterised by 'layers' between each focal point called generations. Dendrimers were first synthesised by Tomalia in the mid 1980's (Tomalia *et al.*, 1990). They can be prepared by two distinct synthetic strategies: the divergent approach developed by Tomalia *et al.* (1985) and Newkome *et al.* (1985) where synthesis starts from the central core and moves out towards the periphery, and the convergent approach developed by Hawker and Fréchet (1990) which starts from the outermost residues moving inward. Dendrimers are structurally well-defined with a low polydispersity in comparison with traditional polymers. They can also be prepared by other non-covalent interactions of some dendrons.

There is now a large and growing number of publications which explore the use of dendrimers in drug, gene and vaccine delivery; the use of some as therapeutic agents in their own right is also being studied (Loup *et al.*, 1999; Gazumyan *et al.*, 2000; Kasai *et al.*, 2002; Shaunak *et al.*, 2004; Solassol *et al.*, 2004).

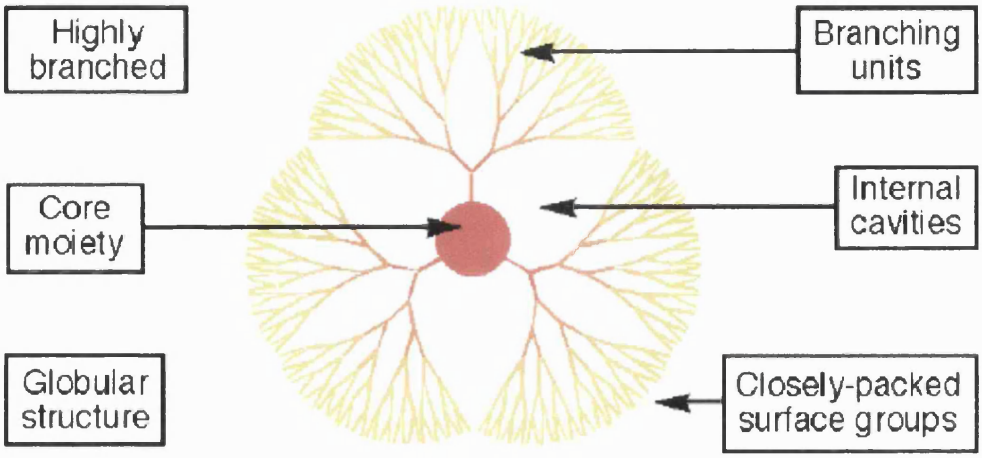

Figure 1.1: Schematic representation of the dendritic structure showing their unique structural aspects. (Reprinted from Matthews *et al.*, 1998)

The oral absorption and organ distribution of dendrimers has been studied (Sakthivel *et al.*, 1999; Nigavekar *et al.*, 2004). The structural and size related toxicity and biocompatibility of many types of dendrimers is being actively researched (Loup *et al.*, 1999; Malik *et al.*, 2000; Krishna and Jayaraman, 2003; Maszewska *et al.*, 2003; Fuchs *et al.*, 2004; Jevprasesphant *et al.*, 2004).

Dendrimers have been found to interact with several drugs, dyes and chemical reagents providing potential applications in areas such as solubilisation of hydrophobic molecules (Newkome *et al.*, 1990; Gopidas *et al.*, 1991; Newkome *et al.*, 1993; Watkins *et al.*, 1997; Milhem *et al.*, 2000), molecular inclusions (Naylor *et al.*, 1989; Twyman *et al.*, 1999), nanoscopic containers (SayedSweet *et al.*, 1997), dendritic boxes (Jansen *et al.*, 1994; Balzani *et al.*, 2002), unimolecular micelles (Baars *et al.*, 2000a), reverse molecular micelles (Stevelmans *et al.*, 1996), pH sensitive controlled drug release systems (Sideratou *et al.*, 2000; Gillies *et al.*, 2004),

catalysts (Piotti *et al.*, 1999; Goetheer *et al.*, 2000) and chromatography (Kuzdzal *et al.*, 1994).

1.1. Supramolecular assembly

There is of course a large and growing spectrum of primary dendron and dendrimer structures, possible because of the almost limitless range of dendritic architectures that can be built around suitable multi-functional core molecules.

The preparation of supramolecular or self-assembled dendrimers via non-covalent interactions has recently been sought to reduce the synthetic effort required in dendrimer synthesis. Such methodology guarantees the accuracy of the structural assembly which can then easily revert to the building blocks with a particular stimuli. The self-assembly process can be a dendron-only process involving hydrogen bonding (Zimmerman *et al.*, 1996), hydrophobic interactions (Percec *et al.*, 2001) or electrostatic interactions (Tomioka *et al.*, 1998; Balzani *et al.*, 2002). Self-assembly can be also directed by a template. The template interacts with functional group(s) on the dendron or dendrimer as shown in **Figure 1.2**. Such interactions can be ligand-metal interactions (Newkome *et al.*, 1999; Gorman and Smith, 2000), hydrogen bonding (Wang *et al.*, 2001) or electrostatic (Bo *et al.*, 1997).

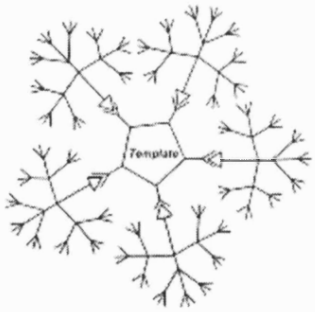

Figure 1.2: Schematic representation of supramolecular dendrimer with individual dendrons assembled around a molecular template. (Reproduced from Dykes and Smith, 2003)

Zimmerman *et al.* (1996) was the first to introduce hydrogen bond mediated assembly of Fréchet-type benzyl ether dendrons with two isophthalic acids at the focal point. The dendrons form hexameric disk-shaped aggregates with a 2 nm thickness and a 9 nm diameter. The dendron or dendrimer structure can direct the assembly process. Baars and co-workers (2000b) reported the non-covalent synthesis of the polyester dendritic "bow-ties" composed of two complementary dendrons based on 2,2-bis(hydroxymethyl)propionic acid with bis-(adamantylurea) or glycinylurea at the focal point. Gillies and Fréchet (2004) showed that the association constant of the parent self-assembled system was dependent on the peripheral functionality as shown by ^{1}H NMR.

Dendritic branches have been also shown to form gel phase materials. Kim *et al.* (2001) reported the thermo-reversible gelation of alkyl modified amide dendrons into organic solvents driven by the intermolecular hydrogen bonding between the amide groups in the dendritic structures and stabilised by hydrophobic interactions among the peripheral alkyl chains. Increasing the dendrimer generation resulted in self-organisation into lamellar or hexagonal columnar structures which self-assembled into fibres. The introduction of polymerisable dendritic blocks such as acetylene moieties added to the nanostructure stability (Kim *et al.*, 2003). Aida *et al.* (2000) also reported the gelation of an aromatic dendron, di-peptidyl core poly(benzyl ether), in organic solvents. The gel contains fibres (1-2 μm diameter) made of smaller fibrils (20 nm diameter). Another type of supramolecular organogels shown in **Figure 1.3** comprised two-components; the polylysine dendritic branches functionalised with acid or crown ethers (Dykes and Smith, 2003) and the aliphatic diamines.

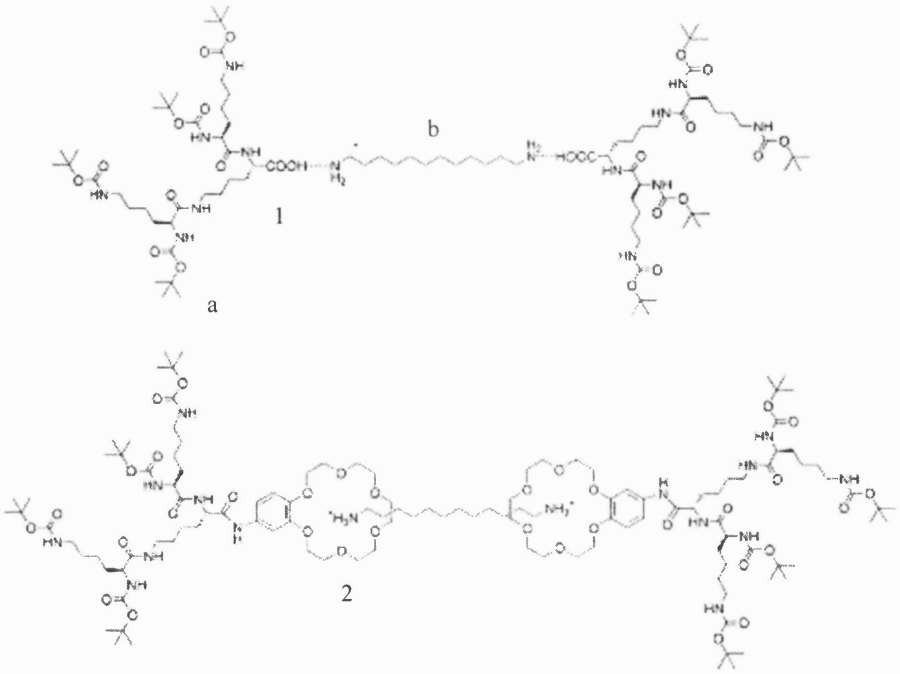

Figure 1.3: Two-component supramolecular dendritic gels made of (a) polylysine dendritic branches functionalised with acid (1) or crown ether (2) and (b) diaminododecane. The network is based on acid-amine or crown-NH_3^+ interactions and the hydrogen bonding between the peptidic groups. (Reprinted from Dykes and Smith (2003), © Elsevier Science Ltd)

Newkome *et al.* (1993) reported the gelation of dumb-bell shaped 'arborols' consisting of two hydrophilic dendrimer spheres and bridged with a lipophilic linker. The length, bulkiness and rigidity of the linker dictate the stacking of some arborols into rod-shape structures.

Other forms of self-assembly include the small vesicular structures with a diameter ranges between 20-200 nm and a bilayer arrangement seen in acidified aqueous solutions of poly(propylene imine) dendrimers modified with 64 hydrophobic alkyl chains (20-200 nm in diameter) (Schenning *et al.*, 1998) and the amide dendron bearing four alkyl chains (160 nm in diameter) in water (Kim *et al.*, 2001).

More water soluble dendrons and dendrimers tend to aggregate into micellar forms. Mizutani and co-workers (2002) reported the aggregation of quaternary dendrimers with methyl and octyl chains into micellar aggregates of 17-36nm diameter. Also

Esumi *et al.* (2002) found that a 4th generation polyamidoamine dendrimer having 64 alkyl groups formed micellar aggregates in water. Gillies and Fréchet (2004) have recently developed micellar carriers, comprised of a linear poly(ethylene oxide) and either a polylysine or polyester dendron, capable of releasing their drug load in response to small changes in pH encountered in the mildly acidic pH of tumour and inflammatory tissues.

The self-assembly of dendrons into liquid crystalline materials is a new approach in supramolecular dendrimers studied by Percec *et al.* (1994; 1995; 1997) and based on the self-assembly of small and well defined tapered or wedge shaped so-called "monodendrons" into macroscopical crystalline and liquid crystalline structures, complex structures which have potential applications in areas as photonics, molecular electronics and catalysis (Ungar *et al.*, 2003).

The correlation between the molecular geometry of the monodendritic molecules and the shape and size of supramolecular structures formed was studied by Ungar *et al.* (2000; 2003). **Figure 1.4** shows that the resulting supramolecular structure was controlled by altering the generation, the size of the core and the width of the aliphatic end. Flat tapered monodendrons based on gallic acid and substituted with three dodecyl chains self-assemble like flat pizza slices and discs, then into cylindrical structures which pack into columnar hexagonal thermotropic solvent free liquid crystals, upon heating to the isotropic melt. Alternatively, cone shaped alkyl substituted second generation dendrons self-assemble into spherical structures instead which further arrange into a cubic liquid crystalline lattice.

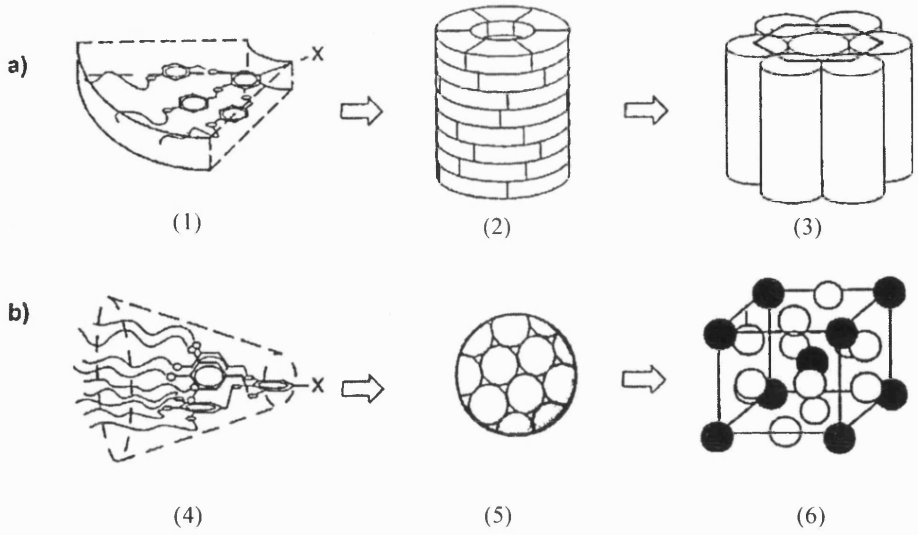

Figure 1.4: a) Schematic representation of the self-assembly of flat tapered monodendrons (1) into a supramolecular cylindrical dendrimer (2) and then into a hexagonal columnar liquid crystal (3); b) self-assembly of conical monodendrons (4) into a supramolecular spherical dendrimer (5) and of the self-organisation of the latter into a cubic liquid crystal (6). (Reprinted from Ungar *et al.*, 2000)

The new concept of receptor functionalised dendrons was studied by Elemans *et al.* (2002) suggesting their use as nanoreactors. Dendrons functionalised at their origins with recognition units, namely clip receptors, formed assemblies with the methyl 3,5-dihydroxybenzoate guest molecules entrapped in the core of the spherical assemblies **(Figure 1.5)**.

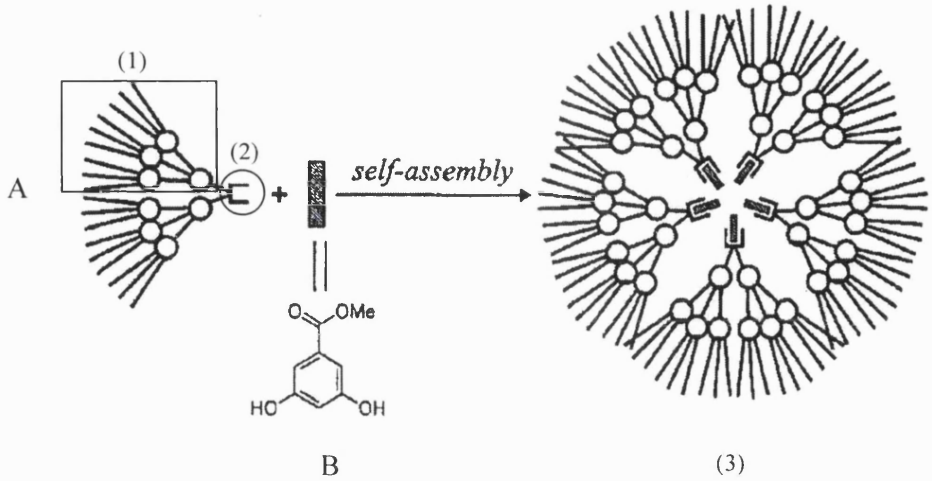

Figure 1.5: a) Schematic representation of the proposed self-assembly of the host-guest complex of (A) a monodendron, based on (1) gallic acid and functionalised with (2) a clip receptor and (B) methyl 3,5-dihydroxybenzoate as a guest. The guest molecules are located in the core of the supramolecular dendrimer (3). (Reprinted from Elemans *et al.*, 2002)

Percec *et al.* (2002) reported the self-assembly of fluorinated dendrons, with a wide range of conducting organic acceptor or donor groups attached to the apex, into supramolecular nano-scale columns which self-organise into hexagonal, centred and rectangular columnar crystals exhibiting high charge carrier mobilities with promising optoelectronic properties.

Other groups have studied dendritic-linear block copolymers which are intermediates between traditional surfactants and amphiphilic block copolymers. Gistov and co-workers (1992) have synthesised amphiphilic diblock (AB) and triblock (ABA) copolymers based on polyether dendrimers and polyethylene glycols and showed that some of them were able to form micelles in some solvents. Polyethylene glycol-Boc-protected polylysine copolymer named hydraamphiphile showed surfactant and

solubilisation properties (Chapman *et al.*, 1994). Similarly a series of the amphiphilic polystyrene (PS)-poly(propylene imine) dendrimer diblock copolymers with varied head group size (Vanhest *et al.*, 1995) showed a generation dependent aggregation pattern in water; the diblock copolymer made of polystyrene and poly(propylene imine) dendrimer with eight surface amine (PS-dendr-$(NH_2)_8$) forms vesicular structures (circa 100 nm in diameter), PS-dendr-$(NH_2)_{16}$ with 16 surface amines forms micellar rods with 12 nm in diameter, PS-dendr-$(NH_2)_{32}$ forms spherical micelles (10-20 nm in diameter). Zhu *et al.* (2001a; 2002) reported another block copolymer of 2nd and 3rd generation polyether dendrimer (non-polar) and the thermoresponsive polymer poly(*N*-isopropylacrylamide) (polar) found to self-assemble in aqueous solution into bilayer spherical aggregates with hydrodynamic diameters of 40- 80 and 140- 250 nm respectively . A phase transition was observed at 37.5 °C with a change in the morphology into entangled nanotubules of several micrometers length. The dendritic polyether – poly(acrylic acid) block copolymer self-assembles into typical vesicular aggregates with a layer thickness of 3-5 nm (Zhu *et al.*, 2001b).

1.2. Dendrimer-surfactant assemblies

Interaction of surfactant molecules with ionic and non-ionic polymers such as poly(acrylic acid) and poly(ethylene oxide) are well known (Robb, 1981; Attwood and Florence, 1983b; Goddard, 1986a; Goddard, 1986b). The nature of interaction as well as the structure of these complexes is of importance in many industrial and biological processes such as the solubilisation of biological membranes, oil recovery, mineral flotation and flocculation. Although many mixed systems of surfactants and polymers have been studied, few dendrimer-surfactant interactions have been investigated. Such studies can provide some information about structural changes of

dendrimers between different generations. For example, poly(amidoamine) dendrimers (PAMAM) possessing external anionic surface groups undergo a change in morphology from an open, branched structures for generations 0.5-3.5 to a closed, increasingly compact surface for generations 4.5-9.5 as shown by molecular simulation (Naylor *et al.*, 1989). Their interaction with the anionic surfactant sodium dodecyl sulphate (SDS) studied by fluorescence spectroscopy (Caminati et al., 1990) leads to the formation of two types of PAMAM-templated surfactant aggregates as a function of generation and size.

In several instances, dendrimers which lack surfactant properties were found to enhance the surface activity and hydrophobicity of some surfactants (Caminati *et al.*, 1990; Esumi *et al.*, 2000; 2001) and vice versa. SDS enhanced the surface activity of the cationic tetrameric PAMAM dendron (G=0) with four octyl chains and four ammonium groups as demonstrated by surface tension measurements (Yoshimura *et al.*, 2002). Light scattering measurements showed an increase in the apparent diameter of the dendron from 1.3 to 171 nm in its aggregated form. Enhanced hydrophobicity and higher pyrene solubilisation of the aggregates compared to SDS micelles alone was observed, possibly due to reducing the electrostatic repulsion due to interactions between ammonium groups and sulphate ions in addition to hydrophobic associations between dendron octyl chains and dodecyl chains of the surfactant. Furthermore, a hydrophobically modified PAMAM dendrimer with 64 octyl chains with an inherent surface activity formed aggregates with a much higher surface activity and an extraordinary capacity for solubilisation of pyrene compared to the dendrimer-dodecyltetrammonium bromide (DTAB) and dendrimer-hexaoxyethylenedodecyl ether ($C_{12}E_6$) systems and twice that of dendrimer alone (Esumi *et al.*, 2002).

Another application is the solubilisation of cascade polymers and dendrimers which are interesting candidates for applications in diagnostics and sensor technology. A large but distinct number of chromophores and biologically active group(s) can be attached to them, but sometimes the hydrophobicity of these structures hinders their use in bioassays since water solubility is a requirement. Dendrimer-detergent association does not require chemical intervention compared to dendrimers carrying covalently attached solubilizing agents to provide water solubility. Recently, an insoluble polyphenylene dendrimer bearing three perylene monoimide chromophores (PMI) and a single biotin group has been synthesised (Minard-Basquin *et al.*, 2003). Non-ionic detergents such as polysorbate 20 and polysorbate 60 have shown promising solubilisation behaviour. Fluorescence correlation spectroscopy (FCS) and dynamic light scattering (DLS) showed a constant hydrodynamic radius of 7.1 nm for dendrimer-detergent complexes at a polysorbate 20: dendrimer molar ratio of 11600:1.

Mixtures of surfactants and amphiphilic dendrimer may provide a wide variety of supramolecular structures (Watkins *et al.*, 1997; Blanzat *et al.*, 2002) depending on temperature, surfactant charge and structure (Caminati *et al.*, 1990; Partearroyo *et al.*, 1992; Esumi *et al.*, 2000; 2002; Minard-Basquin *et al.*, 2003), dendrimer type and generation (Yoshimura *et al.*, 2002; Mizutani *et al.*, 2002) and surfactant/dendrimer molar ratio (Caminati *et al.*, 1990; Esumi *et al.*, 2001; Minard-Basquin *et al.*, 2003).

1.3. Polylysine dendrons and dendrimers

Florence *et al.* (1998) focused on the secondary structures found within a homologous family of polylysine-based dendrons and dendrimers which are cationic, lipidic or amphipathic in nature. By derivatising the surface lysine groups of the dendrimers (and the core of some dendrons) a wide range of solubilities, molecular shapes and solution or suspension behaviour can be obtained. **Figure 1.6** summarized the structures discovered. Sakthivel *et al.* (1998) were the first to discover the asymmetric fibre-like structures formed in aqueous media from lipidic dendrimers **(Figure 1.7)**.

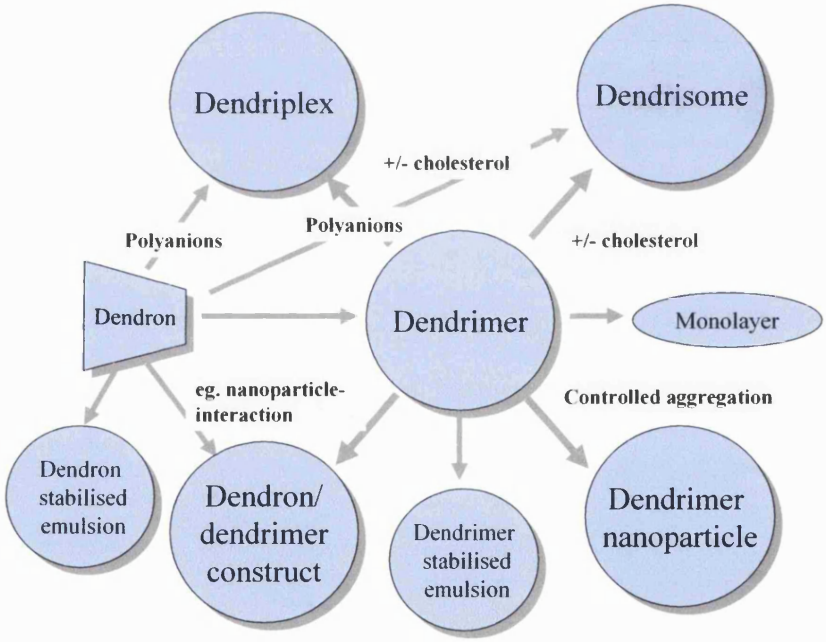

Figure 1.6: A schematic of the relationships between the primary dendron and dendrimer structures and the aggregated states: monolayers, dendrimer nanoparticles, dendrisomes, dendriplexes and dendrimer constructs (e.g. dendrimers adsorbed onto nanoparticles). Perhaps not surprisingly some amphipathic dendrons can stabilise oil in water emulsions.

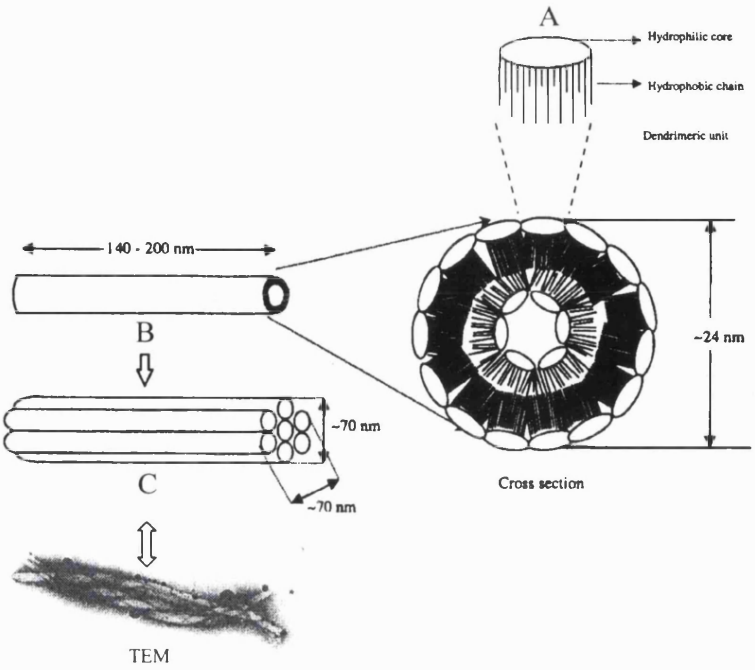

Figure 1.7: Possible models of association of lipophilic dendrimer (A) in aqueous dispersions. A typical tubule (B) with the dimensions of 140-200 nm and 24 nm thickness with the possible association to bundles (C). (Reprinted from Sakthivel *et al.*, 1998)

1.3.1. Surface monolayer formulation

Perhaps the simplest morphology of an array of dendrimers is a monolayer spread at the solid/air, solid/water or air/water interface. Hydrophobic dendrimers can form monolayers at the air/water interface, as shown diagrammatically shown in **Figure 1.8**. The area/dendrimer molecule can be calculated in the normal way from surface pressure - area (π-A) isotherms **(Figure 1.9)**. In one series studied, the calculated areas per dendrimer accurately reflect data from molecular models (Sakthivel *et al.*, 1998). In a later study it became clear that the theoretical diameters and radii derived from such models and the values obtained using surface pressure data were not

always consistent. It was suggested therefore that an "elasticity" or "collapse" potential can be determined as dendrimers are not all rigid spherical structures. The dendrimers appear to transform from more soft structure to less compressible systems. The size of some dendrimers is sensitive to the pH of the medium in which they are dispersed (Pistolis *et al.*, 1999; Zhang *et al.*, 2003; Kim and Bruening, 2003).

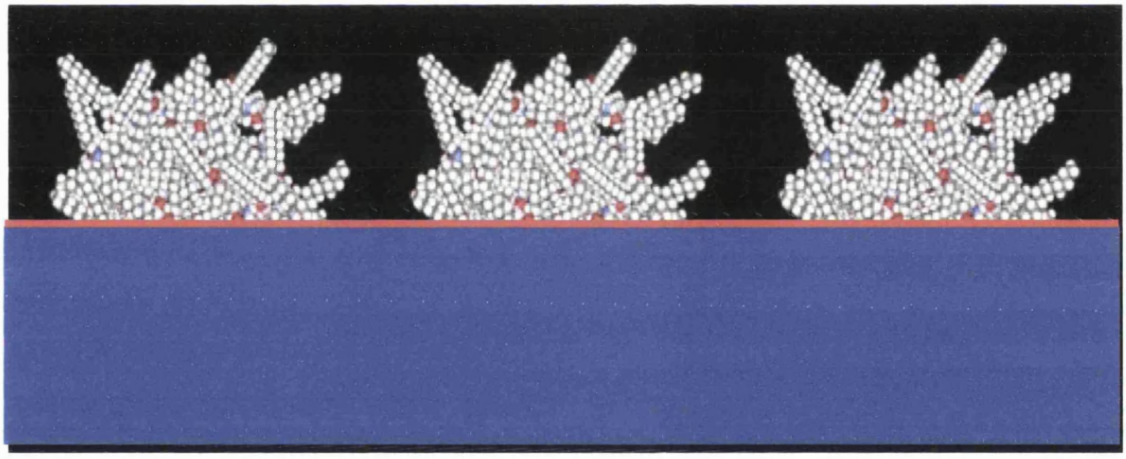

Figure 1.8: A schematic of the adsorption of a lipidic dendrimer spread at the air-water interface. (Courtesy of B. Singh, School of Pharmacy, London).

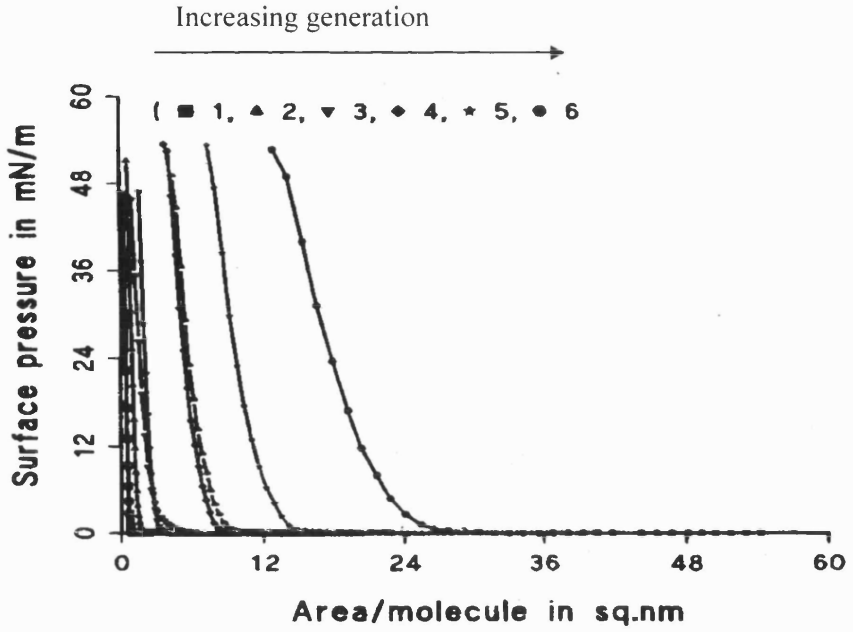

Figure 1.9: Surface pressure-isotherms of lipidic peptide dendrimers (numbers 1 to 6 represents generations 1 to 6 coupled to acetylated α-aminododecanoic acid). Conditions: dendrimers spread on water as solutions in chloroform (50 µl) allowing 10 min for solvent evaporation before commencing compression at a rate of 100 cm^2/min at 25 °C. (Reprinted from Sakthivel *et al.*, 1998)

Amphipathic dendrons adsorb onto polystyrene nanoparticles through hydrophobic interactions: an increase in the cross-sectional area of the branched lysine head group (and hence hydrophilicity) leads to decreased adsorption (Sakthivel and Florence, 2003). Adsorption of cationic dendrons to cellulose membranes is strong but can be minimised by addition of sodium chloride, which acts through charge reduction (Purohit *et al.*, 2003).

1.3.2. Formulation of dendrimer-derived nanoparticles

Dendrimers whose surface groups have been wholly or partially derivatised by hydrophobic groups may aggregate spontaneously in aqueous media. Control of this process is one means of using such individual sub-10nm dendrimers in new morphologies in a larger packed spherical arrangement, whose size can be controlled.

The size and stability of such dendrimer aggregates is dependent on the packing characteristics of the dendrimer. Singh and Florence (unpublished) have studied the concentration-dependent formulation of nanoparticles of interesting morphology from lipidic dendrimers with molecular weights ranging from ~ 6,200-19,800 and differing in generation and length of lipid chain. Controlled aggregates were formulated using the precipitation method of Quintanar-Guerrero *et al.* (1998). Nanoparticles could be prepared in the absence of surfactant. The effect of generation, lipidic chain and molecular weight of the dendrimers on apparent particle size was assessed. A slight increase (from 189nm – 240nm) in the Z-average mean nanoparticle size was observed as the molecular weight of the 6^{th} generation dendrimer increased. This increase might be due to two main factors: the increased length of lipidic chain and the increased intrinsic size of the parent dendrimers. With an increase in lipidic chain length the apparent particle size of the aggregates grew in case of the 6^{th} generation dendrimers as shown in **Figure 1.10**. Results suggest that dendrimers with a longer lipidic chain on the surface are more likely to interact to form denser structures and hence more compact structures are observed.

Using pyrene as a hydrophobic probe (Yanai *et al.*, 2001), an indication of the packing of the dendrimers in the body of the nanoparticles can be determined. At lower dendrimer concentrations (0.07-0.26 mg/ml) the pyrene is in an intermediate hydrophobic environment, after which a plateau is reached, confirming that a compact form of the dendrimer-derived nanoparticles with a hydrophobic interior was attained.

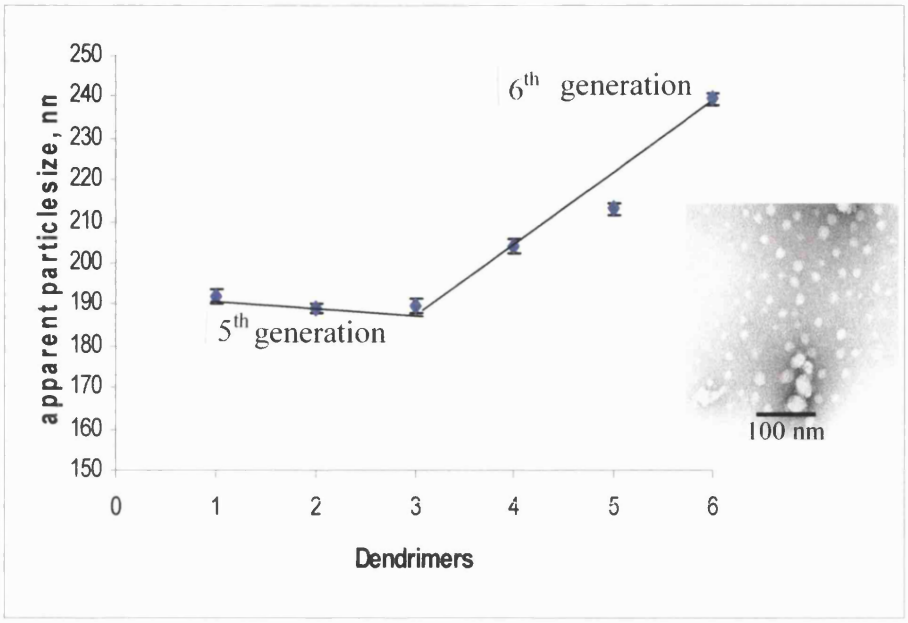

Figure 1.10: Aggregates of lipophilic dendrimers showing the apparent particle size of the order of 190-240nm. Numbers 1-3 and 4-6 represents generations 5 coupled to C_4, C_{10}, C_{12} and generations 6 coupled to C_4, C_{10}, C_{12} respectively. Conditions: The dendrimer was dissolved in dichloromethane (DCM), double deionised water was added and the mixture was sonicated (2x30 sec) to form an emulsion. DCM was evaporated and the aggregates precipitated out into the water phase. The pH of the suspension varied from 5.0-6.0 at ambient temperature. (Singh and Florence, in press)

1.3.3. Polyanionic-cationic dendron/dendrimer complexes

1.3.3.1. Dendron - DNA complexes

The complexes formed between cationic dendrons and polyanions have been termed "dendriplexes" (Ramaswamy *et al.*, 2003a). Their DNA condensation underpins their use as non-viral gene delivery agents. The cationic dendron-DNA complexes have been shown to transfect DNA in a range of cell lines with varying degrees of success (Toth *et al.*, 1999; Shah *et al.*, 2000). Ramaswamy *et al.* (2003a) studied the systematic modification of the terminal lysine branches of dendrons to explore the

structural characteristics that determine their efficiency as non-viral gene vectors. While a cationic charge is paramount, lipid chains on the dendrons enhance the ability to condense DNA: the binding affinity of dendrons is thus ranked $(C_{18})_3Lys_7(NH_2)_8$> $(C_{14})_3Lys_7(NH_2)_8$ > $(C_{10})_3Lys_7(NH_2)_8$ > $Lys_7(NH_2)_8$ (the basic non-lipidic dendron). As the lipidic dendrons form compact complexes with DNA at a lower charge ratio than nonlipidic dendrons, hydrophobic interactions must complement the polyanion-polycation electrostatic interactions. This was confirmed by modelling dendriplexes **(Figure 1.11)** between a 32 bp section of double stranded DNA with four (C18)3Lys7(NH2)8 dendrons, in which clearly the amino groups are in contact with the phosphate groups of the DNA. Dynamics simulation allows the lipidic portions of the dendrons to move towards the DNA backbone through possible hydrophobic interactions. Although these dendrons are of low molecular weight they can form complexes at lower molar quantities than can linear polylysine (of, say, MW 1000). The results suggest that the binding affinity is higher for dendritic polylysine than for their linear counterparts. Transmission electron micrographs (TEM) of some dendriplexes are shown in **(Figure 1.12)**.

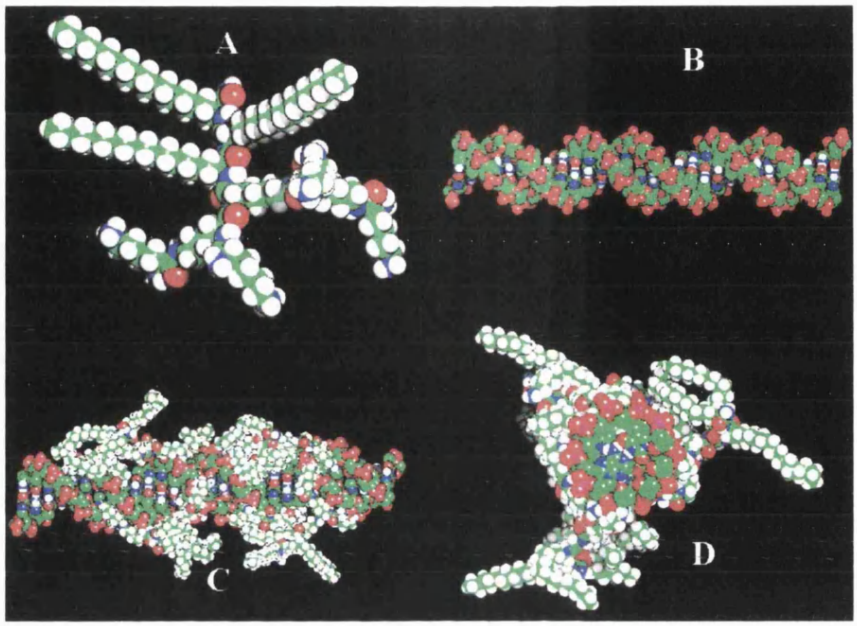

Figure 1.11: Computer generated model of dendriplexes using a 32 base pair segment of DNA. A. $(C_{18})_3Lys_7(NH_2)_8$ dendron B. DNA C and D: two views of the dendriplex. (Courtesy of C. Ramaswamy, School of Pharmacy, London)

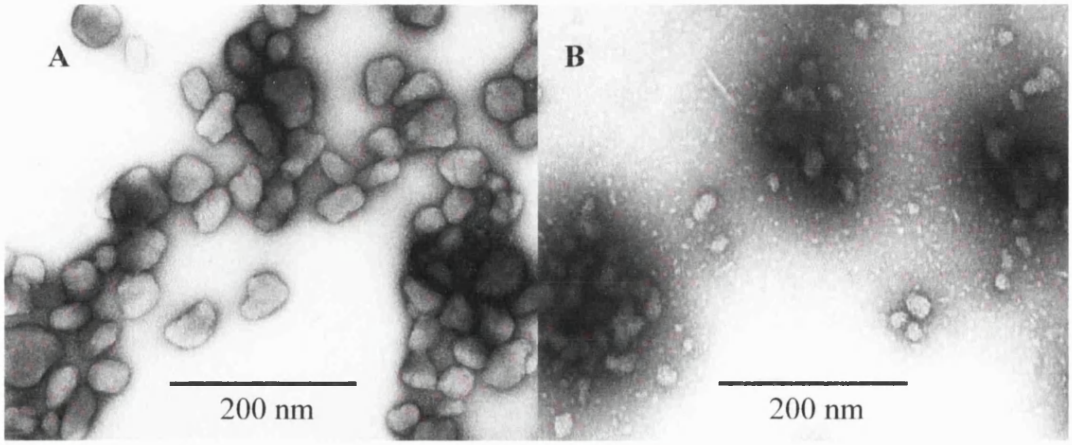

Figure 1.12: a) Transmission electron micrographs of dendriplexes formed by using dendrons without a lipid chain $Lys_7(NH_2)_8$ in water at a 5:1(+/-) charge ratio and b) $(C_{14})_3Lys_7(NH_2)_8$ dendrons in water at a 5:1(+/-) charge ratio. C. Ramaswamy *et al.*(unpublished).

It is not only the condensation of vectors that plays a role in transfection but also the release of DNA from complexes. The release of DNA depends on the stability of the complexes, which can be estimated by challenging the complex with polyanions such as dextrans, poly (aspartic acid), chondroitin sulphate and heparin sulphate (Ruponen *et al.*, 1999). Heparin was used to study the stability and the release of DNA from dendriplexes by measuring the percentage fluorescence recovered by the addition of heparin to dendriplexes and compared with the transfection efficiency (Ramaswamy *et al.*, 2003b). The more stable the complex was, the greater the efficiency, but this is only one factor determining success.

1.3.4. Micellar aggregates

Micelle-like aggregates with a size range of 20-30 nm are formed from more soluble dendrons such as $(C14)_3Lys_7(NH_2)_8$. The electron micrograph in **Figure 1.13a** shows the larger aggregates of approximately 30 nm in diameter which form in the presence of 0.1% NaCl, while **Figure 1.13b** illustrates the somewhat smaller micelles (circa 14 nm in diameter) formed as anticipated in water. The dendrons in this series bearing only one alkyl chain do not form more than dimers .

Figure 1.14 shows the structure of some dendrons which due to their amphipathic nature self-assemble.

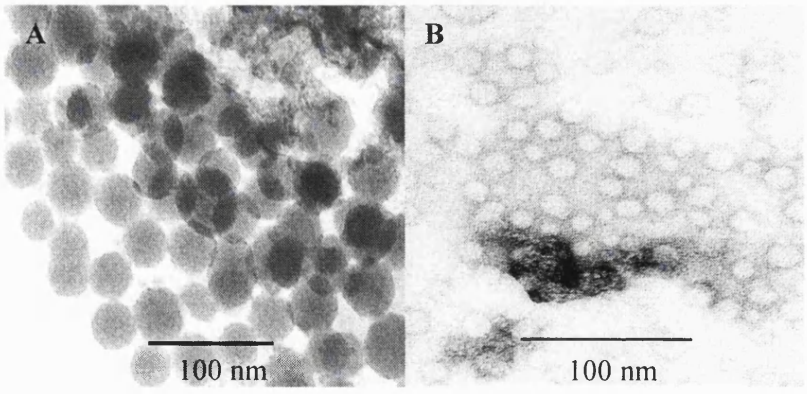

Figure 1.13: TEM photomicrographs of the micellar aggregates of $(C_{14})_3Lys_7(NH_2)_8$: a) in 0.1% sodium chloride solutions and b) in water. C. Ramaswamy *et al.* (unpublished).

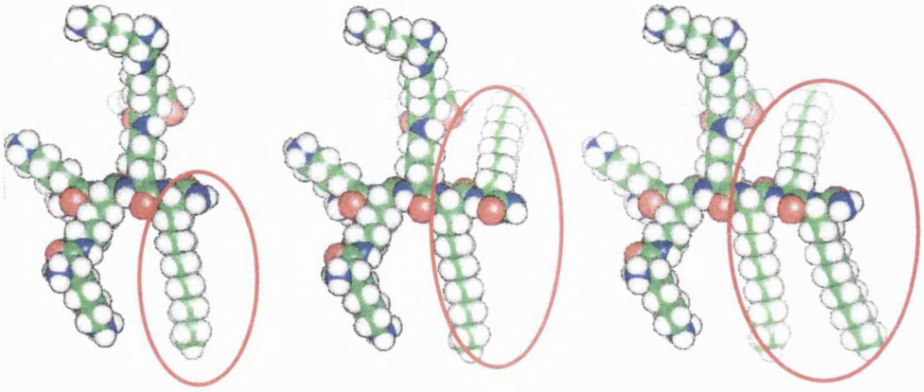

n=1 n=2 n=3

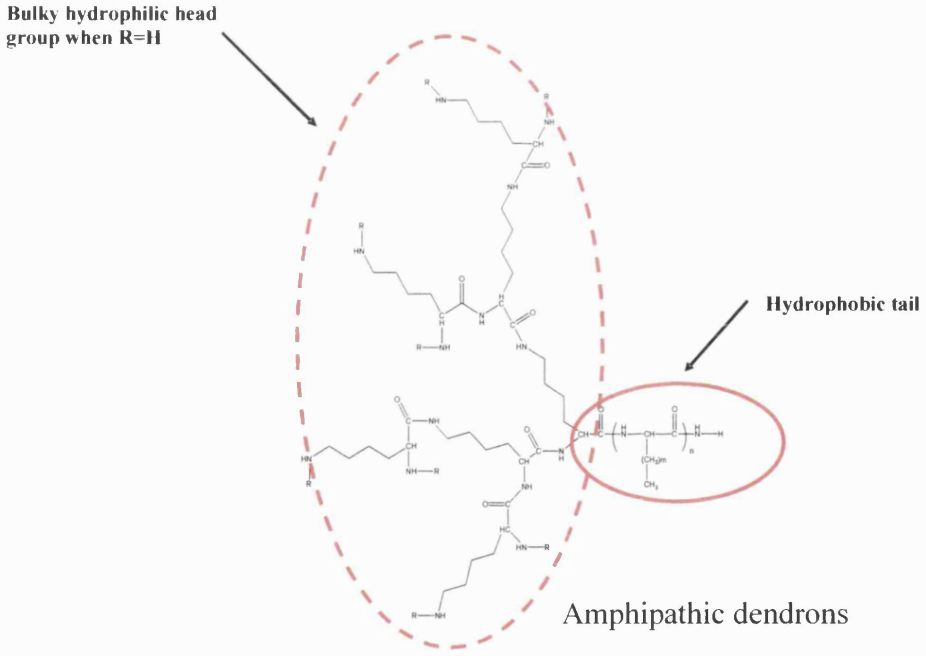

Figure 1.14: Delineation of the general structure of an amphipathic dendrons and specific examples showing the hydrophobic tail and the bulky lysine-based head group.

1.4. Conclusion and correlation to work in the thesis

Further work is necessary to evaluate the thermodynamic parameters associated with the aggregation processes involved in micellization, vesicle, dendriplex and nanoparticle formation in these systems.

Several structures can be formed from dendrons and dendrimers of different chemistry. Polylysine dendrons and dendrimers which are bulky amphiphiles showed controlled aggregation in the form of micelles, dendriplexes and nanoparticles.

Undoubtedly the formation of dendron and dendrimer aggregates overcomes the problem of the large surface to volume ratio or low drug capacity of individual units, whether dendrons or dendrimers. If the systems de-aggregate *in vivo* in a controlled manner then it could be that the supra-molecular forms would have the dual advantage of higher solute carrying capacity and the ability to disperse to small units which can be absorbed and translocate with greater ease than the parent aggregate.

Other forms of supramolecular structures are covered in this thesis. These include dendrisomes as vesicular aggregates, surfactant-dendron assemblies and heparin dendriplexes.

Chapter II

DESIGN AND SYNTHESIS OF CATIONIC LIPIDIC AND NON-LIPIDIC LYSINE-BASED DENDRON AND DENDRIMER DELIVERY SYSTEMS

A group of cationic amphiphilic dendrons and dendrimers of various geometry and lipophilicity were developed and characterised to investigate their potential uses in drug delivery as dictated by their physicochemical properties. These nano-systems are designed as delivery carriers for small molecular weight drugs as well as anionic macromolecules such as heparin.

2.1. Dendrimer synthesis

2.1.1. Solid phase peptide synthesis (SPPS)

Peptide synthesis involves the formation of amide bond between a carboxyl group and an amino group (**Figure 2.1**). Amide bond formation requires a large amount of energy and can be performed at high temperatures. However, this affects the stability of the resulting peptide. Therefore, activation of either the amino or carboxyl terminal is indispensable. *C*-terminal activation is used in all coupling methods. The mechanism of activation involves the substitution of the OH group of the carboxylate group with an electron withdrawing group which renders the carbonyl carbon more

electro-positive and susceptible to nucleophilic attack by the amino group of the second amino acid. A tetrahedral intermediate is formed and stabilised by elimination of the good leaving group (X).

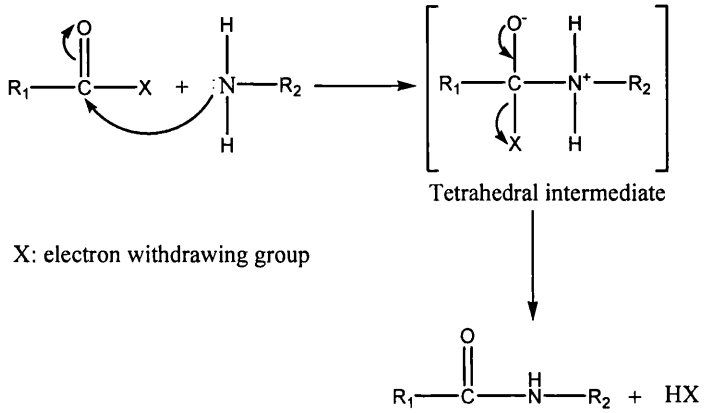

Figure 2.1: General principle of peptide bond formation.

Dendrimers synthesis was carried out using standard solid phase peptide synthesis (SPPS), a technique first proposed by Merrifield (1962; 1963) and now widely used in peptide chemistry.

An overview of a peptide chain assembly using SPPS is shown in **Figure 2.2**. The reactions take place inside the solid support or resin beads which are gels that swell but do not dissolve in particular solvents e.g. *N,N*-dimethylformamide (DMF) (Atherton and Sheppard, 1989). The peptide is anchored to the polymer and built in a stepwise manner by the addition of α-amino and side-chain protected amino acid residues. The acid-labile *tert*-butoxycarbonyl (Boc) group or base-labile 9-fluorenylmethoxycarbonyl (Fmoc) group is used for *N*-protection. After each coupling step, the intermediate protected peptide is separated from starting materials, reagents and by-products by washing the resin with sufficient quantities of solvents such as DMF and isopropanol. The resin swells and contract in successive washing cycles and this allow the removal of excess reagents and by-products.

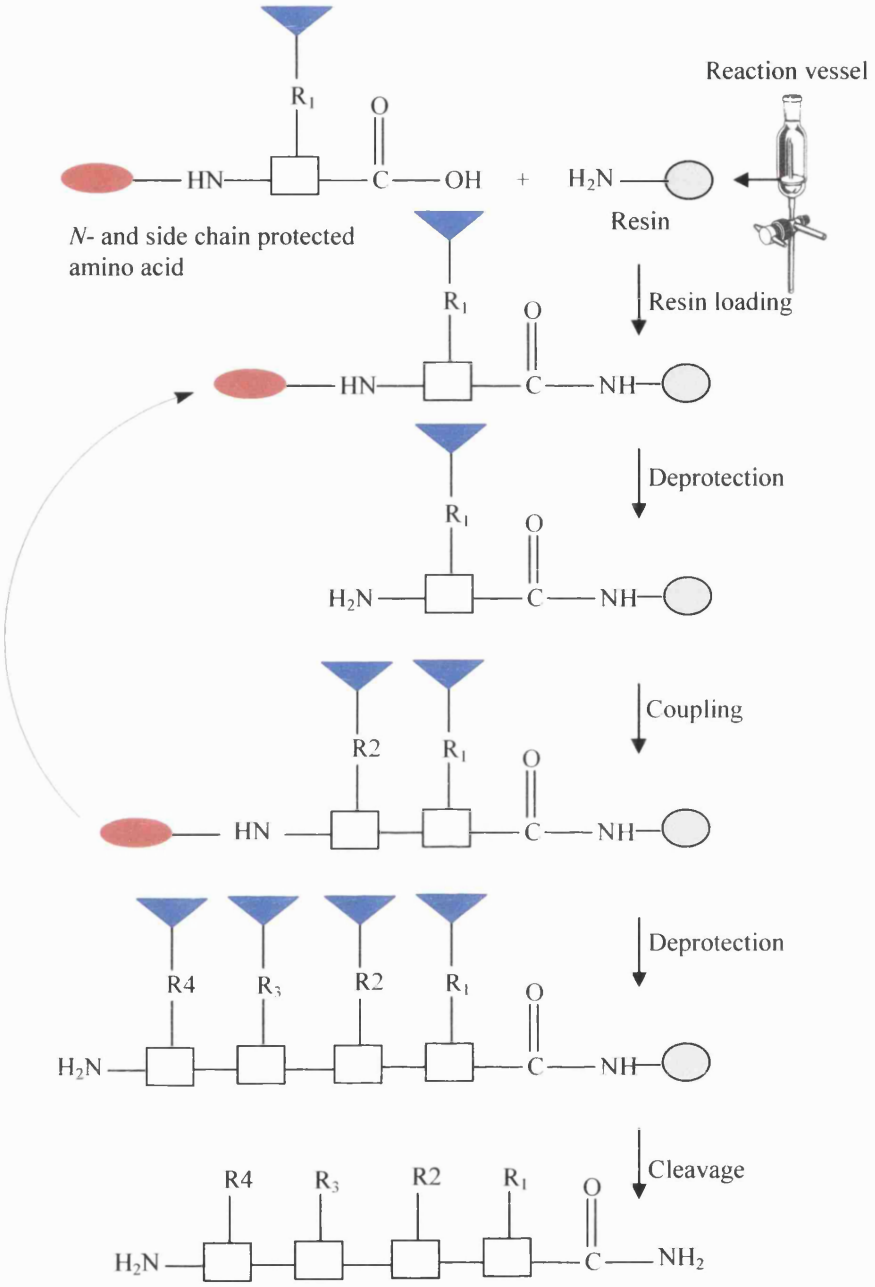

Figure 2.2: Overview of a peptide chain assembly using SPPS.

This is followed by removal of the *N*- protecting groups with reagents that do not affect either the side chain protecting groups or the peptide bond with the polymer. The free amines of the peptide are generated by neutralisation with a tertiary amine and cycles of coupling and deprotection can be repeated. Finally, the completed peptide attached to the resin *via* its *C*-terminus is cleaved from the solid support by

reaction with a strong acid or a weaker acid in Boc or Fmoc methodology, respectively, yielding a peptide acid or amide, depending on peptide-resin linkage. Side-chain protecting groups are cleaved simultaneously with the cleavage from the resin. SPPS is quicker and less tedious than solution-phase synthesis. In the latter, several steps are required after each reaction, involving extraction, filtration, evaporation and purification. However, a limitation of SPPS particularly seen in Boc-methodology is the characterisation of the intermediates. More modern techniques are developed such as FT-IR that characterise intermediates whilst still attached to the resin bead. Also, problems in coupling or deprotection lead to products that are present throughout the rest of the synthesis e.g. deletion peptides.

The various processes to be considered during SPPS are summarised in **Figure 2.3**.

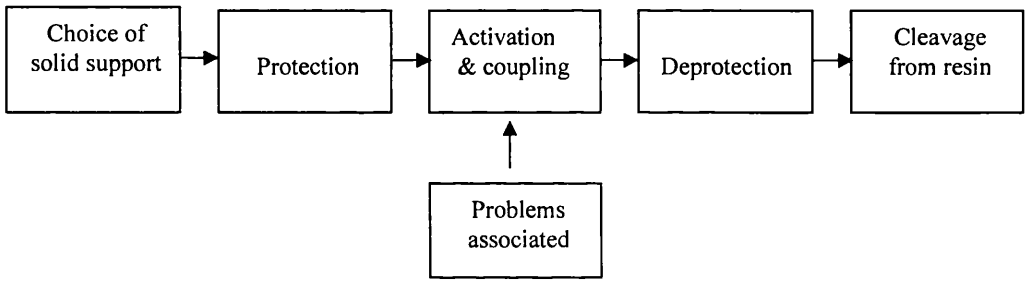

Figure 2.3: Various processes to be considered prior to and after coupling.

2.1.1.1. Resins as solid support

Various materials have been proposed for the solid support. The most commonly used resin suggested by Merrifield (1963) is a polystyrene-divinylbenzene copolymer derivative. Incorporation of divinylbenzene (DVB) as a cross-linker secures resin insolubility in the applied solvents as well as mechanical resistance but it should be lowered to 1-2% to achieve better swelling. Small bead size and high swelling enable them to better accommodate the growing peptide and allow rapid diffusion of the reagents inside. The polymer should be inert to reaction reagents but reactive enough

to be derivatised. Substitution of resin with a reactive functional group that anchors the peptide dictates the loading efficiency of the resin and the type of bond formed between the peptide and the polymer. There are different methods for anchoring the *C*-terminal of the peptide to the resin; for instance resin A and C **(Table 2.1)** form an ester linkage while resin C forms an amide linkage with the peptide. 4-Methyl benzhydralamine (MBHA) resin used in dendrimer synthesis is a polystyrene resin, cross linked with 1% DVB and functionalised with a 4-methylphenyl-aminomethyl group. It is the most widely used resin for the synthesis of peptide carboxamide by the Boc strategy (Matsueda and Stewart, 1981). Deprotection and cleavage take place by treatment with trifluoroacetic acid (TFA) and liquid hydrogen fluoride (HF) respectively. The structures of the most commonly used resins for both Boc and Fmoc strategies are shown in **Table 2.1**.

Table 2.1: Examples of some resins used in SPPS

Functionality	Example(s)	Chemical structure	Anchoring linkage	Cleavage product
(A) Chloro functionalised resins	Merrifield resin † PAM resin†	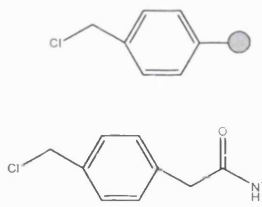	Ester linkage	Peptide acid
(B) Amino functionalised resins	MBHA resin †	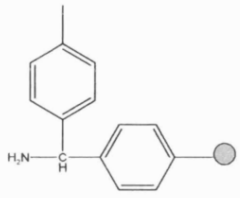	Amide linkage	Peptide carboxamide
(C) Hydroxy functionalised resins	Wang resin‡	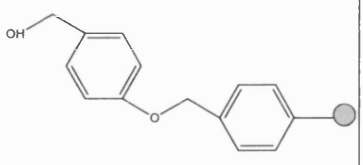	Ester linkage	Peptide acid

† used in Boc strategy
‡ used in Fmoc strategy

2.1.1.2. Protection/deprotection of functional groups

The *N*-protecting group has to be stable to the coupling conditions employed and easily deprotected after the coupling has been accomplished, without affecting the stability of semipermanent side chain protecting groups and the peptide-resin linkage (Kent, 1988). The commonly used Boc protecting group **(Figure 2.4)** (Anderson and McGregor, 1957) is removed by utilising TFA while side chain deprotection and the cleavage of the peptide from the resin takes place only in the presence of a strong acid such as HF. Repetitive use of TFA in Boc-group deprotection may alter sensitive peptide bonds and catalyse side reactions (Atherton and Sheppard, 1989). The introduction of the acid resistant and base sensitive Fmoc group **(Figure 2.4)** (Carpino and Han, 1970; 1972) in SPPS was a major improvement. The amine deprotection is carried out using a secondary amine such as piperidine which has no effect on the acid-sensitive side chain protecting groups and the resin peptide linkage. This linkage and side chain deprotection can then be cleaved under milder acid conditions of TFA, avoiding the harsh and very hazardous conditions of HF which allow the incorporation of sensitive residues. It is noteworthy that the Boc strategy is cheaper and faster but the solubility of Fmoc-protected peptide intermediates and the deprotected amine is reduced compared to Boc-analogues (Bodanszky, 1993).

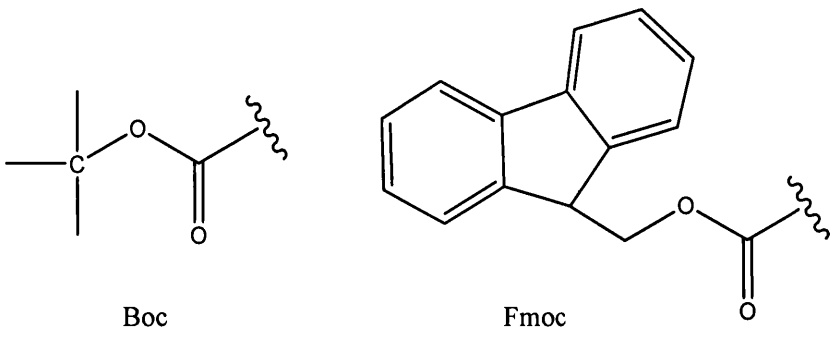

Boc Fmoc

Figure 2.4: Common *N*-protecting groups.

2.1.1.3. Activation and coupling

Different approaches to the formation of peptide bond have been explored. The Azide mediated peptide coupling was one of the earliest method to be introduced (Curtius, 1902) and remains as a classical tool in peptide synthesis. The alkyl ester of the carboxyl group is changed to an acid hydrazide that is then transformed to the reactive azide. Acid chlorides can also be utilised as the reactive species but are now rarely used as a modern synthetic method (Fischer, 1903).

It was not until 1947 when the first report appeared on the application of mixed or unsymmetrical anhydrides in peptide synthesis (Chantrenne, 1947). The most obvious problem using mixed anhydride is the formation of an undesirable acetylation product. Therefore it is necessary to have a considerable difference between the electron densities on the two sides of the anhydride carbonyl with the carbonyl carbon of the protected amino acid being more electrophilic. Mixed anhydride of the protected amino acid and various acids can be designed based on this concept (Albertson, 1962). A solution to this problem was the introduction of symmetrical anhydrides, which generate a single amide type on reaction with an amino component. However, the preparation of isolated symmetrical anhydrides is relatively costly which overrides their reactivity and production of a single acetylation product.

Activated esters of the protected amino acids are the other alternative for the activation of carboxyl group with an electron-withdrawing constituent which cannot act as an acylating agent. Aryl esters such as *p*-nitrophenol (Bodanszky, 1955) **(Figure 2.5a)** and pentafluorophenol (Kovacs *et al.*, 1967) **(Figure 2.5b)** esters of the protected amino acid have been found to be useful in peptide synthesis. *O*-acyl hydroxylamine derivatives have also been proposed in peptide synthesis. However,

only the esters of *N*-hydroxysuccinimide (HOSu) (Anderson *et al.*, 1963) are widely used **(Figure 2.5c)**. Although the *O*-acyl derivative of 1-hydroxybenztriazole (HOBt) (Konig and Geiger, 1970) **(Figure 2.5d)** is not prepared in its isolated form, it is prepared *in situ* where HOBt is used as an additive to suppress side reactions and racemization in carbodiimide-mediated couplings.

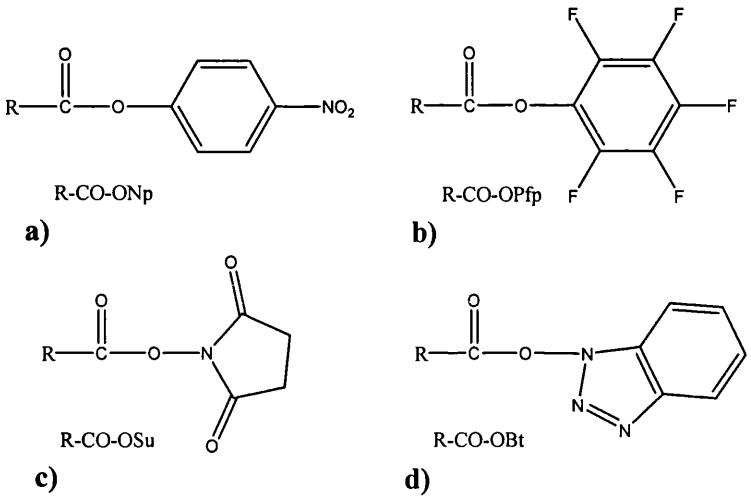

Figure 2.5: Chemical structure of some active aryl and *O*-acyl-hydroxylamine esters.

Coupling or condensing reagents are compounds added to mixtures of both carboxyl and amine components. Ideally, they should activate the carboxyl group and remain inert toward the amine. Such compounds are numerous today. Dicyclohexylcarbodiimide (DCC or DCCI) proposed by Sheehan and Hess (1955) acts by addition to its N=C double bond. The *N,N'*-dicyclohexylurea (DCU) by-product is readily removed from the reaction mixture. Reactive intermediates in the peptide forming step are *O*-acylisourea and symmetrical anhydrides. However, the use of auxiliary nucleophiles such HOSu and HOBt as an additive in DCC-activated couplings leads to *in situ* generation and consumption of active esters of protected amino acids concurrently **(Figure 2.6)**.

An undesirable side reaction encountered in DCC couplings is the intra-molecular rearrangement of the *O*-acylisourea derivative resulted from the attack of the carbonyl group by the adjacent (NH) causing an O→N shift and yielding an *N*-acylurea derivatives by-product which are difficult to remove and causes loss of the valuable carboxylate component. Also activation by DCC can cause racemization of the carboxyl-terminal residue. Racemization or loss of chiral purity occurs in few instances when a single amino acid residue with urethane protecting group is incorporated. The cause of racemization in DCC couplings is based on the basic character of the reactive *O*-acylisourea intermediate which tends to abstract the proton from the chiral centre.

Some shortcomings of the DCC method can be eliminated by the use of the auxiliary nucleophile HOBt. The additive is applied in an equimolar amount with the two components to be coupled and its concentration hardly changes during the coupling reaction as it is continuously regenerated. The highly reactive intermediates such as *O*-acylisourea derivative and symmetrical anhydrides are converted to the less HOBt reactive ester which is less conducive to side reactions such as O→ N acyl migration and racemization reactions but sufficiently reactive to ensure satisfactory acetylation rates. Multiple and alternative pathways involved in DCC coupling, in the presence in the auxiliary nucleophile HOBt, leading to the same product are summarised in **Figure 2.6** (Hudson, 1988).

The use of auxiliary nucleophiles should not be limited to DCC couplings since by reducing the overactivation of other reactive intermediates the overall performance should be improved.

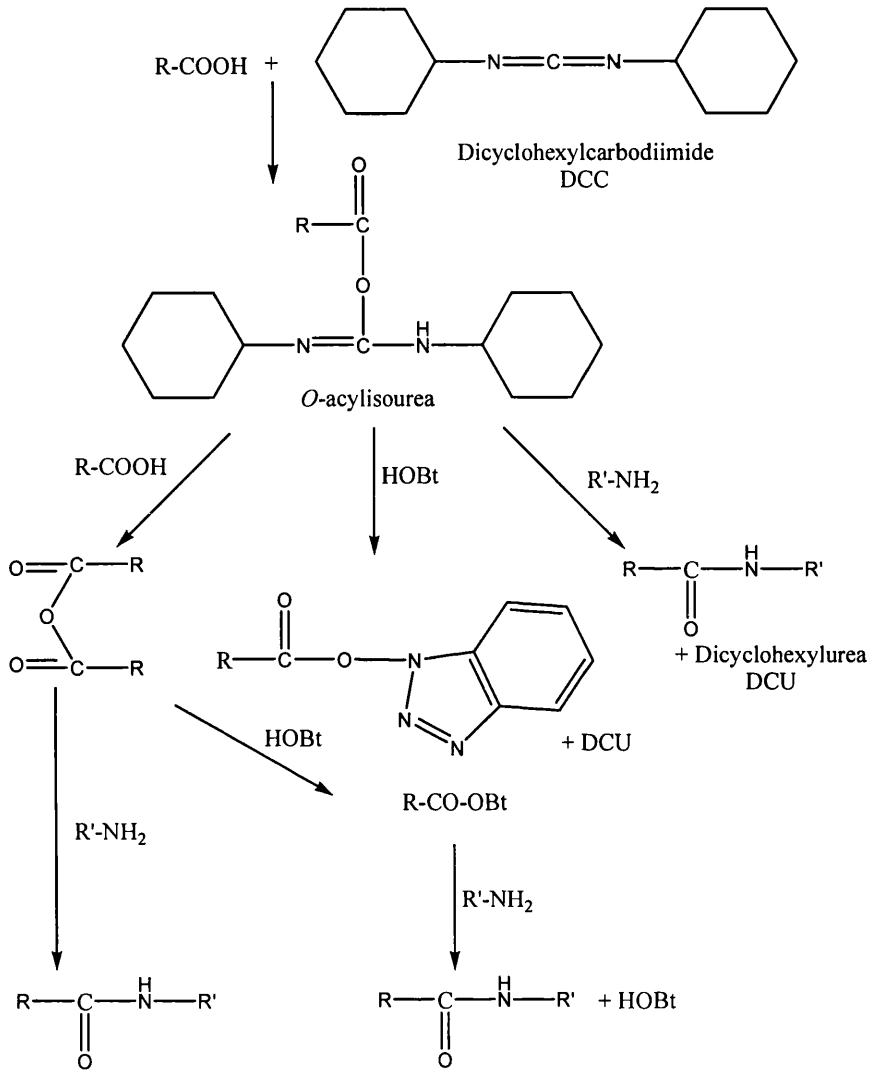

Figure 2.6: Pathways of DCC mediated coupling. Reactive intermediates include *O*-acylisourea, symmetrical anhydrides and HOBt ester of the protected amino acid.

In comparison, Uronium salts (Dourtoglou *et al.*, 1983; Knorr *et al.*, 1989) as coupling reagents cause very little racemization. *O*-benzotriazolyl-*N,N,N',N'*-tetramethyluronium hexafluorophosphate (HBTU) was employed in this work in dendrimer synthesis (see Appendix I). In the presence of a tertiary amine such as

N,N-diisopropylethylamine (DIEA) (this is used to ensure that the carboxylate group is in the anionic form) the carboxylate anion of the *N*-protected amino acid reacts with the uronium cation and generate the highly reactive acyloxyuronium intermediate **(Figure 2.7)** which can be converted directly, as with the carbodiimides, into the reactive esters of HOBt and the symmetrical anhydride, that act as acylating agents to the nucleophilic amine of the peptide chain (Jones, 1999). HBTU should not be used in excess relative to the carboxylic acid as it may lead to the capping of the amino group by converting it into a guanidine group. As mentioned above, HOBt was utilised for to catalyse the reaction and minimise side reactions (Knorr *et al.*, 1989).

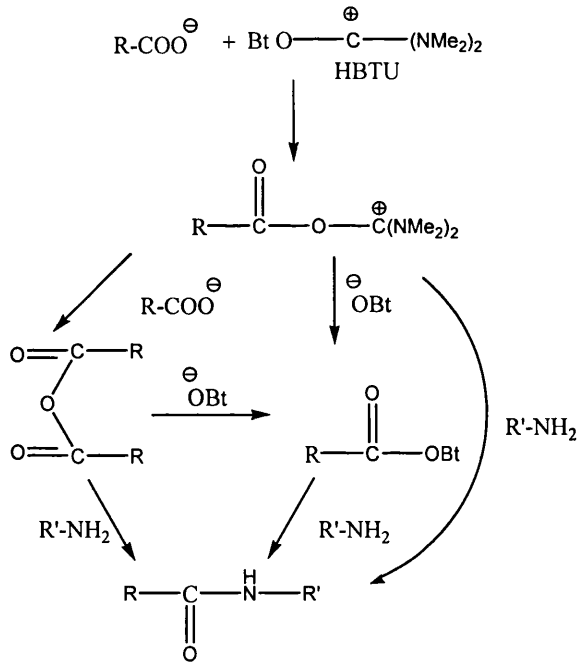

Figure 2.7: HBTU mediated coupling pathways. Reactive intermediates include acyloxyuronium intermediate, symmetrical anhydrides and HOBt ester of the protected amino acid.

2.1.1.4. Cleavage from the solid support

Cleavage of the peptide from Boc-based resins and side chain deprotection requires a strong acid such as HF or trifluoromethanesulfonic acid (TFMSA). HF appears to be

most versatile and least harmful to a wide variety of peptides. However, it is highly toxic and reactive and therefore requires the use of expensive HF-resistant fume hoods and cleavage apparatus.

The *N*-terminal Boc-group must be removed before the HF cleavage to prevent *t*-butylation of susceptible residues during the cleavage and to remove any Boc-amino acid held on the resin by ion-exchange. Standard HF cleavage is carried out at 0-5 °C for 30-60 minutes. Temperature and time control minimises side reactions during the cleavage. Any moisture can be very harmful in HF cleavage. Side-chain deprotection in standard HF cleavage yields highly reactive carbonium ions via an S_N1 mechanism (Tam *et al.*, 1983) so scavengers such as *p*-cresol and anisole are used to prevent the alkylation of susceptible residues but have to be removed from the cleaved peptide. In comparison to standard HF cleavage, low-high HF cleavage uses a low concentration of HF in dimethyl sulphide (DMS) (1:3), which results in deprotection via the S_N2 mechanism which does not involve carbonium ions formation and therefore prevents side-chain alkylation. This procedure deprotects the side chains but does not cleave the peptide from the resin. So HF and DMS are evaporated and followed by standard HF cleavage.

Cleavage of the peptide from Fmoc-based resins is performed simply by using TFA. After cleavage, the peptide is precipitated by cold anhydrous ether to remove scavengers and fluoride ions; the peptide is separated by filtration, then extracted by an appropriate percentage of glacial acetic acid and freeze-dried. Residual acids have to be removed so the compounds are re-suspended in water and dried again to remove all residual acids. The compounds should be kept frozen at -20 °C under nitrogen.

2.1.1.5. Problems associated with peptide synthesis and some useful measures undertaken

Imperfections in acetylation or in the removal of the protecting groups during coupling/deprotection cause the formation of a "failure sequence" or a "deletion sequence" in which one of the amino acid residues is missing. The presence of deficient peptides represents a serious problem as they are difficult to remove because of their similar composition to the desired cleavage compound. This can be as a result of many factors. The polymer choice is very crucial, a less crossed-linked resin showing a more intense swelling and thus a better accessibility to the functional groups. Solubility problems may be overcome by employing Boc-methodology as stated above, Fmoc peptide intermediates are less soluble than their Boc-analogues. The tendency of peptide dendrimers to aggregate by either forming the aggregating beta-structures or due to hydrophobic interactions further reduces the solubility of the intermediates in the reaction solvent. Peptide aggregation is indicated by resin matrix shrinking. Peptide solvation is a crucial condition for efficient peptide synthesis. A solvent mixture of DMF and *N*-methylpyrrolidone (NMP) was advantageous in de-aggregating the beta-structures by competing of NMP's CO-NH bonds with the inter-chain peptide bonds hydrogen bonding. The solvents used have to be pure to avoid side reactions and accumulation of impurities. The principle of excess and extending coupling times were useful to obtain reasonably pure peptide dendrimer. Monitoring the coupling reactions was performed qualitatively or quantitatively with the sensitive colour Kaiser test (Kaiser *et al.*, 1970), a test that gives a dark blue colour with free primary amino groups. Couplings are repeated until a negative test is obtained which ensures complete coupling. However, strongly aggregated sequences occasionally give false negatives, so care should be taken during monitoring

coupling/deprotection efficiency. Minimising side reactions and racemization problems was sought by adopting HBTU activated coupling and addition of the auxiliary nucleophile HOBt.

2.1.2. Dendrimer and dendron design and construction

A peptide vessel shown in **Figure 2.2** constructed from a sintered glass funnel can be used to assemble a simple manual system. MBHA resin LL (100-200 mesh) with 1% DVB was chosen as a solid support. These supports are more sensitive to HF and thus allow release of the peptide with HF at less drastic conditions than other resins. The choice of low loading resin capacity, small bead size and the low degree of cross-linking aimed to achieve better resin swelling, peptide solvation and thus reaction completion. The resin was pre-swollen in DMF which was chosen as a solvent for SPPS. The amino acid and the coupling reagent HBTU were dissolved in DMF. Care was taken not to add HBTU in excess otherwise capping of the amino group would occur. HOBt was added as a catalyst. DIEA was used at double the molar quantities of carboxylic acid and HBTU for two purposes, firstly to neutralise the trifluoroacetate salt of the amino functionalities and secondly to assure that the carboxylate group is in the anionic form to be activated by HBTU. A glycine amino acid or the lipoamino acid was used as a spacer before lysine residues were added.

2.1.2.1. Synthesis of α-amino tetradecanoic acid

The α-lipoamino acids are so called because they combine the structural properties of both lipids (hydrophobic) and amino acids (hydrophilic) **(Figure 2.8)** (Gibbons *et al.*, 1990). They have many applications in drug delivery (Toth, 1994) as well as other areas (Takino *et al.*, 1987; Kitamura *et al.*, 1987). We introduced the lipoamino acids to our dendron and dendrimer delivery systems to control their lipophilicity, by changing the number and length of alkyl chains, while still maintaining their aqueous

solubility. This furnished systems of various HLB values that have different physicochemical properties and which can be tailored to application requirements. Their bi-functional properties that make them superior to normal fatty acids permit their introduction at various stages during dendrimer synthesis; as both intermediate and surface branching units. Surface substitution of polylysine dendrimer with the α-lipoamino acids furnish a surface functionality which can be useful in conjugating the dendrimer which other moieties. Furthermore, α-lipoamino acids previously showed profound advantages in the area of drug delivery such as enhancing stability to chemical and enzymatic degradation (Toth, 1994). However, because they exist as R and S isomers, the possibility of having large number of diasterioisomers is a problem to be considered (Gibbons *et al.*, 1990).

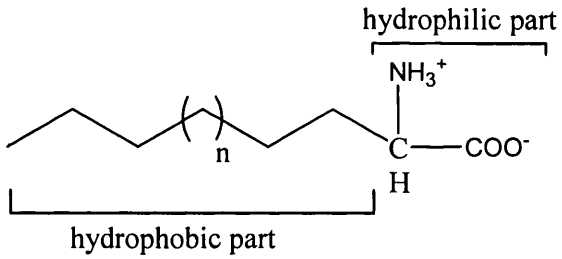

Figure 2.8: Generic chemical structure of a α-lipoamino acid.

α-Lipoamino acids were synthesised according to the method adopted earlier (Albertson, 1946), with some modifications (Gibbons *et al.*, 1990) and demonstrated in **Figure 2.9**. α-Bromoalkane (a) was refluxed with di-ethyl acetamidomalonate (b) in the presence of sodium ethoxide yielding the alkyl diester (c), which was subsequently hydrolysed and partially decarboxylated (d) by refluxing in concentrated HCl. 10% DMF was added to enhance the solubility of the α-lipoamino

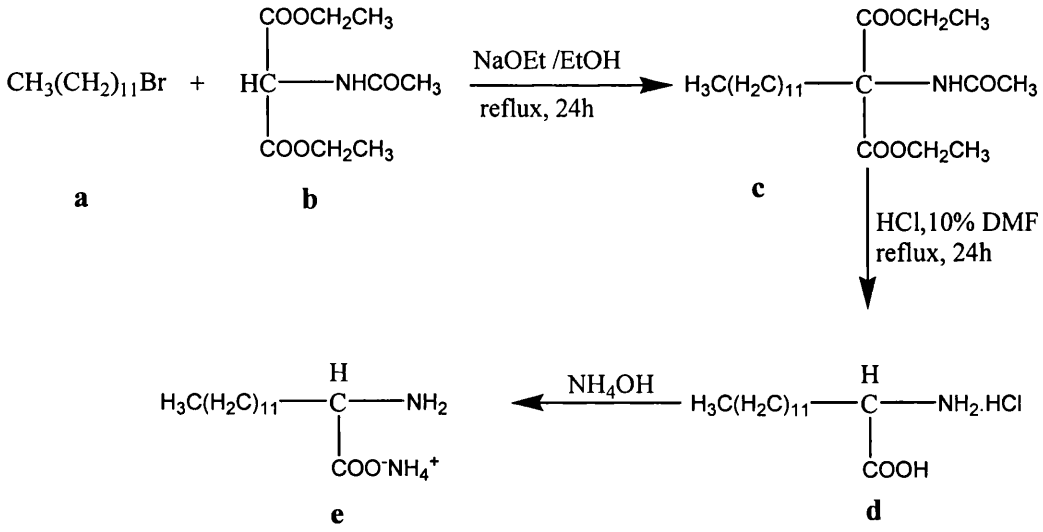

a b c d e

Figure 2.9: Steps involved in the synthesis of α-amino tetradecanoic acid.

acid (Gibbons *et al.*, 1990), and then neutralised with NH_4OH producing the racemic mixture of the lipoamino acid (e) in a good yield.

2.1.2.2. Synthesis of *N*-Boc-α-amino tetradecanoic acid

Figure 2.10 describes the reaction employed in the synthesis of *t*-Boc-protected lipoamino acid. Prolonged stirring of the α-lipoamino acid (a) with di-*tert*-butyl dicarbonate (b) at pH 11 in a water/*tert*-butanol mixture was followed by acidification to pH 3 yielded the *N*-protected amino acid (c). The amino group of the α-lipoamino acid was protected using a Boc group in order to be useful in SPPS of dendrimer (Anderson and McGregor, 1957). A Boc group was preferable to an Fmoc group due to the more economical and facile synthesis (Bodanszky, 1993).

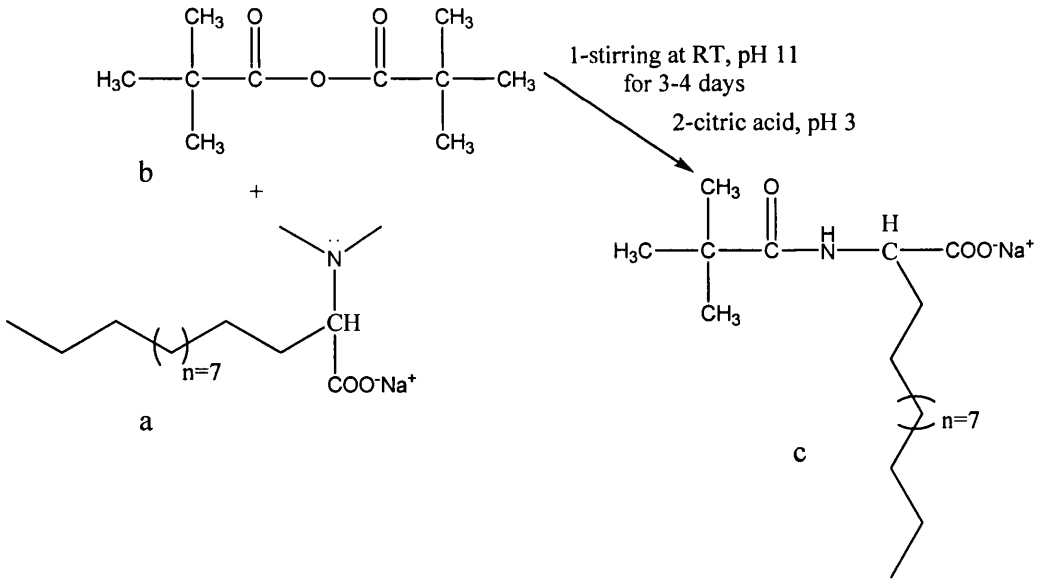

Figure 2.10: Boc-protection of α-amino tetradecanoic acid by reacting it with di-*tert*-butyl dicarbonate.

2.1.2.3. Types of dendrimers synthesised

Our laboratory has established a simple nomenclature to describe our compounds. Compounds names and descriptions are given in **Table 2.2**. For example, **compound 2a** is described as $(C_{14})_3Lys_7(C_{14})_8(NH_2)_8$. $(C_{14})_3$ denotes that the compound has 3 C_{14} alkyl chains in the core coupled to 7 lysine branching units (Lys_7) and that the surface is substituted with 8 C_{14} alkyl chains $(C_{14})_8$ carrying 8 amino groups $(NH_2)_8$. A schematic representation of the SPPS of **compound 2a** is summarised in **Figure 2.11**.

Lipidic (C_{14} substituted) and non-lipidic 5th and 6th generations cationic polylysine dendrimers were synthesised by SPPS. Synthesis details are given in the Appendix I and their chemical structures are shown in **Figure 2.12**.

Table 2.2: A list of the compounds synthesised

Dendron or dendrimer synthesised	Molecular weight (Da)*	Number of lysine units	Number of C_{14} chains	Number of surface amines
Compound 2a $(C_{14})_3Lys_7(C_{14})_8(NH_2)_8$	3388	7	11	8
Compound 2b Gly-$Lys_{31}(NH_2)_{32}$	4047	31	-	32
Compound 2c Gly-$Lys_{63}(NH_2)_{64}$	8149	63	-	64
Compound 2d Gly-$Lys_{31}(C_{14})_{32}(NH_2)_{32}$	11259	31	32	32
Compound 2e Gly-$Lys_{63}(C_{14})_{64}(NH_2)_{64}$	22573	63	64	64

*Molecular weight was calculated by applying the formula:

MW=75× (number of glycine residues) + 146× (number of lysine residues) + 243× (number of lipoamino acid residues) - 18× (number of peptide bonds) + 17

2.1.2.4. Purification of the dendrimers

Purification of the cleaved dendrimer **(compound 2b)** was performed using RP-HPLC based on a C_4 silica-based reverse-phase column. A water/acetonitrile gradient with TFA (0.1%) as acidic ion pairing reagent was used as a mobile phase. Monitoring of elution was performed at 230 nm **(Figure 2.13)**. The large molecular weight of **compound 2c**, which is highly cationic nature, did not allow the compound to be purified by RP-HPLC as it showed poor retention **(Figure 2.13)**. So desalting and removal of small molecular weight impurities was achieved by exhaustive dialysis using 3,500 Da MWCO membranes. Size exclusion chromatography (SEC) using a series of Ultrahydrogel 1000/250Å column and deionised water as a mobile phase did not achieve a good separation in retention

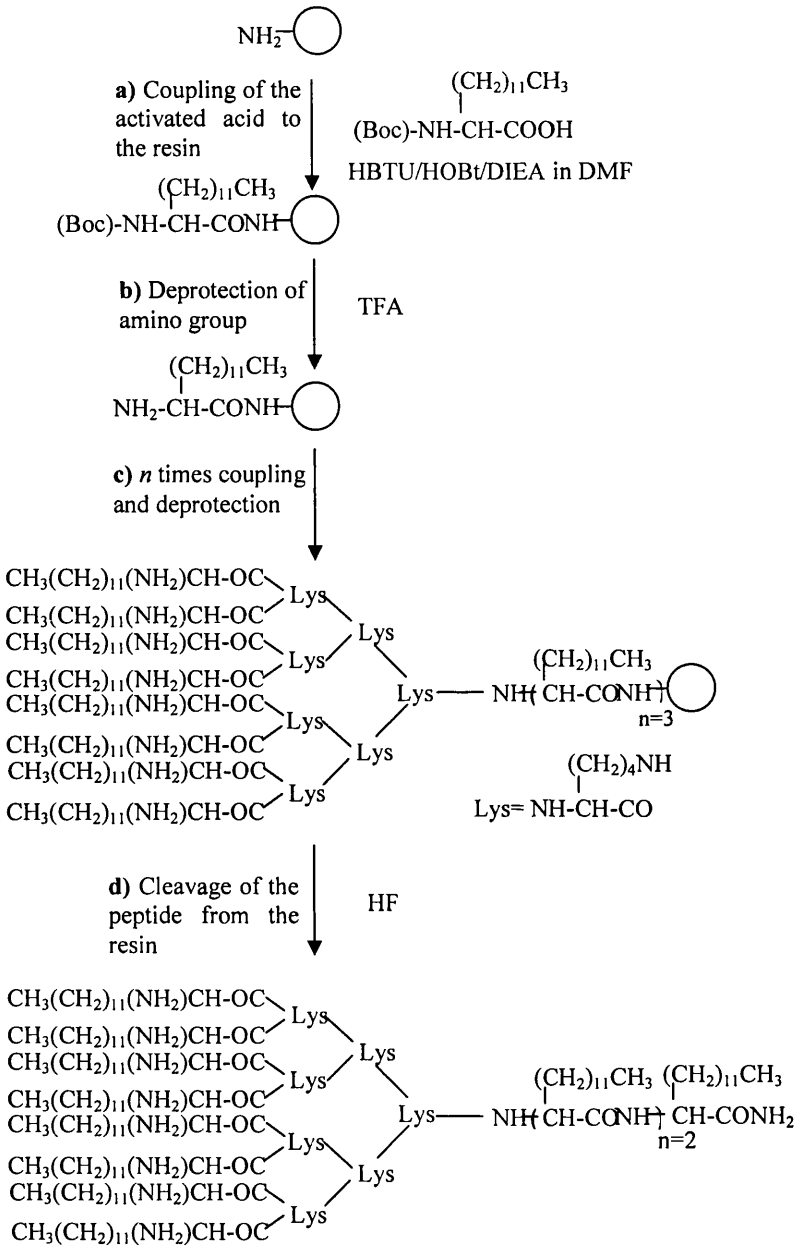

Figure 2.11: Solid phase peptide synthesis of compound 2a $(C_{14})_3Lys_7(C_{14})_8(NH_2)_8$.

times for the 5th and 6th cationic polylysine dendrimers (**compound 2b** and **compound 2c**) **(Figure 2.14)**. Accordingly, the relative molecular weights obtained were similar. However, the use of a series of a smaller pore size diameter e.g. 100Å would achieve better resolution (Bolzacchini *et al.*, 1998). Solubility problems were encountered in **compounds 2a, 2d** and **2e**. So purification could not be performed.

Gel permeation chromatography (GPC) using organic mobile phases such as DMF which dissolves the water insoluble dendrimers can be an alternative. However, in our studies the degree of purity for non-purified dendrimers was estimated using NMR (as discussed later).

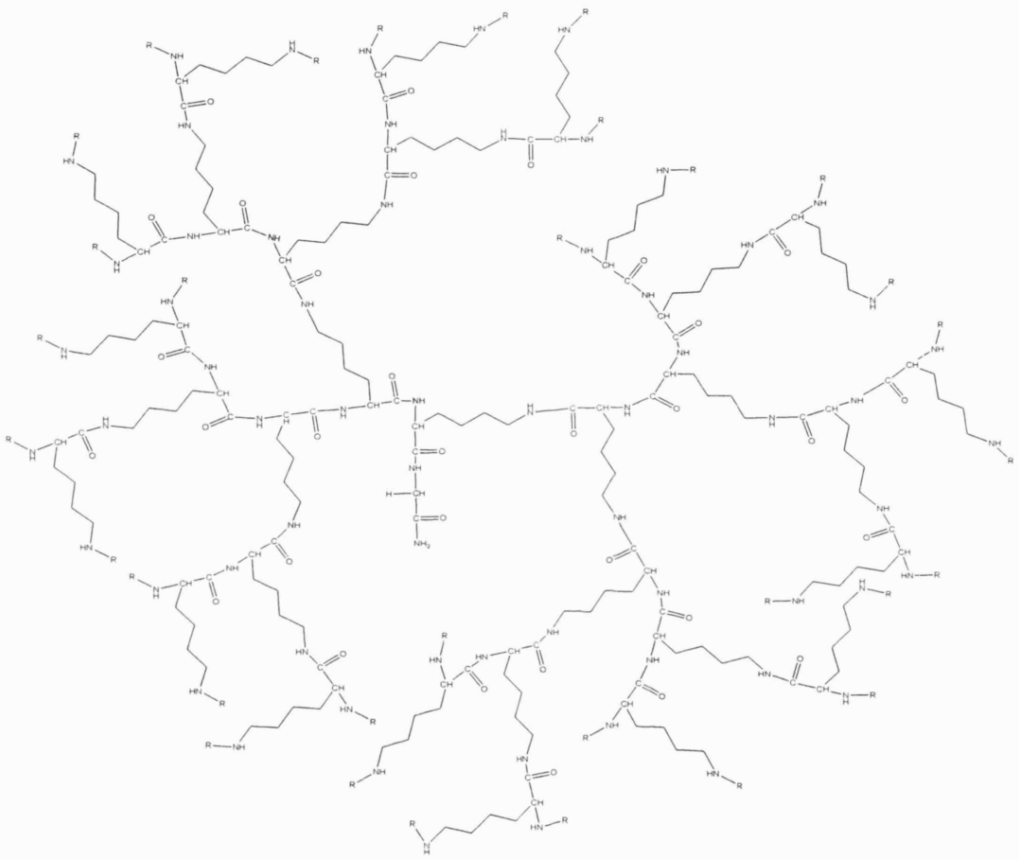

Compound	R
2b	H
2c	$COCH(NH_2)(CH_2)_4NH_2$
2d	$COCH(NH_2)(CH_2)_{11}CH_3$
2e	$COCH(NH[COCH(NH_2)(CH_2)_{11}CH_3])(CH_2)_4NH[COCH(NH_2)(CH_2)_{11}CH_3]$

Figure 2.12: Chemical structures of the cationic lipidic (α-amino tetradecanoic acid substituted) and non-lipidic (lysine substituted) dendrimers with 32 (**compounds 2b** and **2d**) and 64 (**compounds 2c** and **2e**) surface amino groups.

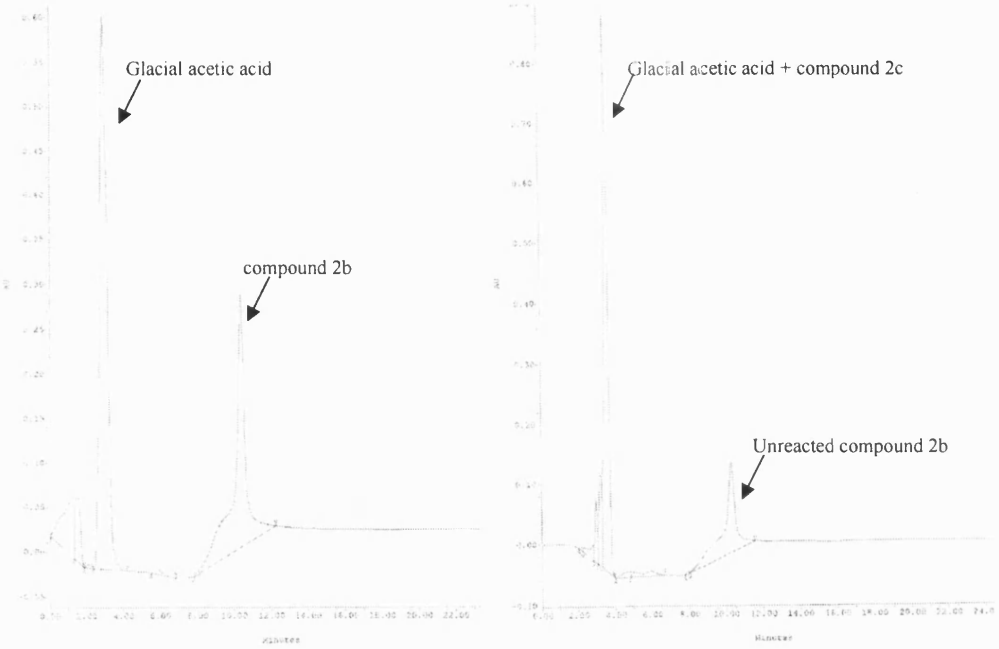

Figure 2.13: RP-HPLC chromatogram of **compounds 2b** (left) and **2c** (right). Conditions: 100µl (1mg/ml); Vydac C_4 column; Solvent A: 0.1% TFA; Solvent B: MeOH; 0% B to 100% B over 10 min, then 100% B to 0% over 10 min. flow rate: 1.0 ml/min; detection at 230 nm.

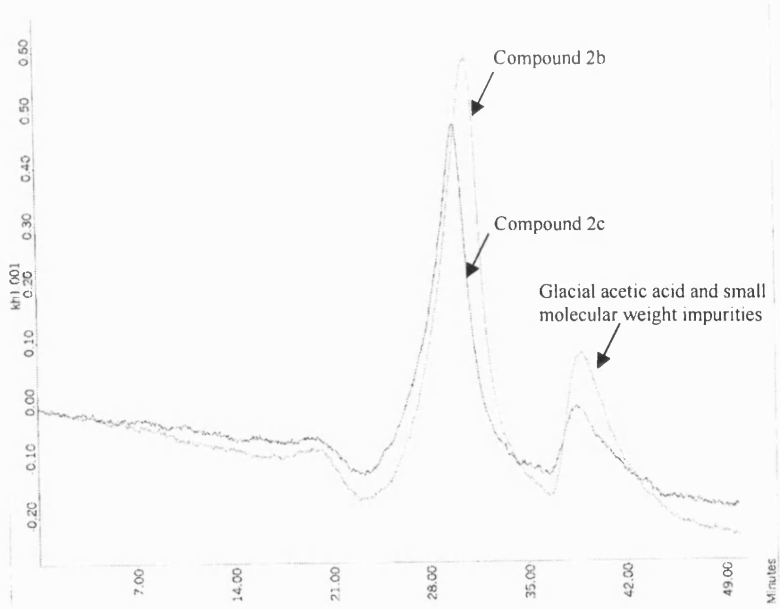

Figure 2.14: SEC chromatogram of **compounds 2b** and **2c**. Conditions: 20µl (5mg/ml); Ultrahydrogel 1000/250Å column; deionised water 0.5ml/min; refractive index detector.

2.1.2.5. Solubility of the compounds synthesised

Compounds 2b and **2c** are soluble in acidic and basic aqueous media. Their aqueous solutions are yellowish-brown in colour, the intensity of colour increases with increasing the number of amino groups and concentration. This association between the yellowish colour and the number of free amines was also observed in synthetic peptides.

Compounds 2a, **2d** and **2e** are water insoluble. **Compound 2a** is soluble in DMF, *t*-butanol and chloroform: diethyl ether (1:1). **Compound 2d** and **2e** are soluble in DMF, methanol and methanol: chloroform (1:1) but not in chloroform alone.

2.1.2.6. Spectrophotometry

The UV spectrum of compound **2c** showed a bathochromic shift in λ_{max} from 207 nm to 223 nm and a decrease in the absorbtivity **(Figure 2.15)** as the pH increases from 1 to 13, possibly due to the change in the protonated state and dendrimer solubility. A PAMAM dendrimer functionalised with α-helices of poly-(L-glutamic acid) synthesised by Higashi *et al.* (2002) showed conformational changes, using circular dichroism, from a helix (pH=3.9) to a random coil structure (pH=8.9) upon increasing the pH.

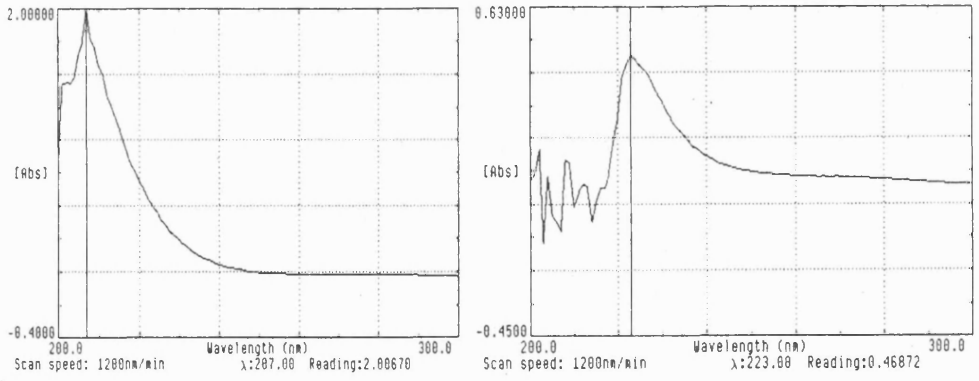

Figure 2.15: UV spectra of **compound 2c** (240 μg/ml) at pH=1 (left) and pH=13 (right). A bathochromic shift in λ_{max} from 207 nm to 223 nm and a decrease in absorbance occurred when pH changed from 1 to 13.

2.1.2.7. NMR

Precise structural elucidation and characterisation of these macromolecules is not as straightforward as in simpler molecules. To characterise our compounds we relied on various techniques such as mass spectroscopy, 1D and 2D NMR spectroscopy. Matrix-assisted laser desorption ionisation time of flight mass spectrometry (MALDI-TOF) and electro-spray ionisation mass spectrometry (ESI-MS) mass spectral analysis revealed the expected molecular weights of the compounds (see Appendix I for mass spectra). Extracts of 1D ^{1}H NMR spectra for **compounds 2b** and **2c** are shown in **Figure 2.16** and **Figure 2.17** respectively. Interpretation of such spectra is obviously difficult particularly when chemical shift values of various protons (H-α, H-β, H-γ, H-δ and H-ε) of both internal and external lysine residues are overlapping. One possible solution was to carry out the two-dimensional correlation spectroscopy (2D-TOCSY) (Braunschweiler and Ernst, 1983), in addition to 1D ^{1}H NMR, which provides additional information in relation to the coupling of protons in close proximity. Coupled protons showed dark shaded regions in the spectrum. For example H-α shows coupling with H-β, H-γ and H-δ , and possibly H-ε. The 2D TOCSY spectra of **compounds 2b** and **2c** are shown in **Figure 2.18** and **Figure 2.19** respectively. 1D and 2D ^{1}H NMR spectroscopy revealed a range of chemical shift values assigned for H-α, H-β, H-γ H-δ and H-ε protons of the dendrimers (Zloh *et al.*, 2005). The error in the experimentally determined proton percentages ranged between 0 to 20 % **(Table 2.3)**. Defects in chemical structure, incomplete coupling, or even entrapped solvent molecules would have a remarkable contribution. We categorised lysine components, according to the environment in which they exist, into interior branching units and exterior residues. This was attributed to the fact that interior lysine have amide protons involved in forming a

peptide bond as compared to surface lysine that have amine protons that are not involved in amide bond formation. A general trend was also observed, H-α and H-ε, shifted downfield in the interior residues as compared to same protons in the exterior ones. For instance, four peaks were observed for H-α and H-ε, two downfield peaks for interior lysine protons and two upfield peaks for exterior lysine protons **(Figure 2.18** and **Figure 2.19)**. However, exterior H-β, H-γ and H-δ protons shifted downfield compared to same interior protons as they are more exposed to an aqueous environment.

Table 2.3: Chemical shifts δ of external and internal lysine protons as assigned by 2D TOCSY

Protons	Chemical shift * compound 2b	Chemical shift * compound 2c	Bands assigned
Internal H_α	4.38-4.56	4.40-4.55	a
External H_α	4.20-4.33	4.09-4.20	b
Internal H_ε	3.31-3.50	3.30-3.50	c
External H_ε	3.18-3.28	3.13-3.25	d
External H_β	2.05-2.20	2.05-2.15	e
Internal H_β, external H_δ	1.89-2.05	1.8-2.05	f, g
Internal H_δ, external H_γ, internal H_γ	1.5-1.8	1.4-1.8	h, i, j

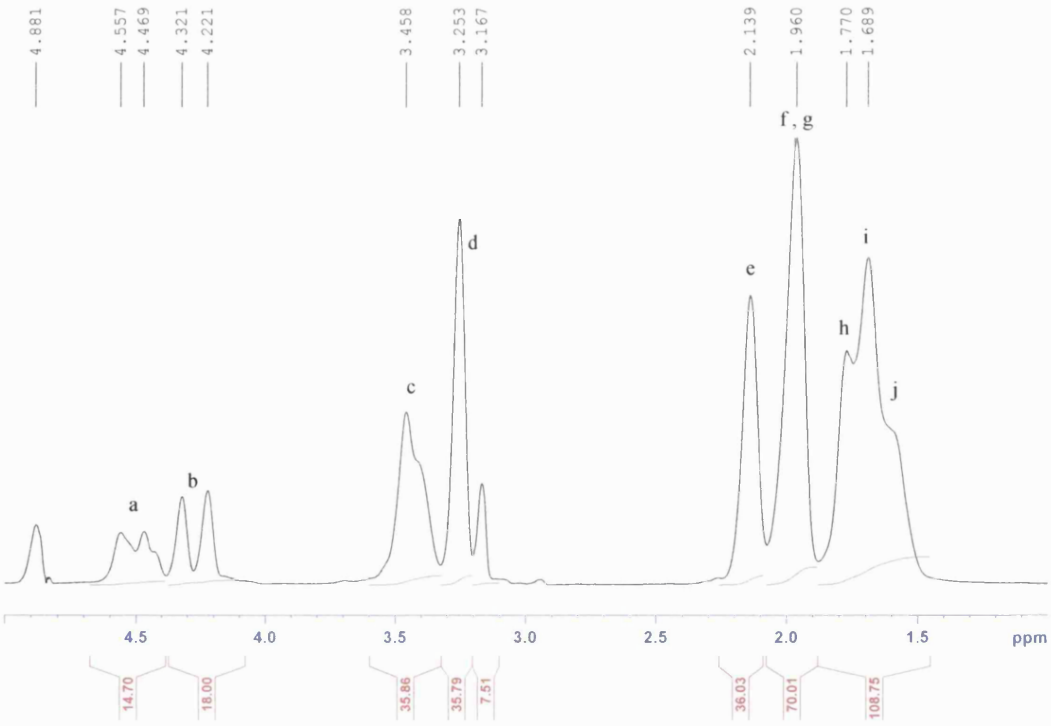

Figure 2.16: ^1H NMR spectrum extract for **compound 2b** in D_2O. It shows overlapping between similar protons. Internal and external H_α are represented by letters a and b. C and d represent internal and external H_ε. E, f, g, h, I, and j represent external and internal H_β, H_δ and H_γ. The error in the experimentally determined proton percentages ranged between 0 to 20 %.

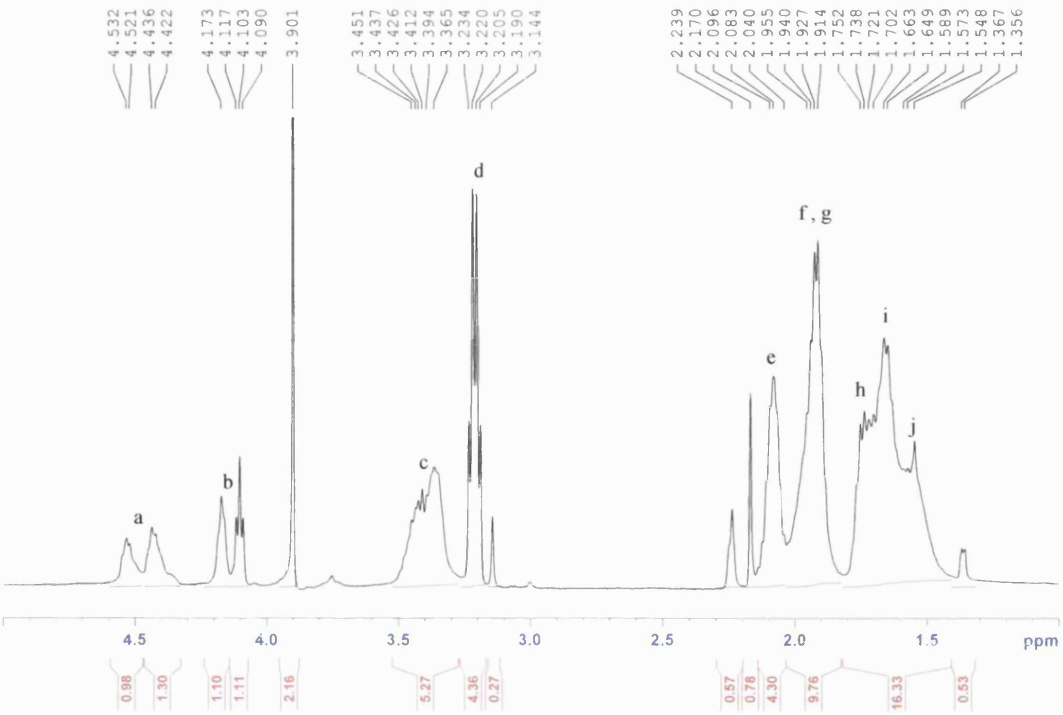

Figure 2.17: ^{1}H NMR spectrum extract for **compound 2c** in D_2O. It shows overlapping between similar protons. Internal and external H_α are represented by letters a and b. C and d represent internal and external H_ε. E, f, g, h, I, and j represent external and internal H_β, H_δ and H_γ. The error in the experimentally determined proton percentages ranged between 0 to 20 %.

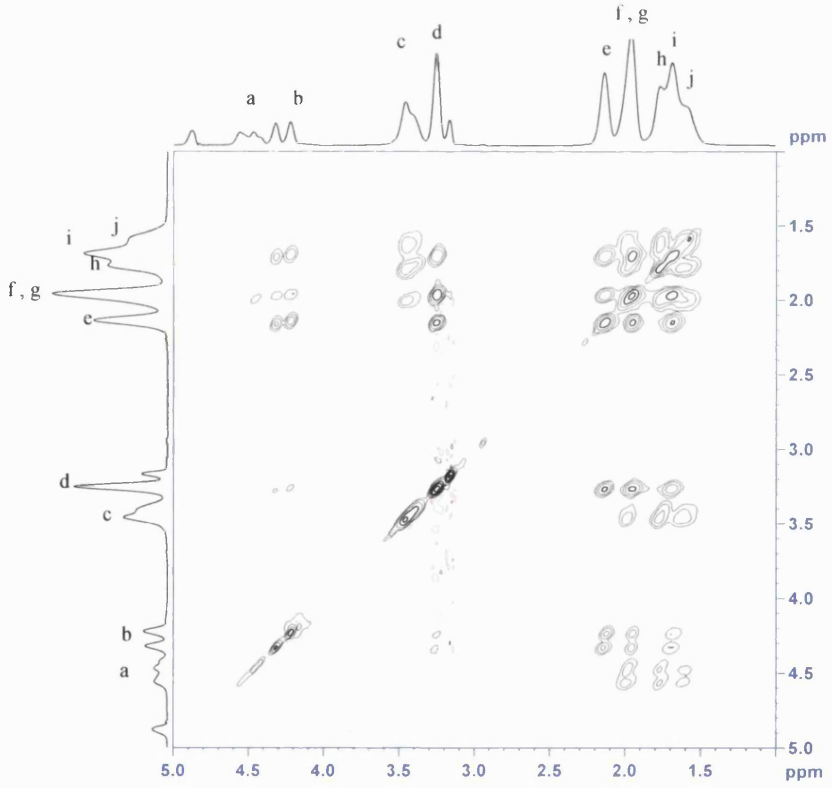

Figure 2.18: 2D NMR TOCSY spectrum for **compound 2b** in D_2O. Coupled protons in close proximity show dark shaded regions in the spectrum.

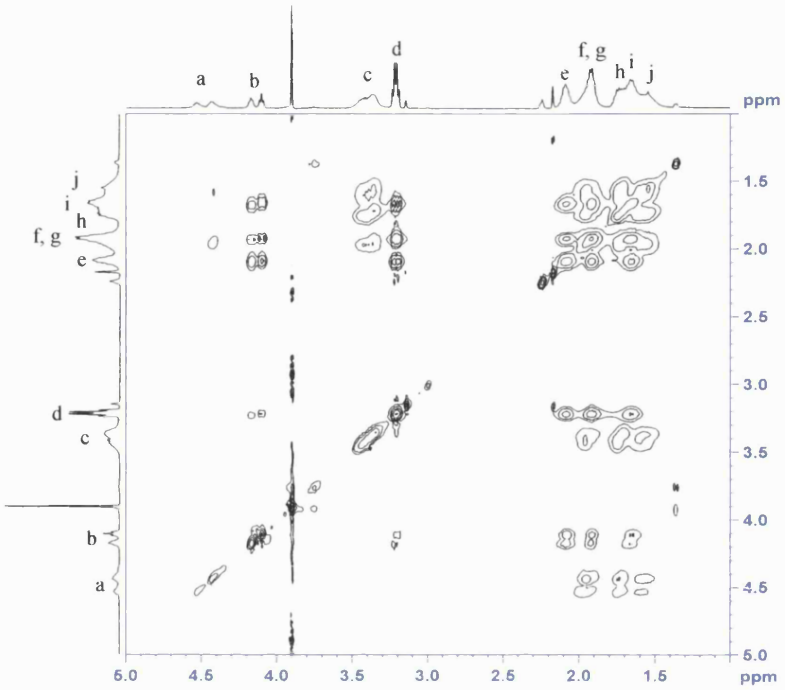

Figure 2.19: 2D NMR TOCSY spectrum for **compound 2c** in D_2O. Coupled protons in close proximity show dark shaded regions in the spectrum.

Chapter III

INTRINSIC FLUORESCENCE OF AMINO TERMINATED POLYAMIDE POLYLYSINE DENDRIMERS AND STUDYING THEIR INTERACTIONS WITH CARBOXYFLUORESCEIN USING SPECTROPHOTOMETRY AND SPECTROFLUORIMETRY

Of the dendrimers synthesised, Gly-$Lys_{31}(NH_2)_{32}$ and Gly-$Lys_{63}(NH_2)_{64}$ (**compounds 2b and 2c**) were the only water soluble derivatives without lipid chains. Due to their water solubility, we were able to study the spectrofluorimetric characteristics of these two compounds, which would be an important property in the study of the cellular uptake of these carriers. The possibility of interference between any intrinsic dendrimer fluorescence and the extrinsic fluorescent probe is an issue. The ability of our dendrimers to sequester small molecules was also verified. The green fluorescent dye, carboxyfluorescein (CF), was chosen due to its negative charge and because the changes in the microenvironment in which it exists can be estimated by studying the excitation and emission spectra of the dye.

3.1. Experimental

3.1.1. Materials

MBHA resin, HBTU, HOBt, the protected Boc-Gly-OH and Boc-Lys(Boc)-OH (DCHA salt) (Novabiochem, UK), DIEA, Magnesium sulphate dried, Potassium hydroxide pellets, Sulphuric acid, Glacial acetic acid, Ethyl acetate (BDH, UK), DMF (Rathburn, UK), TFA (Halocarbon Product Corporation, USA), HF (BOC, UK), pleated dialysis tubing (Snakeskin™) and dialysis cassettes of 3,500 Da MWCO (Pierce Chemical Company, USA), CF (Fluka, USA), Poly-L-lysine hydrobromide (Mw 9,600, 23,800 and 121,000 Da), unfractionated heparin (MW 6,000-30,000 Da) (Sigma, USA), Sephadex G-25 superfine (Amersham Pharmacia Biotech, Sweden).

3.1.2. Synthesis of Gly-$Lys_{31}(NH_2)_{32}$ and Gly-$Lys_{63}(NH_2)_{64}$ dendrimers

The cationic water soluble polylysine dendrimers **(compounds 2b and 2c) (Figure 2.12)** having 32 and 64 surface amino groups, were synthesised (method D) and purified as described in Appendix I.

3.1.3. UV-Vis and fluorescence spectroscopy

The dendrimer Gly-$Lys_{63}(NH_2)_{64}$ was dissolved in water for a final concentration of 3.7×10^{-4}-7.4 $\times10^{-2}$ mM (3-600 μg/ml). Scanning for its excitation and emission maxima was carried out between 200-700 nm. Excitation and emission wavelengths used were 453 nm and 514 nm respectively. Excitation and emission slit widths were 10 nm.

CF solutions were prepared by serial dilution of a stock (80 mM CF in 1M KOH) with water. All solutions were kept protected from light. Fluorescence intensities for CF were reported using 486 nm and 518 nm as the excitation and emission wavelengths respectively and 5 nm as an excitation and emission band widths. CF

(53 nM or 20 ng/ml) was titrated with Gly-$Lys_{63}(NH_2)_{64}$ dendrimer (12.2×10^{-6} - 2.5×10^{-3} mM or 0.1-20 μg/ml) and allowed to equilibrate overnight in the dark at room temperature. All absorption and fluorescence spectra were recorded at 25 °C on a LS50B spectrophotometer (Perkin Elmer, UK) in a 1 ml quartz cuvette.

For spectroscopy, solutions (2ml) containing final concentrations of 10 μM CF and 0.0-10 μM dendrimer were prepared from 20 μM CF and 122.7 μM dendrimer solutions. Absorption spectra for CF, in the presence and absence of dendrimer, were obtained from 400-600 nm at a scan rate of 1200 nm/min in a plastic cuvette using a Beckman DU® 650 Spectrophotometer (USA). The optical densities were measured at 450, 488 and 498 nm. The experiments were repeated at least four times to check the reproducibility of the results.

3.1.4. Molecular modelling of the dendrimer and the dye molecule

The dendrimer model was "constructed" by joining two identical fragments of the dendrimer using the Quanta (MSI) program. The absolute configuration of the lysine residues was "S" and the amino groups of lysine were given a formal charge of +1. Overall energy minimization to a local minimum was carried out manually. Final images were produced using The PyMOL Molecular Graphics system (DeLano Scientific LLC, San Carlos, CA, USA).

3.1.5. Separation of free CF from the entrapped CF

Gel filtration of the samples was carried out using a manually prepared 1 × 30 cm Sephadex G-25 column. 200 μl of the aqueous solution of CF: dendrimer mixture (1 μmole : 1 μmole) or CF (1 μmole) was applied on the top of the gel bed and eluted by deionised water. The flow rate was controlled by gravity. Dialysis was carried out by injecting the sample (2 ml) contains CF: dendrimer mixture (1 μmole: 1 μmole) or CF (1 μmole) into the dialysis cassettes (3,500 MWCO) as recommended by the

supplier and dialyzed against 250 ml water. Fractions eluted from the gel and dialysis samples were analyzed by spectrofluorimetry.

3.2. Results and discussion

3.2.1. Intrinsic dendrimer fluorescence

Aqueous solutions of the 6th generation amine-terminated polylysine dendrimer having 64 primary amines at the surface, Gly-$Lys_{63}(NH_2)_{64}$ having a molecular weight of 8149 Da, showed broad and concentration dependent excitation and emission spectra, different from the solvent background, with an excitation and emission maxima at 234 and 492 nm, respectively. Although excitation of aqueous solutions of dendrimer resulted in a linear relationship between the emission intensity and dendrimer concentration **(Figure 3.1)**, a spectral change in emission spectra occurs at dendrimer concentrations > 80 μg/ml (10 μM) **(Figure 3.2)** and was reflected in a change in the slope of the calibration curve at 10 μM concentration **(Figure 3.1)**.

A lower generation polylysine dendrimer Gly-$Lys_{31}(NH_2)_{32}$ (MW 4047 Da) showed lower emission intensities at the same molar concentrations **(Figure 3.3c)**. Linear polylysine hydrobromide (MW 9,600 – 121,000 Da) showed no detectable fluorescence **(Figure 3.3d)**.

It has been shown by other groups (Caminati *et al.*, 1990; Pistolis *et al.*, 1997; Wade *et al.*, 1999; Larson and Tucker, 2001; Varnavski *et al.*, 2001) that PAMAM dendrimers with carboxylate and amino terminals also have weak but detectable intrinsic fluorescence despite their lack of a fluorophore. Varnavski *et al.*(2001) have observed an absorption maximum of 300 nm when the methanolic solutions of G5 and G9 of the amine-terminated PAMAM dendrimers were excited at 270 nm. Also,

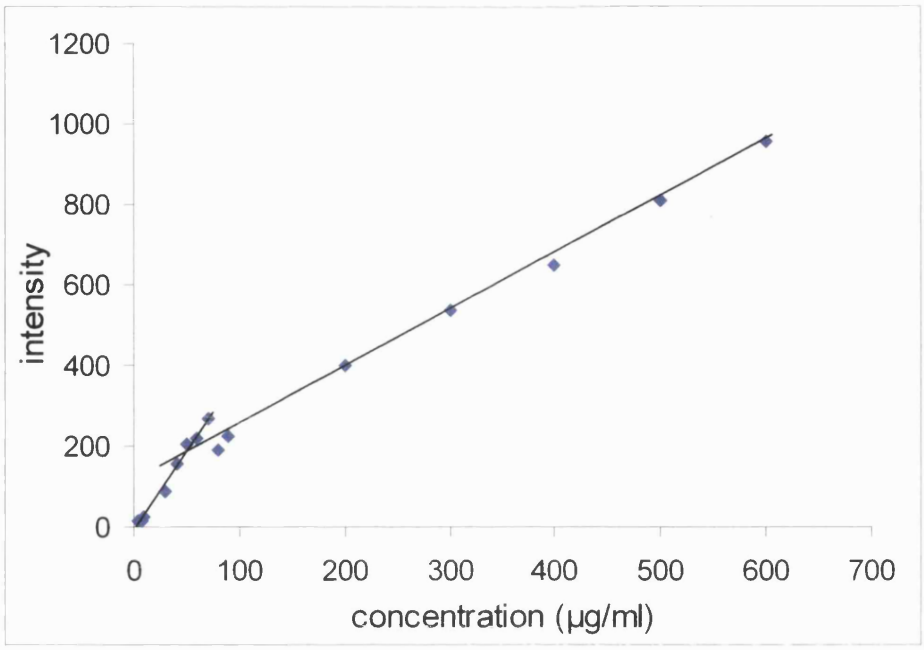

Figure 3.1: Calibration plot of the dendrimer in water ($\lambda_{excitation}$ and $\lambda_{emission}$: 453 nm and 514 nm respectively). A change in the slope is seen at concentrations > 80 µg/ml (10 µM). The excitation and emission band width was 10 nm.

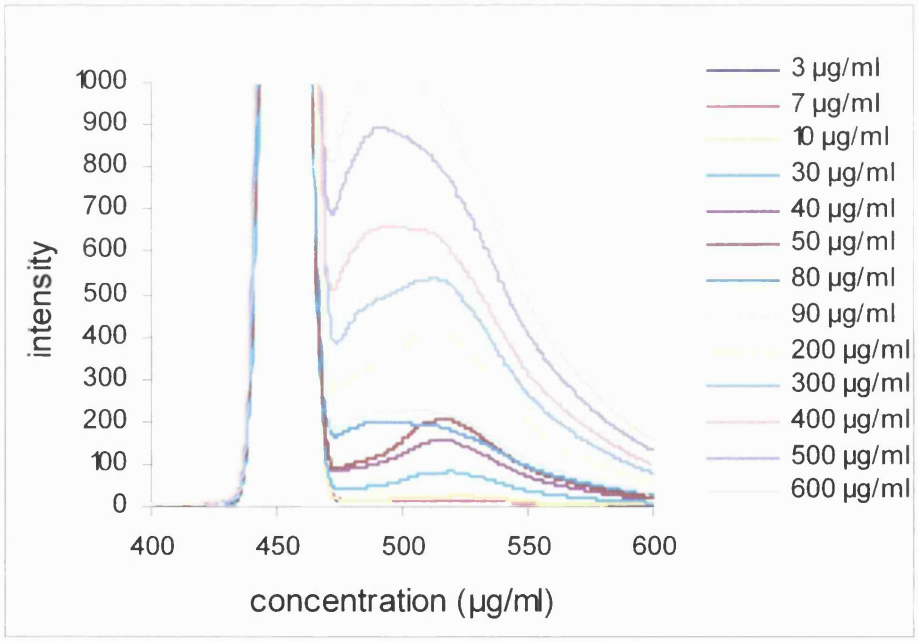

Figure 3.2: Emission spectra of various dendrimer concentrations (3-600 µg/ml or 3.7×10^{-4}-7.4 $\times10^{-2}$ mM) in water at $\lambda_{excitation}$=453 nm showing a spectral change in emission spectra at concentrations > 80 µg/ml (10 µM). The excitation and emission band width was 10 nm.

Figure 3.3: Photographs taken of a range of macromolecules concentrations (0.01-3 mM) for (a) Gly-$Lys_{63}(NH_2)_{64}$ (0.08-24.5 mg/ml) exposed to visible light; (b) Gly-$Lys_{63}(NH_2)_{64}$ (0.08-24.5 mg/ml); (c) Gly-$Lys_{31}(NH_2)_{32}$ (0.04-12.14 mg/ml) and (d) polylysine hydrobromide (MW 9,600 Da) (0.096-28.8 mg/ml) exposed to a UV transilluminator. Under visible light, dendrimer aqueous solutions exhibit a yellow-brownish colour at high concentrations (a). More intense fluorescence is observed by increasing the dendrimer concentration and generation number (b,c). Linear polylysine shows no intrinsic fluorescence behaviour (d).

Pistolis *et al.* (1997) have noted a maximum of 430 nm for the aqueous solutions of G0, G1, and G2 amine-terminated PAMAM dendrimers.

The fluorescence of polylysine dendrimers, another example of fluorescent polyamide dendrimers which lack a traditional fluorophore, validates the assumption made by Larson and Tucker (2001) who suggested that the phenomenon of PAMAM dendrimer fluorescence is due to an $n \rightarrow \pi^*$ transition from the various amido groups throughout the dendrimer structure. The lower generation dendrimer Gly-$Lys_{31}(NH_2)_{32}$ exhibited a lower emission intensity perhaps due to the smaller number of fluorescent centers as suggested by Larson and Tucker (2001). Linear polylysine polymer lacks the polyamide network structure which seems to be involved in the generation of fluorescence.

This phenomenon may have applications in various areas. Firstly, because dendrimers have the ability to sequester small molecules, fluorescent probe techniques are one of the techniques used to study dendrimer architecture (Caminati *et al.*, 1990; Pistolis *et al.*, 1997; Richter-Egger *et al.*, 2000; 2001a; 2001b; Esumi *et al.*, 2001; 2002; Yoshimura *et al.*, 2002; Mizutani *et al.*, 2002). However, the intrinsic fluorescence of dendrimers may interfere with the extrinsic probe excitation and emission especially if the probe is excited near or in dendrimer's excitation region. So such interference should be considered when analyzing this data. Secondly, fluorescence quenching of fluorescent three dimensional hyperbranched polymers has gained popularity as a tool for detecting nitro-compounds used in explosives. Nitro-containing compounds, due to their strong electron withdrawing nature, quench polymer fluorescence. The well-developed network structure of the hyperbranched polymers (Newkome *et al.*, 1985), which have cavities large enough to entrap nitro aromatic compounds (Wade *et al.*, 1999; Wang *et al.*, 2004), suggests dendrimers as suitable candidates for sensor materials. Thirdly, such carriers can be visualized microscopically without the need for fluorescent labelling so their cellular uptake and localization can be quantified.

3.2.2. Dendrimer-CF complexation

The use of several types of dendrimers as nanoscopic devices and drug delivery vehicles has been demonstrated by their ability to capture small molecules in the internal cavities, a process which could be followed by measuring the photophysical state of the molecules (Newkome *et al.*, 1991; Hawker *et al.*, 1993; Jansen *et al.*, 1994; Stevelmans *et al.*, 1996; Watkins *et al.*, 1997; Richter-Egger *et al.*, 2000; 2001a; 2001b; Baars *et al.*, 2000b; Dykes *et al.*, 2001; Balzani *et al.*, 2002; Beezer *et al.*, 2003).

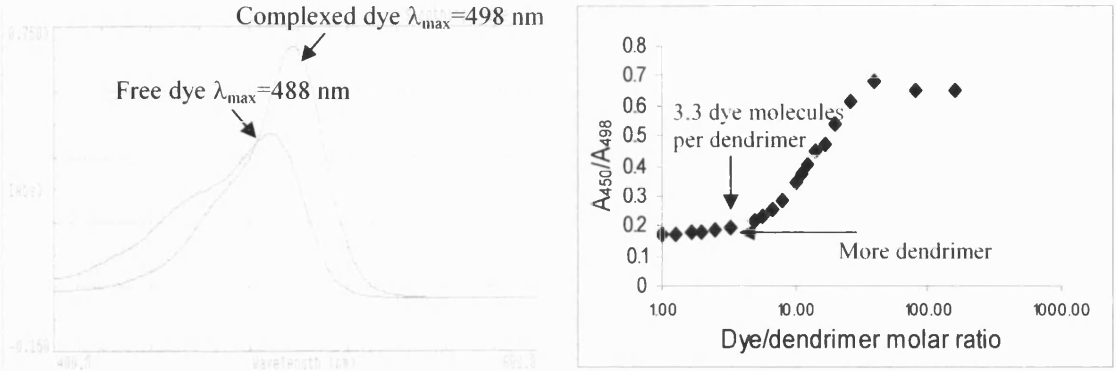

Figure 3.4: Left: UV/Vis spectra of free CF (λ_{max}=488 nm) and complexed CF (λ_{max}=498 nm). The maximum bathochromic shift ($\Delta\lambda_{max}$=10 nm) was observed when the dye (10 μM) is complexed with the dendrimer (3 μM) at 3.3 dye/dendrimer molar ratio. Right: titration of CF (10 μM) with the dendrimer; upon increasing dendrimer concentration (0.0625-10μM), A_{450}/A_{498} decreased (A_{450} and A_{498} are indicatives of free and complexed dye concentration respectively) until it becomes independent of the dendrimer concentration when 3.3 dye molecules are available per dendrimer molecule.

The interaction between the negatively charged green fluorescent dye CF and the cationic 6th generation dendrimer was studied by UV-Vis and fluorescence spectroscopy. CF (10 μM) exhibited a shift in its absorption maximum from 488 nm (yellow) to 498 nm (orange) in the presence of dendrimer. Increasing the dendrimer concentration from 0.0625 to 10 μM decreased A_{450} and increased A_{498}. The A_{450}/A_{498} ratio was used to measure the ratio of free to bound CF in the solution, its value being independent of dendrimer concentration as the dye/dendrimer molar ratio approached 3.3 **(Figure 3.4)**.

The finding that titration of the negatively charged CF with the dendrimer caused a red shift in its absorption maximum ($\Delta\lambda_{max}$=10 nm) indicated complexation between the dye and the dendrimer. A similar bathochromic shift was previously reported for dendrimer-solubilised proflavine hydrochloride (Dykes *et al.*, 2001) because of the increased protonation of the proflavine. Also, phenol blue, a probe used to study

micellar properties, displayed only a slight shift ($\Delta\lambda_{max}$ = 5 nm), with a reduction and broadening, for the absorption band in the vicinity of the unimolecular micelle micellanoate™ due to its complexation (Moorefield and Newkome, 2003).

Fluorescence spectroscopy showed a noticeable increase in the intensity of CF emission as a function of dendrimer concentration **(Figure 3.5)** and a shift in its emission maximum from 518 nm to 523 nm when the dye/dendrimer molar ratio became 0.43 **(Figure 3.5)**. The observation of two values of emission maxima of CF can be explained by two different sites of interaction. It has been previously noted that PPI dendrimers have at least two different sites for inclusion of a spin probe (Jansen and Meijer, 1995), a fact also established by fluorescence lifetime measurements (Balzani *et al.*, 2002).

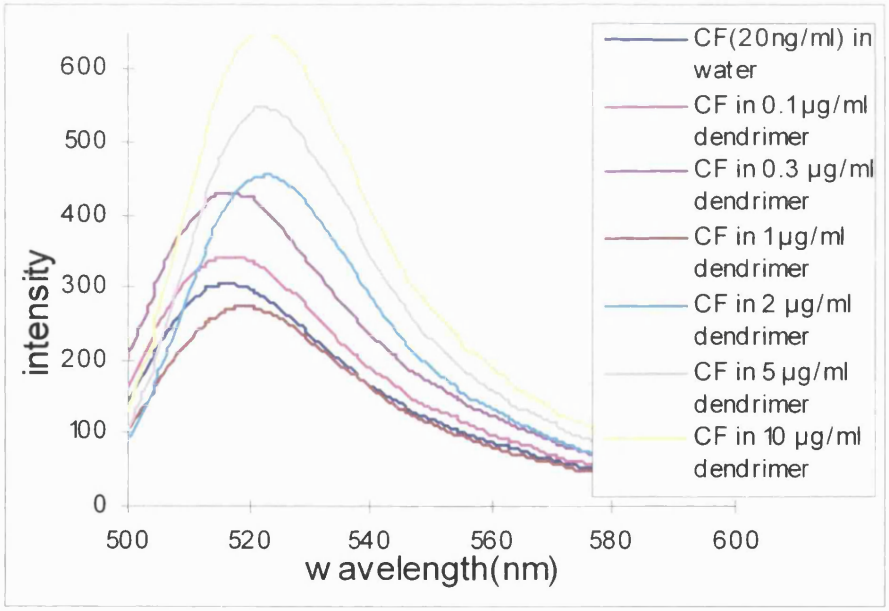

Figure 3.5: Effect of dendrimer concentration on CF fluorescence. Emission spectra of CF (20 ng/ml or 53 nM) in water and in dendrimer solutions at various concentrations ranging from 0.1- 10 µg/ml (12.2- 1.25×10^3 nM) ($\lambda_{excitation}$= 486 nm) showing an enhancement in emission intensity in the presence of dendrimer and a change in the dye emission maximum from 518 nm to 523 nm at dye/dendrimer molar ratio of 0.43.

Fluorescence enhancement could be due to the enhanced solubility of the dye in the dendrimer microenvironment or to the presence, at the dendrimer surface, of primary amines known for their electron donating properties. Electron donating p-methoxy benzene increases the emission intensity of the hyperbranched fluorescent poly(p-phenyl vinylene (PPV) polymer (Wang *et al.*, 2004). On the other hand, nitro-containing compounds quench the fluorescence of the polymer due to the electron withdrawing effect of the nitro group (Wang *et al.*, 2004). PAMAM and poly(propylene imine) (PPI) dendrimers have been found to quench the fluorescence of extrinsic probes due to the electron withdrawing effect of the tertiary amine within their interior (Bartholomew and Davidson, 1971; Pistolis *et al.*, 1997; Wade *et al.*, 1999; Balzani *et al.*, 2002).

3.2.3. Molecular modelling

Molecular modelling of both host and guest was performed and showed that the hyperbranched structure had many cavities in each dendrimer which are 6.48 nm in diameter. The diameter of each cavity was about 1.55 nm, whereas the dye has a diameter of 1.23 nm. We expect the polylysine dendrimer to be able to accommodate CF molecule in their cavities **(Figure 3.6 A)**, but interaction between the dendrimer surface amines and the carboxylate dye can take place at the dendrimer surface without CF internalization **(Figure 3.6 B)**.

3.2.4. Factors affecting dendrimer-dye complexation

3.2.4.1. pH

Fluorescence spectroscopy was also performed over a pH range 3-13 to rule out the effect of pH change on the shift in the CF emission maximum. The solubility of CF in the absence of dendrimer is lowered in acidic media, as reflected by reduced

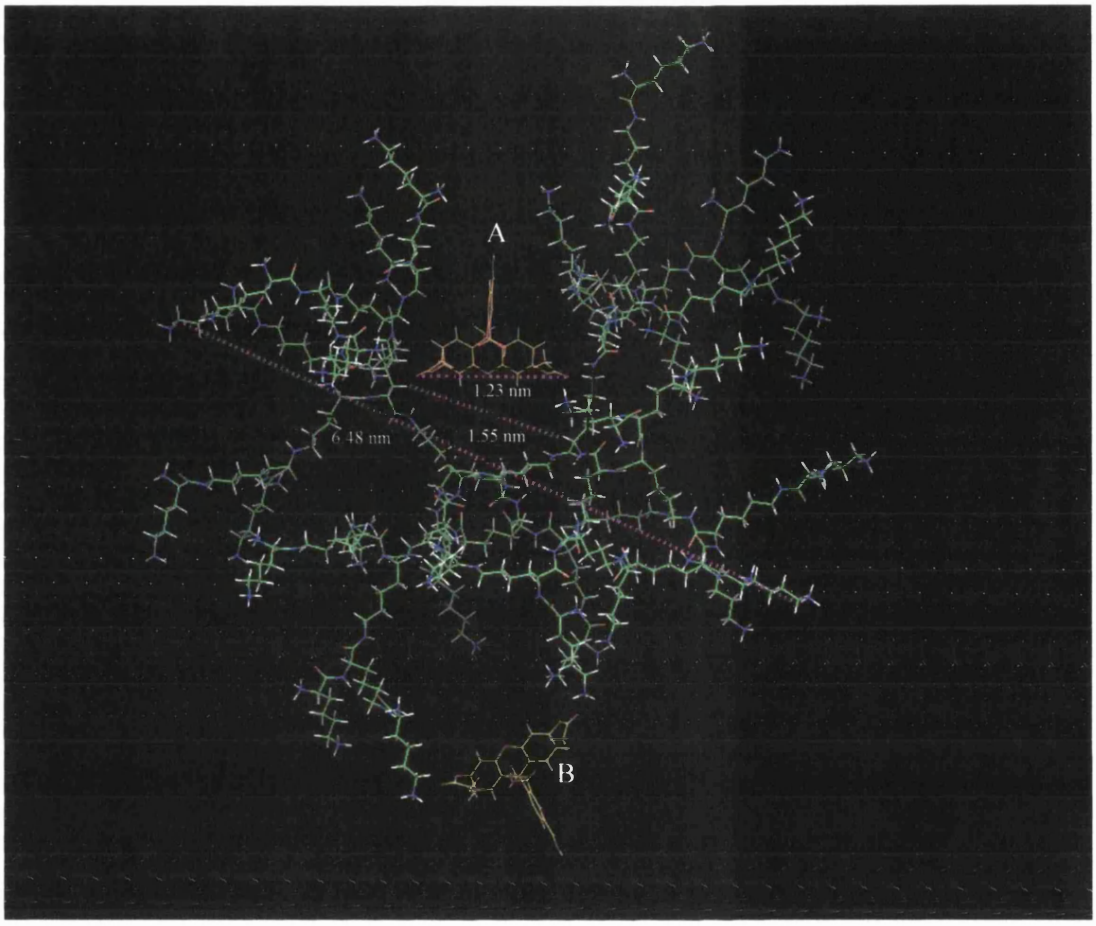

Figure 3.6: Molecular modelling of the dendrimer (host) and CF molecule (guest) shows that (A) the dendrimer has cavities large enough (1.55 nm in diameter) to accommodate the dye molecule in its interior (1.23 nm in diameter) and (B) CF can be retained at the dendrimer surface via electrostatic interactions between the carboxylate and the surface amine groups.

absorbance, but no shift in its emission maximum wavelength over this pH range was observed. When CF was complexed with the dendrimer, the shift occurred at pH 3, 8 and 13, strongly suggesting that the shift in the emission maximum is due to the interaction between dendrimer and dye and not to pH changes. Furthermore, the interaction between CF and the dendrimer occurred over a wide pH range.

3.2.4.2. Ionic strength

The effect of ionic strength on the shift in CF emission maximum was studied using NaCl solutions (0-154 mM). At 154 mM NaCl (0.9%) concentration, no shift was noticed even at very high dendrimer concentrations. At 15.4 mM (0.09%), 10 times the dendrimer concentration was required to cause the shift. This finding is not surprising as Welch and Muthukumar (1998) demonstrated a dramatic change in the dendrimer conformation as a function of the media ionic strength presumably due to a decrease in the water content within the interior of the dendrimer as the ionic strength increases. Hawker et al. (1993) found that solubilisation of pyrene in the hydrophobic core of polyaryl ether dendrimers is favored by NaCl due to improved hydrophobic interactions between the pyrene and dendrimer core when water molecules are withdrawn from dendrimer interior. NaCl is expected to lower the cmc of the cationic dendrimer, if it exists, and thus enhance the solubilisation properties of micelles at lower dendrimer concentrations. However, this was not the case suggests the unimolecular nature of the dendrimer.

3.2.4.3. CF/dendrimer molar ratio

It was also important to establish if the shift phenomenon was dendrimer concentration dependent or dye/dendrimer molar ratio dependent. Titration of different CF concentrations (5 and 10 ng/ml in water) with the dendrimer indicated that the shift is noticeably dependent on the molar ratio rather than the absolute dendrimer concentration.

3.2.5. The reversibility and the stability of the complex

To study the reversibility of complexation, a negatively charged macromolecule heparin found to bind to the dendrimer at a dendrimer: heparin molar ratio 2.2:1, was added to the dye-dendrimer complex (10 μM: 3 μM) at a concentration of 1.5 μM.

The UV/vis spectrum for this ternary mixture is similar to that of free CF i.e. λ_{max} shifted again from 498 nm to 488 nm. This showed that CF complexation with the dendrimer can be reversible upon the addition of a molecule which has higher affinity to the dendrimer than CF.

The stability of the complex was checked by gel filtration. Molecules >5000 Da will not be retained in the gel and elute faster than small molecular weight compounds. Two upper and lower bands were identified when applying the dendrimer-dye complex to the gel, corresponding to free and complexed CF respectively, compared to only one band when CF alone was applied **(Figure 3.7a)**.

The release of CF from the complex was carried out by a dialysis technique using dialysis cassettes of 3,500 Da MWCO. After 24h, 22% of the dye was released through the membrane when no dendrimer was present compared to only 0.12% when the dye was complexed with dendrimer in an equimolar ratio **(Figure 3.7b)**.

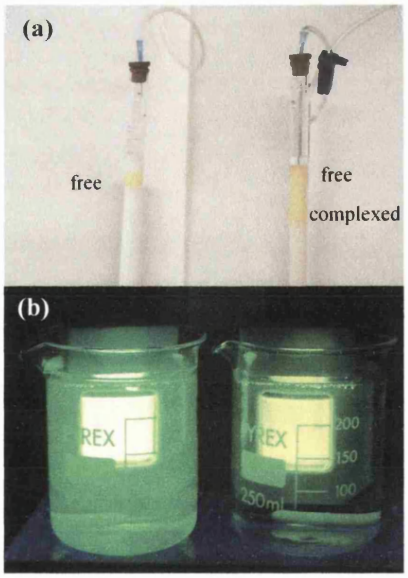

Figure 3.7: (a) Separation of free and complexed CF by gel filtration using a Sephadex G-25 column. A 200 µl sample containing the dye/dendrimer mixture (top right: 1 µmole: 1 µmole) or free CF (top left: 1 µmole) was applied on the top of the gel bed and eluted by deionised water. The flow rate was controlled by the gravity. The upper and lower bands (top right) correspond to free and complexed dye respectively as confirmed by spectrofluorimetry. **(b)** Dialysis was carried out for a 2 ml sample containing either the complex (bottom right: 1 µmole: 1 µmole) or CF alone (bottom left: 1 µmole) using the dialysis cassette (MWCO 3,500 Da) against 250 ml water. After 24h, the percentage release of free dye was 0.12% and 22% from the complexed and free dye solutions respectively.

3.3. Conclusion

The intrinsic fluorescence of polylysine dendrimers, despite the lack of a classical fluorophore, clearly shows the influence of the complex and unique aspects of the dendrimer architecture. This was not only shown by the presence of fluorescence but also by the changes in the signals with the dendrimer generation and concentration. This could be an effective tool in their characterisation and quantification as well as suggesting their use as sensor materials for quenching substrates.

Complexation between the dendrimer Gly-$Lys_{63}(NH_2)_{64}$ and CF further suggests the use of these dendrimers as nanoscopic devices. The difference in the spectroscopic behaviour between the free and the complexed dye (λ_{max}= 488 nm and 498 nm respectively) could be utilised to study the stoichiometry of complexation which was found to be 3.3 CF molecules/dendrimer. Different sites (the surface and the interior of the dendrimer) and mechanisms of interactions (electrostatic interaction, H-bonding and molecular inclusion) were suggested as shown by fluorescence spectroscopy, principally the enhancement and a shift in the emission maximum of CF from 518 nm to 523 nm, in the presence of dendrimers when the dye/dendrimer molar ratio approached 0.43. The fact that NaCl decreased the dendrimer-dye complexation and that the onset in the shift of CF emission maximum was dependent on the dendrimer/dye molar ratio and not on an absolute dendrimer concentration strongly suggest that molecular interactions are involved and that is, the dendrimer is more likely to be present as single molecules 6 nm in diameter rather than in the aggregated form.

Chapter IV

DENDRISOMES: VESICULAR STRUCTURES DERIVED FROM A CATIONIC LIPIDIC DENDRON

Engineering dendrimers and dendrons (partial dendrimers) has been possible by controlling the generation number, branching units and surface functionalities. Dendrimers and dendrons of the appropriate hydrophile-lipophile balance (HLB), size and topology can self-assemble into higher order structures, broadening their potential for use as drug and gene carriers. The cationic lipidic dendron $(C_{14})_3Lys_7(C_{14})_8(NH_2)_8$ was found to self-assemble in water forming small vesicular structures which we have named "dendrisomes". These were characterised and their interaction with cholesterol studied using techniques such as photon correlation spectroscopy (PCS), zeta potential measurement, transmission electron microscopy (TEM) and differential scanning calorimetry (DSC). We also studied the encapsulation and release of benzyl penicillin (penicillin G), used as a model of a negatively charged water soluble drug using neutral liposomes as our comparator.

4.1. Experimental

4.1.1. Materials

Distearoyl phosphatidylcholine (DSPC), cholesterol (CHOL) (Sigma Chemical Company, UK), [^{14}C]-benzyl penicillin potassium salt (penicillin G) (specific radioactivity 59 mCi/mmol) (Amersham Life Science, UK), pleated dialysis tubing (Snakeskin®), 3500 Da MWCO (Pierce Chemical Company, USA), Optiphase 'safe' scintillation cocktail (Perkin-Elmer, UK), 3.05 mm copper grid for TEM (Taab, UK). Materials used in the dendrimer synthesis were mentioned in chapter III.

4.1.2. Synthesis of the amphipathic dendron

The synthesis of *N*-Boc-α-amino tetradecanoic acid was carried out as described in Appendix I (method B). The cationic lipidic polylysine dendron $(C_{14})_3Lys_7(C_{14})_8(NH_2)_8$ **(compounds 2a)** having 11 C_{14} alkyl chains and 8 surface amino groups, was synthesised as described in Appendix I (method C).

4.1.3. Surface pressure study

A chloroformic dendron solution (100µl, 1mg/ml) was spread on a purified water surface in a Langmuir film balance system (Nima 601S, Cambridge, UK) at 25°C. The solvent was allowed to evaporate for 5 min before the monolayer was compressed at a rate of 100 cm^2/min. The surface pressure was measured by a Wilhelmy plate and the compression isotherm recorded.

4.1.4. Molecular modelling of the dendron

The initial topology file for the dendrimer was defined using QUANTA/CHARMm (version 96 and 23.2 respectively) software (Accelrys). Half of the molecule was defined as a fragment and joined to form the complete dendrimer. The absolute configuration of the lysine residues was "S", but with the possibility of the tetradecanoic acid adopting the S or R configurations in the synthesis, 2048

conformers are possible. For the molecular dynamics trials that followed, it was decided to apply an S configuration throughout, and also to apply an alpha helical conformation to the central section of the polymer that forms a stretch of seven lysine residues. The amino groups of lysine were given a formal charge of +1, to become NH_3^+. Minimization in CHARMm using charge templates provided the starting conformation for further dynamics procedures.

For greater control of dynamics parameters, the structure was transferred to the Sybyl (Tripos) program. In order to show that the molecule was not adopting preferred stable conformations, a series of dynamics heating (1000K over 1ps) and annealing (200K over 2.5ps) procedures was carried out.

Dynamic characteristics of the molecule under different conditions of simulated solvation were carried out. Using Sybyl software (version 6.7), the Gasteiger-Huckel method of charge assignment appropriate to a system of single and double bonds was used. After energy minimization, dynamics simulations were set up to run over 40ps (picoseconds), sufficient to allow large internal movements of the molecule to take place. Bond vibrations involving hydrogen atoms were constrained with the "Shake algorithm" to allow a dynamics integration time step of 1fs (femtosecond). To allow for the gross effect of solvent water, a distant dependent dielectric constant of 2 was applied. For comparison, a constant dielectric of 1 was used to simulate *in vacuo* dynamics. The same initial minimized conformation was used as the starting point in each case. All simulations were carried out using a Silicon Graphics Indigo2 workstation.

To remove the bias from the choice of the starting conformation, four initial starting conformations produced by previous annealing experiments were run in duplicates, one to simulate the vacuum and one to simulate the water.

4.1.5. Dendron self-assembly and dendrisome formation

To study the potential of the dendron to form supramolecular aggregates, dendrisomes with different dendron/CHOL molar ratios, namely 1:0 (20 mg dendron: 0.0 mg CHOL), 1:1 (18.03 mg dendron: 1.97 mg CHOL), 1:5 (12.93mg dendron: 7.07 mg CHOL), 1:7 (11.33 mg dendron: 8.67 mg CHOL), 1:9 (10.09mg dendron: 9.91 mg CHOL), were prepared by reverse-phase evaporation (REV) method (New, 1989). After dissolving 20 mg of the total lipid (dendron/CHOL) in 40 ml chloroform: ether (1:1) mixture, 5ml of deionised water was injected into the organic solution, bath sonicated for 2 min and the organic solvent removed under reduced pressure in a rotary evaporator. The dispersion was bath-sonicated at 65 °C for 2 h, a temperature above the transition temperature of the dendron and to remove residual solvent. Liposomes containing DSPC: CHOL (1:1) were prepared using the same technique.

4.1.6. Transmission electron microscopy

A drop of the dendrisome suspension (4mg/ml) was placed onto a grid with a support film of Formvar/carbon previously glow discharged in an Emitech glow discharger unit. Excess material was blotted off with a 50 hardened filter paper and negatively stained with 1% uranyl acetate, a cationic uranyl salt which is, unlike anionic salts, is compatible with the cationic dendrisomes, prior to viewing by Philips CM 120 (Einhoven, Netherlands) Bio Twin transmission electron microscope using a lab 6 emitter and 120 KV. Images were captured on Kodak SO-163 negative film and printed on Ilford multi-grade paper.

4.1.7. Measurement of dendrisome diameter and zeta potential

The hydrodynamic Z-average diameter and zeta potential of all dendrisome preparations in deionised water were measured by PCS using a Zetasizer 3000

(Malvern Instruments, Malvern, UK, He-Ne laser, 90° angle of measurement) after appropriate dilution of the samples. The average of three measurements was used and the results expressed as Z-average (nm) ± S.D and zeta potential (mV) ± S.D.

4.1.8. Phase transition behaviour of the supramolecular aggregates

Samples (4 mg) of dendrisome suspension (molar ratios 1:0 and 1:9 dendron/CHOL, 4 mg/ml) prepared in water were scanned at a rate of 10 °C/min, from -10 °C to 90 °C in a differential scanning calorimeter (DSC60, Shimadzu, Japan).

4.1.9. Dendrisome encapsulation efficiency

While not an ideal drug, [^{14}C]-benzyl penicillin potassium salt (penicillin G) was chosen as it was available in radiolabelled form. It was reconstituted in doubly deionised water to make a final concentration of 0.9μCi/50μl. A mixture of cold (2mg) and radiolabelled (5.7μg or 0.9μCi) drug was dissolved in 5ml water (drug to lipid percentage was 10%) and injected into the lipid solutions (dendron/CHOL molar ratios; 1:0, 1:5, 1:9) prepared as mentioned above. The suspension was ultra-centrifuged in a Sorvall Combi-Plus ultracentrifuge (Sorvall, Dupont, USA) at 40,000 rpm for 1 h at 4 °C, and washed to remove any unentrapped/non-interacting drug. The pellets were suspended in 1 ml water for encapsulation efficiency and release studies. Radioactivity was measured in 10 μg of pellets suspension and supernatant. The weight of entrapped drug was calculated accordingly (0.9μCi is equivalent to 2 mg drug). The percentage entrapment was calculated as mg drug entrapped in 100 mg total lipid (total mass of dendron and cholesterol). Entrapment studies were carried out in triplicate, the results being expressed as percentage ± S.D.

4.1.10. *In vitro* drug release

In vitro release of drug from dendrisomes (dendron/CHOL molar ratios; 1:0, 1:5, 1:9) and the comparator DSPC: CHOL (1:1) liposome formulation was measured

using a dialysis technique. 1 ml of drug-containing dendrisome or liposome suspension was pipetted into the dialysis tubing with a MWCO of 3,500 Da, used without previous treatment and sealed. The tubing was placed in 250 ml of deionised water in a 300 ml conical flask with constant stirring at 25°C. At intervals over 48h, 1 ml samples were taken and replaced with water at the same temperature, the sample added to 4 ml Optiphase 'Safe' scintillation cocktail for quantification (LS 6500 Multi-Purpose Scintillation Counter, Beckman, USA). Release studies were carried out in triplicate, the results being expressed as percentage ± S.D.

4.2. Results and discussion

4.2.1. Design of the amphipathic dendron and molecular modelling

The dendron discussed here **(Figure 4.1)** was synthesised to modify the lipophilicity and properties of the dendrons reported by our group elsewhere (Shah *et al.*, 2000; Ramaswamy *et al.*, 2003a) to investigate the manner in which the lipophilicity and geometry of these molecules affects the process of self-assembly, drug interaction and possibly fate in the body (Florence, 1997; Florence and Hussain, 2001).

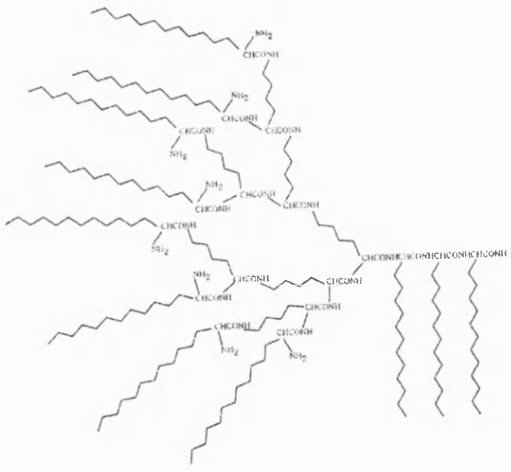

Figure 4.1: The chemical structure of the lipid-lysine dendron synthesised $(C_{14})_3Lys_7(C_{14})_8(NH_2)_8$. The increase in the lipophilicity was achieved by substitution of surface groups with α-amino tetradecanoic acid. The alkyl amino groups remain unacetylated which imparts the cationic nature to the dendron.

Three successive couplings of α-amino tetradecanoic acid to the lysine C-terminal as well as single coupling to the α-amino and ε-amino groups of surface lysine residues were made to provide lipophilicity. Although lysine amino terminals were coupled to the lipoamino acid, the amino groups of the lipid remain unacetylated and thus impart an overall positive charge to the dendron.

To learn more about the behaviour of a single molecule in vacuum and in a polar medium, dynamics simulations were carried out in both environments. **Figure 4.2** shows two frames of dynamics simulations. In **(a)** where dynamics were simulated in vacuum, the lipidic chains show less tendency to aggregate and the molecule expands. In **(b)** the dynamics with a distance dependent dielectric mimicking the effect of a polar environment, the lipidic chains collapse and internalise in the globular structure, the charged amino groups being generally oriented outwards from the centre of the molecule. The frames show the behaviour of a single dendron in non-polar and polar media respectively. The results were not surprising but further indicate that the lipophilicity of the dendron is a driving force for self-assembly. Acetylation of the alkyl amino group results in an extremely insoluble compound which fails to self-assemble in water.

4.2.2. Dendron self-assembly and dendrisome formation

Self-assembling dendrimers with a variety of structures have been reported by several groups. Mizutani *et al.* (2002) reported aggregation of quaternary 4th generation dendrimers with methyl and octyl chains forming loose aggregates with diameters ranging from 17 to 36 nm. Esumi *et al.* (2002) found a 4th generation polyamidoamine dendrimer with 64 alkyl end groups, which adsorbed at the air-water interface, to aggregate in water forming systems of around 53 nm in diameter.

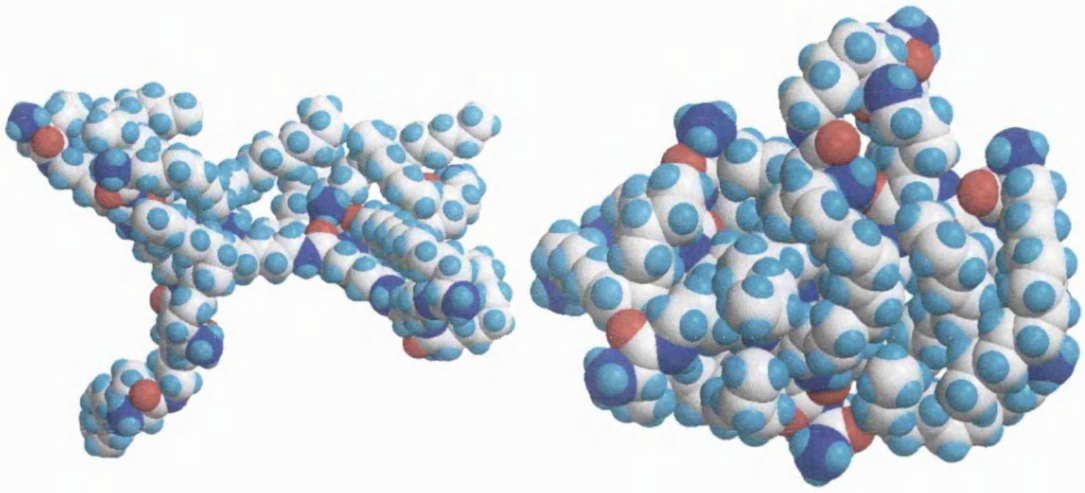

Figure 4.2: Dynamics simulations of the dendron $(C_{14})_3Lys_7(C_{14})_8(NH_2)_8$ were performed over 40 picoseconds using (QUANTA/CHARMm) and Sybyl. Blue and red spheres represent the nitrogen and oxygen atoms, respectively. **a:** dynamics simulated in vacuum, where the lipidic chains show less tendency to aggregate and expansion of the molecule occurs. **b**: dynamics with a distance dependent dielectric mimicking the effect of a polar environment, collapse of the lipidic chains and their internalisation within the globular structure. The charged amino groups are generally oriented outwards from the centre of the molecule.

Poly(propylene imine) with 64 surface palmitoyl chains forms vesicular structures with diameters ranging from 20 to 200 nm in acidic media (Schenning *et al.*, 1998). The lipid-modified cationic dendron self-assembles into vesicular structures (dendron/CHOL molar ratios 1:0) named here dendrisomes. The Z-average hydrodynamic diameter of these was found to be 311 nm ± 8 nm. The zeta-potential (+ 55 mV) was positive. Dendrisomes are reminiscent of cationic liposomes except that no cationic lipid is added to impart a positive charge, as the dendron itself carries eight amino groups which results in a positive zeta potential (+50 mV), investing the structures with properties relevant to interaction with DNA and oligonucleotides.

The TEM micrograph in **Figure 4.3** shows membranes of 6.6-10 nm thickness. We assume bilayer formation, with the hydrophilic polylysine head directed towards the aqueous phase and the hydrophobic alkyl chains associating with the hydrophobic regions of neighbouring dendrons, as shown schematically in **Figure 4.3**. The

diameter, d, was calculated from the molecular area found from the monolayer studies **(Figure 4.4)**. The area per molecule was calculated by extrapolation of surface pressure to zero pressure (400 $Å^2$) (400 $Å^2 = \pi r^2$, d = 2r = 2.26 nm). The length of an alkyl chain, L, based on Corey-Pauling-Koltun (CPK) molecular modelling is approximately 2.2 nm (Schenning *et al.*, 1998). It is possible that the polylysine head makes the membrane bulkier and thicker compared to phospholipid bilayer membranes whose thickness is generally around 5nm.

TEM shows also a population of smaller size (<100 nm) structures compared to the 300 nm Z-average hydrodynamic diameter measured by PCS. In PCS, as stated before the hydrodynamic diameter obtained is an intensity mean size. The intensity of light scattered is proportional to d^6 (d being the particle diameter) from the Rayleigh approximation), so the contribution of the light scattered from small particles to calculation of mean size is minimal compared to that of large particles. Accordingly, the presence of large particles due to a heterogeneous size distribution **(Table 4.1)** or aggregation could bias the result and may explain the difference in diameter obtained by TEM and PCS.

Cholesterol, as is well known, has an interesting modulatory effect on the transition behaviour of lipid vesicles. It broadens the peak of the phase transition from a "gel" state, where the fatty acyl chains of the lipid membranes are closely packed and relatively ordered, to a " fluid " state in which the side chains are capable of rotational motion (Papahadjopoulos *et al.*, 1973).

Incorporation of cholesterol into these vesicles was found to affect the morphology, size, thermal transition behaviour of the aggregates but not their charge.

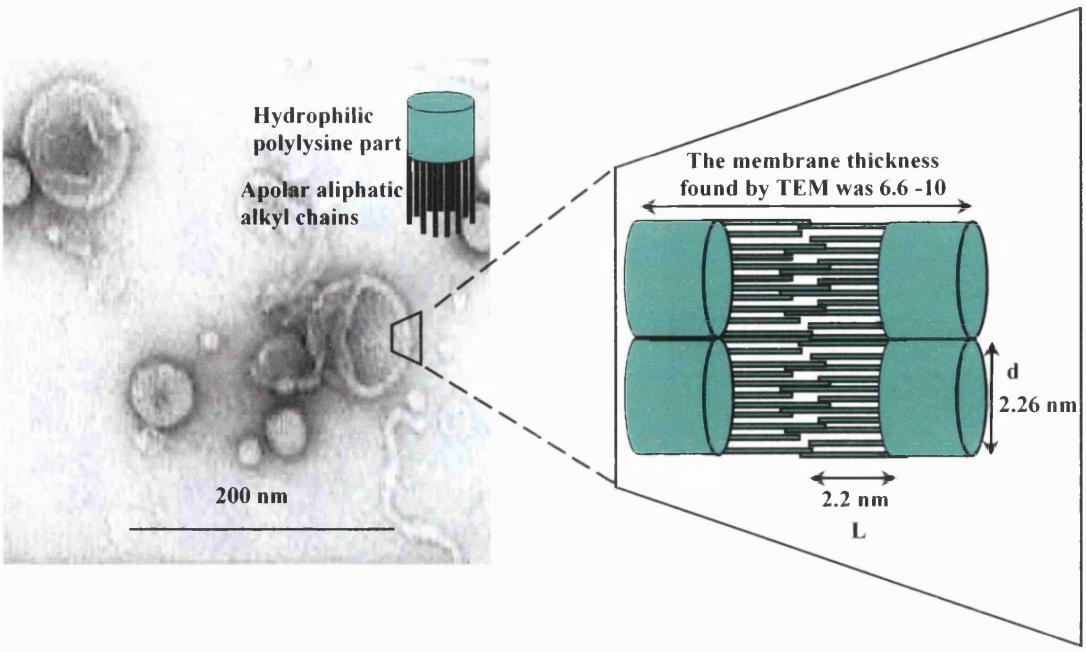

Figure 4.3: Left: Transmission electron micrograph of dendrisomes prepared by the REV technique, demonstrating dendron assembly into unusual vesicular structures with a membrane thickness of from 6.6 to 10 nm. Right: schematic representation of bilayer formation of the lipidic dendron with the assumption that the hydrophilic polylysine head is directed towards the aqueous phase and the hydrophobic alkyl chains interact with the hydrophobic groups of another dendron. The diameter, D, was calculated from the molecular area found by surface pressure studies. The length of the alkyl chain, L, is based on CPK molecular modelling.

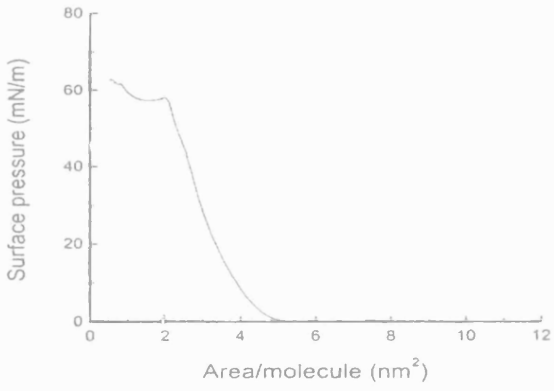

Figure 4.4: A surface pressure-area isotherm of the lipidic dendron $(C_{14})_3Lys_7(C_{14})_8(NH_2)_8$ spread on water. The isotherm shows the characteristics of an expanded monolayer with a calculated limiting surface area of about 4 nm^2 (400 $Å^2$).

Table 4.1 shows dendrisomes in the absence of cholesterol to be smaller and more uniform **(Figure 4.5A)** than dendrisomes with dendron/CHOL molar ratios 1:7 **(Figure 4.5C)**. On the other hand, the effect of cholesterol incorporation was less significant on the zeta potential, which varies from 55.6 ± 3 mV for cholesterol - free dendrisomes to 50.3 ± 2 mV for dendrisomes with the highest cholesterol content.

DSC results **(Figure 4.6)** shows a broad transition for cholesterol-free dendrisomes with maxima at 48.5 °C and 63.2 °C. Although the dendrisomes are comprised of a single lipid component, the broad transition can be attributed to the effect of diasterioisomers, since the lipoamino acid used in the synthesis was a mixture of R and S forms. The origin of such phase transitions cannot be easily explained due to the complex arrangements of the alkyl chains in the dendrisome and lack of information about how these structures self-assemble. The peak obtained by cholesterol-containing dendrisomes (1:9 dendron/CHOL molar ratio) was further broadened with a lower maximum at 32.43 °C.

Table 4.1 Dendrisomes Z-average size and zeta-potential with different cholesterol ratios

Dendron/CHOL molar ratios	Z-average size (nm) ± S.D[a]	Polydispersity index	Zeta-potential (mV) ± S.D[a]
1:0	311 ± 8	0.232	55.6 ± 3
1:1	377 ± 5	0.303	50.4 ± 2
1:5	399 ± 6	0.520	51.4 ± 3
1:7	557 ± 13	0.708	52.1 ± 4
1:9	449 ± 9	0.808	50.3 ± 2

[a] Mean ± S.D; n=3

4.2.3. Encapsulation efficiency and *in vitro* release

Although dendrimers of a wide range of structures have been synthesised by several groups (Denkelwalter *et al.*, 1981; Tomalia *et al.*, 1990; Uhrich *et al.*, 1991; Sakthivel *et al.*, 1998; Sadler and Tam, 2002), relatively few studies of their use as

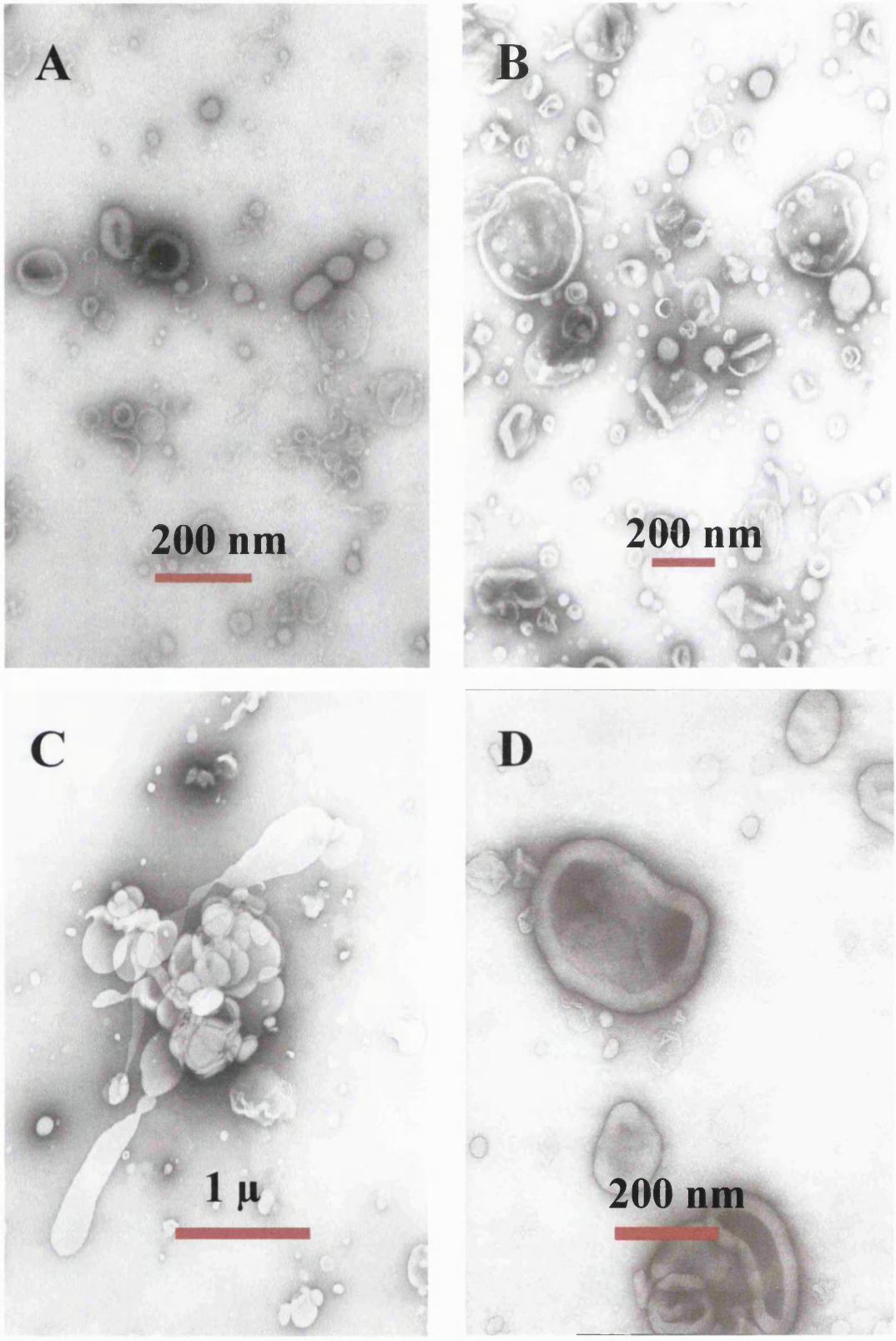

Figure 4.5: Transmission Electron Micrographs of dendrisomes prepared by reverse-phase evaporation technique show the increase in size and shape irregularity with increase in cholesterol content. **(A)** dendron-cholesterol molar ratio 1:0 ; **(B)** molar ratio 1:1; **(C)** molar ratio 1:7 ; **(D)** molar ratio 1:0 encapsulating penicillin G.

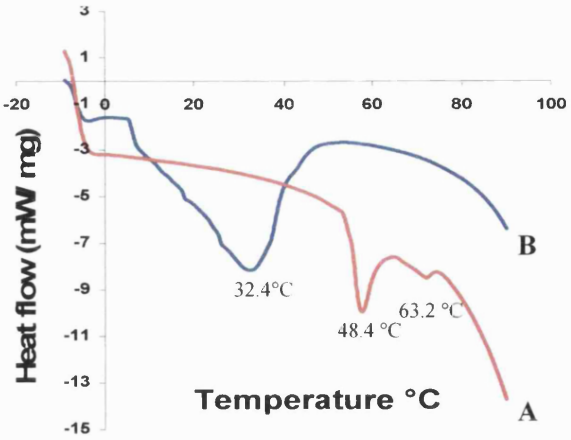

Figure 4.6: (A) DSC trace of dendrisomes (dendron/CHOL molar ratios 1:0) which shows a main endothermic transition at 48.47 °C and a minor one at 63.23 °C. **(B)** A broad endothermic transition at 32.43 °C of dendrisomes (dendron/CHOL molar ratios 1:9)

drug delivery carriers are found in the literature, although the interaction of dendrimers with drugs such as piroxicam (Wiwattanapatapee *et al.*, 1999), 5-fluorouracil (Khopade *et al.*, 1999), ibuprofen (Milhem *et al.*, 2000), indomethacin (Liu and Fréchet, 1999), and propranolol (D'Emanuele *et al.*, 2004) have been reported. Complexation of drugs with dendrimers can affect drug properties in various ways. For example, complexation of some acidic drugs with PAMAM dendrimers was not only successful in slowing drug release *in vitro* but, in some instances, allowed faster cellular uptake, perhaps due to the cationic nature of the dendrimer (Beezer *et al.*, 2003; Kolhe *et al.*, 2003). Furthermore, self-assembling dendrimers could be of use in targeting drugs to tumour tissues since the total molecular weight of the self-assembled system could surpass the enhanced permeation and retention (EPR) threshold, disassembling to lower molecular weight monomers which are removed from the body (Zimmerman *et al.*, 1996; Shultz and Zimmerman, 1999).

Penicillin G was chosen as a model of a negatively charged water soluble drug. The influence of the negatively charged drug, penicillin G, on the morphology of drug-loaded dendrisomes was minimal, as shown by TEM **(Figure 4.5D)**.

Neutral liposomes (hydrodynamic diameter 730 ± 13.5 nm, polydispersity index 0.35, zeta potential -2 mV) were used as a comparator to avoid the complications of electrostatic interaction. Dendrisomes of different compositions were found to have higher encapsulation efficiencies compared to a typical liposome prepared by the same technique. The encapsulation efficiency was directly proportional to the percentage of the dendron in the total lipid "dendron+cholesterol". **Figure 4.7** shows that cholesterol-free dendrisomes have the maximum entrapment efficiency (6.15 %w/w drug in total lipid) although they are smaller in size. Lower entrapment efficiencies were achieved by decreasing the percentage of dendron, despite size increases. Percentage entrapments of 4.7 and 4.0 in case of 1:5 and 1:9 dendron/CHOL molar ratios were achieved respectively, compared to 1.4% in neutral REV liposomes.

Penicillin G is a weak acid (pKa 2.7 at 25 °C) while the dendron is weakly basic due to its lysine content and the surface amino groups. Many cationic polymers possess amines protonated at neutral pH (Ohsaki *et al.*, 2002). The pH of water during the experiment was 6.4. Buffer was not used to avoid the presence of electrolytes which affect the self assembly of the dendron. According to the Henderson-Hasselbalch equation and because of the polycationic nature of the dendron, both the penicillin and the dendron should be ionised over a wide pH range. The mechanism of interaction is likely to be via electrostatic interactions or H-bonding between the drug carboxylate group and terminal amino groups of the dendron, but drug entrapment within the dendritic branches of the dendrisome cannot be excluded.

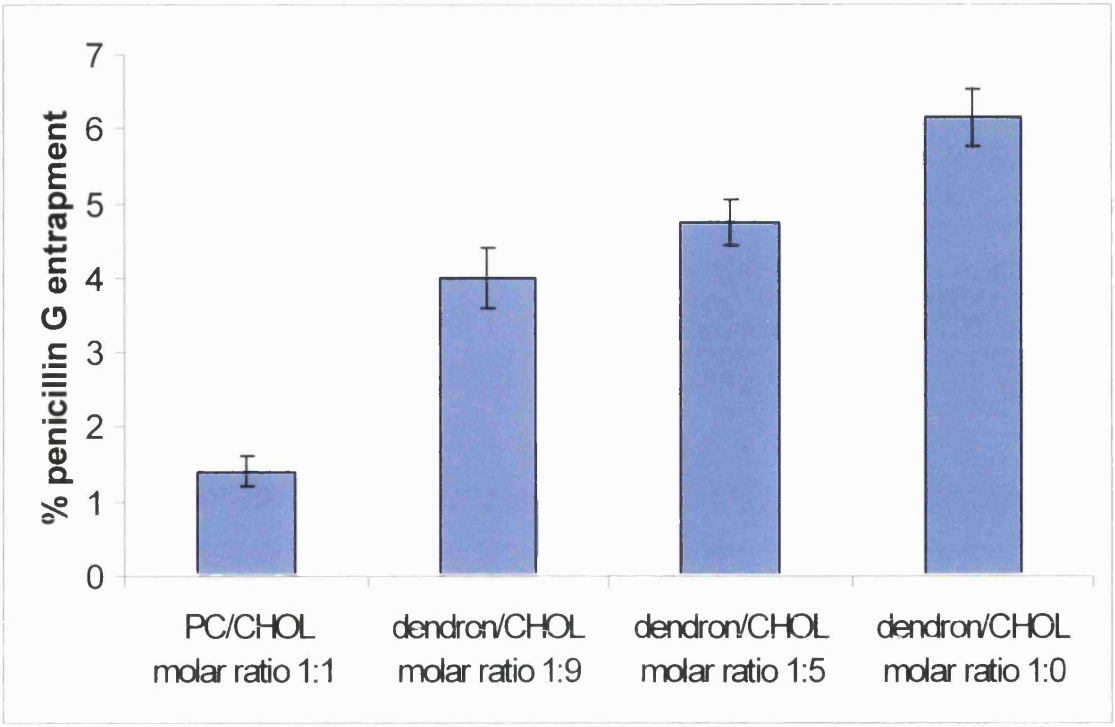

Figure 4.7: Percentage penicillin G entrapment calculated as mg drug entrapped in 100 mg total lipid (cholesterol/DSPC or cholesterol/dendron). Dendron: cholesterol ratios varied in the amount of total lipid (20 mg). The effect of cholesterol is to decrease the percentage entrapment, despite an increase in dendrisome size. The results were expressed as % penicillin G entrapment ± S.D (n=3).

Dykes and coworkers (2001) reported the solubilisation of proflavine hydrochloride and aurin tricarboxylic acid by L-lysine amino acid-based dendrimers and found that dye incorporation was enhanced by acid-base coordination. Control experiments with unbranched hosts showed very little dye uptake, which suggests the importance of dendritic branching in the solubilisation process. Interestingly, the drug/dendron molar ratio in our experiments was also directly proportional to dendrisome size, as shown in **Figure 4.8**.

In vitro release data are shown in **Figure 4.9**, where it is seen that a plateau is reached before complete release as sink conditions were not maintained; in addition the membrane has its own resistance. The dialysis membranes used have a MWCO

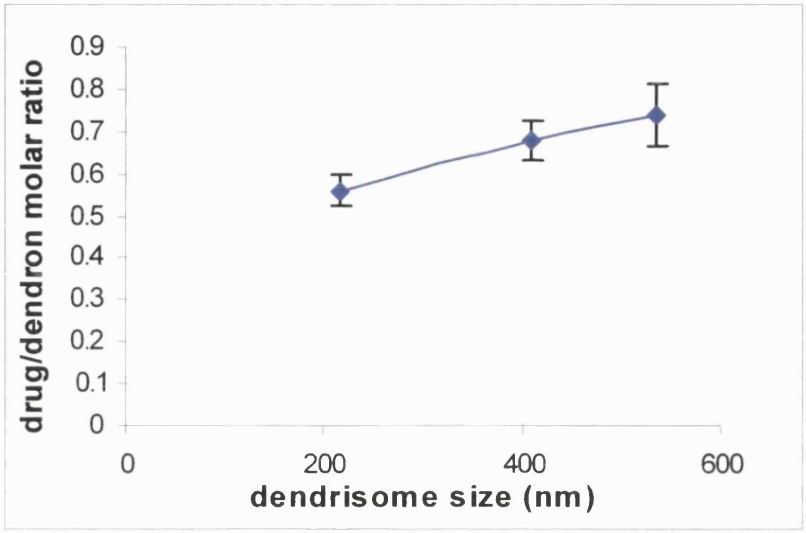

Figure 4.8: The relationship between drug/dendron molar ratio and dendrisome size. Drug:dendron molar ratios were calculated using drug:dendron weight ratios obtained from entrapment studies using the equation:

$$\frac{drug}{dendron} \quad molar\ ratio = \frac{drug}{dendron} \quad weight\ ratio \times \frac{dendron\ MW}{drug\ MW}$$

Dendrisomes with the largest Z-average diameter (highest cholesterol content) had a maximum drug/dendron interaction molar ratio. The results were expressed as drug:dendron weight ratio ± S.D (n=3).

of 3,500 which makes them permeable to unentrapped drug molecules but not to dendrons primarily because they exist as aggregates.

Dendrisomes showed slower release rates than the liposome formulation at 25 °C. Release after 24 h was approximately 24.5% from liposomes but only 4.6% from cholesterol-free dendrisomes possibly due to electrostatic interactions. The release rate is almost doubled when cholesterol is added to the dendrisomes. Presumably, the dendrons are in a less ordered state in the presence of cholesterol or could simply be the replacement of dendrons (i.e. the drug binding molecules) with cholesterol (which presumably do not bind the drug). It is established that the addition of cholesterol to liposomes causes the bilayers to be less ordered and more permeable at temperatures below the transition temperature (Papahadjopoulos *et al.*, 1973).

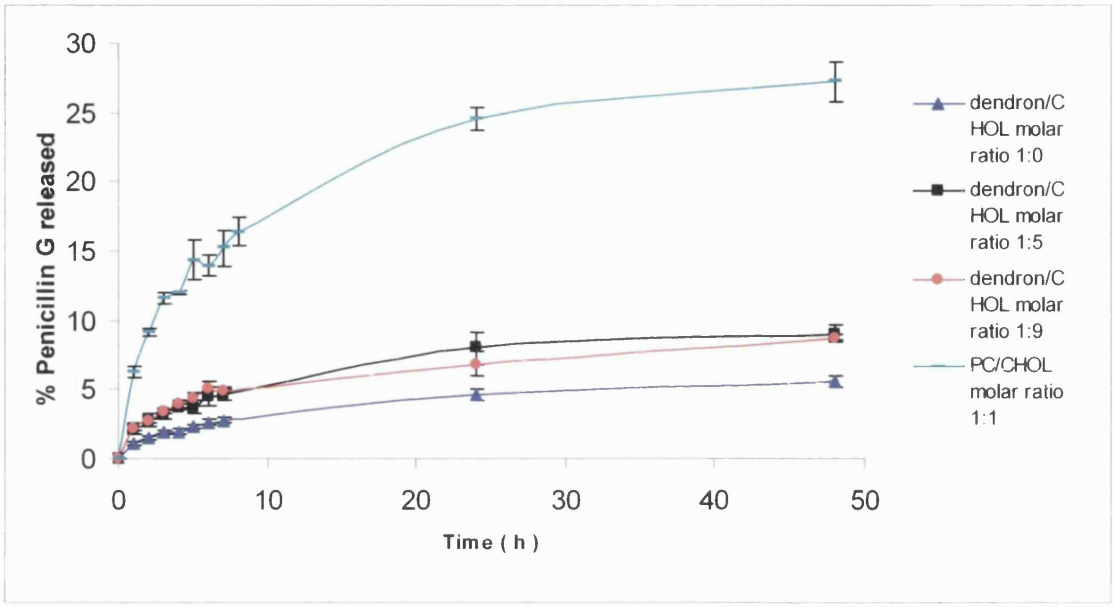

Figure 4.9: *In vitro* release of penicillin G from dendrisomes (dendron/CHOL molar ratios 1:0, 1:5 and 1:9) and liposome PC/CHOL molar ratio1:1. Conditions: pellets of each drug containing dendrisome suspension and liposome were reconstituted in 1 ml deionised water and then the suspension was dialysed against 250 ml of deionised water at 25°C under constant stirring. The percentage was calculated from the original amount entrapped in that particular preparation and expressed as % penicillin G released ± S.D (n=3). The release rate was the lowest in dendrisomes with the highest dendron content. Dendrisomes generally show slower release rates than the neutral liposome formulation studied. A positive control (free penicillin G alone) was not included as the drug is soluble with a small molecular weight and different encapsulation efficiencies among the four formulations studied.

4.3. Conclusion

Engineering the structure of dendrimers and dendrons can affect their behaviour in aqueous media. Understanding molecular aggregation of dendrimers and dendrons in aqueous solution and the behaviour of dendrimer monolayers at the air/water interface are important in the design of novel supramolecular carrier systems for the delivery of challenging drug molecules including proteins and polynucleotides. Dendrisomes of all compositions have higher encapsulation efficiencies and slower release rates compared to the comparator. Cholesterol was found both to increase the size of the aggregates and shape irregularities but did not change the positive zeta potential. Cholesterol decreases penicillin G entrapment efficiency but increases solute leakage at 25 °C.

Electrostatic interactions and hydrogen bonding as well as physical entrapment are important mechanisms involved in dendrisome-drug interactions. Penicillin G was chosen as a *model* of a negatively charged drug but many other drugs can be substituted. Further work is needed to investigate the loading and release of other neutral and negatively charged drugs to gain better understanding of dendrisome-drug interactions. The self- assembled dendrisomes discussed in this chapter broaden the potential use of dendrimers and dendrons in drug delivery and offer potential for further *in vitro* and *in vivo* evaluation.

Chapter V

SOLUBILISATION AND TRANSFORMATION OF DENDRISOMES INTO MIXED MICELLES

The present chapter explores the molecular interaction between the surfactant Triton X-100 and dendrisomes and the transformation of dendrisomes into isotropic surfactant/dendron mixed micelles. The interaction was studied using techniques such as turbidimetry, photon correlation spectroscopy (PCS) and transmission electron microscopy (TEM). Direct quantification of the solubilised dendron was achieved by use of the bicinchoninic acid (BCA) assay.

5.1. Experimental

5.1.1. Materials

Triton X-100, BCA protein assay kit (Sigma Chemical Company, UK). Diethyl acetamido malonate, 1-Bomododecane, Di-*tert*-butyl dicarbonate and Citric acid (Lancaster, UK), 2-Methyl-2-propanol (Aldrich, USA). Materials used in the dendrimer synthesis were mentioned in chapter III.

5.1.2. Synthesis of the amphipathic dendron

The synthesis of *N*-Boc-α-amino tetradecanoic acid was carried out as described in Appendix I (method B). The cationic lipidic polylysine dendron

$(C_{14})_3Lys_7(C_{14})_8(NH_2)_8$ **(compounds 2a)** having 11 C_{14} alkyl chains and 8 surface amino groups, was synthesised as described in Appendix I (method C).

5.1.3. Preparation of dendrisome -Triton X-100 mixtures

Dendrisomes, without cholesterol, were prepared using the REV method as described in chapter IV. Dendrisomes were suspended in water or surfactant solution giving a final concentration of 2 mg/ml (0.6 mM). The non-ionic detergent Triton X-100 was added to obtain final concentrations from 0.1-100 mM (0.0065-6.47% (w/v)). The mixtures were shaken on a platform shaker at 20 rpm at room temperature for 24 h.

5.1.4. Observation and size measurement of the supramolecular aggregates

The dendron-surfactant aggregates were observed by TEM. The sample preparation was as discussed in chapter IV. The hydrodynamic Z-average diameters of the systems were measured using a PCS 4600 Malvern Submicron Analyser (Malvern Instruments, Malvern, UK; He-Ne laser, the angle of measurement: 90°). The aperture size at Triton X-100 concentrations 0.1 mM- 6 mM, 8 mM -10 mM, and 12 mM-100 mM was 50, 100 and 200 respectively. The average of three measurements provided results expressed as Z-average diameter (nm) ± S.D.

5.1.5. Turbidimetry

The turbidity of the dendrisome dispersions at different Triton X-100 concentrations (Triton X-100: dendron molar ratio varied from 0.170-170) was measured at 400 nm in a plastic cuvette using a Beckman DU® 650 Spectrophotometer (USA). The results (n=3) were expressed as optical density (O.D) ± S.D.

5.1.6. Quantification of the solubilised lipidic peptide dendron

To quantify the amount of dendron solubilised in the mixed micelles, mixed micelles were separated from the unsolubilised aggregates by ultracentrifugation (Sorvall Combi-Plus, Dupont, USA) at 40,000 rpm for 1 h at 4 °C. The supernatant was

assumed to contain the mixed micelles. Quantification of the solubilised peptide was carried out using the standard BCA assay protocol used for protein estimation.

The supernatant (0.2 ml) was mixed with 2 ml of BCA working reagent (50 parts alkaline BCA solution and 1 part copper(II) sulphate pentahydrate 4% (w/v) solution) in a test tube, incubated for 30 min at 37 °C, the optical density was measured at 562 nm in a plastic cuvette. Maximum dendron solubilisation was found to be obtained at a concentration of 60 mM surfactant (taken as 100%). The percentage relative dendron solubilised was calculated from the ratio of the absorbance at 562 nm at a particular surfactant concentration to that of dendron in 60 mM Triton X-100 multiplied by 100. The inherent solubility of the dendron in water was blanked. Results (n=3) were expressed as percentage relative dendron solubilised ± S.D.

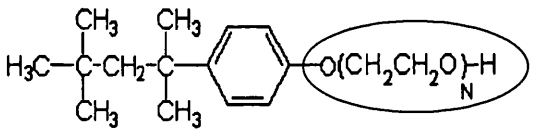

Figure 5.1: The chemical structure of the detergent iso-octyl phenyl poly(10)oxyethylene (Triton X-100). The hydrophilic region (polyoxyethylene chains) is marked.

5.2. Results and discussion

5.2.1. Dendrisomes and Triton X-100

The dendron **(Figure 4.1)** discussed in section 4.2.2 (chapter IV) was found to form higher order vesicular structures or dendrisomes. The dendrisomes combine the properties of both liposomes, because of their vesicular nature, and dendritic macromolecules because they are formed from individual dendrons.

Triton X-100 ([*p*-1,1,3,3,-tetramethylbutyl)phenyl]poly(oxyethylene) with an average of 9.5 oxyethylene groups **(Figure 5.1)** is one of the most widely used non-ionic detergents. It is used in membrane solubilisation and the separation of cellular components. When liposomes or phospholipid vesicles are mixed with a detergent such as Triton X-100, they generally form mixed detergent-phospholipid aggregates a process which is followed by transformation into mixed micelles in which the lipid is considered to be solubilised when excess detergent is added (Dennis, 1974; Robson and Dennis, 1979).

5.2.2. Turbidity measurement

Solubilisation of vesicles by surfactants can be assessed by the decrease in the light scattering or turbidity of the vesicle suspension by measuring the optical density (OD) of the dispersion at a wavelength not absorbed by the suspension (Goni and Alonso, 2000). Mixed micelles scatter much less light than vesicles (Ahmed *et al.*, 1997; Xu and London, 2000).

Figure 5.2 shows the effect of increasing the surfactant concentration on the reduction of turbidity of dendrisome suspension. Increasing the surfactant concentration above 0.8 mM (1.4:1 Triton X-100: dendron molar ratio) causes a

drastic decrease in the turbidity until the dispersion appears to be isotropic at 8 mM (13.4:1 Triton X-100: dendron molar ratio). This suggests a structural change in the aggregate and gradual transformation into a mixed micellar system.

5.2.3. Size measurement and TEM of the aggregates

Figure 5.2 shows that the hydrodynamic diameter of the dendrisomes was unchanged up to molar ratios of 1.4:1 Triton X-100 (0.8 mM): dendron. The CMC of the surfactant is 0.2-0.3 mM.

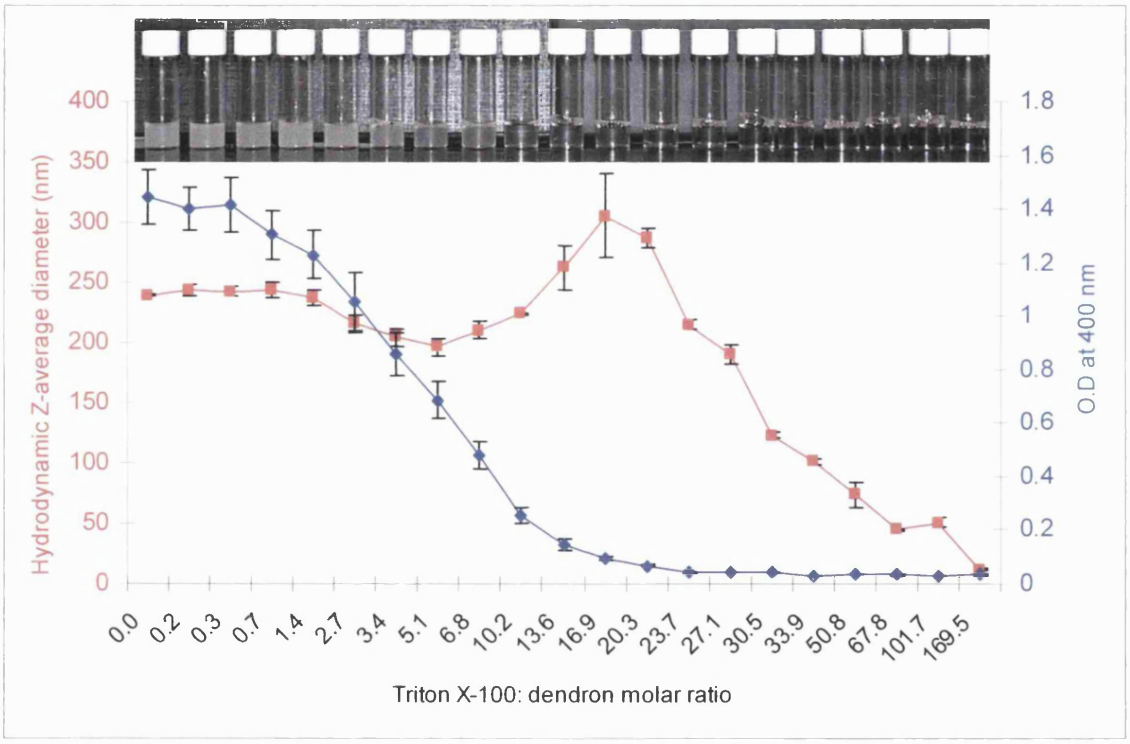

Figure 5.2: The turbidity of dendrisome-surfactant suspensions (the blue line) was obtained by measuring the O.D at 400 nm (a photograph of the dispersions is shown at the top). The hydrodynamic Z-average diameter of the dendrisome-surfactant aggregates was measured by PCS (the red line). Triton X-100: dendron molar ratio varied from 0.17-170. The results were expressed as O.D ± S.D and Z-average diameter (nm) ± S.D (n=3). The dispersion became optically clear at 13.4:1 molar ratio. The Z-average diameter of the dendrisomes (circa 240 ± 1.1 nm) increased to about 305 ± 35 nm at Triton X-100: dendron molar ratio of 17 although the dispersion was isotropic (see text for explanation). The mean size then started to decrease to 50 ± 4.1 nm and 11.6 ± 0.6 nm at Triton X-100: dendron molar ratios of 100 and 170, respectively.

The hydrodynamic size began to decrease to 196 ± 7.2 nm before increasing to a maximum of 305 ± 35 nm. Continual addition of the surfactant up to 100-170:1 Triton X-100: dendron molar ratio (60-100 mM) decreased the size of the aggregates to that in the pure micellar range, namely 11.6-50 nm. TEM showed the transformation of dendrisomes **(Figure 5.3A)** into smaller aggregates **(Figure 5.3B)**.

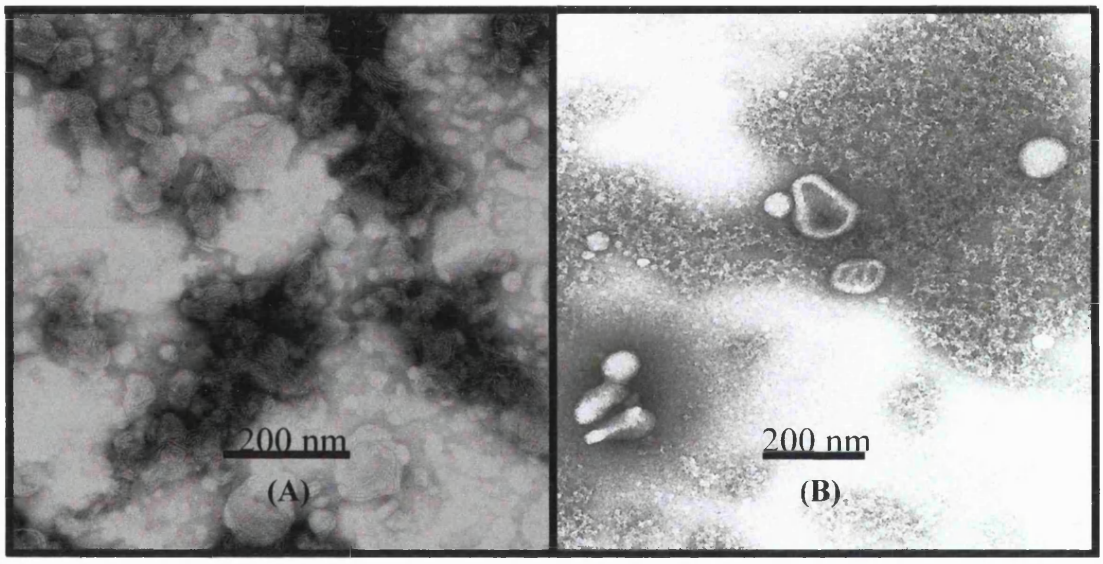

Figure 5.3: (A) TEM of dendrisomes in water. (B) TEM of dendrisomes at a 6.7:1 Triton X-100: dendron molar ratio. 43% of the dendron was solubilised as estimated by BCA assay. PCS suggests a 210 ± 7.3 nm hydrodynamic diameter under these conditions.

The steps involved in the solubilisation process are proposed in **Figure 5.4**. The apparent increase in the aggregate size at low surfactant concentration could be due to three possible effects, i) to the incorporation of surfactant molecules in the membrane which increases the number of molecules per vesicle **(Figure 5.4B)** (Partearroyo *et al.*, 1992; De La and Parra, 1994), ii) to vesicle fusion or iii) the aggregation of small structures or a mixture of all three processes. The addition of

more surfactant molecules caused a transformation of the dendrisomes into surfactant-dendron mixed micelles (11.6-50 nm). Mixed micelles may have gradually been formed by solubilisation of dendron clusters within the mixed micelles (50-100 nm). This increase in the hydrodynamic size was not accompanied by an increase in the turbidity since the dispersion tends to be isotropic at molar ratios above 13.4:1. This difference between turbidity and size measurement data is due to the fact that PCS measures the hydrodynamic diameter, an intensity mean size. The intensity of light scattered is proportional to d^6 (where d is the particle diameter, from the Rayleigh approximation). The contribution of the light scattered from small particles (mixed micelles in this case) to the mean size is minimal compared to that of large particles (real or aggregates of small particles) even if the latter were few in number. Polydispersity increases to 0.45-0.6 when the Triton X-100 concentration has increased to 4-10 mM presumably because two size populations are present. The polydispersity fell to 0.24 when the aggregate size approached 11.6 nm.

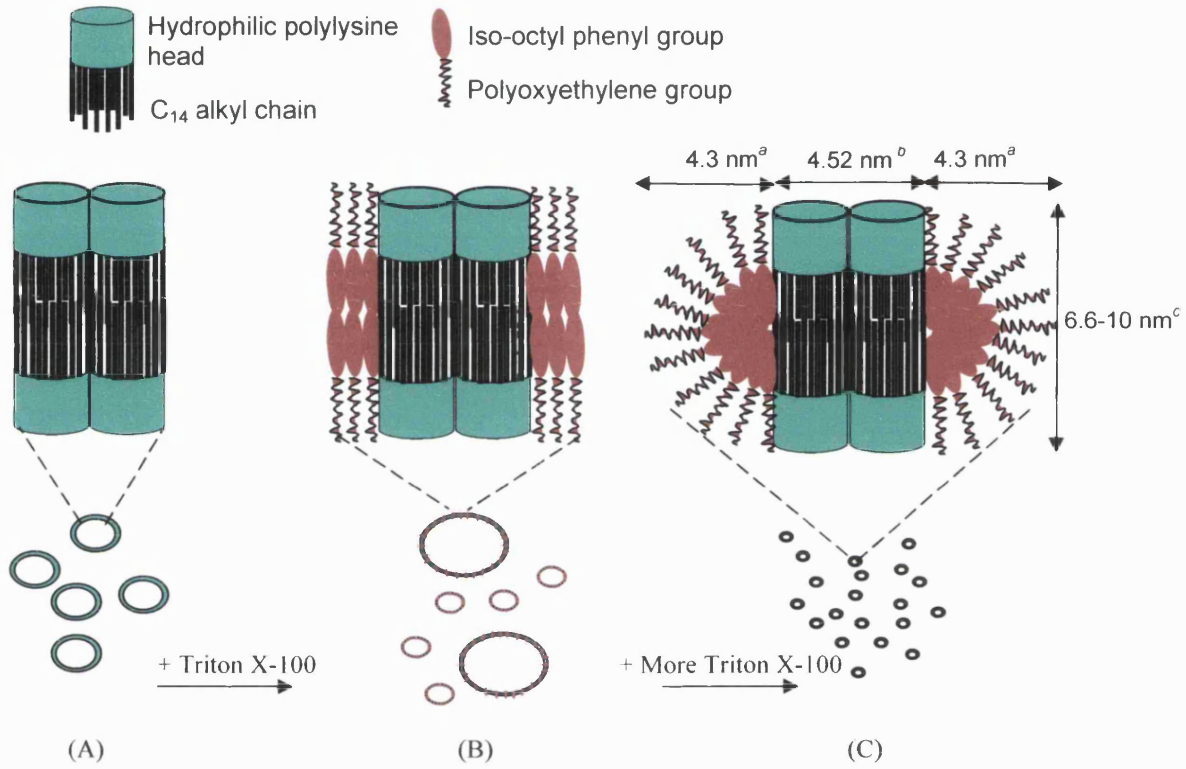

Figure 5.4: A schematic illustration showing the various stages of solubilisation proposed. (A) *Dendrons assemble into bilayer structures* (hydrodynamic diameter, 240 ± 1.1 nm) (see TEM in **Figure 4.5A**). (B) *The hydrodynamic diameter of the aggregates increases to about 305 nm* at surfactant concentrations above the CMC, but not sufficiently high to solubilise all the dendrisomes i.e. 17:1 Triton X-100: dendron molar ratio (10 mM), presumably due to (i) incorporation of surfactant molecules in the dendrisome membrane which increases the number of molecules per vesicle (shown schematically) or (ii) fusion or aggregation of small aggregates besides the formation of smaller mixed aggregates. (C) *Solubilisation of dendrisomes into mixed micelles* upon addition of more surfactant. This may gradually have happened by solubilisation of dendron clusters within a mixed surfactant/dendron aggregates (hydrodynamic diameter 50-100 nm), followed by complete transformation into mixed detergent/dendron micelles 11.6-50 nm at 100-170 Triton X-100: dendron molar ratio. *a* Reported by Attwood and Florence (1983a), *b* and *c* are as calculated in **Figure 4.3**.

5.2.4. BCA assay of the supernatants

Solubilisation data from turbidity measurements are supplemented by quantitative assessment of the solubilised dendron. The BCA assay (Wiechelman *et al.*, 1988; Minard-Basquin *et al.*, 2003) was used here to estimate the amount of the polylysine dendron which is solubilised, after separation of the insoluble fraction by ultracentrifugation as mixed micelles can not be pelleted by ultracentrifugation, and dendrisomes are more dense than the solution. The BCA assay is one of the most commonly used assays for protein determination. The principle of the BCA assay relies on the formation of a Cu^{2+}-protein complex under alkaline conditions, followed by reduction of the Cu^{2+} to Cu^{1+} by cysteine, cystine, tryptophan, tyrosine and peptide bond (the mechanism employed here). It forms a purple-blue complex, which has an absorbance at 562 nm. Maximum solubilisation was achieved at 60 mM Triton X-100 (3.9%) which was considered to be 100%. As shown in **Figure 5.5**, while 20-90 % of the dendron is solubilised in the surfactant concentration range 1.6-30 mM (2.7-50 Triton X-100: dendron molar ratio), only 14 % of the dendron is solubilised at 0.8 mM (1.4 Triton X-100: dendron molar ratio).

For solubilisation to occur the dendron-detergent interaction should be more energetically favoured compared to dendron-dendron and surfactant-surfactant interactions. The molar ratio at which the lipid is solubilised depends mainly on the lipid and detergent used. For example, the minimum solubilizing detergent: lipid molar ratio for cholate: egg yolk lecithin system is 0.75:1, 5:1 for alkyl glycosides surfactant n-octyl-β-D-glucoside (New, 1989) and 3:1 for Triton X-100 (Partearroyo *et al.*, 1992).

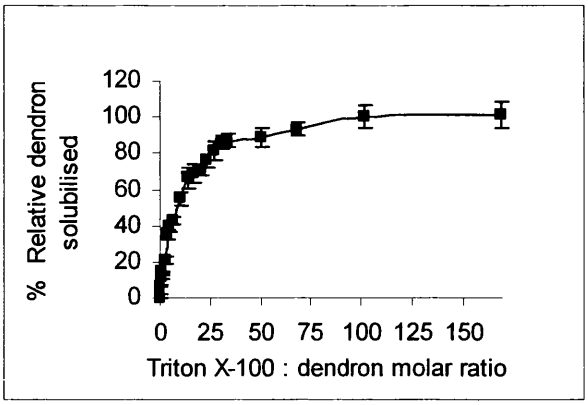

Figure 5.5: Estimation of the percentage relative dendron solubilised into mixed micelles (using the BCA assay) after separating the soluble mixed micelles from the insoluble aggregates by ultracentrifugation. The percentage is relative to 100% solubilisation at 60 mM. The inherent dendron solubility in water (2.3%) was subtracted from the total solubility to calculate the fraction solubilised. The results were expressed as percentage relative dendron solubilised ± S.D. 20-90% of the dendron was solubilised at 2.7-50 Triton X-100: dendron molar ratio, complete solubilisation was obtained at Triton X-100: dendron molar ratio above 100.

5.3. Conclusion

All the techniques showed that dendrisomes were transformed into surfactant-dendron mixed micelles. The dispersion became optically clear at a 13.4:1 Triton X-100: dendron molar ratio. Complete dendron solubilisation was obtained between 100-170:1 Triton X-100: dendron molar ratio when the aggregate diameter reduced to the micellar range, namely 12 to 50 nm. The mechanism of solubilisation of the dendrisomes by the non-ionic surfactant can simply be explained by the general rule that Triton X-100 has a higher affinity for the dendrons than for the pure detergent micelle.

Exploring such types of non-electrostatic molecular interactions between dendritic molecules and other molecules should shed the light on the mechanisms by which these carriers self assemble into higher order structures or interact with other substrates, on which their use as carriers depends.

Also the transformation of water-insoluble dendrisome suspensions into the water-soluble isotropic mixed micelle systems broadens the scope of possible dendritic molecules based supramolecular structures. Such assemblies will have physicochemical properties different from that of the dendrisomes and the pure surfactant micelles. Enhanced hydrophobicity and higher pyrene solubilisation of the SDS-cationic tetrameric PAMAM dendron aggregates compared to SDS micelles alone was previously reported (Yoshimura *et al.*, 2002).

Water solubility is a requirement in diagnostics and sensoring technology where dendrimers are interesting candidates. Dendrimer-detergent association does not require chemical intervention compared to dendrimers carrying covalently attached solubilizing agents to provide water solubility (Minard-Basquin *et al.*, 2003).

Chapter VI

TRANSEPITHELIAL TRANSPORT OF A POLYLYSINE DENDRIMER ACROSS CACO-2 MONOLAYERS

The objective of the work described in this chapter was to investigate the influence of concentration and incubation time on the permeability of the 6th generation water soluble cationic dendrimer Gly-$Lys_{63}(NH_2)_{64}$ across Caco-2 monolayers. Cytotoxicity was also determined by the MTT assay. The influence of the [^{3}H] labelled dendrimer on the integrity of Caco-2 cells and paracellular permeability was monitored by measuring, respectively, the transepithelial electrical resistance (TEER) and PEG 4000 permeability.

6.1. Experimental

6.1.1. Materials

Dimethylsulfoxide (DMSO), 3-(4,5-dimethylthiazol-2-yl)-2,5-diphenyltetrazolium bromide (MTT), Toluidine blue, Trypan blue solution (0.4%), Polyethylene glycol MW 3,350 Da (PEG) (Sigma, USA), L-[4,5-^{3}H] Lysine monohydrochloride (specific radioactivity 87.0 Ci/mmol) (Amersham Pharmacia Biotech, UK), [^{14}C]-PEG 4000 (specific radioactivity 11.2 mCi/g) (Amersham Life Science, UK), Dulbecco's modified Eagle medium with Glutamax-I (DMEM), OptiMEM-1 serum free medium, Gentamicin solution (10 mg/ml), Non-essential amino-acids solution 100X (NEAA), Foetal calf serum (FCS), Phosphate Buffered Saline (PBS) (pH 7.4, 10 X), Hank's balanced salt solution (HBSS), Trypsin/EDTA (1X) (Gibco Invitrogen Corporation, UK), 75 cm^2 tissue culture flasks with filtered screw caps (TPP, Switzerland), Costar Transwell™ polycarbonate cell culture inserts (12 mm diameter, growth area 1.13 cm^2, pore diameter 3.0 μm), 96- and 12-well plates (Corning Costar Corporation, USA), Optiphase 'safe' scintillation cocktail (Perkin-Elmer, UK). Materials used in the dendrimer synthesis were mentioned in chapter III.

6.1.2. Synthesis of Gly-Lys$_{63}$(NH$_2$)$_{64}$ dendrimer

The synthesis of the unlabelled and [^{3}H] labelled (for biological studies) cationic water soluble dendrimer **(compound 2c) (Figure 2.12)** having 64 surface amino groups was performed using method D and F respectively and purified as described in Appendix I.

6.1.3. Caco-2 cell culture

Caco-2 cells were obtained from the European Collection of Animal Cell Culture (Wiltshire, UK). Cells were maintained in DMEM supplemented with 1% NEAA, 10% FCS and gentamicin (50μg/ml) at 37 °C, 5% CO_2, in 95% relative humidity.

Caco-2 passage number 80-91 was used. The cells were expanded in tissue culture flasks (75 cm^2 growth area). The medium was changed every other day and passed before reaching confluence (80% confluence). The cells were washed twice with 5ml of warm PBS (calcium and magnesium free) to remove any traces of serum which may interfere with the action of trypsin/EDTA. The cells were detached from the flask using 5 ml warm trypsin/EDTA for 1 min, 4 ml was aspirated and 1 ml was left for 5 min. The trypsinization was stopped by adding 9 ml of serum containing DMEM. The cells were centrifuged for 5 min at 1000 rpm at 4 °C, the pellets were resuspended in 10 ml serum containing medium for cell viability and permeability studies.

6.1.4. Cell viability (MTT assay)

Caco-2 cells seeded into a 96-well plate at a density of 100,000 cells per well using a cell suspension (1×10^6 cells /ml as assessed by the trypan blue exclusion method). The medium was changed every second day. After three days the cells incubated with 100 µl of dendrimer solution (0.5-10 mg/ml) in DMEM for 4h at 37 °C, then the media was aspirated and the cells were incubated with 160 µl of fresh medium (10 µl 5mg/ml MTT and 150 µl DMEM) for 2.5 h at 37 °C (protected from light due to MTT photosensitivity). The plates were inverted to remove media and gently tapped onto absorbent paper. DMSO (200 µl) was added to each well then placed on a rotary shaker for 20 min to solubilise the crystals. The absorbance was read at 550 nm and 630 nm as (a blank to exclude the effect of cell debris). The results were expressed as the percentage viability (n=8; ±SD). The percentage viability was calculated using the formula:

$$\%\ Viability = \frac{(A_{550}\text{-}A_{630})\ of\ treated\ wells}{(A_{550}\text{-}A_{630})\ of\ untreated\ wells} \times 100$$

Heparin, known to be non-toxic, was used as a comparator. MTT assay steps are summarised in **Figure 6.1**.

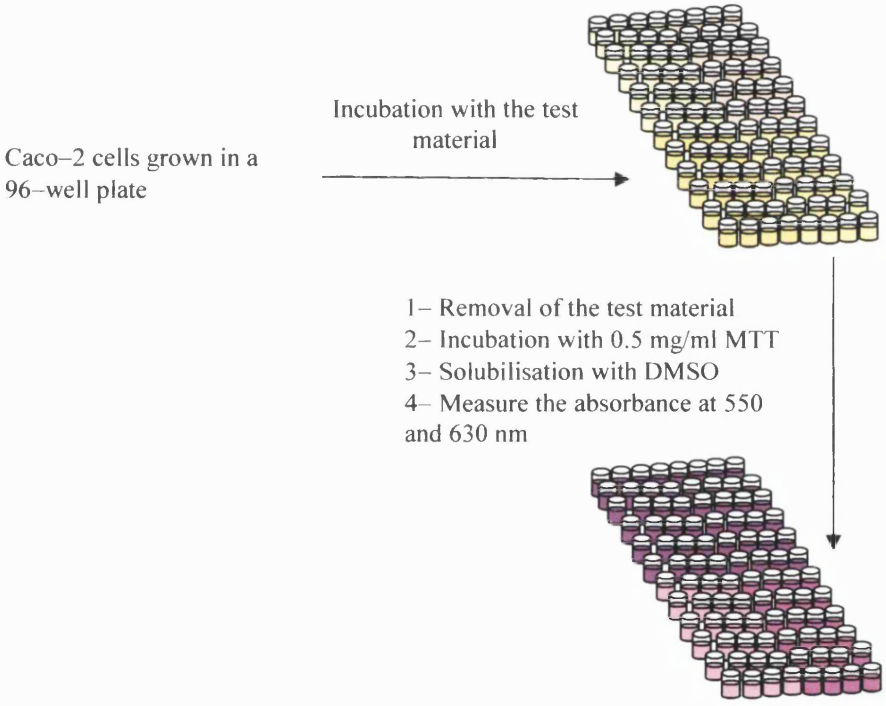

Figure 6.1: A summary of MTT assay procedures.

6.1.5. Permeability of [^{3}H] labelled dendrimer across Caco-2 monolayer

A cell suspension (1× 10^6 cells) was used to culture the cells on permeable polycarbonate inserts as mentioned elsewhere (Artursson and Magnusson, 1990; Artursson, 1990), of which 0.5 ml was added to the apical sides of Costar Transwell™ cell culture inserts (pore diameter 3 μm). Although a pore diameter 0.4 μm is preferred to avoid transmigration of Caco-2 cells from the apical to the basolateral side, 3 μm was used so that the pore size does not restrict the transport of dendrimer monomers or aggregates across the polycarbonate filters. The cells were grown for 21 days, changing the media every other day. The monolayers were used when the TEER was in the range of 600-1000 ohms×cm^2. The cell culture medium in both apical and basolateral chambers was replaced with the serum-free transport medium OptiMEM-1, 30 min before the experiment. This medium was chosen for the transport study to provide nutrients to the cells in the absence of serum, components of which may interact with dendrimer.

[^{3}H]-dendrimer solutions (0.5ml) prepared in OptiMEM-1 at non-toxic concentrations (0, 0.4, 2.0, 5.0 mg/ml, 1×10^5 dpm per insert) were added to the apical chamber. At time points 0, 30, 60, 120, 180 and 240 min, the inserts were transferred to clusters containing fresh OptiMEM-1 (1.5 ml) to maintain sink condition (i.e., before >10% of the drug had been transported). The basolateral samples were assayed in LS6500 Multi-Purpose Scintillation Counter (Beckman, USA) using Optiphase 'safe' scintillation cocktail (9 ml). The permeability of the studied dendrimer was expressed as the percentage [^{3}H]-dendrimer transported and the P*app* (cm/sec) was calculated (n=3; ±SD) at steady state (t=4h) as described by Artursson (1990) with slight modification.

The equation used was:

$$P_{app} = \frac{\Delta Q}{\Delta t \times A \times C_o}$$

Where $\Delta Q/\Delta t$ is the appearance rate of the dendrimer in the acceptor compartment (mg/sec), A is the surface area exposed to the donor chamber (i.e. 1.13 cm^2) and Co is the donor substance concentration (mg/ml). In case of a time lag (t_L):

$$\Delta t = t - t_L$$

So measurement of t_L provides a mean of calculating D presuming knowing *h* (Martin, 1993). t_L is given by:

$$t_L = \frac{h^2}{6D}$$

Where t_L (sec) is the time required for a penetrant to establish a uniform concentration gradient within the membrane separating the donor from the acceptor compartment, *h* is the thickness of the diffusion layer (cm), D is the diffusion coefficient or diffusivity (cm^2/sec). D depends on the resistance to passage of a diffusing molecule and may change in value at high concentrations and is affected by temperature, pressure, solvent properties and the chemical nature of the diffusant. One can also calculate *h* if P*app* was known using the equation:

$$t_L = \frac{h}{6P}$$

6.1.6. TEER and PEG 4000 permeability

The integrity of the monolayer and the paracellular transport was monitored by measurement of the potential difference between the apical and the basolateral sides of the monolayer and by following the transepithelial transport of the hydrophilic marker [^{14}C]-PEG 4000, respectively. Caco-2 cells were maintained and cultured on

Costar Transwell™ polycarbonate inserts as discussed in section 6.1.5. The apical solutions (0, 0.2, 2.0, 5.0, 10.0 mg/ml dendrimer) were prepared in OptiMEM-1, each containing 50μg/ml [^{14}C]-PEG 4000 (12.5 μM, 1×10^5 dpm per insert). OptiMEM-1 (containing 50μg/ml [^{14}C]-PEG 4000) and 1% Triton X-100 were used as negative and positive control respectively. PEG 4000 was added to the negative control to cancel its effect on Caco-2 monolayers.

At time points 0, 15, 30, 60, 120, 180 and 240 min, the transepithelial electrical resistance (TEER) was measured in the cell culture inserts with specially designed electrodes (World Precision Instrument, USA), and the inserts were transferred to clusters containing fresh OptiMEM-1 (1.5 ml) to maintain sink condition. The basolateral samples (1.5 ml) were assayed by liquid scintillation counting. After 240 min, the medium in the apical chamber was removed; the cells were rinsed with PBS and re-incubated in DMEM for 24 h at 37°C for recovery studies. Caco-2 monolayer assembly and a summary of the procedure is shown in **Figure 6.2**.

The TEER was expressed as transmembrane resistance (ohms×cm^2) after subtraction of the intrinsic resistance of the control (i.e. the resistance obtained with cell-free inserts). TEER was expressed as a percentage of TEER at t=0. PEG 4000 permeability was expressed as the percentage of PEG 4000 and P*app* (cm/sec) at the time points studied (n=3; ±SD).

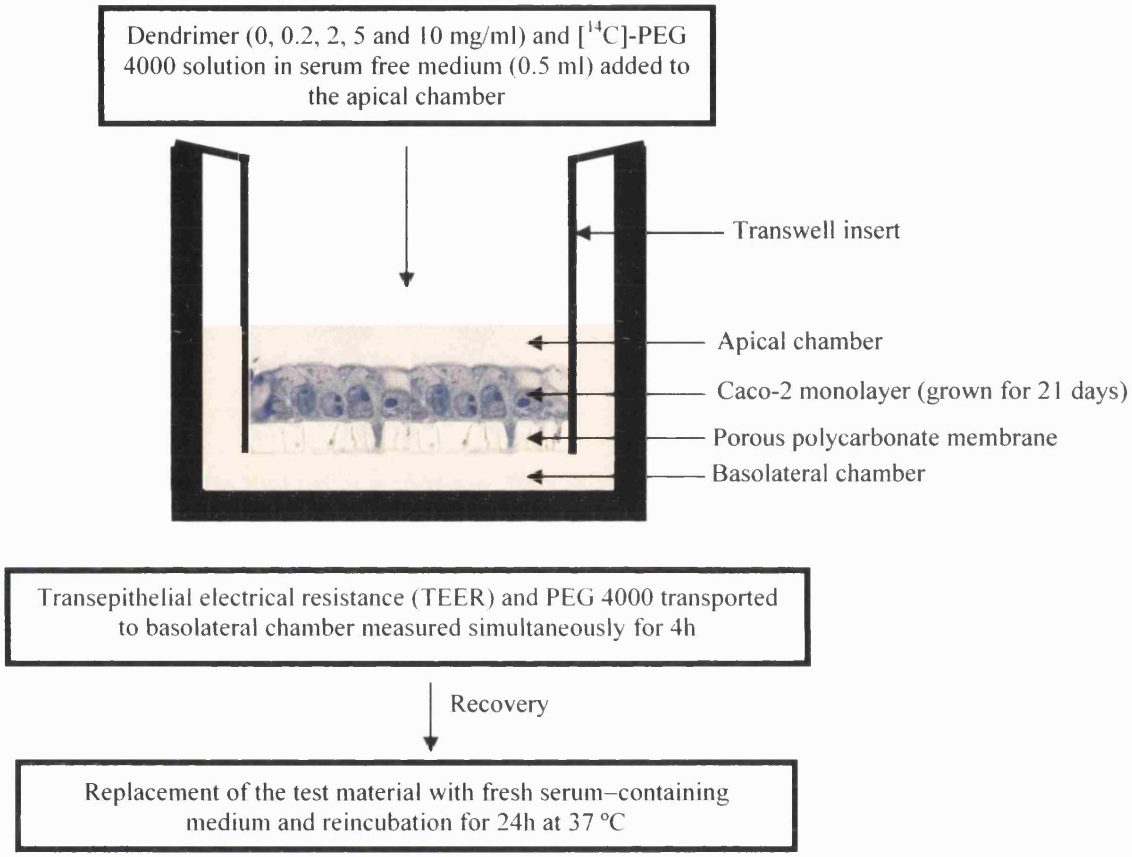

Figure 6.2: Caco-2 monolayer assembly; Caco-2 cells have been cultivated on permeable filters made of uncoated polycarbonate. The cells were allowed to grow and differentiate into a continuous monolayer for up to 21 days. The apical and basolateral chambers represent the donor and acceptor compartments respectively.

6.2. Results and discussion

6.2.1. MTT toxicity assay

In this experiment, we investigated the cytotoxicity of the highest generation water soluble polylysine dendrimer synthesised Gly-$Lys_{63}(NH_2)_{64}$ using human intestinal adenocarcinoma cell-line (Caco-2) a commonly used *in vitro* model in absorption studies, because of its similarity to the human intestinal epithelium (Artursson and Magnusson, 1990; Artursson, 1990).

The effect of the dendrimer concentration (0.5-10 mg/ml) on the cell viability in DMEM after 4h exposure has been determined using MTT assay (Mosmann, 1983). MTT is a tetrazolium salt that is reduced by mitochondrial dehydrogenase in living cells but not dead cells to give dark blue crystals, formazan.

Little effect was noted **(Figure 6.3)** until 5 mg/ml, a concentration above which a decrease in viability was clearly seen. However, below this concentration, the apparent viability of Caco-2 cells was slightly raised up to 110%. Similar stimulation of growth was obtained by Taylor and Folkman (1982), there was a 55% and 37% increase in the growth of V2 carcinoma and Lewis lung cells above the control when exposed to protamine, a cationic polypeptide, at concentrations of 100 and 500µg/ml respectively. Heparin, an innocuous polyanion used as a comparator, did not affect significantly cell viability as shown in **Figure 6.3**.

Several studies reported on the cytotoxicity of derivatised PAMAM dendrimers (Roberts *et al.*, 1996; Malik *et al.*, 2000; El-Sayed *et al.*, 2002; Jevprasesphant *et al.*, 2003; Fuchs *et al.*, 2004). In general, *in vitro* and *in vivo* dendrimer cytotoxicity was charge-, concentration- and generation dependent. The observed toxicity of the cationic G3 and G4 PAMAM dendrimers toward the B16F10 mouse melanoma cell line compared to the anionic G1.5, G2.5, and G3.5, which showed no toxicity, was

attributed to their polycationic nature (Malik *et al.*, 2000). Jevprasesphant (2003) reduced the toxicity of the cationic PAMAM dendrimers by neutralizing the positive charge through conjugation to the absorption enhancer lauroyl chloride.

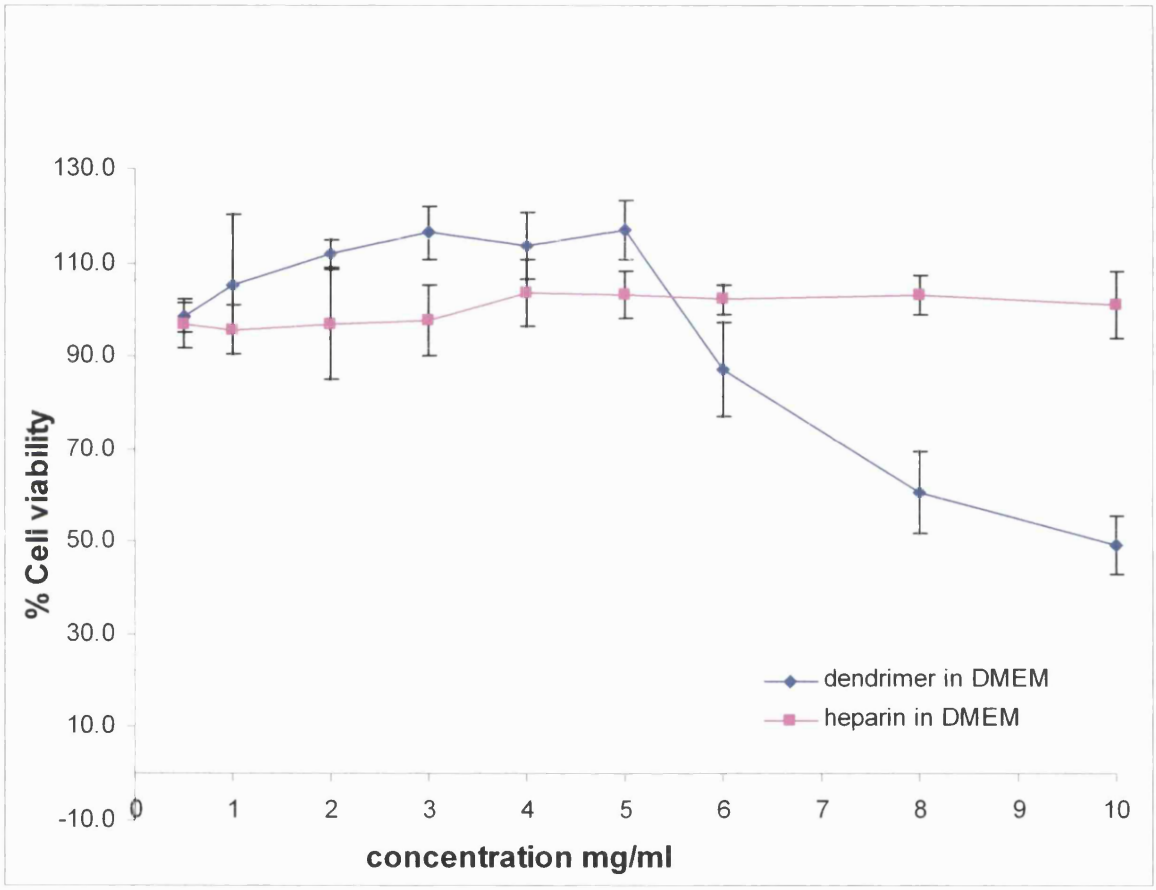

Figure 6.3: Percentage cell viability of confluent Caco-2 cells after exposure to various concentrations of dendrimer (blue line) and heparin (pink line) in DMEM for 4h. The dendrimer was innocuous to Caco-2 cells at concentrations less than 5 mg/ml. Heparin which is known to be non-toxic did not affect much the cell viability. (n=8; ±SD)

6.2.2. TEER, dendrimer and PEG 4000 permeability

Oral uptake is a requirement of an ideal oral drug delivery carrier. The oral bioavailability of some polymeric drug carriers can be impaired by their large size and molecular weight. Macromolecules and particulate materials could be transported across the intestine via either the paracellular route (intercellular junctions) (Nellans, 1991) or the transcellular route (via enterocytes or M-cells in the Peyer's patches) (Florence, 1997; Florence *et al.*, 2000). Small hydrophilic and charged molecules are transported via the paracellular route. The size limit for this pathway is around 3 nm (Pantzar *et al.*, 1994). Theoretically the studied dendrimer of 6.48 nm diameter (as obtained by molecular modelling in chapter III) might be absorbed via intercellular junctions if they (the dendrimers) have the ability to reversibly open the tight junctions (Jevprasesphant *et al.*, 2003).

To avoid overestimation of the dendrimer permeability across Caco-2 monolayers which could also occur due to the monolayer disruption, the effect of the cationic dendrimer on the monolayer integrity, by measuring the TEER, was studied at the concentration range used (0-10 mg/ml). Although 10 mg/ml was known to be unsafe to the monolayers, we wanted to establish a correlation between the toxic effect of the dendrimer and its permeation. OptiMEM-1 containing PEG 4000 and 1% Triton X-100 were used as the negative and positive controls respectively.

TEER values decreased in a time and concentration-dependent manner (up to 4h) as shown in **Figure 6.4**. At 10 mg/ml, within the first 30 min, the TEER value dropped to about 40% of the initial value. A similar reduction occurred only after 2h exposure to 5mg/ml.

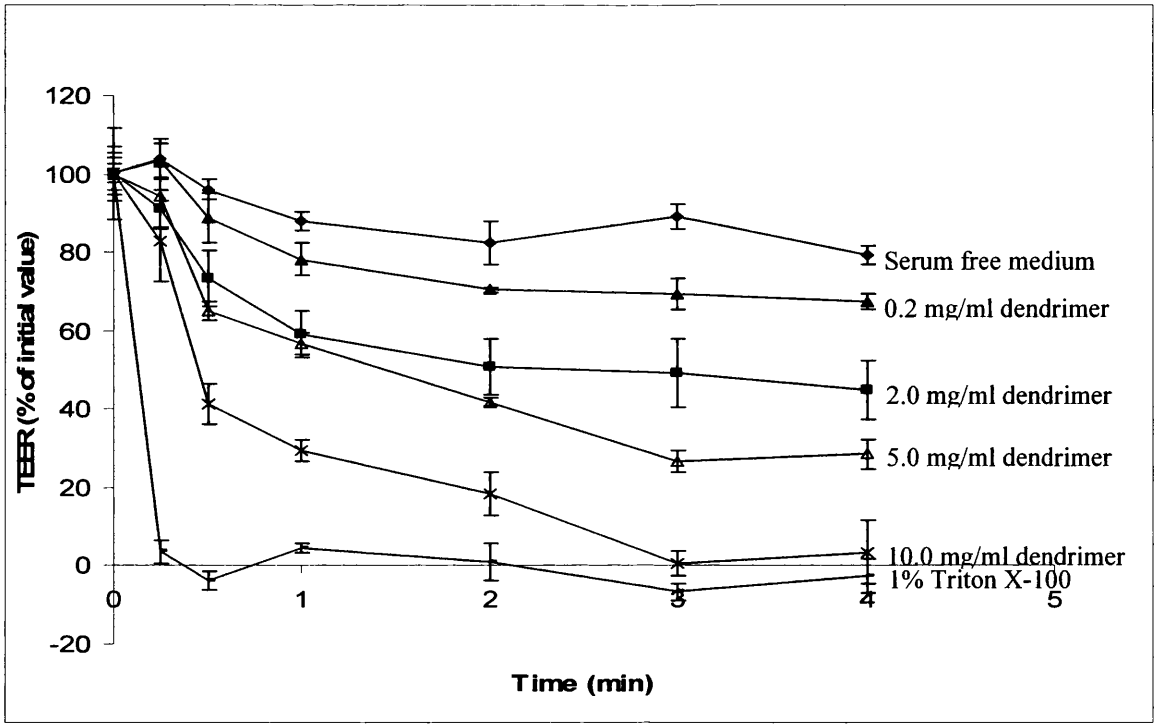

Figure 6.4: Effect of dendrimer concentrations on TEER measurement of Caco-2 monolayer. (◆) serum free medium OptiMEM-1 (negative control), (▲) 0.2 mg/ml, (■) 2.0 mg/ml, (△) 5.0 mg/ml, (×) 10 mg/ml (dendrimer in OptiMEM-1) and (-) 1% TritonX-100 (positive control) (n=3; ± S.D). PEG 4000 was added to all concentrations and the negative control so that the reduction in TEER could be attributed to the effect of dendrimer or Triton X-100 and not PEG 4000. TEER reduction was concentration and time dependent.

The reversibility of dendrimer effect on the TEER measurement was studied by re-incubation in dendrimer-free serum containing media for 24h. **Figure 6.5** showed that re-incubation of the monolayers in the dendrimer-free serum-containing media for 24 h slightly reversed the TEER value at 5 mg/ml but not at 10 mg/ml. On the other hand, at 2 mg/ml the TEER value increased from 44% to 76% (a value obtained by the negative control). This indicates the reversibility of the dendrimer effect at and below this concentration. Complexation of 2 mg/ml cationic dendrimer with heparin polyanion (discussed in chapter VII) resulted in a drop of the TEER to 80% of the initial TEER after 4h, compared to 44% in case of the free dendrimer. Protamine increased the permeability of cultured epithelial monolayers but had no

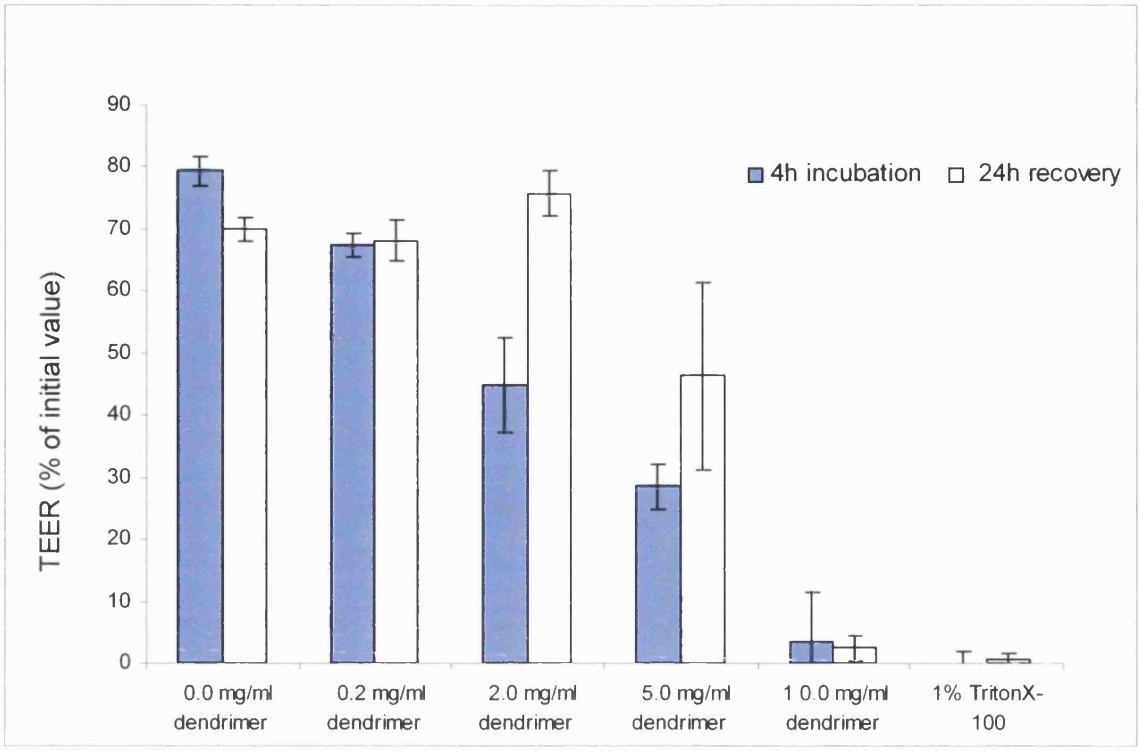

Figure 6.5: TEER recovery after removal of the dendrimer and re-incubation in serum-containing media for 24 h. TEER slightly increased at 5 mg/ml but not at 10 mg/ml. At 2 mg/ml, TEER increased again similar to that of the negative control (n=3; ±SD).

effect in the presence of heparin (Peterson and Gruenhaupt, 1990), suggesting the involvement of the positive charge in affecting the membrane integrity through interaction with the negatively charged membranes.

PEG is a neutral polymer transported via the paracellular route. Its permeability decreases as the molecular weight increases. Only very small amounts of PEG 4000 are transported across Caco-2 monolayers (Yee, 1997; Knipp *et al.*, 1997). The permeability of the cationic dendrimer was compared to that of the neutral PEG 4000. PEG 4000 permeability in the presence and absence of the dendrimer was tested across the cell-free polycarbonate filters, 78- 82% of the PEG 4000 diffused through the filters as shown in **Figure 6.6**. This test was carried out to exclude any interaction between PEG 4000, the dendrimer and the filter.

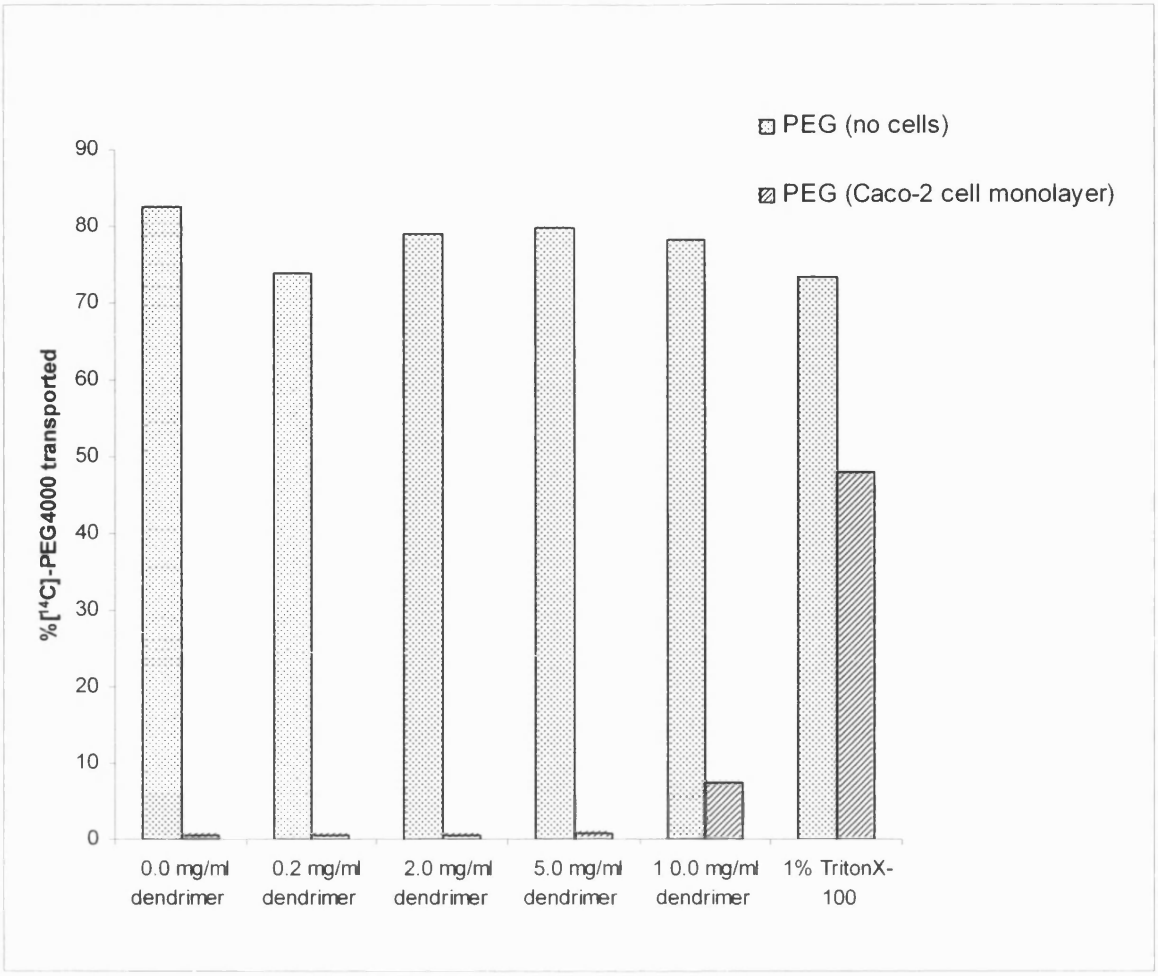

Figure 6.6: Percentage cumulative [^{14}C]-PEG 4000 transport over filters with and without Caco-2 cells with various concentrations of dendrimer after 4h. 78%- 82% of the PEG 4000 diffused through the filters excluding any interaction between PEG 4000, the dendrimer and the filter.

Figure 6.7 shows that after 4h incubation, cells treated with 10 mg/ml dendrimer showed a 14 fold increase (7.3%) in the percentage PEG 4000 transported compared to 90 fold (48%) in the positive control (1% Triton X-100). Lower dendrimer concentrations (0-5 mg/ml), which exhibited no apparent toxicity to the monolayer as found by MTT assay, showed a less significant effect on PEG 4000 permeability i.e. 1.2 and 1.5 fold increase at 2 mg/ml (45% of the initial TEER value) and 5 mg/ml (30% of the initial TEER value) respectively. In a study carried out by Tajarobi *et al.* (2001), mannitol permeability across MDCK monolayer increased by nine-fold in the presence of the fourth generation PAMAM dendrimer which can be attributed to the

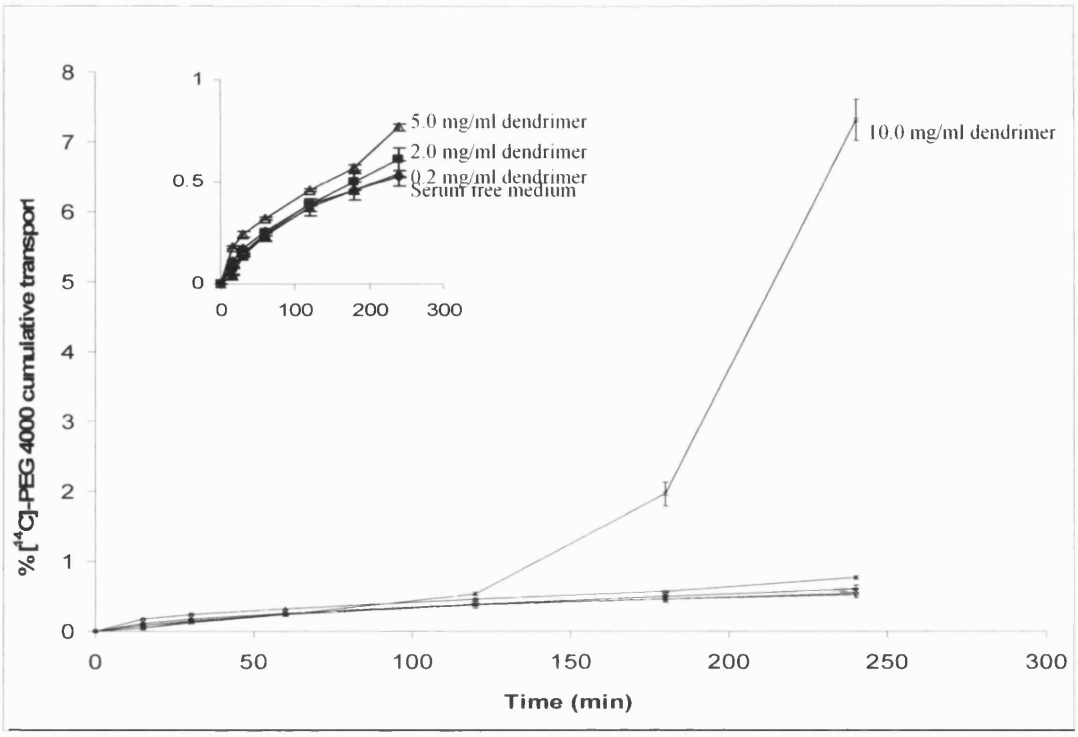

Figure 6.7: Percentage cumulative transport of [^{14}C]PEG 4000 across Caco-2 monolayers; (◆) control, (▲) 0.2 mg/ml dendrimer, (■) 2.0 mg/ml, (△) 5.0 mg/ml, (×) 10 mg/ml (n=3; ±SD). A 14 fold increase in the percentage PEG 4000 transported compared to only 1.2 and 1.5 at 2 mg/ml (45% of the initial TEER value) and 5 mg/ml (30% of the initial TEER value) respectively. A magnified depiction of PEG 4000 percentage cumulative transport is shown on the top left of the figure.

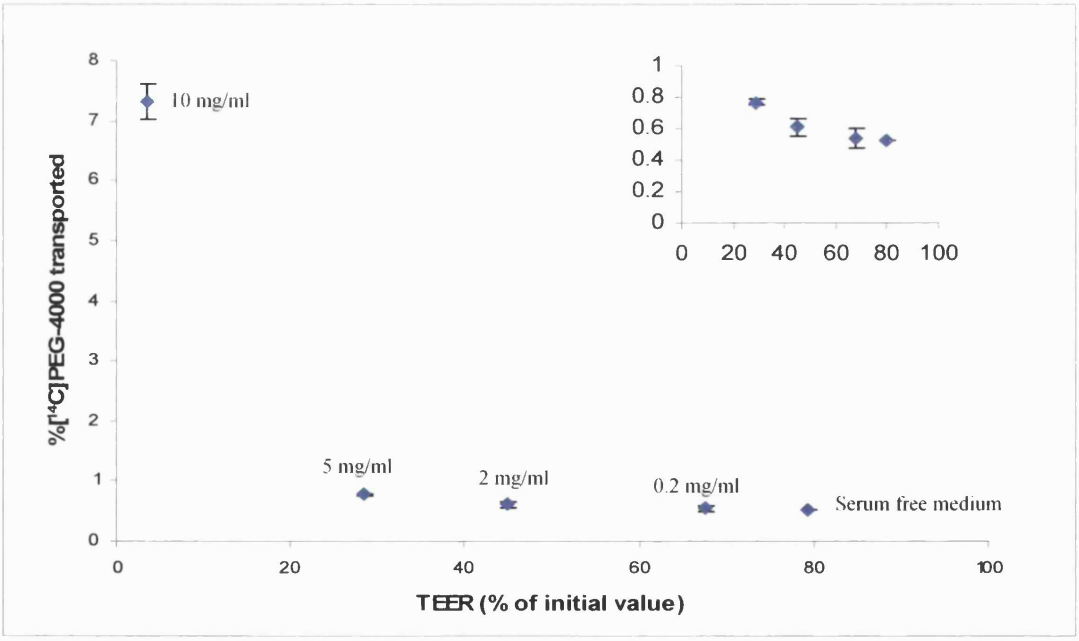

Figure 6.8: The correlation between the TEER and the percentage [^{14}C]-PEG 4000 transported across the monolayer. TEER values were obtained after incubation with a range of dendrimer concentrations for 4h. (n=3; ±SD). A magnified depiction of PEG 4000 percentage transport is shown on the top right of the figure.

small molecular weight of mannitol (182 Da) compared to that of PEG 4000 (4000 Da). A correlation was made between the TEER value and the permeability of [^{14}C]PEG 4000 across the monolayer **(Figure 6.8)**.

Herein we studied the permeability of the aforementioned dendrimer at non-toxic concentration. The inherent toxicity towards Caco-2 cells was investigated using MTT assay and thus the concentrations known to be non-toxic (0-5 mg) were chosen to study the dendrimer permeability. To facilitate study of dendrimer transport, dendrimers were radiolabelled using tritium. **Figure 6.9** shows the percentage cumulative transport of the dendrimer across Caco-2 monolayers and the cell-free polycarbonate membrane. This control experiment was carried out to confirm the permeability of the dendrimer across the filters. Caco-2 monolayer was found to be the limiting factor for dendrimer transport.

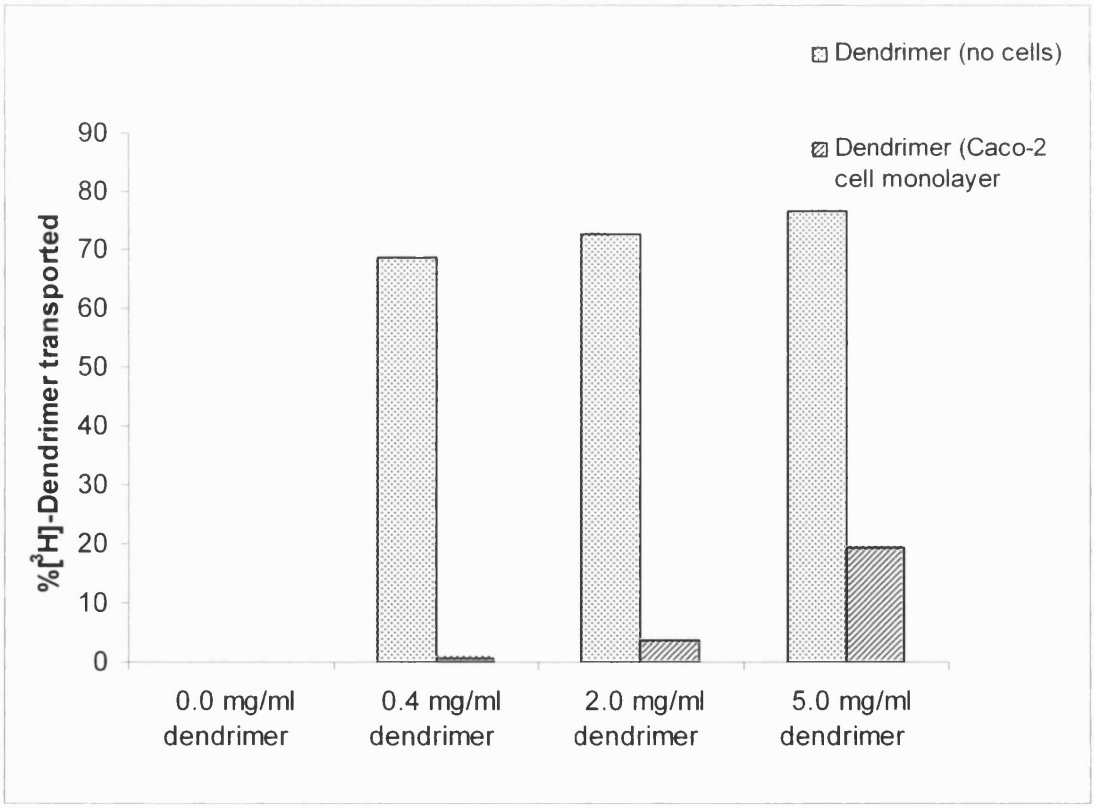

Figure 6.9: Percentage cumulative [^{3}H]-dendrimer transport over filters with and without Caco-2 cells after 4h.

Dendrimer permeability was expressed as the percentage cumulative dendrimer transport. **Figure 6.10** shows that the permeability of the dendrimer increased with the increase in the donor concentration and incubation time and a steady state diffusion of the dendrimer across the monolayers was established after a lag time of 175 and 130 min for 2 and 5 mg/ml respectively. The lag time observed was probably due to the mechanism of uptake i.e., the effect of the cationic dendrimer on widening the tight junctions and thus enhancing its own permeation via the paracellular route. P*app* was calculated at steady state i.e., after 4h and was 4.2 and 12.9×10^{-6} cm/sec for 2 and 5 mg/ml respectively.

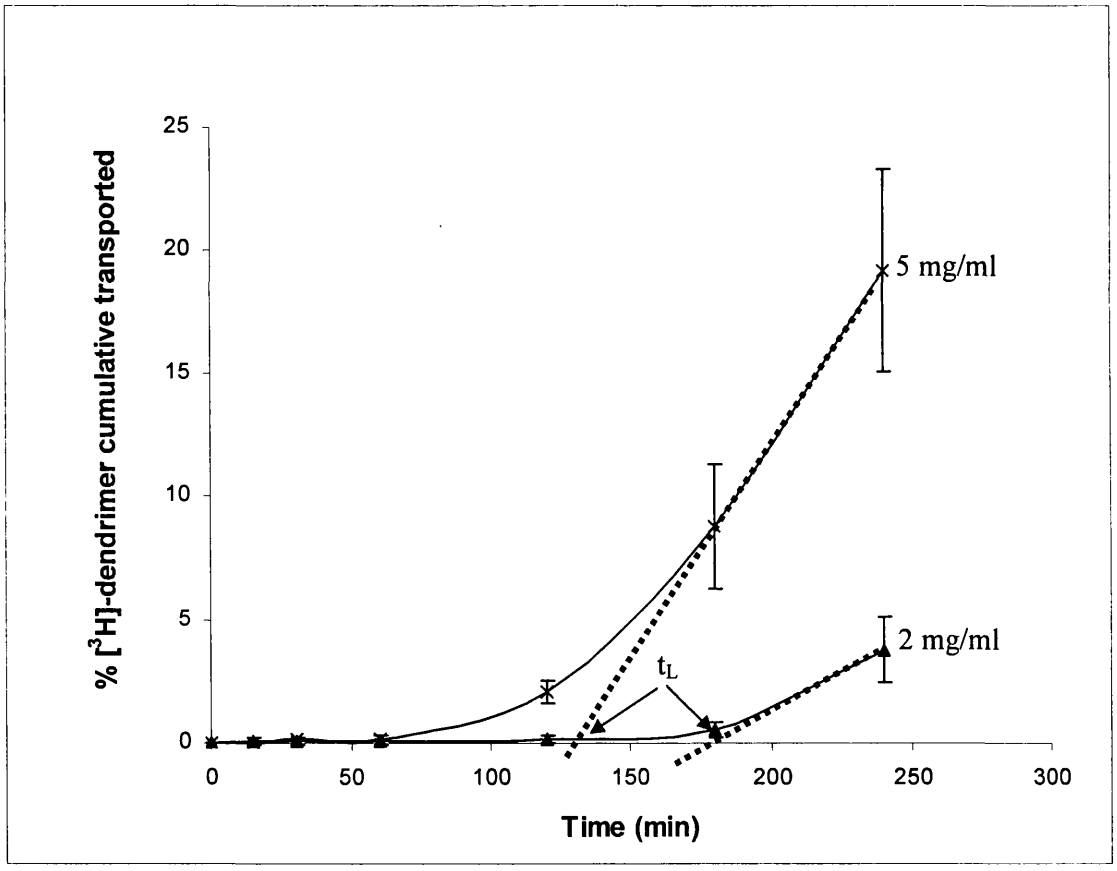

Figure 6.10: Percentage cumulative transport of [^{3}H]-dendrimer across Caco-2 monolayers; (▲) 2 mg/ml, (×) 5 mg/ml (n=3; ±SD). There was a lag time (t_L) required for the dendrimer to establish a uniform concentration gradient within Caco-2 monolayers separating the apical and basolateral chambers. t_L was 175 and 130 min for 2 and 5 mg/ml respectively. Measurement of t_L provides a means of calculating The diffusion coefficient D presuming knowing the thickness of the diffusion layer *h*, as explained in the text.

The increase in permeability with increasing concentration of dendrimer and incubation time was expected due to the increase in the number of positively charged surface amines and the prolonged interaction of the dendrimer with Caco-2 epithelia respectively, resulting in a more pronounced modulation of the tight junctions which was supported by the reduction in TEER measurements.

The permeability of some dendrimer-based systems across cell barriers has already been established (Sakthivel *et al.*, 1999; Wiwattanapatapee *et al.*, 2000; Malik *et al.*, 2000; Tajarobi *et al.*, 2001; El-Sayed *et al.*, 2002; Jevprasesphant *et al.*, 2003; Nigavekar *et al.*, 2004). Tajarobi *et al.* (2001) reported P*app* value of 16.1×10^{-6} cm/sec for PAMAM dendrimers with 64 amino groups across Madin-Darby canine kidney (MDCK) cells and showed that it was concentration dependent.

These data also coincide with that of El-Sayed *et al.*(2002) who found that P*app* of the cationic PAMAM dendrimers increased with increasing donor concentration and incubation time. Jevprasesphant *et al.* (2003) reported the P*app* of cationic, anionic and lauroyl modified PAMAM dendrimers to be in the range of 0.02- 8.0×10^{-6} cm/sec which was generation and concentration dependent.

Finding the value of P*app*, we were able to calculate the thickness of the diffusion layer *h* which ranged between 2695- 6021 μm. Karlsson and Artursson (1991) reported an *h* value of 1544 μm for testosterone permeating Caco-2 monolayers in the absence of agitation, the contribution of resistance of the aqueous boundary layer to the total diffusional resistance was 70%. *h* was then employed to calculate the diffusion coefficient of the dendrimer across Caco-2 monolayer in OptiMEM-1 medium. D values were 1.15 and 7.75×10^{-6} cm^2/sec for 2 and 5 mg/ml respectively. Salicylates diffusion across cellulose membrane had a membrane diffusion coefficient value of 1.69×10^{-6} cm^2/sec (Farng and Nelson, 1977).

Dendrimers, like other macromolecules, can pass the gastrointestinal barrier by two routes: the transcellular route (by endocytosis) and the paracellular route (through the intercellular spaces). The paracellular route occupies a very small surface area and is sealed by the junctional complex with a mean pore diameter of only few angstroms. However, various studies indicate that these junctions are dynamic structures and their permeability can be modulated in response to various stimuli. The reversible opening of the tight junctions is an interesting approach in drug delivery to improve the absorption of hydrophilic drugs. Some cationic dendrimers and polycationic polymers such as chitosan exhibited a reversible opening of the tight junctions as our dendrimer also proved (Artursson *et al.*, 1994; Jevprasesphant *et al.*, 2003). The effect of the dendrimer studied on TEER reduction of the monolayers was also established **(Figure 6.5)** and was reversible up to 2 mg/ml dendrimer concentration. Theoretically, the globular dendrimer of a small diameter might use paracellular pathway especially with their shown capacity to open transiently the tight junctions. Although the exact mechanism of dendrimer uptake is not fully established, it has been shown that anionic and cationic PAMAM dendrimers were endocytosed by the enterocytes of everted rat intestinal sacs *in vitro* (Wiwattanapatapee *et al.*, 2000). Anionic dendrimer showed a higher serosal transfer rate and less tissue adsorption than cationic dendrimer. El-Sayed *et al.* (2002) suggested the paracellular route for cationic PAMAM transport across Caco-2 cells monolayers. A study carried out by Jevprasesphant *et al.* (2003) suggested that PAMAM transport across Caco-2 monolayers occur via both the paracellular and transcellular routes as the permeability was temperature sensitive and significantly reduced by the endocytosis inhibitor colchicine.

Table 6.1: The effect of dendrimer concentration on the P*app* (10^6 cm/sec) of [^{3}H]-dendrimer and [^{14}C]PEG 4000 across the monolayer after 4h incubation (n=3; ±SD).

Dendrimer concentration (mg/ml)	Dendrimer P*app* (10^6 cm/sec)	PEG 4000 P*app* (10^6 cm/sec)
0.4	0.605 ± 0.09	0.39 ± 0.03
2	4.2 ± 0.14	0.42 ± 0.03
5	12.9± 2.6	0.54 ± 0.04

Table 6.1 showed a comparison of P*app* values of the dendrimer and PEG 4000 after 4h incubation. Despite the fact that the dendrimer had almost twice the molecular weight of the linear polymer PEG, it has a rigid globular structure in solution with relatively fixed diameter. In general, the P*app* of the cationic dendrimer was higher than that of PEG 4000. PEG 4000 has been used as a paracellular marker so we expect its permeability to increase if the dendrimer has influenced the TEER and modulated the tight junctions, however, our cationic globular dendrimer had a higher permeability than neutral linear PEG 4000, whose permeability did not increase much by increasing the dendrimer concentration and incubation time. This suggests two things: firstly the positively charged dendrimer has higher affinity to the negatively charged cell membrane compared to the non-ionic PEG 4000 and thus competes with the latter for paracellular transport; secondly, the dendrimer has been transcytosed by enterocytes in addition to its paracellular transport while PEG 4000 was only transported paracellularly. It has been reported that positively charged molecules permeate Caco-2 monolayers at a higher rate than neutral or anionic molecules due to a favourable electrostatic interaction with the negatively charged epithelial cells (Knipp *et al.*, 1997). The finding that dendrimer uptake increased with the increase in its concentration suggests the involvement of endocytosis. The

permeability of molecules which are absorbed by passive diffusion only should not be concentration dependent.

However these studies do not necessarily correlate with human epithelia, as studies have shown that the tight junctions of Caco-2 monolayers and the human small intestine are different, Caco-2 monolayer tight junctions being more restrictive (Collett *et al.*, 1996).

6.3. Conclusion

Polylysine dendrimer with 64 amino groups showed moderate permeability across the human intestinal Caco-2 monolayers comparable to that of PAMAM dendrimers. Their reversible effect on the tight junction, in addition to being innocuous at useful concentrations strongly suggests their use as oral drug delivery carriers.

Chapter VII

DENDRIPLEXES: HEPARIN-DENDRIMER COMPLEXES

Heparin is a polydisperse negatively charged polysaccharide (6,000-30,000 Da). Its relatively high content of sulphate groups (anionic groups) is mainly responsible for its anticoagulant activity, pro-angiogenic character and poor oral absorption.

Heparin dendriplexes were prepared by the complexation of heparin with the water soluble cationic dendrimer Gly-$Lys_{63}(NH_2)_{64}$ (8149 Da) via electrostatic interactions. A change in the dendrimer characteristics as well as in heparin anticoagulant and uptake properties were anticipated upon complexation.

In this chapter, the preparation and characterization of heparin dendriplexes is described. The *in vitro* anticoagulant activity of the dendriplexes was compared to that of heparin using an anti-factor Xa assay. Also a comparison was made between the *in vitro* transport of the dendriplexes and the free heparin across Caco-2 monolayers.

7.1. Experimental

7.1.1. Materials

Unfractionated heparin sodium salt grade I-A from Porcine Intestinal Mucosa 187 USP units/mg (MW 6,000-30,000 Da) (Sigma, USA), Methylene blue (Fisher Scientific, USA), Accucolor™ heparin and Accuclot™ reference plasma (Sigma Diagnostics, USA), [^{3}H]-Heparin (sodium salt) (specific radioactivity 0.32 mCi/mg) (Perkin Elmer, USA). Materials used in cell culture experiments were mentioned in chapter VI.

7.1.2. Synthesis of Gly-Lys$_{63}$(NH$_2$)$_{64}$ dendrimer

The synthesis of the water soluble polylysine dendrimer **(compound 2c) (Figure 2.12)** having 64 surface amino groups was performed using method D and purified as described in Appendix I.

7.1.3. Preparation of heparin dendriplexes

The dendriplexes were formed spontaneously by mixing equal volumes (1 ml) of heparin (1 mg/ml) and the dendrimer (0.5, 1, 2, 3, 4 and 5 mg/ml) aqueous solutions, followed by a gentle shaking of the colloidal dispersions on a platform shaker at 30 rev/min for 1h to get a thorough mixing of the two components.

7.1.4. TEM, size and zeta potential measurement

Heparin dendriplexes were observed by TEM. The sample preparation for TEM was as described in chapter IV.

The mixtures were diluted 5 times in deionised water and sized using a PCS 4700 Malvern submicron particle analyzer (Malvern Instruments, Malvern, UK, He-Ne laser, 90° angle of measurement). The measurement was repeated for seven consecutive days and after two weeks to check for aggregation. Zeta potential of the

aggregates was measured using a Zetasizer 3000 (Malvern Instruments, Malvern, UK). The dispersion (2ml) was diluted 5, 10 and 20 times for 0.5-1, 2.0-3.0, and 4.0-5.0 mg/ml dendrimer dispersions, respectively, for zeta measurement. The average of three measurements was used and the results expressed as Z-average (nm) ± S.D and zeta potential (mV) ± S.D.

7.1.5. MB spectroscopy

A solution containing heparin-MB complex was titrated with the dendrimer. Heparin-MB complex (2ml) was prepared by mixing MB solution (1ml, 20 μM), heparin solution (0.5ml, 2.7 μM) and the calculated volume of dendrimer solution (122.7 μM). MB, heparin and dendrimer final concentrations were 10, 0.725 and 0.16-10 μM respectively. Absorption spectra for MB/heparin, before and after titration with the dendrimer, were obtained between 400-800 nm at a scan rate of 1200 nm/min using a plastic cuvette in a Beckman DU® 650 Spectrophotometer (USA). A_{664}/A_{568} ratio was used to calculate the ratio at maximum association. The experiments were repeated for at least four times to check the reproducibility of the results.

7.1.6. Antifactor Xa assay

The *in vitro* anticoagulant activity of heparin and the complexes was assayed using Accucolor™ heparin using micro-plate method. Lyophilized human antithrombine III (AT III), bovine factor Xa and factor Xa substrate were reconstituted in deionised water as directed by the manufacturer. Lyophilized Accuclot™ reference plasma was reconstituted in deionised water immediately before use.

A solution of heparin in saline was prepared as a stock (8 USP unit/ml or 44 μg/ml) and a calibration curve of heparin (0.1-0.8 U/ml) was prepared by serial dilution of the stock in standard human plasma. Calibration curves for heparin complexes were

prepared similarly except that the dendrimer was added to the stock in dendrimer: heparin mass ratios of 0.1, 0.5, 1, 2, 3, 4 and 5:1. An additional 1:2 dilution of all standards was made by diluting 100 µl of the plasma standard with 100 µl saline before running the assay.

AT III (75µl) was dispensed to individual wells of a 96-well microstate plate and incubated with the diluted standard (25µl), Factor Xa (75µl) and Factor Xa substrate (75µl) were subsequently added and incubated at 37 °C for 2, 1 and 10 min after each addition, respectively. The reaction was stopped with 20% acetic acid (75µl). A_{405} was blanked using these reagents in the following order; acetic acid, AT III, plasma, Factor Xa and the substrate and measured using a Dynex MRX Microplate Reader 133 (Dynex, UK). A_{405} was plotted against heparin concentration (units/ml), the anticoagulant activity was inversely proportional to A_{405}. The measurements were done in triplicates and expressed as $A_{405}\pm$ S.D.

7.1.7. Association of heparin dendriplexes to Caco-2 monolayers

Caco-2 cells seeded into a 24-well plate at a density of 100,000 cells per well. The medium (0.6 ml) was changed every second day. After three days, the media was aspirated and the confluent cells were treated for 4 and 24h at 37 °C with 0.7 ml [^{3}H]-heparin [0.2 and 1.0 mg/ml] (1×10^5 dpm per well) in DMEM or OptiMEM-1 with or without dendrimer [0.5, 1, 2:1 mass ratio]. The [^{3}H]-heparin containing solution was incubated with the dendrimer at 37 °C for 30 min before its addition to the cell cultures to allow for [^{3}H]-heparin dendriplexes to be formed. Heparin concentrations were chosen from the toxicity study (chapter VI) so as dendrimer concentration used for complexation is innocuous to the cells. Two incubation periods and media (with or without serum) were used for comparison. After incubation, the cells were rinsed thrice with PBS to remove any precipitated complex

and lysed for liquid scintillation counting, by incubation for 2 min in a hypotonic solution (450 µl) and a lysis medium (50 µl). (Hypotonic solution: 0.03% magnesium chloride in 0.24% HEPES buffer, lysis solution: 5% ethylhexadecyldimethylammonium bromide in 3% glacial acetic acid). The results were expressed as cell-associated [^{3}H]-heparin dendriplexes percentage of the dose (n=3; ±SD).

7.1.8. Transport of heparin dendriplexes across Caco-2 monolayer

Caco-2 cells were harvested and plated on Costar Transwell™ cell culture inserts (12 wells, 1.13 cm^2 and 3 µm pore diameter) as described in chapter VI. The monolayers were treated on the apical side at 37 °C with 0.5 ml [^{3}H]-heparin [1.0 mg/ml] (1×10^5 dpm per insert) in OptiMEM-1 with or without dendrimer [0.5, 1, 2, 3 and 5:1 mass ratio]. The [^{3}H]-heparin containing solution was incubated at 37 °C for 30 min before its addition to the cell cultures to allow for [^{3}H]-heparin dendriplexes to be formed. At time points 0, 30, 60, 120, 180, 240 and 1440 min, the TEER was measured and the inserts were transferred to clusters containing fresh OptiMEM-1 (1.5 ml) to maintain sink condition. The basolateral samples were assayed for radioactivity using liquid scintillation counting. The permeability and the integrity were expressed as the percentage [^{3}H]-heparin dendriplexes transported and the percentage TEER at t = 0 respectively (n=3; ±SD).

7.2. Results and discussion

7.2.1. Shape, size and zeta potential measurement of the dendriplexes

Heparin is a polydisperse polyanionic copolymer composed of alternating D-glucouronic acid which is frequently O-sulphated at C2, and D-glucosamine-N-sulphate with an additional sulphate group on C6 linked via α-1,4 glycosidic linkage **(Figure 7.1)**.

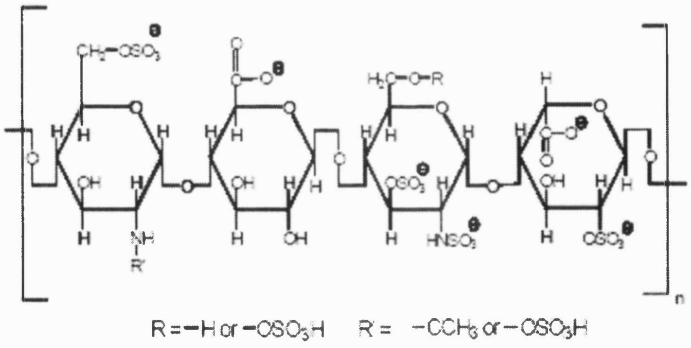

Figure 7.1: The chemical structure of sulphated heparin, a copolymer composed of D-glucouronic acid and D-glucosamine-*N*-sulphate linked via α-1,4 glycosidic linkages.

Molecular weights range from 6,000-30,000 Da. Heparin used in this experiment had a mean number molecular weight in the range of 17,000-19,000 Da as specified by the manufacturer. Gelman and Blackwell (1973) reported 2.33 sulphate groups per disaccharide and showed a maximum interaction between the linear poly(Lys) and the heparin at 2.3:1 amino acid: disaccharide ratio. The complex adapted an α-helical conformation.

Heparin-dendrimer complexes, named heparin dendriplexes, were spontaneously formed upon mixing heparin and the cationic dendrimer in aqueous solutions, presumably via electrostatic interactions. The spherical aggregates shown by TEM in **Figure 7.2** were not observed in simple heparin and dendrimer solutions individually. The mean intensity hydrodynamic diameter of the dendriplexes found by the PCS ranged from 99 ± 4 nm to 147 ± 3 nm **(Table 7.1)**. The minimum and maximum change in the original diameter, after fourteen days and from the first day of the preparation, was 0.5% and 16% at 5:1 and 0.5:1 mass ratio respectively **(Figure 7.3)**.

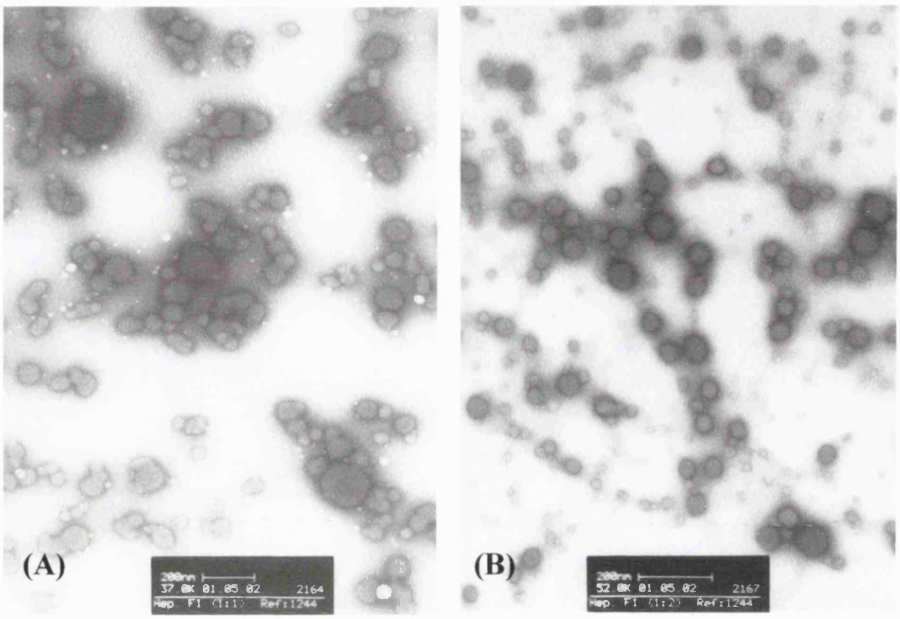

Figure 7.2: Transmission Electron Micrographs of the dendriplexes showing spherical aggregates in the nano-size range. **(A)** 1:1 dendrimer:heparin mass ratio; 2.2:1 molar ratio; 2:1 +/- charge ratio; -47 mV zeta potential **(B)** 2:1 dendrimer:heparin mass ratio; 4.4:1 molar ratio; 4.1:1 +/- charge ratio; +52 mV zeta potential.

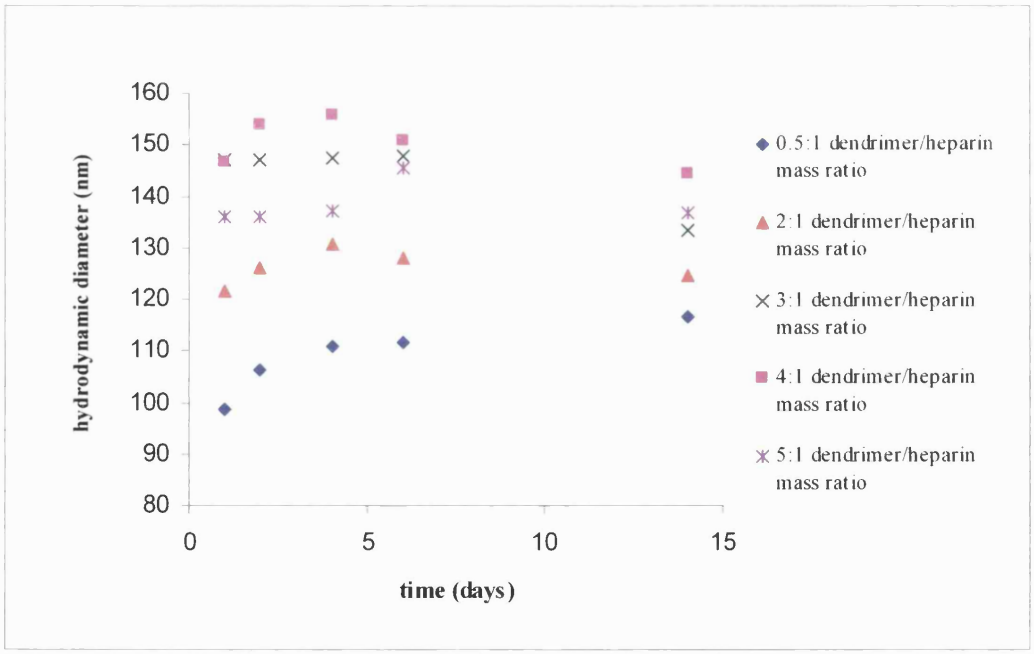

Figure 7.3: Heparin dendriplexes size (nm) versus time. The percentage change of the original diameter was the minimum (0.5%) at 5:1 dendrimer/heparin mass ratio (+60± 2 mV) and the maximum (16%) at 0.5:1 dendrimer/heparin mass ratio (-38 ± 1.6 mV).

We calculated the dendrimer/heparin charge ratio based on the assumption of 18,000 Da average heparin molecular weight and 2.3 sulfate groups per disaccharide. The maximum association between the dendrimer and the heparin occurred at 1:1 mass ratio (2.2 molar ratio or 2.05 +/- ratio). However, the dendriplexes exhibited a negative zeta potential (- 47 mV) at this ratio. The zeta potential became positive (+ 52 mV) at 2:1 mass ratio (4.1:1 +/- charge ratio) **(Table 7.1)**. The reason that the maximum association in dendrimer/heparin systems occurred at 2.05 +/- compared to 1:1 +/- in linear polylysine/dendrimer systems (Gelman and Blackwell, 1973) could be due to unavailability of all the amino groups of the dendrimers for the interaction with the sulfate groups. This could be due to steric hindrance of the terminal amines with the hyperbranched dendrimer structure or due to pH dependent ionization of the dendrimer amino groups. This can also be attributed to the fact that the heparin used was a polydisperse mixture of heparin chains while the assumption in calculating the +/- ratio was based on a single molecular weight.

Table 7.1 Z-average size and zeta-potential of dendriplexes of various dendrimer:heparin ratios

Dendrimer:heparin mass ratio	Dendrimer:heparin molar ratio[a]	+/- charge ratio[b]	Z-average size (nm) ± S.D[c]	Zeta-potential (mV) ± S.D[c]
0.5:1	1.1	1.02	99 ± 4	-38 ± 1.6
1:1	2.2	2.05	122 ± 1	-47 ± 2
2:1	4.4	4.1	121 ± 2	+52 ± 3
3:1	6.6	6.15	147 ± 3	+55 ± 4
4:1	8.8	8.2	147 ± 1.5	+56 ± 2
5:1	11:1	10.25	136± 2	+60± 2

[a] Based on the assumption that heparin has an 18,000 Da average molecular weight.
[b] Based on the assumption that there is 69 negative charges per heparin chain and 64 positive charges per dendrimer. +/- charge ratio was calculated using the equations:

$$+/- \ Ratio = 2.05 \times \frac{Dendrimer\ [weight]}{Heparin\ [weight]} \text{ or } +/- \ Ratio = 0.92 \times \frac{Dendrimer [moles]}{Heparin\ [moles]}$$

[c] Mean ± S.D; n=3

7.2.2. MB/heparin assay

Methylene blue (MB) is a cationic metachromatic dye known for its affinity for polyanions such as heparin (Leone-Bay *et al.*, 1998). Unbound MB has λ_{max} of 664 nm whereas MB bound to heparin (MB/heparin) has λ_{max} of 568 nm. Dendrimer addition to MB/heparin caused a shift in λ_{max} from 568 to 664 nm **(Figure 7.4)**. Furthermore, MB and MB/dendrimers had the same UV/Vis spectra (λ_{max}=664) which excludes any interaction between MB and the dendrimer. MB spectroscopy (A_{664}/A_{568} ratio) was used to find the ratio at which maximum dendrimer/heparin association occurred.

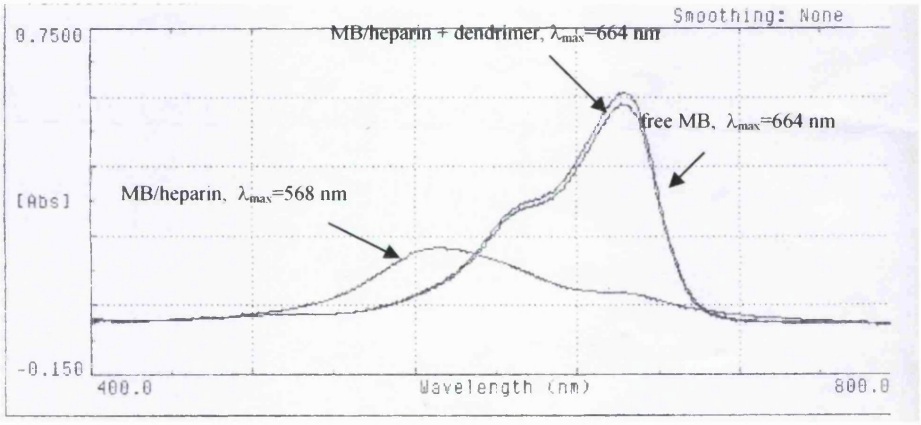

Figure 7.4: UV/Vis spectra of free MB (λ_{max}=664 nm) and MB/heparin (λ_{max}=568 nm). Upon dendrimer addition, MB λ_{max} shifted to 664 nm which indicated MB release from heparin due to dendrimer/heparin complexation.

Firstly, the optimum heparin concentration required to produce a minimum $A_{664/568}$ ratio was experimentally found i.e. all MB molecules (10 μM) are bound to heparin with no excess heparin (0.725 μM) in the solution. Excess free heparin in the medium would give an inaccurate dendrimer/heparin association ratio. The MB/heparin mixture was titrated with dendrimer (0.16-10 μM) as shown in **Figure 7.5**. A maximum A_{664}/A_{568} ratio was obtained at 2.05 +/- charge ratio (1:1 or 2.2:1 dendrimer/heparin mass or molar ratio respectively).

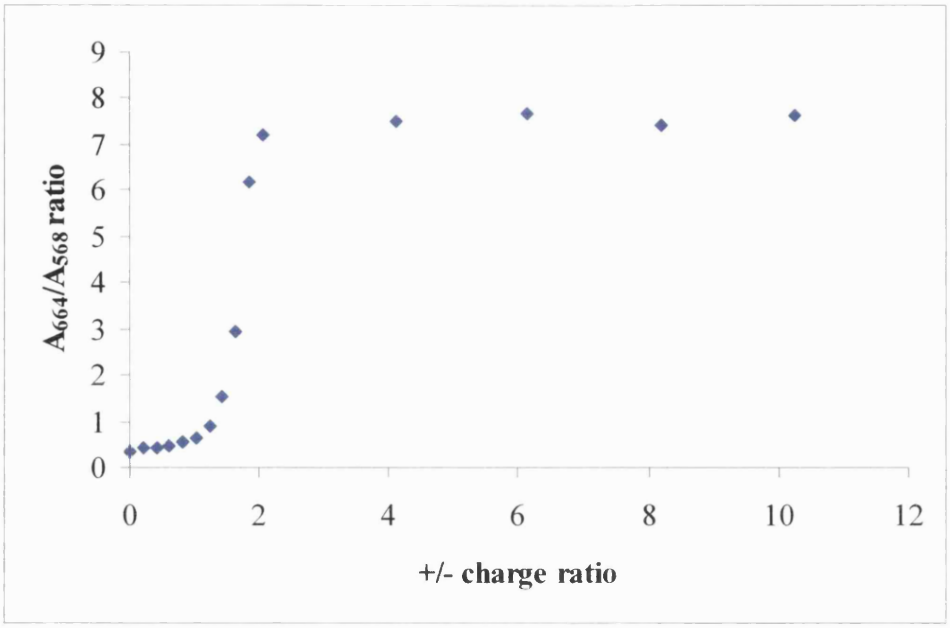

Figure 7.5: Titration of a MB/heparin mixture (10 μM/0.725 μM) with the dendrimer (0.16-10 μM). A maximum A_{664}/A_{568} ratio was obtained at 2.05 +/- charge ratio (1:1 or 2.2:1 dendrimer/heparin mass or molar ratio respectively). This was considered the ratio at which a maximum dendrimer/heparin association occurred.

7.2.3. *In vitro* anticoagulant activity of heparin dendriplexes

Heparin exists in the mammalian circulatory system as an anticoagulant. The U.S.P unit is the measure of the anticoagulant activity of a given heparin product, heparin used in this work has 180 U.S.P units/ mg.

Antithrombine III (AT-III) is a natural inhibitor of thrombin, factor Xa and other coagulation proteases in the plasma. The rate of inhibition is slow but can be increased by several thousands by heparin. Thus the anti-factor Xa assay is a useful test to assay the anticoagulant activity of heparin. Since both factor Xa and antithrombine III are present in excess in the kit, the rate of factor Xa inhibition is directly proportional to active heparin concentration. The residual activity of factor Xa, as measured by absorbance of its chromogenic substrate at 405 nm, is inversely proportional to heparin anticoagulant activity in plasma.

We employed this assay to study the effect of complexation on the *in vitro* anticoagulant activity of heparin. We found that dendrimer binds to heparin and neutralizes its activity **(Figure 7.6)**; Heparin spiked (0.8 IU/ml) in human plasma was inactive at a 1:1 heparin: dendrimer mass ratio. This further confirmed the result obtained by MB spectroscopy which showed that the maximum association between the heparin and dendrimer occurred at the same ratio. The new conformation of the heparin must abolish the negative charge and make it inaccessible to AT III and the coagulation proteases i.e. prothrombine III and factor Xa, a process which cancels its anticoagulant activity.

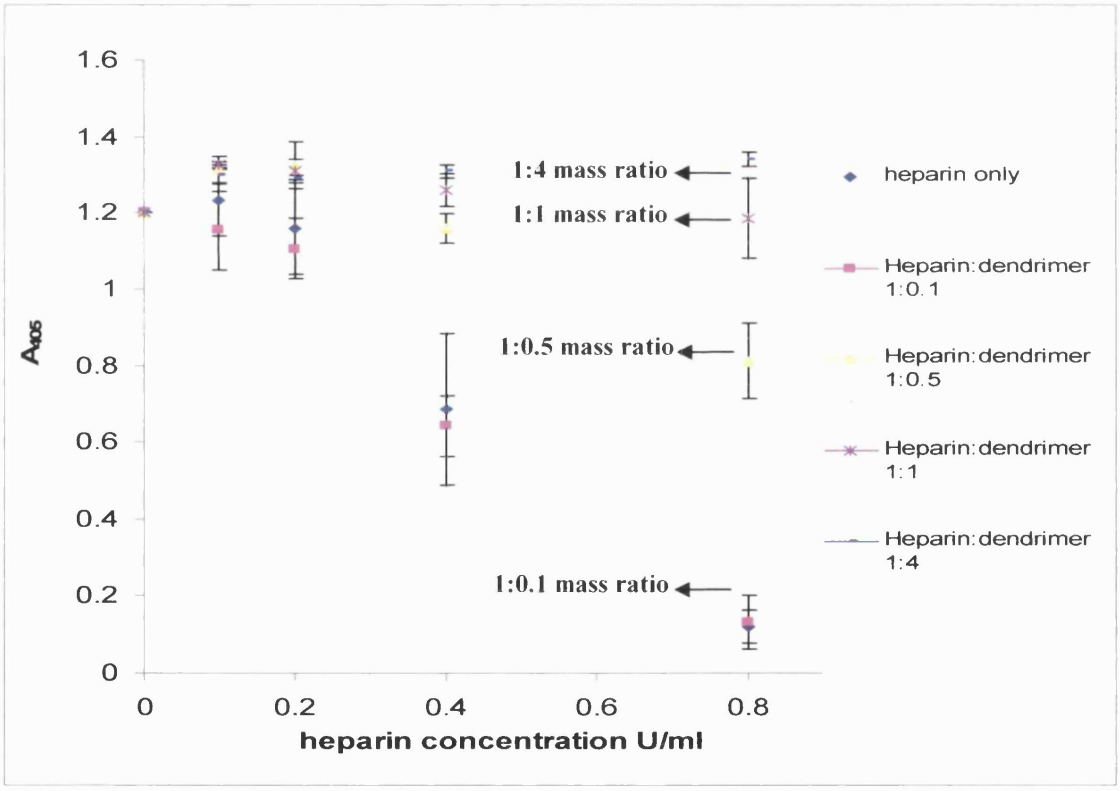

Figure 7.6: Heparin anticoagulant activity as measured by anti-factor Xa assay. A_{405} is inversely proportional to active heparin concentration. Heparin activity was reduced as the dendrimer concentration increased. Heparin activity (0.8 U/ml) began to decrease (A_{405} increased) as the heparin: dendrimer mass ratio increased from 1:0.1 to 1:4.

Suggested applications include the development of a less toxic heparin antidote than the cationic polypeptide protamine which has undesirable side effects (Schick *et al.*, 2001; Liang *et al.*, 2003). Another area is in angiogenesis therapeutics. Interestingly, apart from the heparin anticoagulant effect, heparin can play an important role in angiogenesis. Tumour growth is to a large extent dependent on angiogenesis, the biological process leading to locoregional recruitment of epithelial cells and the growth of new capillary blood vessels. In healthy tissues angiogenesis is kept in a balance between endogenous pro-angiogenic and anti-angiogenic factors (Kerbel, 2000). However in growing tumours excessive angiogenesis is initiated to create a new vascular system which will provide adequate blood supply for growth (Folkman, 1995). The process of angiogenesis is stimulated by various cytokines, such as vascular endothelial growth factor (VEGF) and basic fibroblast growth factor (bFGF). The interaction of cytokines with their endothelial receptors depends on the presence of the extracelluar macromolecule heparin or heparan sulphate proteoglycan (HSPG)(Azizkhan *et al.*, 1980).

The development of anti-angiogenic tumour therapeutics has become an area of intense research interest (Srinivasan and Harris, 2002). It has been recognized that heparin potentiates the activity of growth factors although the mechanism is not yet clearly described (Folkman and Klagsbrun, 1987). Moreover, Azizkhan and coworkers reported that heparin released by mast cells accumulates at the tumour site, enhancing the migration of capillary endothelial cells prior to the in-growth of new blood capillaries (Azizkhan *et al.*, 1980). Heparin has been validated previously as a potential target for anti-angiogenesis therapy by allowing protamine, an arginine-rich basic protein of 4,300 Da molecular weight, to bind to heparin leading to inhibition of angiogenic growth factor activity (Taylor and Folkman, 1982).

Subcutaneous protamine administration inhibits tumour angiogenesis with no toxicity when administered for one year at 60 mg/kg every 12h. However, its systemic administration is limited due to its severe toxicity including symptoms of lethargy, weakness or even death. Compounds similar to protamine in structure and charge density such as poly-L-lysine, poly-L-arginine and poly-L-glutamic acid did not show anti-angiogenic effects *in vitro* except for polylysine at excessive concentrations (five times that used for protamine) (Taylor and Folkman, 1982).

A cationic poly-arginine dendrimer with 16 surface arginine residues has been designed by Kasai et al. (2002) to resemble the structure of the endogenous angiogenesis inhibitor endostatin. They reported effective antiangiogenic *in vivo* activity using the CAM assay (non-tumour angiogenesis model), suggesting that the mechanism of action is due to efficient dendrimer competition with angiogenic factors for binding sites on heparin.

The high affinity of these cationic dendrimers towards heparin and the stability of these dendriplexes in the plasma *in vitro* and *in vivo* (shown in chapter VIII) suggest their potential use as anti-angiogenic therapeutics. The therapeutic activity of the heparin-binding dendrimers as active moieties and as carriers of other types of therapeutics (cytotoxic drugs, plasmid DNA) towards the development of combined anti-angiogenic treatments, as shown recently is worth investigating (Arrieta *et al.*, 1998; Toth *et al.*, 1999; Abdollahi *et al.*, 2003; Vincent *et al.*, 2003). Polylysine polymers (Sakharov *et al.*, 2001) and cationic liposomes have recently shown higher accumulation into the vascular endothelium, a target in angiogenesis treatment (El-Sayed *et al.*, 2001; Sakharov *et al.*, 2001; Hood *et al.*, 2002; Krasnici *et al.*, 2003). Also, functionalization of our heparin-binding cationic dendrimers by attachment of vascular targeting moieties (e.g. endothelial cell integrins) onto their surface might

also allow further improvements in specifically targeting tumour neovascualture (Hood *et al.*, 2002). The intrinsic fluorescence phenomenon (discussed in chapter III) was employed as an investigative tool in studying the localization of dendrimer in Caco-2 cells (Ruenraroengsak and Florence, unpublished). Intra-vital microscopy (Jain *et al.*, 1997) is thought to be a non-invasive technique that can be used in studying the accumulation of intrinsically-fluorescent dendrimers in the vascular endothelium in living animal models and in a dynamic pattern.

7.2.4. Association of heparin dendriplexes to Caco-2 monolayer

Heparin association to Caco-2 cells in the presence [0.5, 1, 2:1 mass ratio] and absence of dendrimer was studied in serum-free (OptiMEM-1) and serum-containing (DMEM) media for 4 and 24h using different heparin concentrations (0.2 and 1.0 mg/ml). The results are expressed as the cell-associated [^{3}H]-heparin dendriplexes percentage of the dose and shown in **Figures 7.7**. Cell association referred to both membrane bound or internalized heparin. Whether association was followed by internalization into the cells or not can not be answered by this experiment. Complexation of heparin with the cationic dendrimer at 1:1 (-47 ± 2 mV) and 2:1 (+52 ± 3) mass ratios dramatically enhanced cell association. There was no clear effect on the cell association by changing heparin concentration, the incubation time or the presence or absence of serum. Bleiberg *et al.* (1981) reported that enhanced binding and internalization of heparin by macrophages in the presence of polycations (protamine, histone, poly(DL-lysine) and poly(L-ornithine)) was due to charge neutralization. Since the cells are generally negatively charged, the enhanced uptake of the negatively charged compounds observed previously in the presence of polycations has been attributed to charge neutralization (Deierkauf *et al.*, 1977; Fabian *et al.*, 1978; Shen and Ryser, 1978; Duncan *et al.*, 1979).

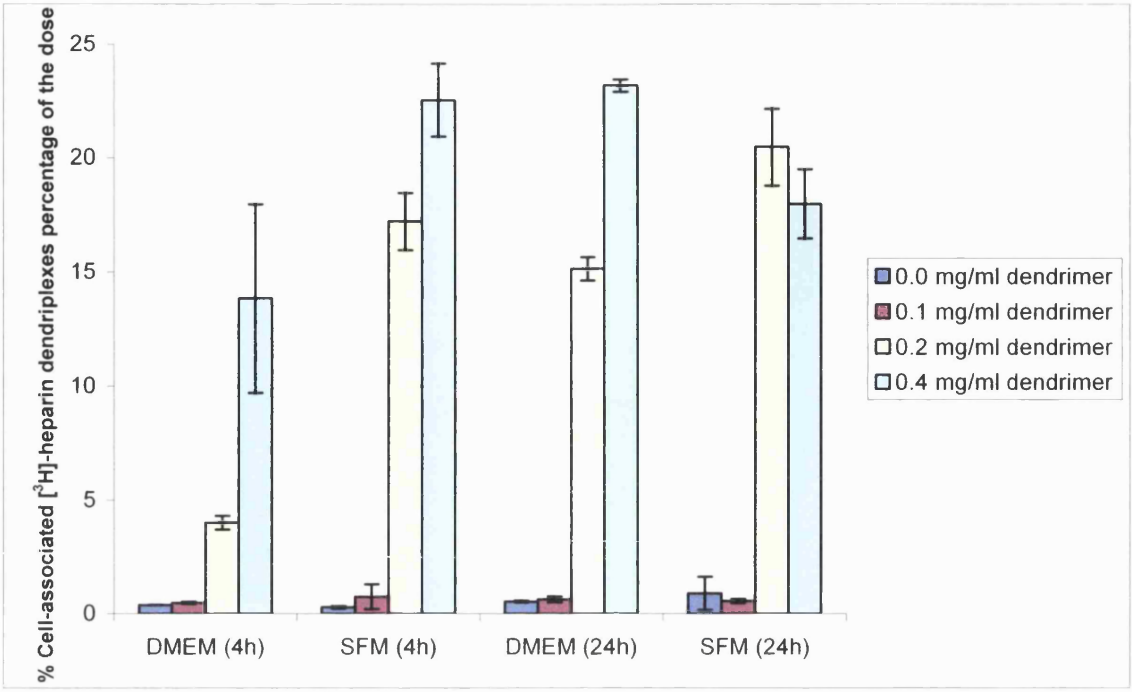

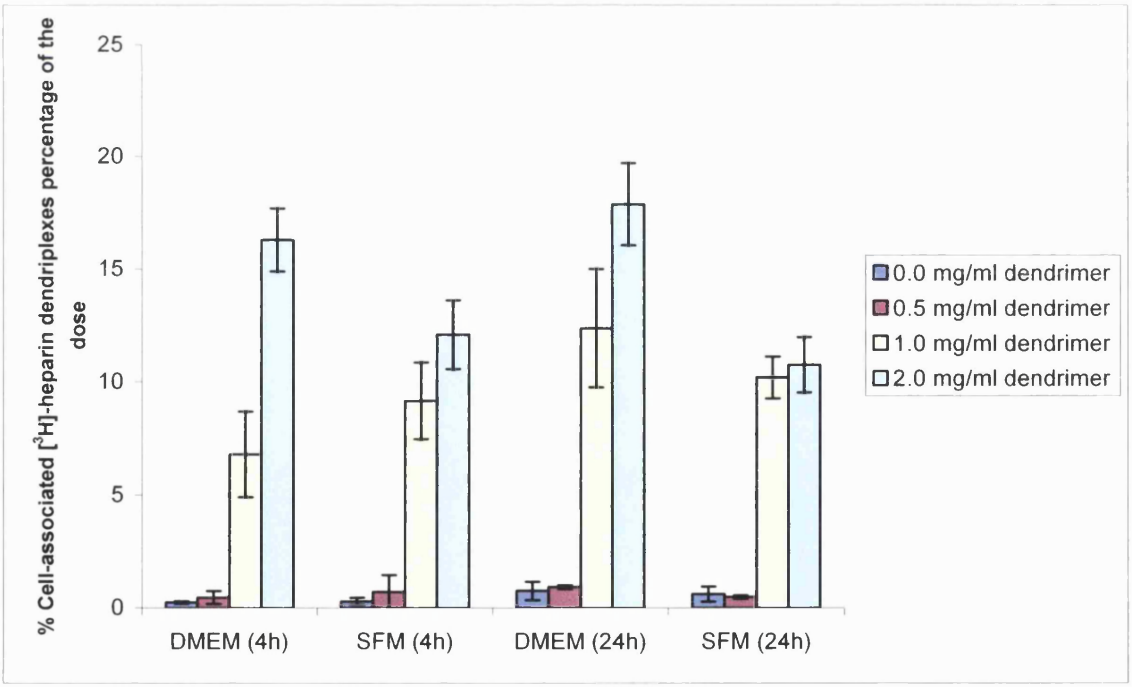

Figure 7.7: Percentage of [^{3}H]-heparin associated with a Caco-2 monolayer. [^{3}H]-heparin [0.2 or 1.0 mg/ml, top and bottom graphs respectively], free and complexed with the dendrimer [0.5, 1, 2:1 mass ratio], was incubated with the confluent monolayers in DMEM or OptiMEM-1 for 4 and 24h. The cells were lysed and the associated heparin was quantified by liquid scintillation counting (n=3; ± S.D). Complexation of heparin with the dendrimer at 1 and 2:1 mass ratios enhanced dramatically cell association.

7.2.5. Transport of heparin dendriplexes across Caco-2 monolayers

Transport experiments using Caco-2 monolayers were carried out to examine whether the dendriplex binding to cells was followed by uptake, whether the percentage uptake was dependent on the concentration of the complexed heparin or the free dendrimer and the possible route(s) involved i.e. paracellular or transcellular. Caco-2 monolayers were seeded on polycarbonate filters (3μm pore diameter) to resemble the intestinal barriers. The percentage of [^{3}H]-heparin dendriplexes transported to the basolateral chamber was quantified.

It was found that incubation of the monolayers with low heparin concentration (0.2 mg/ml) in the presence of the dendrimer (0.5-3:1 mass ratio) in OptimMEM-1 for 4h had little effect on the percentage of heparin transported and was similar to that of the negative control (free heparin) **(Figure 7.8)**. Similarly, no effect was observed on the TEER of the monolayers probably because of the low dendrimer concentration (0.1-0.6 mg/ml) utilised **(Figure 7.9)**. However, association studies showed that the complexation at 1 and 2:1 mass ratio caused, respectively, a 60 and 78-fold increase in the percentage heparin associated with the cell.

The effect of complexation was more noticeable at higher heparin concentration (1mg/ml) **(Figure 7.10 and 7.11)**. Heparin uptake was enhanced the most at 5:1 mass ratio (this was the highest mass ratio used to avoid the toxic effect) by only a factor of 1.3 and 5 after 4 and 24h respectively **(Figure 7.12)** but the latter was accompanied by a loss in TEER. The fact that the enhanced uptake occurred at 1 mg/ml and not at 0.2 mg/ml heparin, and its correlation with TEER reduction suggests two things: firstly, the enhanced transport was mainly a consequence of the interaction between the free dendrimer, rather than complex, with the cells. Secondly, the transport of the complex occurred mainly via the paracellular route.

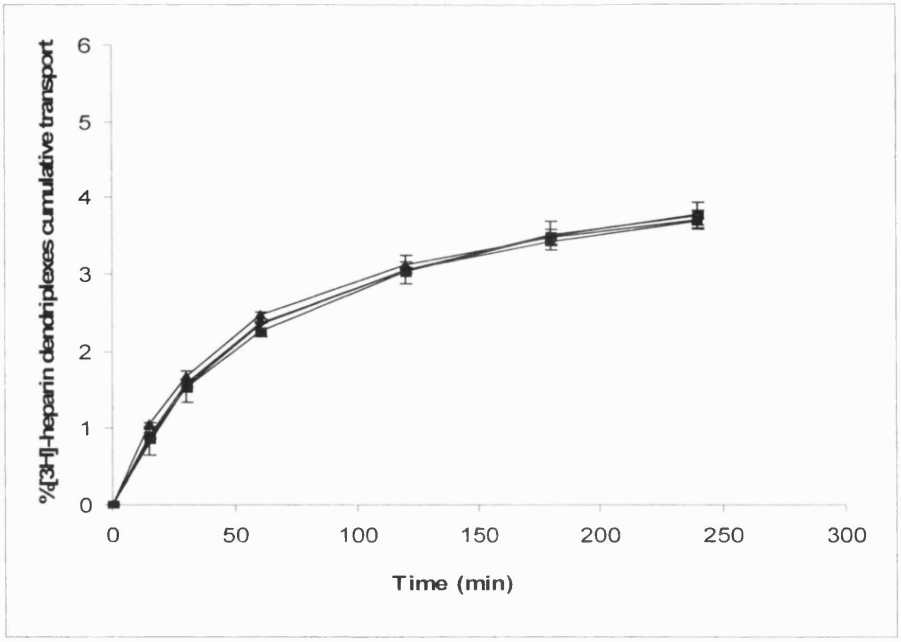

Figure 7.8: Percentage cumulative transport of [^{3}H]-heparin dendriplexes across Caco-2 monolayers as a function of time. Heparin (0.2 mg/ml) was complexed with (◆) 0.0 mg/ml dendrimer, (▲) 0.1 mg/ml, (×) 0.2 mg/ml, (•) 0.6 mg/ml (n=3; ± S.D). Complexation had little effect on heparin transport.

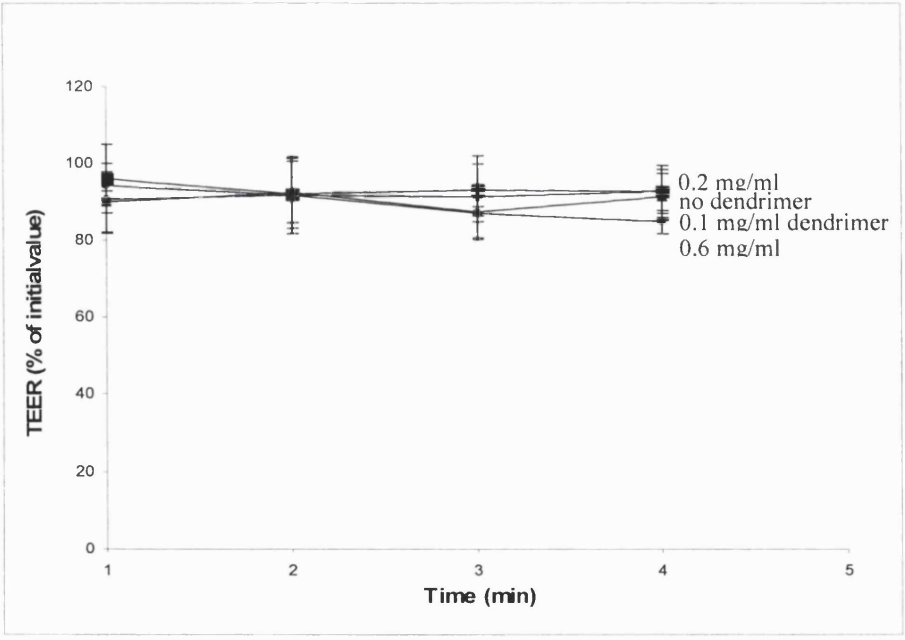

Figure 7.9: Effect of heparin:dendrimer complexation ratio on TEER of Caco-2 monolayers as a function of time. Heparin (0.2 mg/ml) was complexed with (◆) 0.0 mg/ml dendrimer, (▲) 0.1 mg/ml, (×) 0.2 mg/ml, (•) 0.6 mg/ml (n=3; ± S.D). The complexes showed little effect on TEER.

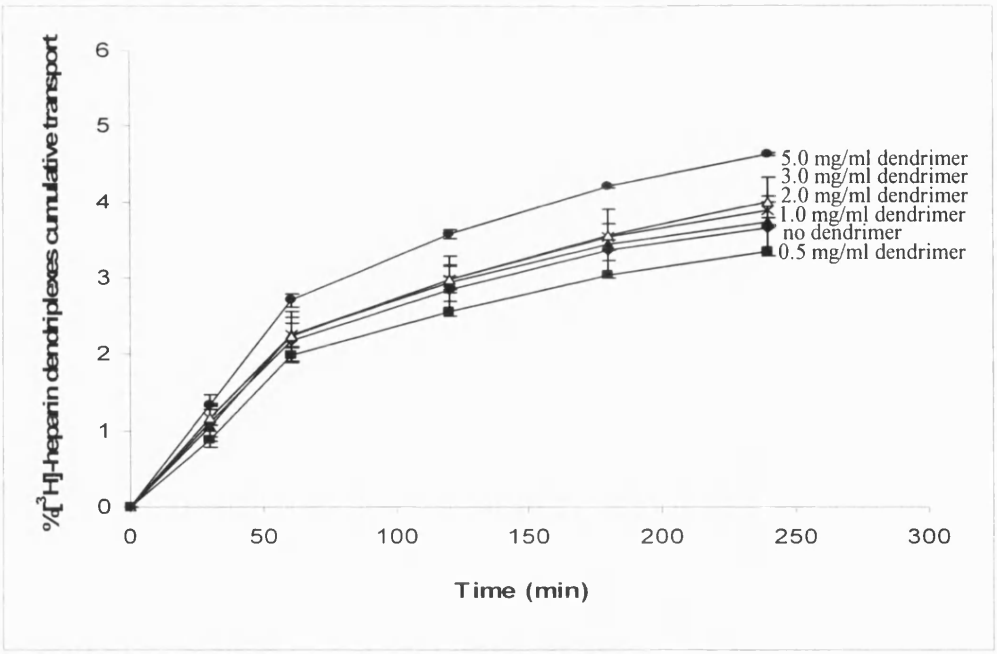

Figure 7.10: Percentage cumulative transport of [^{3}H]-heparin dendriplexes across Caco-2 monolayers as a function of time. Heparin (1 mg/ml) was complexed with (◆) 0.0 mg/ml dendrimer, (■) 0.5 mg/ml dendrimer, (▲) 1 mg/ml, (×) 2 mg/ml, (△) 3.0 mg/ml, (•) 5.0 mg/ml (n=3; ± S.D). Complexation enhanced heparin uptake the most at 5:1 mass ratio and by only a factor of 1.3.

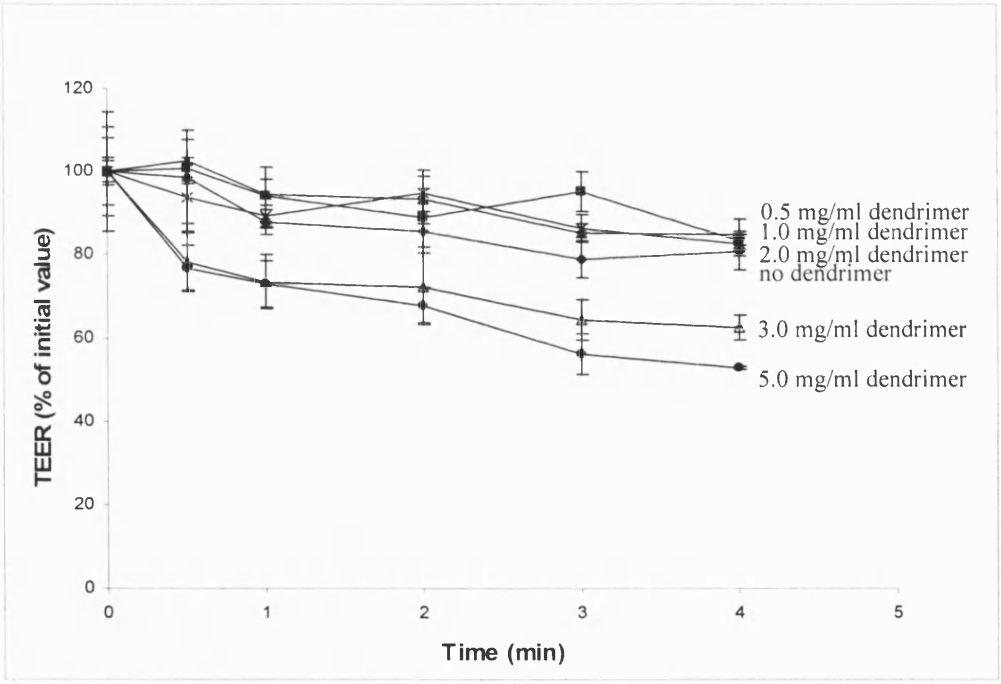

Figure 7.11: Effect of heparin:dendrimer complexation ratio on TEER of Caco-2 monolayers as a function of time. Heparin (1 mg/ml) was complexed with (◆) 0.0 mg/ml dendrimer, (■) 0.5 mg/ml dendrimer, (▲) 1 mg/ml, (×) 2 mg/ml, (△) 3.0 mg/ml, (•) 5.0 mg/ml (n=3; ± S.D). Complexed dendrimer had less effect on TEER compared to free dendrimers as shown in **Figure 6.4**.

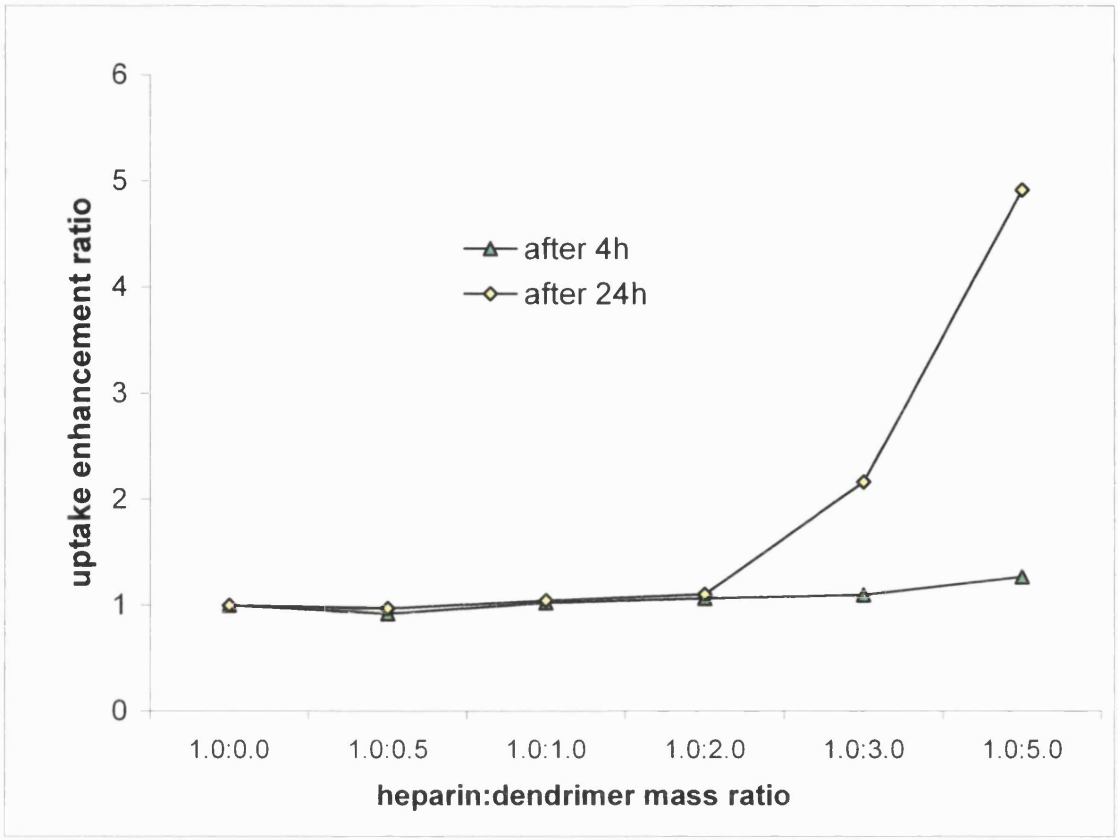

Figure 7.12: Uptake enhancement ratio (percentage transport of the heparin dendriplexes to free heparin) as a function of heparin:dendrimer mass ratios (1 mg/ml heparin was used) after 4h and 24h incubation. Higher uptake enhancement ratios were obtained at higher dendrimer concentrations after 24h compared to 4h incubation probably due to the prolonged exposure of the monolayers to the dendrimer, and its effect on the monolayer integrity.

Complexation did not only affect the biological activity of heparin, but also dendrimer interaction with Caco-2 monolayers was also reduced. The cationic dendrimer studied here has already revealed its effect on TEER of Caco-2 monolayers in chapter VI **(Figure 6.4)**. This effect was much reduced when the dendrimer was complexed with heparin **(Figure 7.10)**, which may be attributed to the partial charge neutralization of the dendrimer. Shen and Ryser (1981) have reported that heparin at low concentration reduced the endocytosis of polycation polylysine-methotrexate conjugates by Chinese hamster ovarian cells due to polycation-heparin complexation.

7.3. Conclusion

Maximum association occurred between heparin and the cationic dendrimer at 1:1 heparin:dendrimer mass ratio. Electrostatic interaction is most likely to be the mechanism involved. The biological properties of both the dendrimer and heparin have changed upon complexation i.e. heparin lost its anticoagulant activity and dendrimer effect on the TEER of Caco-2 monolayers was also reduced. Cell-association of heparin was increased, results which can be attributed to the decrease in its negativity. The strong binding affinity of the dendrimer to heparin suggests investigating their use as heparin antidotes. In addition, the use of heparin-binding dendrimers *per se* and in combination with antiangiogenic modalities i.e. anti-angiogenic drugs and DNA delivery, is a novel approach. Dendrimer-heparin dendriplexes can be also tested for their use as nanoparticulate drug carriers since complexation inactivates both components.

Chapter VIII

BIODISTRIBUTION OF HEPARIN DENDRIPLEXES AND DENDRIMER IN RATS

As we saw in chapter VII complexation of heparin with the dendrimer Gly-$Lys_{63}(NH_2)_{64}$ led to the neutralisation of the anticoagulant activity of heparin *in vitro*. In addition the permeability of heparin dendriplexes across Caco-2 monolayer was only slightly higher than the negative control of free heparin. Furthermore, the permeation enhancing effect of the dendrimer was reduced in the presence of heparin. In the work described in this chapter, an *in vivo* study was carried out to evaluate the anticoagulant activity of the dendriplexes after subcutaneous administration in Sprague-Dawley rats and then compare this to the activity of free heparin. Although the dendriplexes were detected in various organs and in the plasma in a trend similar to the free heparin, it exhibited no anticoagulant activity, which suggests the stability of the complex *in vivo*.

The biodistribution of heparin, heparin dendriplexes and the dendrimer into various organs of Sprague-Dawley rats was studied after oral gavage into the stomach. The dendriplexes and the free dendrimer achieved higher lung tissue concentrations (2.9-3% of the dose administered found in a gram of tissue) compared to heparin (0.03%). Orally administrated heparin and its dendriplexes revealed no anticoagulant activity in the plasma.

8.1. Experimental

8.1.1. Materials

Unfractionated heparin sodium salt grade I-A from Porcine Intestinal Mucosa 187 USP units/mg (MW 6,000-30,000 Da), Hydrogen peroxide, Isoamyl alcohol (Sigma, USA), Accucolor™ heparin (Sigma Diagnostics, USA), [^{3}H]-Heparin (sodium salt) (specific radioactivity 0.32 mCi/mg) (Perkin Elmer, USA).

8.1.2. Synthesis of Gly-Lys$_{63}$(NH$_2$)$_{64}$ dendrimer

The synthesis of the unlabelled and [^{3}H]-labelled cationic water soluble dendrimer **(compound 2c) (Figure 2.12)** having 64 surface amino groups was performed using method D and F respectively and purified as mentioned in appendix I.

8.1.3. Preparation of heparin dendriplexes

The complex was prepared as mentioned in chapter VII (section 7.1.3) except that the concentrations were modified as per the dose. The suspension was kept in suspension during the dosing period by mixing on a vortex.

8.1.4. Animals

Female, Sprague-Dawley rats (176.4 gm ± 10.5gm) were caged in groups of 3 to 8 (B and K Universal Ltd, UK). Animals were fasted for 12 h before dosing with free access to water. A temperature of 19–22 °C was maintained, with a relative humidity of 45–65%, and a 12-h light/dark cycle. Animals were acclimatized for 7 days before each experiment. All procedures followed the Home Office Code of Practice for the Housing and Care of Animals used in Scientific Procedures.

8.1.5. Experimental design and dosing

A subcutaneous heparin dose used was as recommended by Borchard (1990). The oral heparin dose was determined from dose-response studies conducted by Leone-

Bay *et al.* (1998). Dose volumes were chosen as recommended in the literature (Diehl *et al.*, 2001) .

Oral dendrimer uptake study: 20 rats were randomized into 5 groups and gavaged with a single dose of [^{3}H]-dendrimer (177 mg/Kg, 1μCi, 2 ml). Groups of 4 rats each were sacrificed at 0 (control), 1, 3, 6 and 24 h after administration.

Oral heparin uptake study: 20 rats were randomized into 5 groups and gavaged with a single dose of [^{3}H]-heparin (100 mg/Kg, 1μCi, 2 ml). Groups of 4 rats each were sacrificed at 0 (control), 1, 3, 6 and 24 h after administration.

Oral heparin dendriplexes 100/300 uptake study: 15 rats were randomized into 5 groups and gavaged with a single dose of [^{3}H]-heparin complexed with unlabelled dendrimer (100 and 300 mg/Kg respectively, 1μCi, 2 ml). Groups of 3 rats each were sacrificed at 0 (control), 1, 3, 6 and 24 h after administration.

Subcutaneous heparin uptake study: 20 rats were randomized into 5 groups and injected subcutaneously with a single dose of [^{3}H]-heparin (10 mg/Kg, 1μCi, 0.2 ml). Groups of 4 rats each were sacrificed at 0 (control), 1, 3, 6 and 24 h after administration.

Subcutaneous dendriplexes 10/30 uptake study: 15 rats were randomized into 5 groups and injected subcutaneously with a single dose of [^{3}H]-heparin complexed with unlabelled dendrimer (10 and 30 mg/Kg respectively, 1μCi, 0.2 ml). Groups of 3 rats each were sacrificed at 0 (control), 1, 3, 6 and 24 h after administration.

8.1.6. Blood collection and radioactivity in organs

The animals were anesthetised by intraperitoneal (ip) injection of pentobarbitone sodium B.P (72 mg/rat) (Sagatal ®, 60 mg/ml, Rhone Merieux, UK). At different time intervals (0, 1, 3, 6 and 24 h), the blood was withdrawn from the abdominal aorta using BD Eclipse™ needle and collected into 2.7 ml BD vacutainer™ tubes

which contain 0.129 M sodium citrate (3.8%, 9:1 blood: sodium citrate ratio) as anticoagulant (Beckton Dickinson, USA). The tubes were transferred into ice, centrifuged (2500g, 10 min) at room temperature, plasma was then harvested as soon as possible and stored at -20 °C. Immediately after sacrifice, organs such as the heart, lungs, liver, spleen, kidneys, stomach, small (SI) and large intestine (LI) were dissected and homogenized in water for 3min, using a tissue homogenizer (model PT-10, Switzerland). The intestinal tissues were washed gently with distilled water to remove any unabsorbed material. All samples were solubilised before counting to measure the low energy radiation emitted by tritium; an aliquot of 0.6 ml or 200 µg of the tissue homogenate was solubilised with 1.0 ml of the tissue solubiliser Biosol® (National Diagnostic, UK), shaken overnight at 55 °C, then combined with 17 ml of the self-acidified Bioscint® scintillation cocktail, to eliminate chemiluminescence, and kept in a dark cold room for 72 h before counting in a LS6500 Multi-Purpose Scintillation Counter (Beckman, USA). Colored samples were decolorized with 200-400 µl of 30% hydrogen peroxide and isoamyl alcohol was added to stop foaming. The plasma volume of the rat was calculated in the range of 6.1- 7.6 ml based on the formula 36-45 ml plasma per Kg of a rat (Altman and Dittmer, 1974). The results were expressed as the percent recovered per organ and the percent recovered per gram of wet tissue ± S.D (n=3-4). The plasma volume instead of the weight was used in all the calculations.

8.1.7. Anti-factor Xa assay

Accucolor™ heparin is intended for the quantitative determination of therapeutic heparin in human plasma. Due to variation between human and rat plasma, the standard curve of heparin in rat plasma was established using the same procedure for human plasma mentioned in chapter VII (section 7.1.6) except that 50µl of undiluted

rat plasma was used instead of 25µl of diluted human plasma. A standard curve was prepared by spiking heparin in control pooled platelet free rat plasma (0.1-1.6 IU/ml). Test plasma samples was used within 2 h of collection or alternatively stored at -20 °C and thawed once at 37 °C, 30 min before use.

8.2. Results and discussion

8.2.1. *In vivo* anticoagulant activity of heparin and heparin dendriplexes after oral and subcutaneous administration

Heparin is a potent anticoagulant used in the treatment of patients who have a high risk of deep venous thrombosis and pulmonary embolism. It is available to patients only by parental administration since it is hydrophilic, highly negatively charged and has a high molecular weight (6-30 KDa) (Gonze *et al.*, 1998). Furthermore, heparin has a tendency to desulphate and undergo glycoside metabolism under the acidic conditions of the stomach (Jandik *et al.*, 1996).

Heparin anticoagulant activity in the platelet-free rat plasma was estimated in all the study groups at 0, 1, 3, 6 and 24 h post-injection using an anti-factor Xa assay. Blood stasis or contamination with tissue fluids during blood sampling should be avoided because platelet contamination in plasma samples, particularly after freezing and thawing, may result in the release of platelet factor 4 (PF4), a potent heparin neutralizing protein which may result in underestimation of heparin concentration. Blood obtained by tail bleeding was prone to stasis even in the presence of 3.8% sodium citrate as an anticoagulant. So it was preferable to obtain the blood directly from the abdominal aorta.

The heparin calibration curve in platelet-free pooled rat plasma was plotted in **Figure 8.1** and the active heparin concentration in the plasma was determined. Estimation of

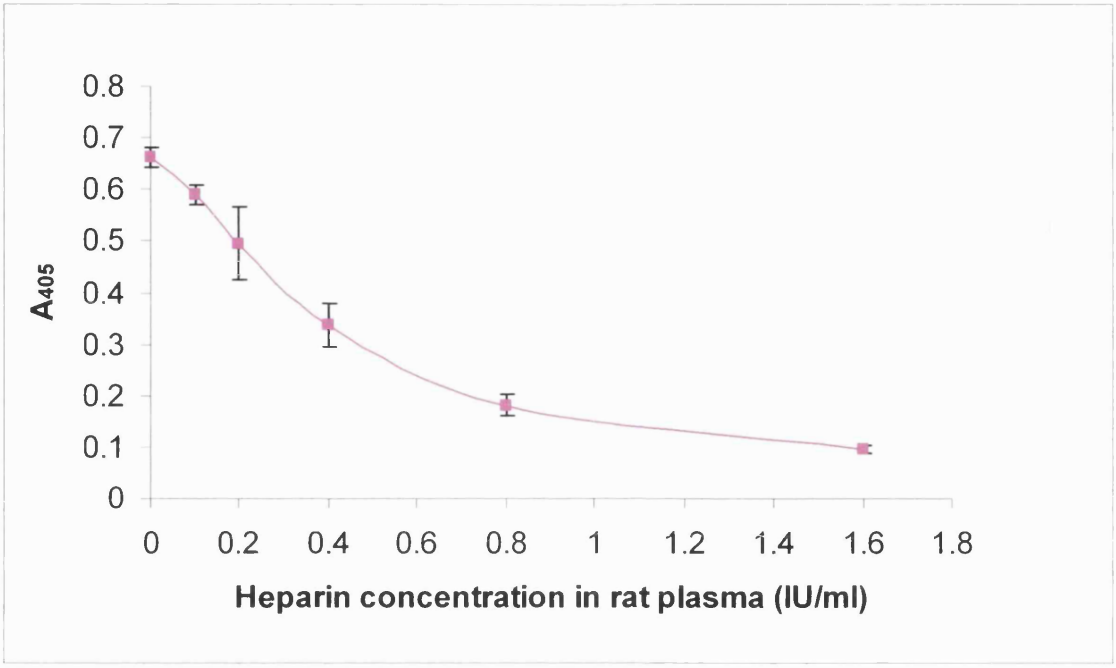

Figure 8.1: The heparin calibration curve of absorbance at 405 nm versus heparin concentration (0.0-1.6 IU/ml) in control pooled platelet free Sprague-Dawley rat plasma using the anti-factor Xa assay (n=4; ± S.D).

the total heparin concentration (both active and inactive) was achieved by measuring the radioactivity of heparin in the plasma. **Figure 8.2** showed that heparin injected subcutaneously at a dose of 10 mg/Kg possessed anticoagulant activity up to 24h while heparin complexed with the dendrimer before injection, at a 1:3 heparin:dendrimer mass ratio (10/30 mg/Kg), resulted in an inactive complex *in vivo*. The new conformation of the heparin must abolish the negative charge and make it unaccessible to antithrombine III and the coagulation proteases i.e. prothrombine III and factor Xa. Heparin inactivity in the plasma may also be attributed to precipitation of the aggregates at the site of injection.

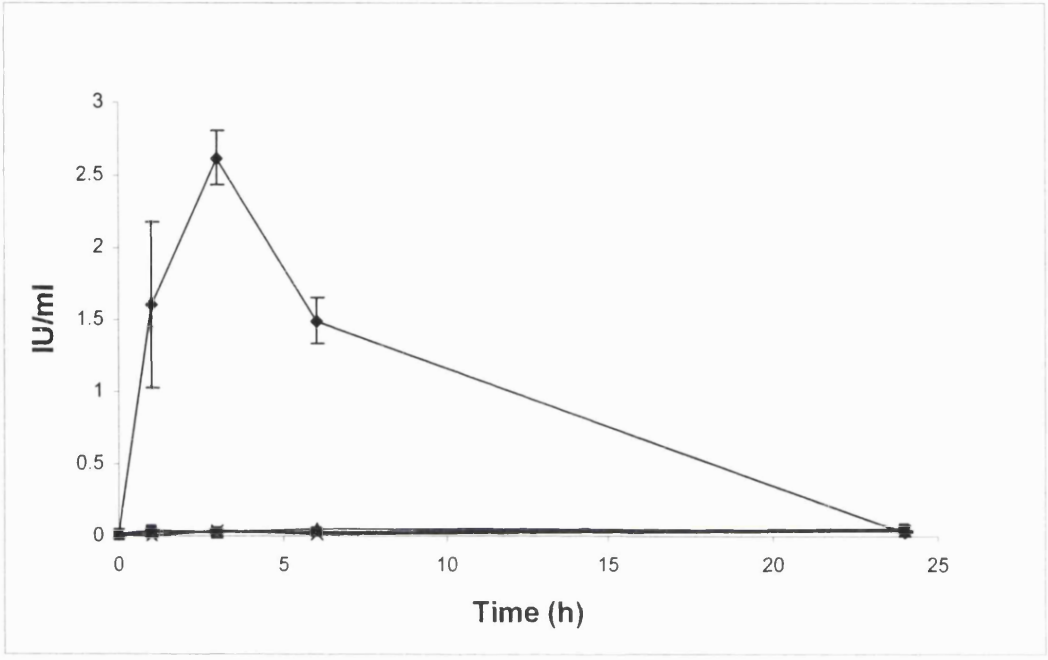

Figure 8.2: Active heparin plasma concentration (IU/ml) versus time (h) in sprague-dawley rats quantified using antifactor Xa assay. SC heparin (10 mg/Kg) (♦); SC heparin dendriplexes (10/30 mg/Kg) (■); oral heparin (100 mg/Kg) (×) and oral heparin dendriplexes (▲) (n=3-4). Uncomplexed heparin injected SC was the only active formulation.

However, data obtained from radioactivity measurements **(Table 8.1)** suggested that both free and complexed **(Figure 8.3)** were heparin detected in the plasma and other organs which implied that heparin inactivity was attributed to its complexation and not to its precipitation at the site of administration.

Table 8.1: Organ biodistribution of subcutaneous heparin injected in the (1) free form (10 mg/kg) and (2) complexed form (10/30 mg/kg). Tritiated heparin was assayed in the organs by liquid scintillation counting after sacrificing the animal at 1, 3, 6 and 24h post injection. The results are expressed as the percent injected dose recovered per organ (n=3-4; ± S.D).

	1h		3h		6h		24h	
ORGAN	(1)	(2)	(1)	(2)	(1)	(2)	(1)	(2)
plasma	1.8±0.64	1.33±0.04	0.83±0.19	0.86±0.15	0.55±0.08	0.7±0.13	0.45±0.04	0.37±0.06
Heart	0.11±0.04	0.07±0.01	0.12±0.08	0.06±0.00	0.07±0.01	0.07±0.01	0.11±0.04	0.05±0.00
Lungs	0.18±0.06	0.08±0.01	0.15±0.03	0.09±0.00	0.14±0.02	0.09±0.01	0.12±0.01	0.06±0.00
Liver	1.14±0.17	0.90±0.06	0.87±0.05	1.13±0.13	0.83±0.02	1.57±0.46	0.85±0.18	1.62±0.36
Spleen	0.05±0.01	0.06±0.02	0.03±0.007	0.06±0.01	0.07±0.06	0.06±0.00	0.05±0.02	0.06±0.01
Kidneys	1.87±0.95	0.87±0.03	1.47±0.28	0.70±0.07	1.49±0.69	0.74±0.20	1.16±0.10	0.72±0.11
Stomach	0.14±0.05	0.14±0.06	0.18±0.07	0.09±0.00	0.27±0.11	0.07±0.01	0.12±0.04	0.03±0.02
S.I	0.85±0.25	0.60±0.56	0.90±0.38	0.38±0.17	0.57±0.08	0.22±0.02	0.43±0.06	0.17±0.06
L.I	0.37±0.03	0.12±0.01	0.36±0.06	0.18±0.00	0.42±0.13	0.18±0.02	0.34±0.06	0.12±0.03

Table 8.2: Organ biodistribution of heparin in the free form (100 mg/kg) (3), complexed with the dendrimer Gly-$Lys_{63}(NH_2)_{64}$ (100/300 mg/kg) (4) and the tritiated free dendrimer (5) after oral administration. Radioactivity was assayed in the organs by liquid scintillation counting after sacrificing the animal at 1, 3, 6 and 24h post injection. The results are expressed as the percent injected dose recovered per organ (n=3-4; ± S.D).

	1h			3h			6h			24h		
ORGAN	(3)	(4)	(5)	(3)	(4)	(5)	(3)	(4)	(5)	(3)	(4)	(5)
plasma	0.38±0.08	0.21±0.04	0.00±0.00	0.57±0.04	0.50±0.12	0.00±0.00	0.85±0.24	1.27±0.16	0.01±0.00	0.96±0.18	1.44±0.20	0.04±0.01
Heart	0.02±0.01	0.03±0.02	0.00±0.00	0.01±0.01	0.02±0.01	0.00±0.00	0.06±0.01	0.09±0.04	0.02±0.00	0.09±0.02	0.10±0.01	0.05±0.00
Lungs	0.03±0.02	4.0±0.35	3.17±1.4	0.06±0.01	0.65±0.58	0.58±0.37	0.08±0.00	0.23±0.18	0.04±0.01	0.09±0.01	0.14±0.02	0.04±0.00
Liver	0.41±0.07	0.51±0.09	0.27±0.35	0.66±0.08	0.64±0.1	0.17±0.07	0.69±0.11	0.85±0.06	0.22±0.11	0.78±0.21	1.38±0.04	0.16±0.03
Spleen	0.01±0.01	0.04±0.01	0.04±0.02	0.02±0.00	0.04±0.01	0.02±0.08	0.04±0.03	0.05±0.01	0.04±0.04	0.04±0.01	0.09±0.00	0.06±0.00
Kidneys	0.01±0.01	0.08±0.01	0.03±0.03	0.11±0.02	0.13±0.04	0.02±0.01	0.48±0.7	0.24±0.05	0.03±0.01	0.15±0.04	0.23±0.12	0.05±0.01
Stomach	1.23±0.67	2.70±1.43	0.83±0.21	0.28±0.07	1.70±0.37	0.82±0.60	0.17±0.11	0.87±0.83	0.41±0.34	0.09±0.03	0.14±0.03	0.11±0.13
S.I	9.4±2.13	2.56±1.09	1.10±1.70	2.11±0.39	3.8±1.1	0.29±0.07	1.37±0.47	3.7±0.95	0.57±0.56	0.26±0.14	0.48±0.04	0.12±0.08
L.I	0.56±0.3	0.36±0.14	0.25±0.38	2.43±0.95	1.1±0.49	0.12±0.06	1.11±0.14	1.47±0.24	0.14±0.06	0.25±0.10	0.40±0.03	0.15±0.08

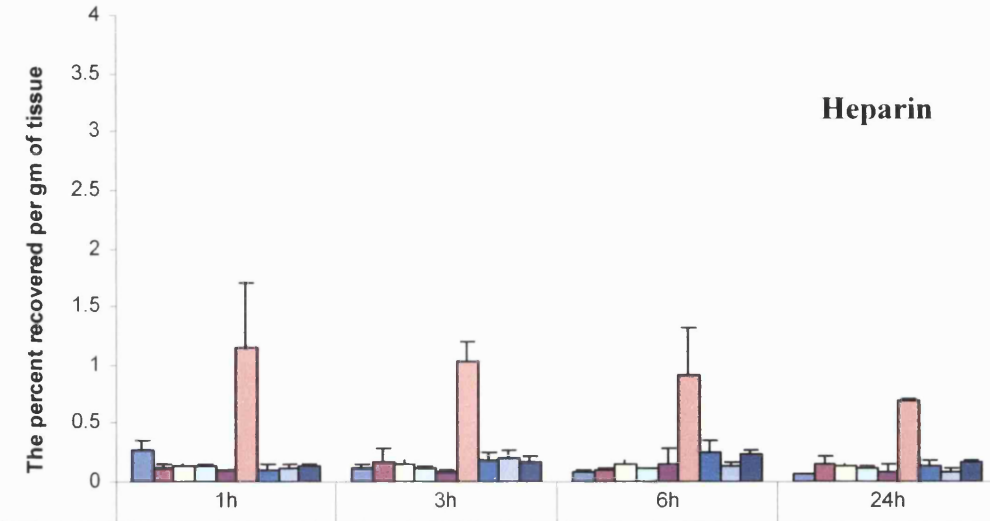

	1h	3h	6h	24h
plasma	0.262	0.121	0.081	0.066
heart	0.124	0.161	0.098	0.150
lungs	0.127	0.152	0.156	0.129
liver	0.140	0.119	0.113	0.113
spleen	0.093	0.077	0.147	0.092
kidneys	1.142	1.029	0.914	0.698
stomach	0.093	0.178	0.249	0.131
S.i	0.124	0.209	0.131	0.091
L.i	0.137	0.177	0.244	0.166

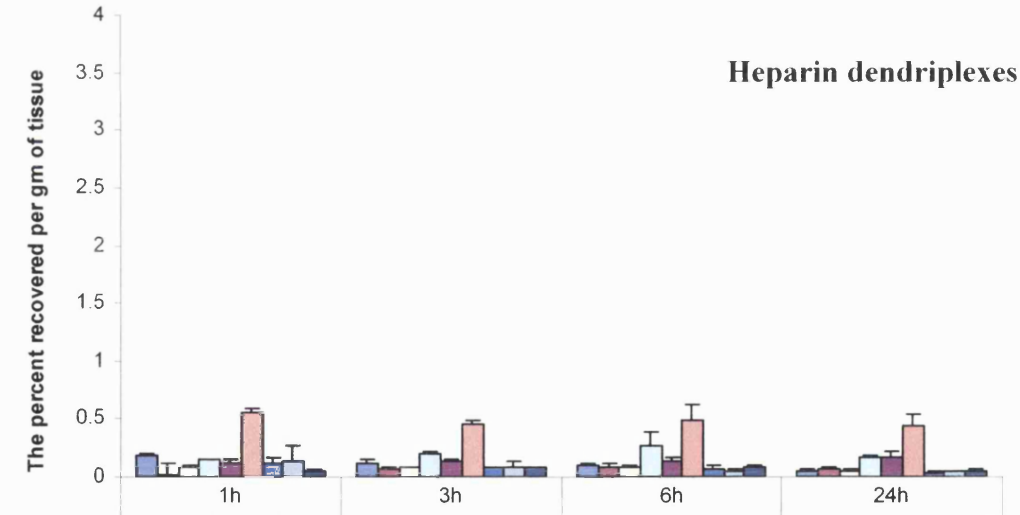

	1h	3h	6h	24h
plasma	0.193	0.125	0.103	0.053
heart	0.014	0.074	0.093	0.062
lungs	0.081	0.086	0.084	0.058
liver	0.148	0.196	0.278	0.171
spleen	0.114	0.131	0.134	0.162
kidneys	0.550	0.458	0.489	0.441
stomach	0.122	0.084	0.074	0.031
S.i	0.133	0.086	0.052	0.043
L.i	0.058	0.084	0.083	0.055

Figure 8.3: Organ biodistribution of subcutaneous heparin (10 mg/kg) (top) and the dendriplexes (10/30 mg/Kg) (bottom). Radioactivity was assayed in the organs by liquid scintillation counting after sacrificing the animal at 1, 3, 6 and 24h post injection. The results are expressed as the percent injected dose recovered per gram of tissue (n=4; ± S.D).

Another observation was that heparin injected subcutaneously resulted in bleeding and formation of a haematoma (a collection of blood outside the vessel as a result of a vessel rupture and haemorrhage) at the injection site. No bleeding occurred in the case of the complex **(Figure 8.4)**. Pisano *et al.* (2005) reported the synthesis of an antiangiogenic heparin derivative with no anticoagulant activity and showed that animals treated with 100mg/kg heparin had pronounced bleeding and oedema formation at the subcutaneous injection site and 25% died soon after treatment. However animals treated with the test compounds showed no similar side effects.

Oral administration of 100 mg/Kg heparin and its dendriplexes (100/300 mg/Kg) showed an anticoagulant activity *in vivo*.

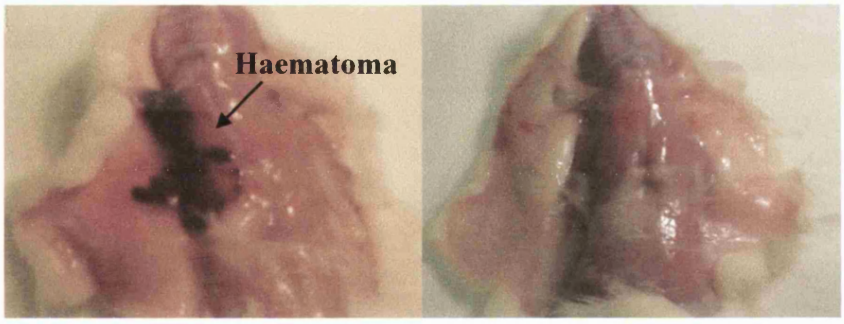

Figure 8.4: The subcutaneous injection site 1h after injection with (A) 10 mg/Kg heparin showing formation of a haematoma (B) 10/30 mg/Kg heparin/dendrimer complex showing no bleeding.

8.2.2. Oral uptake of heparin, the cationic dendrimer and heparin dendriplexes

Several approaches to develop an oral heparin formulation have been attempted with limited success. These included enteric-coated heparin-amine combinations, heparin complexes or salts prepared with organic acids, heparin derivatives produced by partial desulphation and methylation, mixed micelles, oil/water emulsions, absorption enhancers, heparin based on hydrophobic organic bases such as spermine and lysine salts, liposomes, hydrogel nanospheres, or bile salts (Morton *et al.*, 1981; Ueno *et al.*, 1982; Ziv *et al.*, 1983; Guarini and Ferrari, 1985; Kim *et al.*, 1986; Dal *et al.*, 1989; Caramazza *et al.*, 1991; Dunn and Hollister, 1995; Thanou *et al.*, 2001b). A polyampholytic chitosan derivative, mono-*N*-carboxymethyl chitosan, enhanced the intestinal absorption of low molecular weight heparin across intestinal epithelia *in vitro* and *in vivo*. The absorption-enhancing property of the chitosan was attributed to its interaction with the negative sites of the tight junctions, significantly decreasing the TEER and increasing the paracellular permeation of the hydrophilic compound (Thanou *et al.*, 2001a). The quaternized chitosan derivative *N*-trimethyl chitosan (TMC) was found to increase the paracellular permeability of peptide drugs in Caco-2 monolayers and in rats (Thanou *et al.*, 2000) but a strong aggregation and subsequent fibre formation occurred when low molecular weight heparin (LMWH) was added to TMC.

A recent approach using drug delivery agents, such as sodium N-[8-(2-hydroxybenzoyl)amino]caprylate (SNAC) which promote the oral absorption of heparin has shown some success (Rivera *et al.*, 1997; Lee *et al.*, 2000). This type of drug delivery system is based on the formation of non-covalent complexes between the *N*-acylated non-α-amino acids and/or *N*-acylated amino alkanoic acids and the

macromolecules such as heparin. These complexes are able to pass the intestinal barrier and then dissociate to yield the active molecules.

The enhanced uptake of heparin and other negatively charged compounds was observed *in vitro* in the presence of polycations and was attributed to charge neutralization (Deierkauf *et al.*, 1977; Fabian *et al.*, 1978; Shen and Ryser, 1978; Duncan *et al.*, 1979; Bleiberg *et al.*, 1981).

The cationic dendrimer studied showed its effect on the tight junctions of Caco-2 monolayers besides neutralizing the negative charge of heparin. In this chapter described the effect of heparin-dendrimer complexation on the oral uptake of both uncomplexed heparin and the dendrimer is described. Drug-carrier interactions may lead to drug deactivation which hence hinders the use of the carrier. However, such deactivation can sometime be favorable and may find useful applications.

Table 8.2 shows that the percent uptake of oral heparin dendriplexes **(Figure 8.5)** in the organs studied; plasma, heart, lung, liver, spleen, kidney, stomach, SI and LI was almost similar to that of heparin **(Figure 8.6)** administered using the same route except for the lung data.

In order to compare the results obtained by different compounds and doses, organ biodistribution data was also expressed as the percent recovered per gram of wet tissue.

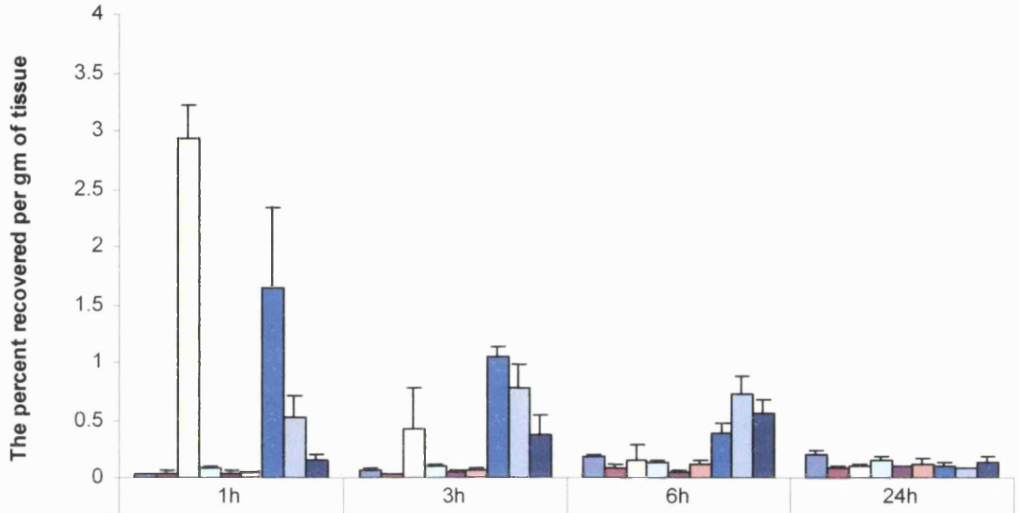

	1h	3h	6h	24h
plasma	0.032	0.073	0.185	0.210
heart	0.037	0.028	0.080	0.089
lungs	2.934	0.416	0.159	0.102
liver	0.080	0.103	0.139	0.152
spleen	0.042	0.050	0.059	0.093
kidneys	0.043	0.064	0.126	0.117
stomach	1.645	1.058	0.382	0.102
S.i	0.527	0.778	0.736	0.081
L.i	0.151	0.380	0.561	0.136

Figure 8.5: Organ biodistribution of tritiated heparin administered orally after complexation with the dendrimer (100/300 mg/kg). Radioactivity was assayed in the organs by liquid scintillation counting after sacrificing the animal at 1, 3, 6 and 24h post-injection. The results are expressed as the percent dose recovered per gram of tissue (n=3; ± S.D). The peak concentrations were obtained in lungs and stomach after 1h; in S.I after 3h; in kidneys and L.I after 6h; in plasma, heart, liver and spleen after 24h. After 3h, the uptake of the dendriplexes into organs was in the following order: stomach> S.I> lungs> L.I> liver> plasma> spleen> heart> kidneys.

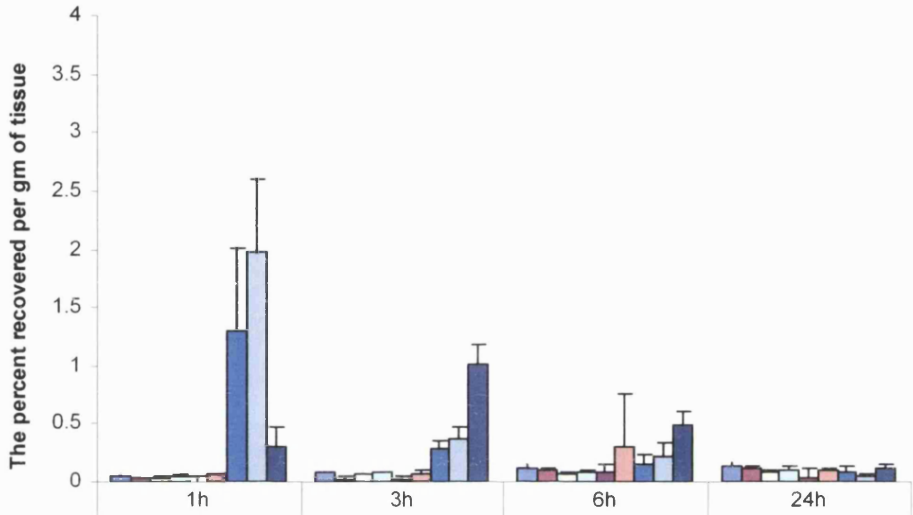

	1h	3h	6h	24h
plasma	0.056	0.083	0.123	0.140
heart	0.028	0.019	0.093	0.114
lungs	0.034	0.061	0.075	0.084
liver	0.051	0.080	0.089	0.097
spleen	0.005	0.021	0.086	0.027
kidneys	0.066	0.075	0.309	0.098
stomach	1.307	0.280	0.155	0.091
S.i	1.971	0.379	0.228	0.047
L.i	0.300	1.009	0.484	0.111

Figure 8.6: Organ biodistribution of tritiated heparin administered orally (100 mg/kg). Radioactivity was assayed in the organs by liquid scintillation counting after sacrificing the animal at 1, 3, 6 and 24h post-injection. The results are expressed as the percent dose recovered per gram of tissue (n=4; ± S.D). The peak concentrations were obtained in stomach and S.I after 1h; in L.I after 3h; in kidneys and spleen after 6h; in plasma, heart, liver and lungs after 24h. After 3h, the uptake of heparin into organs was in the following order: L.I> S.I> stomach> plasma> liver> kidneys> lungs> spleen> heart.

Heparin complexation with the dendrimer increased heparin biodistribution into the lungs compared to free heparin (about 90 times after 1h) **(Figure 8.7A)**. The tritiated dendrimer also showed high lung deposition similar to that of the complex **(Figure 8.7B)**. The percentage and pattern of uptake of the systems studied (in lungs and plasma for comparison) were shown in **(Figure 8.8)** The fact that the complex was made of tritiated heparin and the unlabelled dendrimer whereas tritiated dendrimer was used in dendrimer uptake studies, led to a conclusion that heparin found in the lung was in the complexed form. One may suggest that the appearance of the dendrimer and the dendriplexes in the lungs was as an artefact due to dosing i.e. intra-tracheal instead of oral administration, however, since all the oral formulations tested (heparin, dendrimer and heparin dendriplexes) were administered using the same technique but only the cationic dendrimer and the cationic dendriplexes, but not the anionic heparin, showed high lung uptake, we suggested that the results were genuine and not a dosing artefact. Whether the positive charge of both the dendrimer and the dendriplex are involved with lung uptake has to be further studied. A similar observation was made by Nigavekar *et al.*(2004) who found that positively charged [^{3}H]-PAMAM dendrimers had 5-10 times increase in lungs deposition compared to neutral dendrimers, with the highest levels observed in lungs, liver and kidney in both species. Both the free and complexed heparin showed no anticoagulant activity in the plasma after oral administration **(Figure 8.2)**. Heparin deactivation can be attributed to the strong electrostatic interaction with dendrimer. Heparin desulphation and metabolism under the acidic conditions of the stomach cannot be ruled out, however heparin deactivation was also noticed after subcutaneous administration of the complex where the complex was not exposed to the acidic conditions of the stomach which supports the electrostatic interaction hypothesis.

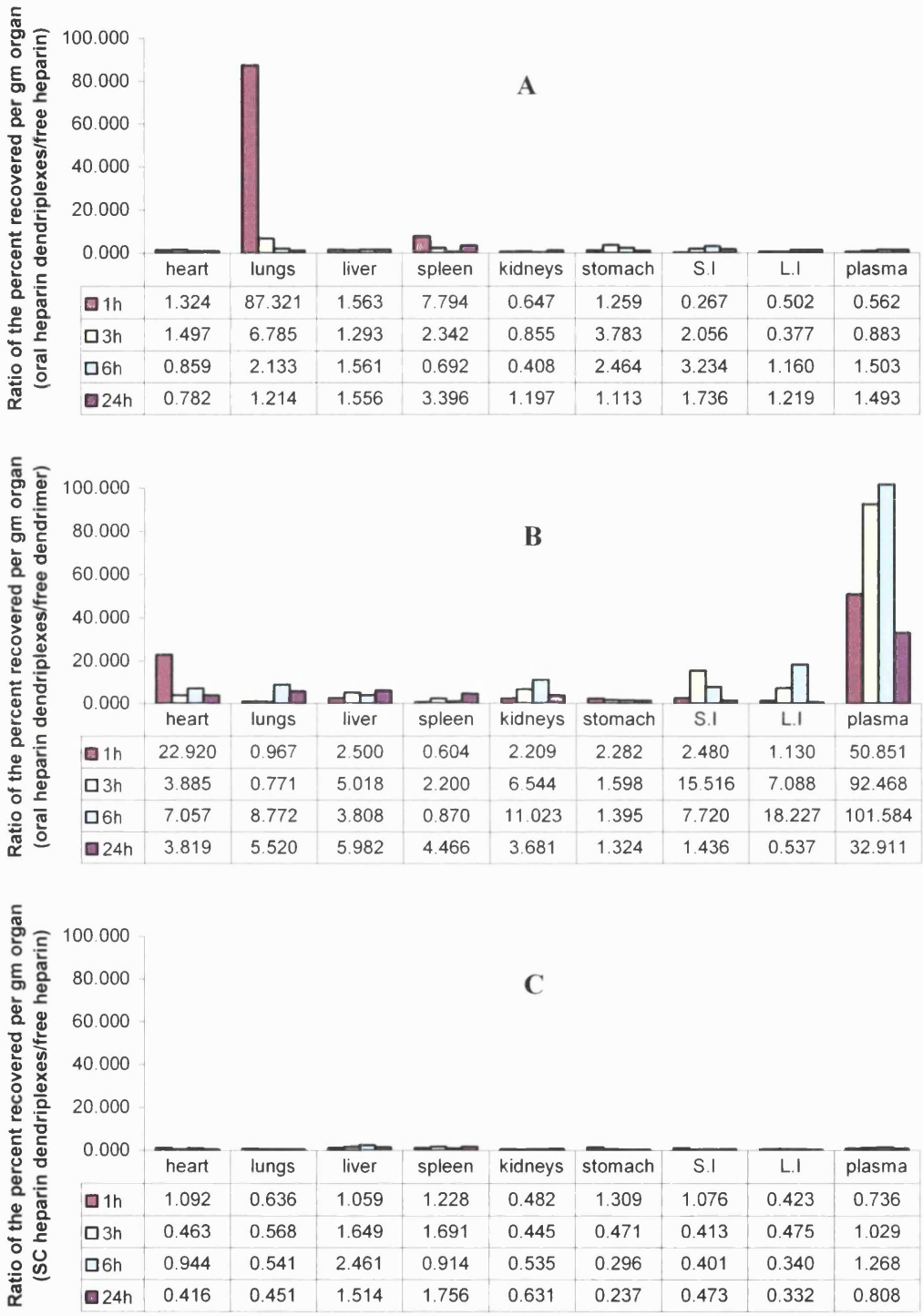

Figure 8.7: Ratio of the percent recovered per gram of organ of (A) heparin dendriplexes (100/300 mg/kg) to free heparin (100 mg/kg); (B) heparin dendriplexes (100/300 mg/kg) to free dendrimer (177 mg/Kg) administered orally showing higher dendriplexes and dendrimer biodistribution into the lungs compared to free heparin; (C) heparin dendriplexes (10/30 mg/kg) to free heparin (10 mg/kg) administered subcutaneously showing slightly lower but evident absorption of the dendriplex compared to heparin .

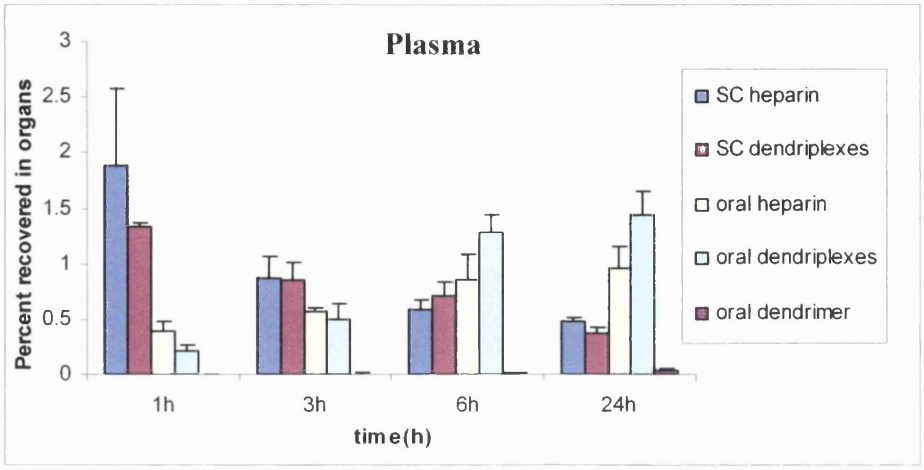

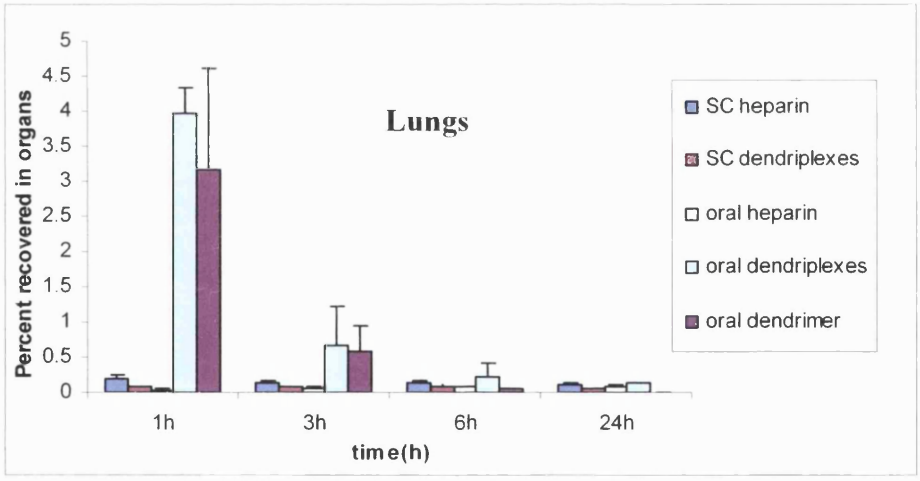

Figure 8.8: The percentage of recovered into plasma (top) and lungs (bottom) of the formulations studied as a function of time (h); subcutaneous heparin (10 mg/kg), subcutaneous dendriplexes (10/30 mg/kg), oral heparin (100 mg/kg), oral heparin dendriplexes (100/300 mg/kg) and oral dendrimer (177 mg/Kg). **Plasma:** subcutaneous administration of heparin and its dendriplexes achieved higher plasma concentration than the oral route despite one-tenth the dose. Plasma concentrations decreased and increased with time after SC and oral administration respectively. **Lungs:** oral heparin and its dendriplexes showed the highest lung recovery among the rest which decreased as a function of time.

Dendrimer biodistribution **(Figures 8.9)** into rat organs was enhanced when complexed with heparin **(Figure 8.7B)**. Dendrimer complexation with the heparin was expected to reduce the interaction of dendrimer with the cell due to charge neutralization. Shen and Ryser (1981) have reported that heparin at low concentrations reduces the endocytosis of polylysine-methotrexate polycation conjugates by Chinese hamster ovarian cells due to polycation-heparin complexation. However, this does not contradict our results since the dendrimer was much in excess and the complex had an overall positive charge.

Despite the fact that both the dendrimer and the dendriplexes did not achieve high plasma concentrations, it was noticeable that the plasma concentration of the dendriplexes was 30-100 times greater than that of the free dendrimer **(Figure 8.7B)**. A study carried out by Nigavekar *et al.* (2004) showed that both neutral and positively charged PAMAM dendrimers were cleared rapidly from the blood after intravenous administration.

The use of heparin dendriplexes can be investigated as nanoparticulate drug carriers. In the past, heparin was used in the preparation of various drug delivery systems (Cremers *et al.*, 1994; Passirani *et al.*, 1998; Liang *et al.*, 2002). Nanoparticles bearing heparin covalently bound to poly(methyl methacrylate) (PMMA) have been prepared by Passirani *et al.* (1998) and these showed prolonged circulation *in vivo*. This was explained by the "stealth" effect of the heparin which probably inhibited complement activation. It would be interesting to assess the entrapment of drug molecules in the heparin dendriplexes and harness their use in targeted drug delivery.

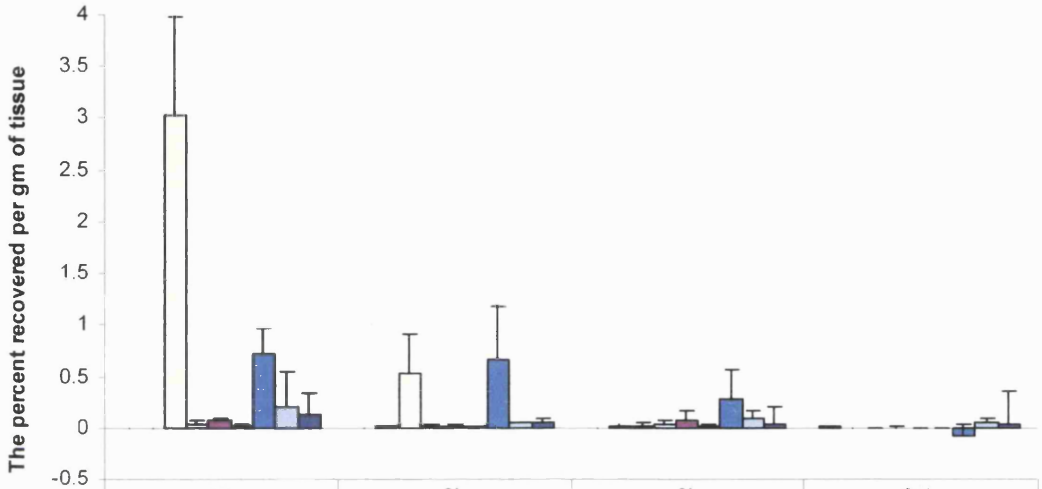

	1h	3h	6h	24h
plasma	0.001	0.001	0.002	0.006
heart	-0.002	0.007	0.011	0.002
lungs	3.035	0.539	0.018	0.002
liver	0.032	0.021	0.036	0.003
spleen	0.070	0.023	0.068	-0.002
kidneys	0.019	0.010	0.011	-0.003
stomach	0.721	0.662	0.274	-0.077
S.i	0.212	0.050	0.095	0.057
L.i	0.134	0.054	0.031	0.025

Figure 8.9: Organ biodistribution of tritiated dendrimer administered orally (177 mg/kg). Radioactivity was assayed in the organs by liquid scintillation counting after sacrificing the animal at 1, 3, 6 and 24h post-injection. The results are expressed as the percent injected dose recovered per gram of tissue (n=4; ± S.D). The peak concentrations were obtained in stomach and S.I after 1h; in L.I after 3h; in kidneys and spleen after 6h; in plasma, heart, liver and lungs after 24h. After 3h, the uptake of heparin into organs was in the following order: stomach> lungs> L.I> S.I> spleen>liver> kidneys> heart> plasma.

8.3. Conclusion

Complexation of heparin with the dendrimer did not improve its oral uptake in Sprague-Dawley rats. Oral heparin formulation remains a big challenge in drug delivery. However, the heparin-binding dendrimer studied possessed a heparin-blockade activity both *in vitro* and *in vivo*, a property that should be investigated in areas such as designing new heparin antidotes and antiangiogenic therapeutics.

Chapter IX

REFLECTIONS

In this thesis each chapter ends with a brief conclusion so it will be redundant to recapitulate here. It might be sufficient to state that even the relatively few dendrimers and dendrons described in this thesis and on which the research was conducted have resulted in a large number of ideas, leading to new findings in this relatively new area in drug delivery.

The versatility of dendrimers and dendrons that can be synthesised is infinite. However, the six cationic dendrimers and dendrons which were synthesised varied in size and lipophilicity, features controlled by the generation number, the number of surface amino groups and the number of C_{14} chains attached. The work dealt with has perhaps concentrated on a rather limited range of dendritic structures but the variety of potential chemical structures can lead possibly to an unlimited array of supramolecular forms. Structures covered in this thesis include: water soluble cationic dendrimer *per se*, dendrisomes as novel supramolecular vesicular structures comprised of cationic lipidic dendron, dendron-surfactant aggregates and mixed micelle systems stabilised by hydrogen bonding and hydrophobic interactions and finally dendrimer-heparin dendriplexes formed by electrostatic interactions.

Each single category of these structures has more and more aspects to be discovered as time was not sufficient to delve into each set in more depth. But it has provided some insight in a potential future work:

- The work in the thesis started out investigating the use of dendrimers as drug delivery carriers. However, the apparent insolubility of some dendrimers gave us the idea of solubilizing these molecules using surfactants or studying their aggregation in water to find if these structures had any special arrangements in solution. We found that some of these dendritic molecules depending on their size, HLB and topology can form controlled aggregates such as dendrisomes; this process was not random as engineering the dendrons and dendrimers can affect their aggregation process. So studying the self-assembly of these compounds under different conditions by changing salt concentration, pH and the solvent may give further information on factors controlling self-assembly.
- The entrapment capacity and thermal properties of dendrisomes have been shown to be modulated by changing cholesterol content. The use of dendrisomes as DNA carriers has not yet been investigated. Dendrisomes comprise the properties of both dendritic molecules and cationic liposomes except that no external cationic lipid is added during preparation. Such properties may distinguish them from other DNA delivery systems studied so far. Although the thermal behaviour of the dendrisomes is not clearly understood, further studies can be carried out to check the suitability of these systems as heat-responsive drug delivery carriers.
- We then moved on to study the solubilisation of these aggregates using the non-ionic surfactant Triton X-100. The gradual transformation of dendrisomes into isotropic surfactant dendron mixed micelle systems opens a new area, not of dendrimer-surfactant interactions themselves but maybe the use of these systems as drug solubilizing agents especially knowing that other

PAMAM-surfactant systems showed an extraordinary solubilizing capacity for pyrene which was more than that of the surfactant alone.

- Some studies not reported in this thesis have shown that the 3rd generation polylysine dendrimer with 32 C_{14} chains can stabilise o/w emulsions only in alkaline media (0.1 N NH_4OH). Stabilisation of emulsions with soluble macromolecules and insoluble particulate materials is already established. But dendrimers are not yet reported as emulsion stabilisers. Further studies need to be conducted in order to understand this phenomenon.
- The intrinsic fluorescence of our dendrimers without a fluorophore, a property discovered in these molecules which was also generation dependent, can be a very useful tool in studying the uptake of these molecules in cells. Such work has already been started by our group. Visualisation of these molecules localised in the nucleus may shed some light about the usefulness of these molecules in DNA delivery to the nucleus.
- Dendrimers have shown to act as nanocarrier devices, carboxyfluorescein was used as a model only but other drugs such as cytotoxic and anti-angiogenic drugs are potential targets, especially with the discovery of heparin binding and deactivation properties of some dendrimers. A heparin-binding polyarginine dendrimer was found to have some anti-angiogenic properties in egg membranes. We discussed in chapter VII how these dendrimers can be good candidates in anti-angiogenesis therapeutics especially if they prove to be effective molecules *per se.* Also the anti-angiogenic drug can be chemically bound to the dendrimer or physically entrapped with the choice of attaching an endothelial targeting molecule such as integrin to the dendrimer surface. This work is planned to start in October.

- The use of dendrimers as an approach to enhance heparin absorption orally was not successful due to the low uptake enhancement ratio and heparin inactivation. However, this strong interaction with heparin suggests use as heparin antidotes. Engineering the chemical structure and molecular weight while maintaining this property may lead to the preparation of a less toxic range of heparin antidotes than protamine, the only available antidote.
- Biodistribution studies in rats showed the affinity of dendrons and dendriplexes to lung tissues, a phenomenon not unusual with cationic molecules but one needs to be further studied so it can be considered as a disadvantage (sign of toxicity) or as an advantage (in lung delivery).

APPENDIX I

^{1}H NMR: ^{1}H NMR spectra were acquired in D_2O or $CDCl_3/CD_3OD$ depending on the compound solubility. All spectra were obtained using a Bruker AVANCE 500 MHz spectrometer at 298 K, Windows 2000 computer and X-WIN 3.1 software. 1D proton NMR spectra were obtained with 32768 data points in the t2 domain. 2D NMR TOCSY spectra was acquired in a phase-sensitive manner using time-proportional phase instrumentation for quadrature detection in F_1 and had 128 increments in the t1 with 2048 data points in the t2 domain. TOCSY spectra were recorded with a spin-lock mixing time of 60 ms. Chemical shifts are reported in ppm downfield from internal TMS.

Electro-Spray Ionisation mass spectrometry (ESI-MS): Mass spectra were obtained using a Finnigan MassLab Navigator quadropole mass spectrometer. (N2 flow, 400 L/h; temperature, 150 °C; cone voltage 25V; capillary voltage 3V).

Matrix-Assisted Laser Desorption Ionisation Time of Flight mass spectrometry (MALDI-TOF): Mass spectra for the compounds were run on a Voyager-DE PRO MALDI-TOF mass spectrometer (Biospectrometry Workstation, Applied Biosystems). 10µl of dilute sample solution of compounds (10^{-10} M dissolved in 1:1 acetonitrile/0.1%TFA) was mixed with 10µl of saturated cyano-4-hydroxycinnamic acid solution, and then 1µl of solution was loaded on the sample plate. The mixture was allowed to air dry until all solvent is evaporated, and then was run on the instrument.

Thin layer chromatography (TLC): Reaction progress of compounds 1a and 1b was monitored by TLC on Kieselgel 60 F_{254} using the mobile phase indicated. Visualisation was achieved by UV light and by charing with sulphuric acid.

High pressure liquid chromatography (HPLC): Analytical RP-HPLC was carried out on Vydac C4 Protein column (5 μm, 4.6 mm, 250 mm). Separation of compound 2b was achieved using a linear gradient at a flow-rate of 1.0 ml/min affected by a Water 600S controller and 616 pump running Solvent A: 0.1% TFA; Solvent B: methanol; 0% B to 100% B over 10 min, then 100% B to 0% over 10 min. HPLC grade methanol and water were filtered through 23 μm membrane filter and degassed with helium flow, prior to column application. Separation was monitored with a Waters 486 absorbance detector at 230 nm. Retention time (R_t) and purity were determined using Waters Millennium Chromatography Manager software.

Size exclusion chromatography (SEC): SEC for aqueous soluble dendrimers comprised of Waters Ultrahydrogel 250° and 1000° (7.8 × 300 mm) columns coupled to a Gibson 133 refractive index detector. Water was used as an eluent at 37°C. The SEC system was operated with Polymer Laboratories software (USA).

Spectrophotometry and spectrofluorimetry: UV spectrophotometry was performed using a Beckman DU® 650 Spectrophotometer, USA. Fluorescence spectra were recorded using a LS50B, Perkin Elmer, UK.

Dialysis: Purification of compound 2c was performed by exhaustive dialysis using pleated dialysis tubing (Snakeskin™), 3500 Da MWCO, 22 mm dry diameter (ID) (Pierce Chemical Company, USA), used without previous treatment; the freeze-dried water soluble dendrimer was dissolved in water at a concentration of 5 mg/ml, and then passed through 0.2 μm hydrophobic filter, 30 ml of the solution was pipetted into a 12 cm-long dialysis tubing (3.7 ml sample per cm of dry tubing) and sealed using dialysis clips by folding dry tubing over twice. The tubing was placed in 1L of deionised water in a 1L-beaker and kept stirring at 25°C over 3 days; the water was changed twice a day.

Synthesised compounds

Synthesis of α-amino tetradecanoic acid [method A] (compound 1a)

To a pre-cooled oven-dried 500 ml round bottom flask (in an ice bath) containing absolute ethanol (85 ml), dried over standard drying agents and freshly distilled, and added sodium pellets (5 g, 0.22 mol), stirred until sodium pellets dissolved. Diethyl acetamido malonate (24.3 g, 0.11 mol) and 1-bomododecane (34.39 g, 0.15 mol) were added and heated under reflux for 24 h, keeping the reaction mixture free of moisture with a calcium chloride drying tube. Upon cooling, the mixture was poured onto ice/water (160 ml) and the precipitate filtered and washed with water. The crude solid was placed into a 500 ml round bottom flask, concentrated hydrochloric acid (180 ml) and DMF (20 ml) added, and then heated with reflux for 24 h. The mixture was allowed to cool, poured into a solution of ethanol/water (3:1) and neutralised with concentrated aqueous NH_3. The precipitate was filtered off and washed with ethanol/water (2 × 100ml) and finally rinsed with cold hexane to get rid of the bromoalkane.

Yield: 95%

ESI MS $C_{14}H_{29}O_2N$ (243.29) *m/z* (%) 244 [M+H](95%), 198.1 (100).

Synthesis of α-(*tert*-Boc)tetradecanoic acid [method B] (compound 1b)

The solid DL-α-amino tetradecanoic acid (15.01 g, 61.7 mmol) was suspended in a 2:3 mixture of *tert*-butyl alcohol/water (240 ml) and 8 M aqueous NaOH added drop-wise and the pH was corrected to 13. Di-*tert*-butyl dicarbonate (20 g, 91.6 mmol) in *tert*-butyl alcohol (40 ml) was added at room temperature. The pH value was adjusted to 11-12 and the reaction mixture was subsequently stirred for 4-5 days. Following dilution of the reaction mixture with water (50 ml), solid citric acid was

added and made pH 3. The oil was extracted with ethyl acetate (3×150 ml) and was washed with brine (1 × 250 ml). The solution was then dried over anhydrous $MgSO_4$, filtered and evaporated. The product was purified by recrystallization from cold acetonitrile, filtered and then dried under silica. The reaction progress was monitored by thin layer chromatography (TLC).

Yield: 84 %

R_F =0.26 hexane:ethyl acetate 4:1 (v/v)

^{1}H-NMR ($CDCl_3$) δ 5.00 (s, 1H, OCONH), 4.28 (m, 1H, α-CH), 1.40 [s, 9H, $C(CH_3)_3$], 1.24 (m, 22H, $11CH_2$), 0.87 (t, 3H, CH_3).

ESI MS $C_{19}H_{37}O_4N$ (343.5) *m/z* (%) 288 $[M\text{-}BOC\text{-}H+2Na]^+$ (100), 366 $[M+Na]^+$ (28), 344 $[M+H]^+$ (40), 244 $[M\text{-}BOC+H]^+$ (38).

SPPS of cationic lipid-lysine dendron $(C_{14})_3Lys_7(C_{14})_8(NH_2)_8$ (compound 2a) [method C]

The peptide dendron **(compound 2a)** was synthesised by stepwise solid-phase peptide synthesis on a MBHA resin (1g, substitution 0.67 mmol/g) using Boc-methodology. The resin was allowed to swell in DMF (three times resin volume) at room temperature prior the synthesis in the reaction vessel. The resin was never allowed to dry. Four fold excess HBTU activated Boc-aminoacids in DMF was used to achieve each coupling. α-(Boc)tetradecanoic acid (4 equivalents), HBTU (4 equivalents), HOBt (4 equivalents) were dissolved in the minimum volume of DMF necessary to dissolve all the components and finally DIEA (8 equivalents) was added to the solution (the colour of the solution changes to yellow or orange). The efficiency of coupling was checked by Kaiser test (method G) during the first 30 min of coupling, typical free primary amino groups give dark blue colour with this test. If the reaction was not complete, another coupling was carried out before the

subsequent deprotection. *N*-termini deprotection was carried out with 100% TFA (2 × 1 min). Three successive couplings with the activated lipoamino acid, each followed by *N*-deprotection and washed twice with DMF before and after deprotection. This was then followed by three successive couplings/deprotections with Boc-Lys(Boc)-OH.DCHA (method F) (4,8,16 equivalents respectively) under the same conditions, then the coupling/deprotection with the lipoamino acid (32 equivalents). The resin was washed twice with DCM and dried under vacuum over KOH or P_2O_5 as moisture can be very harmful in HF cleavage. The compound was cleaved from the resin using a standard HF method (1g resin peptide, 10ml HF, 1.5h in a salted ice bath at -5°C). After cleavage, the resin was washed with 95% glacial acetic acid and freeze-dried followed by drying over P_2O_5 for three days and stored under silica gel.

Compound 2a:

Yield: 32.1 %

MALDI-TOF MS $C_{196}H_{384}O_{18}N_{26}$ (3388.0) *m/z* (%) 2402 (55), 2627 (55), 2853 (98), 2939 (40), 3163 (45), 3388 [M](100).

^{1}H-NMR ($CDCl_3/CD_3OD$) δ 3.8-4.5 (t, 18H, α-CH)*, 2.9-3.5 (t, 14H ,ε-CH)*, 1.1-2.1 (m, 284H, CH_2)*, 0.8-0.9 (t, 33H, CH_3).

*All peaks except CH_3 protons showed broad peaks due to overlapping of protons having various chemical shifts as they exist in different environments.

SPPS of cationic lysine dendrimers Gly-$Lys_{31}(NH_2)_{32}$ (compound 2b) and Gly-$Lys_{63}(NH_2)_{64}$ (compound 2c) [method D]:

The peptide dendrimers **(compounds 2b, 2c)** were synthesised by stepwise solid-phase peptide synthesis on a MBHA resin under the same conditions mentioned in method C. Boc-Gly-OH (4 equivalents relative to resin loading), HBTU (4

equivalents), HOBt (4 equivalents) were dissolved in the minimum volume of DMF necessary to dissolve all the components and finally DIEA (8 equivalents) was added to the solution to make the first coupling. The efficiency of coupling was checked by Kaiser test (method G) during the first 30 min of coupling with this test. If the reaction was not complete, another coupling was carried out before the subsequent deprotection. *N*-termini deprotection was carried out with 100% TFA (2 × 1 min). Five and six successive couplings/deprotections using four fold excess HBTU activated Boc-Lys(Boc)-OH.DCHA (method H) (4,8,16,32,64 and 4,8,16,32,64,128 equivalents), HBTU (4,8,16,32,64 and 4,8,16,32,64,128 equivalents), HOBt (4,8,16,32,64 and 4,8,16,32,64,128 equivalents) and DIEA (8,16,32,64,128 and 8,16,32,64,128,256 equivalents) for **compounds 2b** and **2c** respectively. After the 3rd lysine coupling, a mixture of DMF/NMP (1:1) was used instead of DMF alone to achieve better resin swelling and a more efficient coupling. The resin was washed twice with DCM and dried under vacuum. The compound was cleaved from the resin by HF as mentioned in method C. After cleavage, the dendrimer was precipitated with ether to remove fluoride salt. The precipitated dendrimer and resin were filtered, and washed with 20% glacial acetic acid or water and freeze-dried, drying over P_2O_5 for three days and stored over silica gel.

Compound 2b:

Yield: 33.4 %

$C_{188}H_{378}O_{32}N_{64}$ (4047.48) *m/z* (%) 4049 (100)4031(55)4069(50).

^{1}H-NMR (D_2O) δ 4.2-4.7 (t, 33H, α-CH), 3.15-3.6 (t, 62H, ,ε-CH), 1.5-2.2 (m, 186H, β, γ , δ-CH) †.

Compound 2c:

Yield: 20.67 %

$C_{380}H_{762}O_{64}N_{128}$ (8149.05) An envelope was obtained.

^{1}H-NMR (D_2O) δ 4.08-4.6 (t, 65H, α-CH), 3.13-3.6 (t, 126H ,ε-CH), 1.4-2.25 (m, 378H, β, γ, δ-CH) †.

†The coupling was not observed instead broad peaks are obtained

SPPS of cationic lipid-lysine dendrimers Gly-$Lys_{31}(C_{14})_{32}(NH_2)_{32}$ (compound 2d) and Gly-$Lys_{63}(C_{14})_{64}(NH_2)_{64}$ (compound 2e) [method E]:

The peptide dendrimers **(compounds 2d, 2e)** were synthesised using method D except that a final coupling/deprotection with the α-(Boc) tetradecanoic acid (64 and 128 equivalents), HBTU (64 and 128 equivalents), HOBt (64 and 128 equivalents) and DIEA (128 and 256 equivalents) for compounds 2d and 2e respectively. The resin was washed twice with DCM and dried under vacuum. The compound was cleaved from the resin by HF as mentioned in method C. After cleavage, the resin was washed with 95% glacial acetic acid and freeze-dried, drying over P_2O_5 for three days and stored over silica gel.

Compound 2d:

Yield: 40 %

$C_{636}H_{1242}O_{64}N_{96}$ (11259.47) An envelope was obtained as the sample was not purified. But the peak for the expected molecular weight is observed.

^{1}H-NMR ($CDCl_3/CD_3OD$) δ 3.5-4.5 (t, 65H, α-CH), 2.7-3.4 (t, 62H ,ε-CH), 1.0-2.0 (m, 890H, CH_2), 0.8-0.95 (t, 96H, CH_3)‡.

Compound 2e:

Yield: 5.4 %

$C_{1276}H_{2490}O_{128}N_{192}$ (22573.02) An envelope was obtained as the sample was not purified. But the peak for the expected molecular weight is observed.

^{1}H-NMR ($CDCl_3/CD_3OD$) δ 3.45-4.5 (t, 129H, α-CH), 2.7-3.4 (t, 126H ,ε-CH), 1.0-2.0 (m, 1786H, CH_2), 0.7-1.0 (t, 192H, CH_3) ‡.

‡ All peaks except CH_3 protons showed broad peaks due to overlapping of protons having various chemical shifts as they exist in different environments.

SPPS of cationic radio-labelled lysine dendrimer Gly-$Lys_{63}(NH_2)_{64}$ for biological studies (compound 2c) [method F]:

The synthesis of [^{3}H] labelled Boc-Lys(Boc)-OH was first carried out. To a 100 ml round bottom flask containing 12 ml of 1 M NaOH, cold lysine.HCl (2 g, 10.87 mmol), [^{3}H] lysine.HCl (5 mCi) were added and stirred at ambient temperature and then diluted with *tert*-butyl alcohol (9 ml). To a well-stirred, clear solution di-*tert*-butyl dicarbonate (4.9 g, 21.97 mmol) was added dropwise within 1h and kept stirring for 24 h. A white precipitate appears during addition of di-tert-butyl dicarbonate. The reaction mixture was extracted with hexane (2 × 3 ml), and then the hexane layer was extracted with saturated $NaHCO_3$ solution (3 × 20 ml). The combined aqueous layers were acidified to pH 1-1.5 by careful addition of solution of 1.5 g of KHSO4 in 10 ml water. The turbid reaction mixture is then extracted with ethyl acetate (4 × 20 ml). The combined organic layers were then washed with water (2 × 40 ml), dried over anhydrous $MgSO_4$ and filtered. The solvent is removed under reduced pressure using a rotary evaporator. Radio-labelled Boc-Lys(Boc)-OH.HCl was yielded at 31% in the form of oil and dissolved in DMF for the dendrimer synthesis. The synthesis of **compound 2c** was carried out using method D starting with 0.25 g MBHA resin using one fold excess HBTU activated hot Boc-Lys(Boc)-OH.HCl (8.5×10^7 dpm/58 mg or equivalent), and followed by a coupling using four fold excess HBTU activated cold Boc-Lys(Boc)-OH.DCHA as mentioned in method

D. The labelling was performed at 1st, 2nd, 3rd and 4th lysine coupling, yielding 35% radioactivity.

Kaiser test reagents [method G]:

1. 5 g of ninhydrin was dissolved in 100 ml ethanol.
2. 80 g of liquefied phenol was dissolved in 20 ml of ethanol.
3. 2 ml of 0.001 M aqueous solution of potassium cyanide was added to 98 ml pyridine.
4. Few resin beads were sampled in a sintered glass filter, washed several times with methanol:DCM (1:1) and then transferred to a small glass tube and 2 drops of each of the solutions above were added.
5. The mixture was heated to 120 °C for 4-6 min, and diluted with 5 ml of 60% ethanol. A positive test is indicated by blue resin beads.

Activation of Boc-Lys(OH)-Boc.DCHA salt [method H]:

1. 2.68 mmol (1.4 g) of Boc-Lys(Boc)-OH.DCHA was suspended in 10.4 ml ethyl acetate in a separating funnel.
2. 3.2 mmol (3.12 ml) of ice-cold 2 M H_2SO_4 was added and shaken until dissolved.
3. The top (ethyl acetate) layer was removed and kept a side. The aqueous layer was diluted with 10 ml of cold water and extracted with 2×10 ml of ethyl acetate.
4. All the ethyl acetate layers were combined and washed with 2×10 ml of water, dried with $MgSO_4$. The ethyl acetate was filtered and then removed in a rotary evaporator at not more than 40 °C. Complete solvent removal was performed under high vacuum in a desiccator with fresh NaOH.

Standard HF cleavage [method I]:

1. The dried resin, a Teflon-coated stirring bar and the scavenger were placed in a Teflon reaction vessel.
2. The cap was screwed on the reaction vessel and cooled in liquid nitrogen for at least 5 min before distilling HF.
3. 10 ml HF per gram of the resin was distilled. The temperature was maintained at 0-5 °C by using a salted ice-bath for 90 min.
4. HF was evaporated under reduced pressure, once all HF was evaporated, the reaction vessel was kept under vacuum for another 20 min.
5. The peptide and the resin were precipitated with cold diethyl ether (8-10 volumes) added dropwise.
6. The peptide and the resin were removed by filtration under reduced pressure using a sintered glass filter.
7. The peptide was isolated, dissolved by stirring in either water or the appropriate dilution of glacial acetic acid and lyophilised.

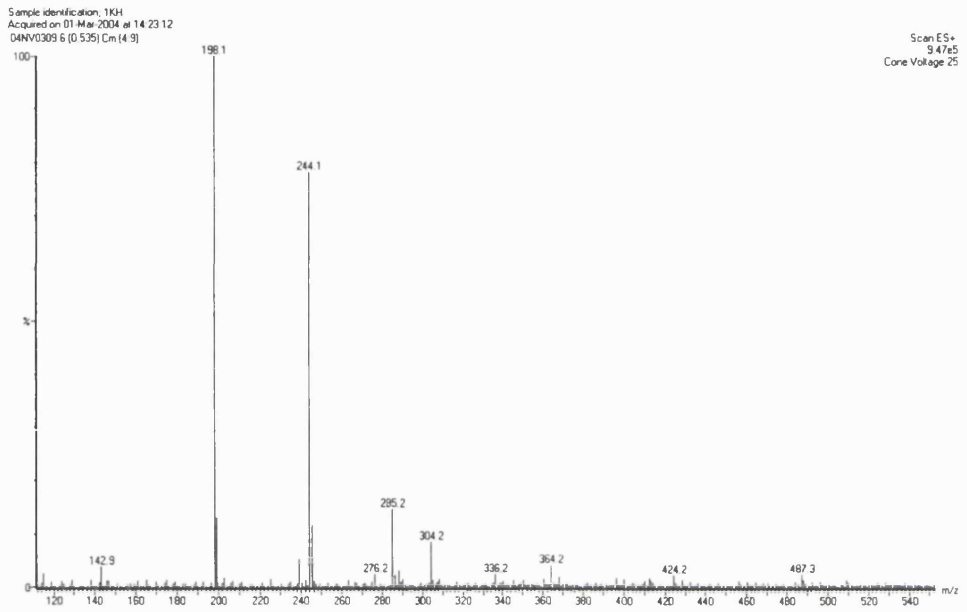

ESI-MS of **compound 1a** (MW 243.29 Da)

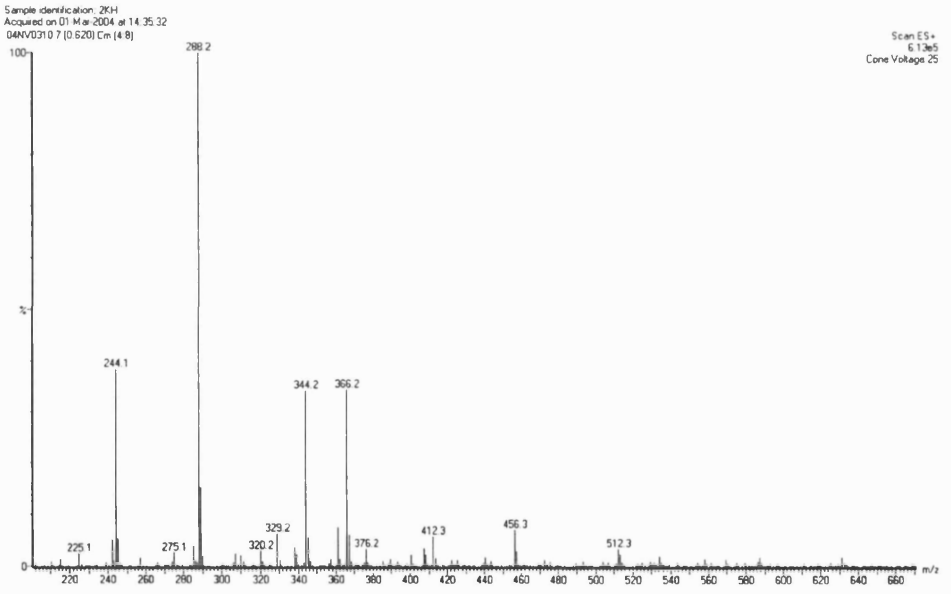

ESI-MS of **compound 1b** (MW 343.5 Da)

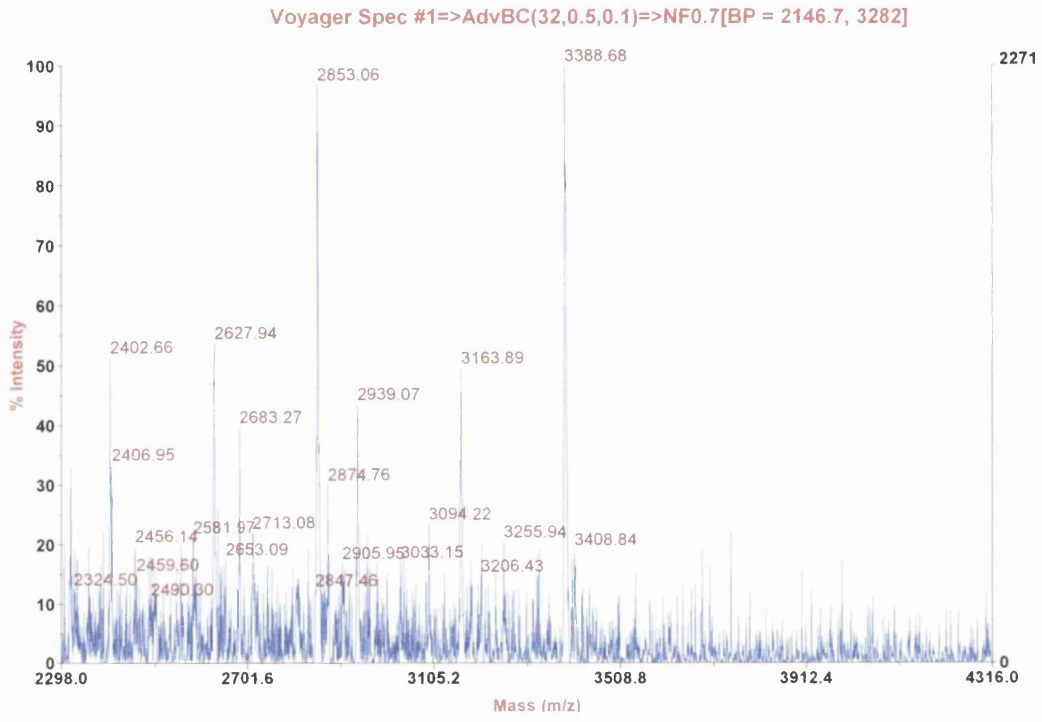

MALDI-TOF of **compound 2a** (MW 3388 Da)

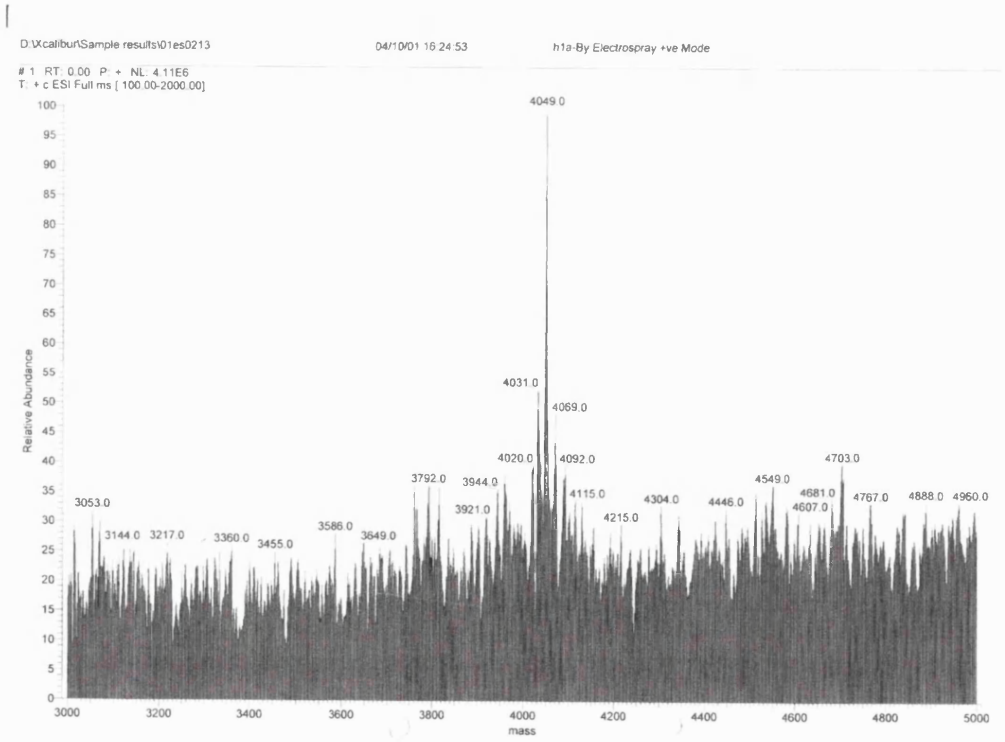

ESI-MS of **compound 2b** (MW 4047 Da)

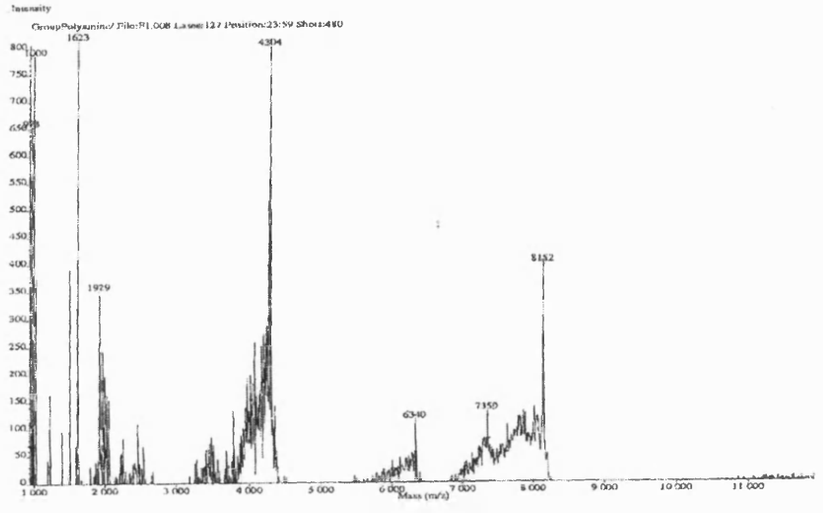

MALDI-TOF of **compound 2c** (MW 8149 Da)

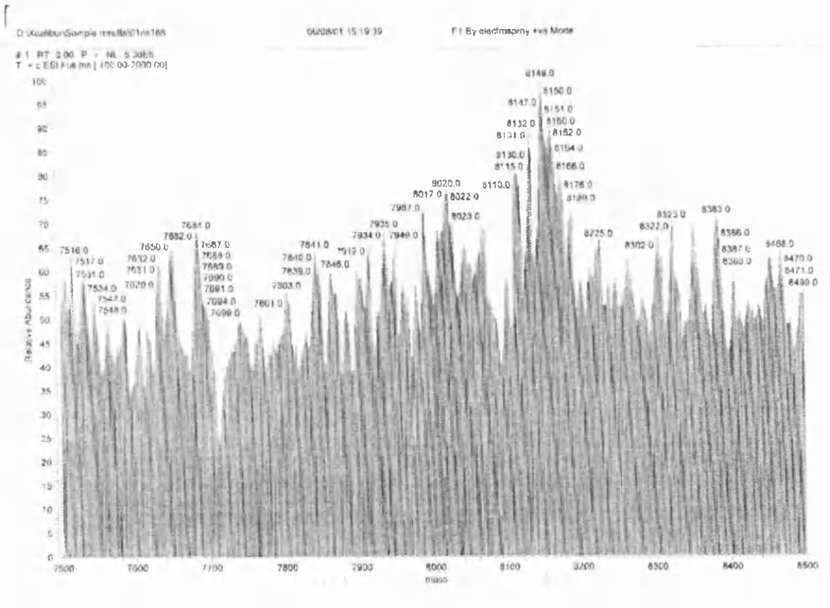

ESI-MS of **compound 2c** (MW 8149 Da)

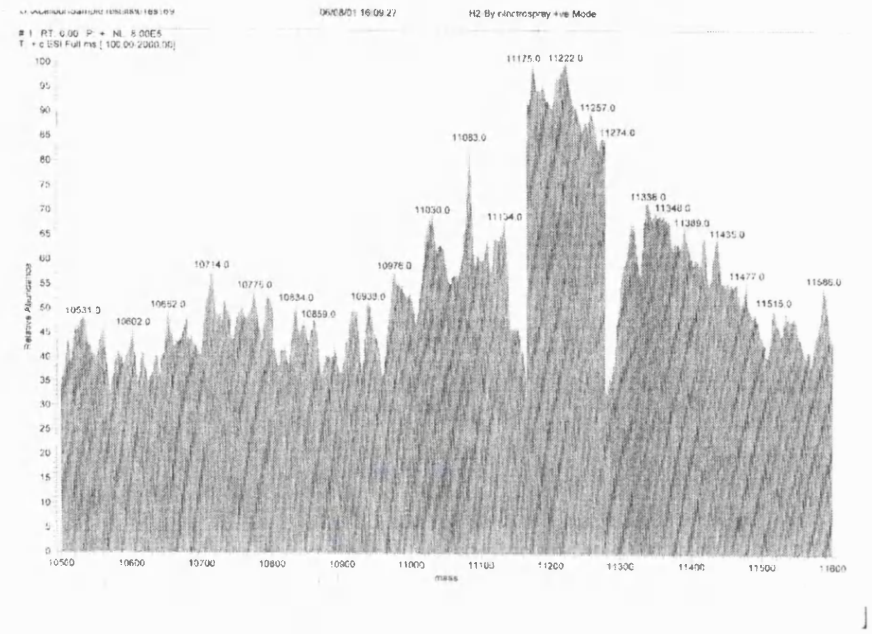

ESI-MS of **compound 2d** (MW 11259 Da)

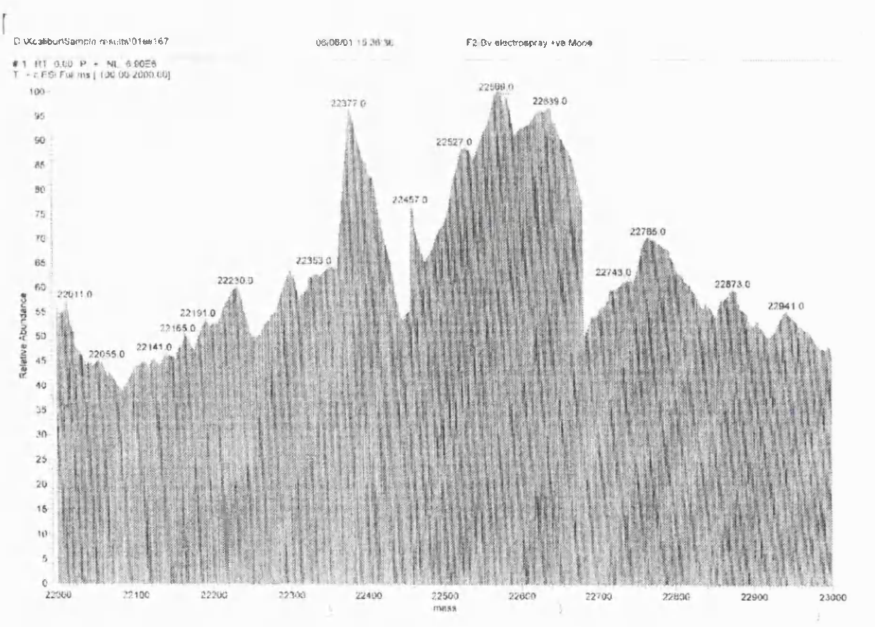

ESI-MS of **compound 2e** (MW 22573 Da)

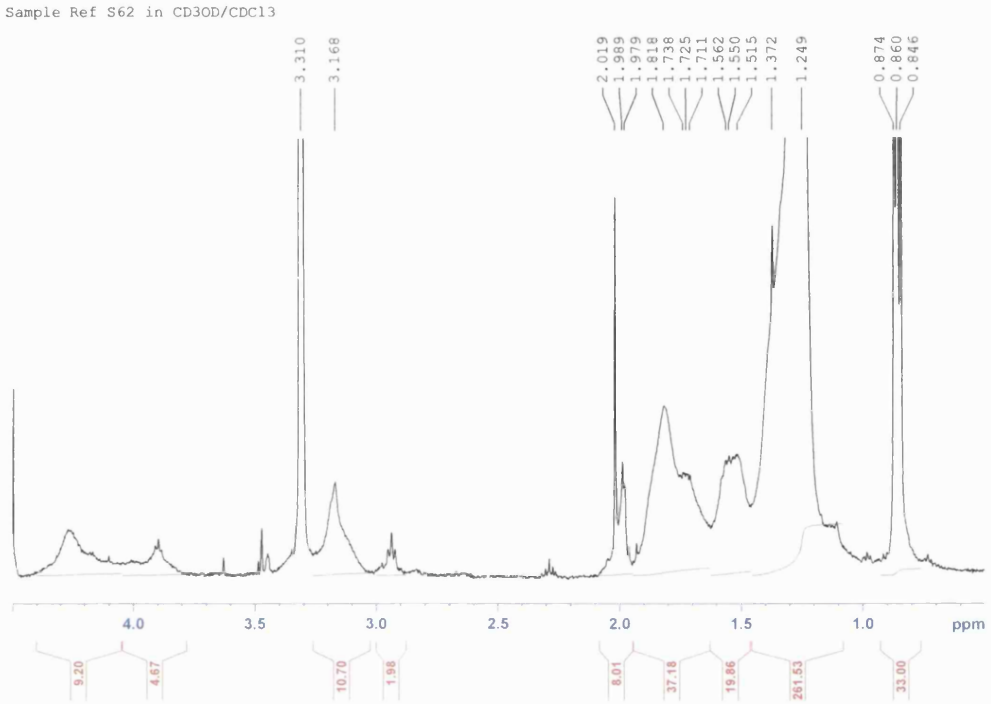

^{1}H NMR of **compound 2a** in $CD_3OD/CDCl_3$. It shows overlapping between similar protons. Chemical shift δ=3.8-4.5 (H_α of lysine and alkyl chain), 2.9-3.5 (H_ε of lysine), 1.1-2.1 (H_β, H_δ and H_γ of lysine and C-H of alkyl chain), 0.8-0.9 (CH_3 of alkyl chain).

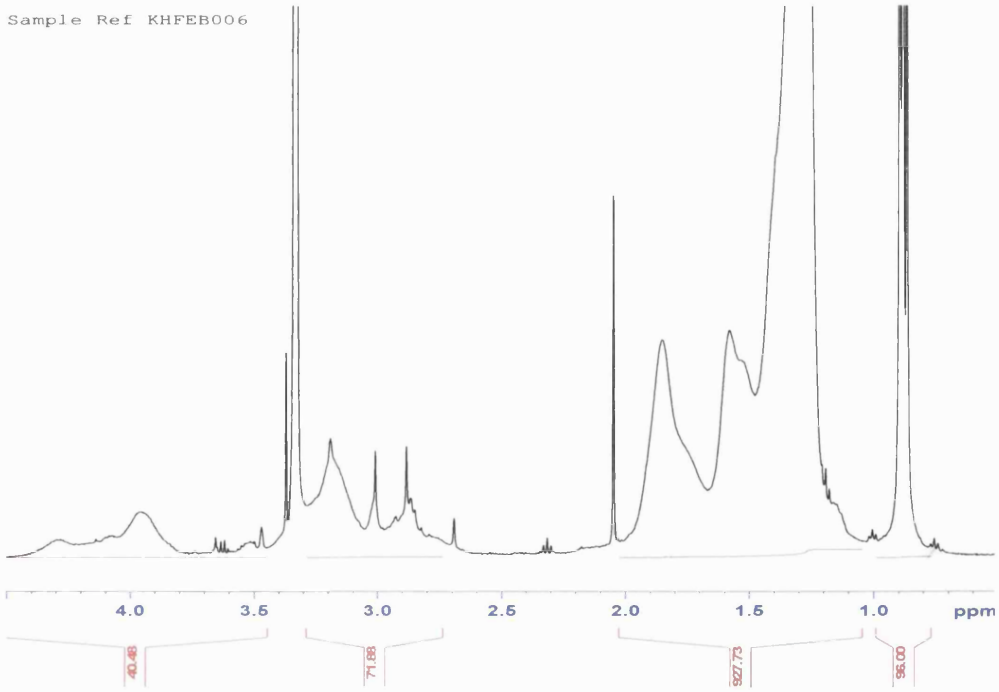

^{1}H NMR of **compound 2d** in $CD_3OD/CDCl_3$. It shows overlapping between similar protons. Chemical shift δ=3.5-4.5 (H_α of lysine, glycine and alkyl chain), 2.7-3.4 (H_ε of lysine), 1.0-2.0 (H_β, H_δ and H_γ of lysine and C-H of alkyl chain), 0.8-0.95 (CH_3 of alkyl chain).

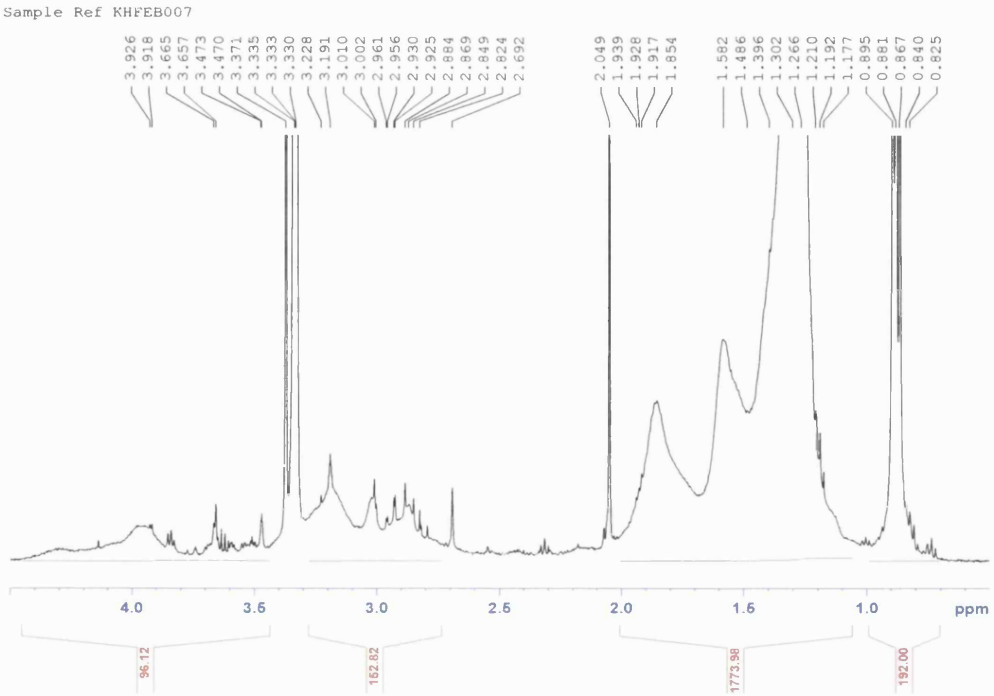

^{1}H NMR of **compound 2e** in $CD_3OD/CDCl_3$. It shows overlapping between similar protons. Chemical shift δ=3.45-4.5 (H_α of lysine, glycine and alkyl chain), 2.7-3.4 (H_ε of lysine), 1.0-2.0 (H_β, H_δ and H_γ of lysine and C-H of alkyl chain), 0.7-1.0 (CH_3 of alkyl chain).

BIBLIOGRAPHY

Abdollahi, A., Lipson, K. E., Sckell, A., Zieher, H., Klenke, F., Poerschke, D., Roth, A., Han, X., Krix, M., Bischof, M. H. P., Grone, H.-J., Debus, J., Hlatky, L., Huber, P. E., 2003. Combined therapy with direct and indirect angiogenesis inhibition results in enhanced antiangiogenic and antitumour effects. *Cancer research*, **63**, 8890-8898.

Ahmed, S. N., Brown, D. A., London, E., 1997. On the origin of sphingolipid/cholesterol-rich detergent-insoluble cell membranes: physiological concentrations of cholesterol and sphingolipid induce formation of a detergent-insoluble, liquid-ordered lipid phase in model membranes. *Biochemistry*, **36**, 10944-10953.

Albertson, N. F.1962. Organic Reactions. Wiley, New York.

Albertson, N. F., 1946. The synthesis of amino acids from ethyl acetamidomalonate and ethyl acetamidocyanoacetate. III. The use of primary halides. *J. Am. Chem. Soc.*, **68**, 450-453.

Altman, P. K. and Dittmer, D. S. Biological handbooks: Biology data book.Volume III, in: Bethesda, M. D., Federation of American Societies for Experimental Biology, 1974, pp1987-2008-2041.

Anderson, G. W., McGregor, A. C., 1957. *t*-Butyloxycarbonylamino acids and their use in peptide synthesis. *J. Am. Chem. Soc.*, **79**, 6180-6183.

Anderson, G. W., Zimmermann, J. E., Callahan, F. M., 1963. *N*-hydroxycuccinimide esters in peptide synthesis. *J. Am. Chem. Soc.*, **85**, 3039.

Arrieta, O., Guevara, P., Reyes, S., Ortiz, A., Rembao, D., Sotelo, J., 1998. Protamine inhibits angiogenesis and growth of C6 rat glioma; a synergistic effect when combined with carmustine. *Eur. J. Cancer*, **34**, 2101-2106.

Artursson, P., 1990. Epithelial transport of drugs in cell culture. I: A model for studying the passive diffusion of drugs over intestinal absorptive (Caco-2) cells. *J. Pharm. Sci.*, **79**, 476-482.

Artursson, P., Lindmark, T., Davis, S. S., Illum, L., 1994. Effect of chitosan on the permeability of monolayers of intestinal epithelial cells (Caco-2). *Pharm. Res.*, **11**, 1358-1361.

Artursson, P., Magnusson, C., 1990. Epithelial transport of drugs in cell culture. II: Effect of extracellular calcium concentration on the paracellular transport of drugs of different lipophilicities across monolayers of intestinal epithelial (Caco-2) cells. *J. Pharm. Sci.*, **79**, 595-600.

Atherton, E. and Sheppard, R. C.1989. Solid Phase Peptide Synthesis- a Practical Approach. IRL Press, Oxford.

Attwood, D. and Florence, A. T. Pharmaceutical aspects of solubilisation, *Surfactant Systems: Their Chemistry, Pharmacy and Biology,* Chapman and Hall, London, 1983b, pp361-370.

Attwood, D. and Florence, A. T. Micellization, *Surfactant Systems. Their Chemistry, Pharmacy and Biology,* Chapman and Hall, London, 1983a, pp72-117.

Azizkhan, R. G., Azizkhan, J. C., Zetter, B. R., Folkman, J., 1980. Mast cell heparin stimulates migration of capillary endothelial cells in vitro. *J. Exp. Med.*, **152**, 931-944.

Baars, M. W. P. L., Karlsson, A. J., Sorokin, V., de Waal, B. F. W., Meijer, E. W., 2000a. Supramolecular modification of the periphery of dendrimers resulting in rigidity and functionality. *Angew. Chem. Int. Ed.*, **39**, 4262-4264.

Baars, M. W. P. L., Kleppinger, R., Koch, M. H. J., Yeu, S. L., Meijer, E. W., 2000b. The localization of guests in water-soluble oligoethyleneoxy- modified poly(propylene imine) dendrimers. *Angew. Chem. Int. Ed.*, **39**, 1285-1288.

Balagurusamy, V. S. K., Ungar, G., Percec, V., Johansson, G., 1997. Rational design of the first spherical supramolecular dendrimers self-organized in a novel thermotropic cubic liquid-crystalline phase and the determination of their shape by X-ray analysis. *J. Am. Chem. Soc.*, **119**, 1539-1555.

Balzani, V., Ceroni, P., Gestermann, S., Gorka, M., Kauffmann, C., Vogtle, F., 2002. Fluorescent guests hosted in fluorescent dendrimers. *Tetrahedron*, **58**, 629-637.

Bartholomew, R. F., Davidson, R. S., 1971. The photosensitised oxidation of amines part II: the use of dyes as photosensitisers: evidence that singlet oxygen is not involved. *J. Chem. Soc. C*, 2347-2350.

Beezer, A. E., King, A. S. H., Martin, I. K., Mitchel, J. C., Twyman, L. J., Wain, C. F., 2003. Dendrimers as potential drug carriers; encapsulation of acidic hydrophobes within water soluble PAMAM derivatives. *Tetrahedron*, **59**, 3873-3880.

Blanzat, M., Turrin, C. O., Perez, E., Rico-Lattes, I., Caminade, A. M., Majoral, J. P., 2002. Phosphorus-containing dendrimers bearing galactosylceramide analogs: self-assembly properties. *Chem. Commun. (Camb.)*, **17**, 1864-1865.

Bleiberg, I., Fabian, I., Aronson, M., 1981. Mode of binding and internalization into mouse macrophages of heparin complexed with polycations. *Biochim. Biophys. Acta*, **674**, 345-353.

Bo, Z. S., Zhang, X., Yang, M. L., Shen, J. C., 1997. The self-assembled dendritic supramolecular complex based on electrostatic attraction. *Chemical Journal of Chinese Universities-Chinese*, **18**, 326-328.

Bodanszky, M., 1955. Synthesis of peptides by aminolysis of nitrophenyl esters. *Nature*, **175**, 685.

Bodanszky, M.1993. Principles of Peptide Synthesis. Second Edition, Springer-Verlag, Berlin.

Bolzacchini, E., Consonni, V., Lucini, R., Orlandi, M., Rindone, B., 1998. High-performance size-exclusion chromatographic behaviour of substituted benzoylpoly-L-lysines by principal component analysis and molecular dynamics simulation. *J. Chromatogr.*, **813**, 255-265.

Borchard, R. E., Barnes, C. D., and Eltherington, L. G.1990. Drug Dosage in Laboratory Animals: A Handbook. The Telford Press, Caldwell, NJ.

Braunschweiler, L., Ernst, R. R., 1983. Coherence transfer by isotropic mixing-application to proton correlation spectroscopy. *J. Magn. Reson.*, **53**, 521-528.

Caminati, G., Turro, N. J., Tomalia, D. A., 1990. Photophysical investigation of starburst dendrimers and their interactions with anionic and cationic surfactants. *J. Am. Chem. Soc.*, **112**, 8515-8522.

Caramazza, I., D'Atri, G., Bossi, M. L., De, P. F., D'Angelo, L., Crema, A., 1991. Intraduodenal absorption of the new UF-heparin salt ITF 1057 in the conscious dog. *Thromb. Res.*, **62**, 785-789.

Carpino, L. A., Han, G. Y., 1970. The 9-fluorenylmethoxycarbonyl function, a new base-sensitive amino protecting group. *J. Am. Chem. Soc.*, **92**, 5748-5749.

Carpino, L. A., Han, G. Y., 1972. The 9-fluorenylmethoxycarbonyl amino-protecting group. *J. Org. Chem.*, **37**, 3404-3409.

Chantrenne, H., 1947. Hippuric acid formation from glycine and dibenzoylphosphate. *Nature*, **160**, 603-604.

Chapman, T. M., Hillyer, G. L., Mahan, E. J., Shaffer, K. A., 1994. Hydraamphiphiles: novel linear dendritic block copolymer surfactants. *J. Am. Chem. Soc.*, **116**, 11195-11196.

Collett, A., Sims, E., Walker, D., He, Y. L., Ayrton, J., Rowland, M., Warhurst, G., 1996. Comparison of HT29-18-C1 and Caco-2 cell lines as models for studying intestinal paracellular drug absorption. *Pharm. Res.*, **13**, 216-221.

Cremers, H. F., Kwon, G., Bae, Y. H., Kim, S. W., Verrijk, R., Noteborn, H. P., Feijen, J., 1994. Preparation and characterization of albumin-heparin microspheres. *Biomaterials*, **15**, 38-48.

Curtius, Th., 1902. Synthetische versuche mit hippurazid. *Ber. dtsch. Chem. Ges.*, **35**, 3226-3228.

D'Emanuele, A., Jevprasesphant, R., Penny, J., Attwood, D., 2004. The use of a dendrimer-propranolol prodrug to bypass efflux transporters and enhance oral bioavailability. *J. Control. Rel.*, **95**, 447-453.

Dal, P. A., Acquasaliente, M., Geron, M. R., Andriuoli, G., 1989. New heparin complexes active by intestinal absorption: I-multiple ion pairs with basic organic compounds. *Thromb. Res.*, **56**, 119-124.

De La, M. A., Parra, J. L., 1994. Vesicle-micelle structural transition of phosphatidylcholine bilayers and Triton X-100. *Biochem. J.*, **303**, 907-914.

Deierkauf, F. A., Beukers, H., Deierkauf, M., Riemersma, J. C., 1977. Phagocytosis by rabbit polymorphonuclear leukocytes: the effect of albumin and polyamino acids on latex uptake. *J. Cell Physiol*, **92**, 169-175.

Denkelwalter, R. G., Kolc, J., Lukasavage, W. J., 1981. Macromolecular highly branched homogenous compound based on lysine units. *U. S. Patent. 4 289 872.*

Dennis, E. A., 1974. Formation and characterization of mixed micelles of the nonionic surfactant Triton X-100 with egg, dipalmitoyl, and dimyristoyl phosphatidylcholines. *Arch. Biochem. Biophys.*, **165**, 764-773.

Diehl, K. H., Hull, R., Morton, D., Pfister, R., Rabemampianina, Y., Smith, D., Vidal, J. M., van, d., V, 2001. A good practice guide to the administration of substances and removal of blood, including routes and volumes. *J. Appl. Toxicol.*, **21**, 15-23.

Dourtoglou, V., Gross, B., Lambropoulou, V., Zioudrou, C., 1983. *O*-Benzotriazolyl-N,N,N',N'-tetramethyluronium hexafluorophosphate as coupling reagent for the synthesis of peptides of biological interest. *Synthesis-Stuttgart*, **7**, 572-574.

Duncan, R., Pratten, M. K., Lloyd, J. B., 1979. Mechanism of polycation stimulation of pinocytosis. *Biochim. Biophys. Acta*, **587**, 463-475.

Dunn, J. M., Hollister, A. S., 1995. Oral bioavailability of heparin using a novel delivery system. *Curr. Ther. Res. Clin. E*, **56**, 738-745.

Dykes, G. M., Brierley, L. J., Smith, D. K., McGrail, P. T., Seeley, G. J., 2001. Supramolecular solubilisation of hydrophilic dyes by using individual dendritic branches. *Chem. Eur. J.*, **7**, 4730-4739.

Dykes, G. M., Smith, D. K., 2003. Supramolecular dendrimer chemistry: using dendritic crown ethers to reversibly generate functional assemblies. *Tetrahedron*, **59**, 3999-4009.

El-Sayed, M., Ginski, M., Rhodes, C., Ghandehari, H., 2002. Transepithelial transport of poly(amidoamine) dendrimers across Caco-2 cell monolayers. *J. Control. Release*, **81**, 355-365.

El-Sayed, M., Kiani, M. F., Naimark, M. D., Hikal, A. H., Ghandehari, H., 2001. Extravasation of Poly(amidoamine) (PAMAM) dendrimers across microvascular network endothelium. *Pharm. Res.*, **18**, 23-28.

Elemans, J. A., Boerakker, M. J., Holder, S. J., Rowan, A. E., Cho, W. D., Percec, V., Nolte, R. J., 2002. Plastic- and liquid-crystalline architectures from dendritic receptor molecules. *Proc. Natl. Acad. Sci. U. S A*, **99**, 5093-5098.

Esumi, K., Chiba, T., Mizutani, H., Shoji, K., Torigoe, K., 2001. Physicochemical properties of aqueous mixed solutions of sugar-persubstituted poly(amidoamine)dendrimers and anionic surfactants. *Colloids Surf. A*, **179**, 103-109.

Esumi, K., Kuwabara, K., Chiba, T., Kobayashi, F., Mizutani, H., Torigoe, K., 2002. Interactions between a hydrophobically modified poly(amidoamine)dendrimer and surfactants in aqueous solutions. *Colloids Surf. A*, **197**, 141-146.

Esumi, K., Saika, R., Miyazaki, M., Torigoe, K., Koide, Y., 2000. Interactions of poly(amidoamine)dendrimers having surface carboxyl groups with cationic surfactants. *Colloids Surf. A*, **166**, 115-121.

Fabian, I., Bleiberg, I., Aronson, M., 1978. Increased uptake and desulphation of heparin by mouse macrophages in the presence of polycations. *Biochim. Biophys. Acta*, **544**, 69-76.

Farng, K. F., Nelson, K. G., 1977. Effects of polyelectrolytes on drug transport II: permeation. *J. Pharm. Sci.*, **66**, 1611-1614.

Fischer, E., 1903. Synthese von derivaten der polypeptide. *Ber. dtsch. Chem. Ges.*, **36**, 2094-2106.

Florence, A. T., 1997. The oral absorption of micro- and nanoparticulates: neither exceptional nor unusual. *Pharm. Res.*, **14**, 259-266.

Florence, A. T., Hussain, N., 2001. Transcytosis of nanoparticle and dendrimer delivery systems: evolving vistas. *Adv. Drug Deliv. Rev.*, **50**, S69-S89.

Florence, A. T., Sakthivel, T., Toth, I., 2000. Oral uptake and translocation of a polylysine dendrimer with a lipid surface. *J. Control Release*, **65**, 253-259.

Folkman, J., 1995. Clinical applications of research on angiogenesis. *N. Engl. J. Med.*, **333**, 1757-1763.

Folkman, J., Klagsbrun, M., 1987. Angiogenic factors. *Science*, **235**, 442-447.

Fuchs, S., Kapp, T., Otto, H., Schöneberg, T., Franke, P., Gust, R., Schlüter, A. D., 2004. A surface-modified dendrimer set for potential application as drug delivery vehicles: synthesis, in vitro toxicity, and intracellular localization. *Chem. Eur. J.*, **10**, 1167-1192.

Gazumyan, A., Mitsner, B., Ellestad, G. A., 2000. Novel anti-RSV dianionic dendrimer-like compounds: design, synthesis and biological evaluation. *Curr. Pharm. Des*, **6**, 525-546.

Gelman, R. A., Blackwell, J., 1973. Heparin-polypeptide interactions in aqueous solution. *Arch. Biochem. Biophys.*, **159**, 427-433.

Gibbons, W. A., Hughes, R. A., Charalambous, M., Christodoulou, M., Szeto, A., Aulabaugh, A. E., Mascagni, P., Toth, I., 1990. Lipidic peptides, I: synthesis, resolution and structural elucidation of lipidic amino acids and their homo- and hetero-oligomers. *Liebigs Ann. Chem.*,**12**, 1175-1183.

Gillies, E. R., Fréchet, J. M. J., 2004. Development of acid-sensitive copolymer micelles for drug delivery. *Pure and Applied Chemistry*, **76**, 1295-1307.

Gillies, E. R., Jonsson, T. B., Fréchet, J. M., 2004. Stimuli-responsive supramolecular assemblies of linear-dendritic copolymers. *J. Am. Chem Soc.*, **126**, 11936-11943.

Gitsov, I., Wooley, K. L., Fréchet, J. M. J., 1992. Novel polyether copolymers consisting of linear and dendritic blocks. *Angew. Chem. Int. Ed. Engl.*, **31**, 1200-1202.

Goddard, E. D., 1986b. Polymer-Surfactant Interaction Part II. Polymer and Surfactant of Opposite Charge. *Colloids Surf.*, **19**, 301-329.

Goddard, E. D., 1986a. Polymer-Surfactant Interaction Part I. Uncharged Water-Soluble Polymers and Charged Surfactants. *Colloids Surf.*, **19**, 255-299.

Goetheer, E. L. V., Baars, M. W. P. L., van den Broeke, L. J. P., Meijer, E. W., Keurentjes, J. T. F., 2000. Functionalised poly(propylene imine) dendrimers as novel phase transfer catalysts in supercritical carbon dioxide. *Industrial & Engineering Chemistry Research*, **39**, 4634-4640.

Goni, F. M., Alonso, A., 2000. Spectroscopic techniques in the study of membrane solubilisation, reconstitution and permeabilization by detergents. *Biochim. Biophys. Acta*, **1508**, 51-68.

Gonze, M. D., Manord, J. D., Leone-Bay, A., Baughman, R. A., Garrard, C. L., Sternbergh, W. C., III, Money, S. R., 1998. Orally administered heparin for preventing deep venous thrombosis. *Am. J. Surg.*, **176**, 176-178.

Gopidas, K. R., Leheny, A. R., Caminati, G., Turro, N. J., Tomalia, D. A., 1991. Photophysical Investigation of Similarities Between Starburst Dendrimers and Anionic Micelles. *J. Am. Chem Soc.*, **113**, 7335-7342.

Gorman, C. B., Smith, J. C., 2000. Iron-sulfur core dendrimers display dramatically different electrochemical behaviour in films compared to solution. *J. Am. Chem Soc.*, **122**, 9342-9343.

Guarini, S., Ferrari, W., 1985. Sodium deoxycholate promotes the absorption of heparin administered orally, probably by acting on gastrointestinal mucosa, in rats. *Experientia*, **41**, 350-352.

Hawker, C. J., Fréchet, J. M. J., 1990. Preparation of polymers with controlled molecular architecture - a new convergent approach to dendritic macromolecules. *J. Am. Chem Soc.*, **112**, 7638-7647.

Hawker, C. J., Wooley, K. L., Fréchet, J. M. J., 1993. Unimolecular micelles and globular amphiphiles: dendritic macromolecules as novel recyclable solubilisation agents. *J. Chem. Soc. Perkin Trans. I*, **12**, 1287-1297.

Higashi, N., Koga, T., Niwa, M., 2002. Enantioselective binding and stable encapsulation of alpha-amino acids in a helical poly(L-glutamic acid)-shelled dendrimer in aqueous solutions. *Chem. Bio. Chem.*, **3**, 448-454.

Hood, J. D., Bednarski, M., Frausto, R., Guccione, S., Reisfeld, R. A., Xiang, R., Cheresh, D. A., 2002. Tumour regression by targeted gene delivery to the neovasculature. *Science*, **296**, 2404-2407.

Hudson, D., 1988. Methodological implications of simultaneous solid-phase synthesis. 1. comparison of different coupling procedures. *J. Org. Chem.*, **53**, 617-624.

Jain, R. K., Schlenger, K., Hockel, M., Yuan, F., 1997. Quantitative angiogenesis assays:progress and problems. *Nature Med.*, **11**, 1203-1208.

Jandik, K. A., Kruep, D., Cartier, M., Linhardt, R. J., 1996. Accelerated stability studies of heparin. *J. Pharm. Sci.*, **85**, 45-51.

Jang, W. D., Jiang, D. L., Aida, T., 2000. Dendritic physical gel: hierarchical self-organization of a peptide-core dendrimer to form a micrometer-scale fibrous assembly. *J. Am. Chem. Soc.*, **122**, 3232-3233.

Jansen, J. F. G. A., Debrabandervandenberg, E. M. M., Meijer, E. W., 1994. Encapsulation of Guest Molecules Into A Dendritic Box. *Science*, **266**, 1226-1229.

Jansen, J. F. G. A., Meijer, E. W., 1995. The dendritic box: shape-selective liberation of encapsulated guests. *J. Am. Chem. Soc.*, **117**, 4417.

Jevprasesphant, R., Penny, J., Attwood, D., D'Emanuele, A., 2004. Transport of dendrimer nanocarriers through epithelial cells via the transcellular route. *J. Control. Release*, **97**, 259-267.

Jevprasesphant, R., Penny, J., Attwood, D., McKeown, N. B., D'Emanuele, A., 2003. Engineering of dendrimer surfaces to enhance transepithelial transport and reduce cytotoxicity. *Pharm. Res.*, **20**, 1543-1550.

Jones, J.1999. Amino Acid and Peptide Synthesis. Oxford University Press, Oxford.

Kaiser, E., Colescott, R. L., Bossinger, C. D., Cook, P., 1970. Color test for detection of free terminal amino groups in the solid-phase synthesis of peptides. *Anal. Biochem.*, **34**, 595-598.

Karlsson, J., Artursson, P., 1991. A Method for the determination of cellular permeability coefficients and aqueous boundary-layer thickness in monolayers of intestinal epithelial (Caco-2) cells grown in permeable filter chambers. *Int. J. Pharm.*, **71**, 55-64.

Kasai, S., Nagasawa, H., Shimamura, M., Uto, Y., Hori, H., 2002. Design and synthesis of antiangiogenic/heparin-binding arginine dendrimer mimicking the surface of endostatin. *Bioorg. Med. Chem. Lett.*, **12**, 951-954.

Kent, S. B. H., 1988. Chemical synthesis of peptides and proteins. *Ann. Rev. Biochem.*, **57**, 957-989.

Kerbel, R. S., 2000. Tumour angiogenesis: past, present and the near future. *Carcinogenesis*, **21**, 505-515.

Khopade, S. A., Khopade, A. J., Chauhan, A. S., Tripathi, P., Jain, N. K., 1999. A unimolecular reverse micellar dendrimer for oral delivery of 5-Flurouracil. *Proc. Int. Symp. Control. Rel. Bioact. Mater.*, **26**, 6354.

Kim, B. Y., Bruening, M. L., 2003. pH-dependent growth and morphology of multilayer dendrimer/poly(acrylic acid) films. *Langmuir*, **19**, 94-99.

Kim, C., Kim, K. T., Chang, Y., Song, H. H., Cho, T. Y., Jeon, H. J., 2001. Supramolecular assembly of amide dendrons. *J. Am. Chem Soc.*, **123**, 5586-5587.

Kim, C., Lee, S. J., Lee, I. H., Kim, K. T., 2003. Stabilization of supramolecular nanostructures induced by self-assembly of dendritic building blocks. *Chem. Mater.*, **15**, 3638-3642.

Kim, T. D., Sakon, M., Kawasaki, T., Kambayashi, J., Ohshiro, T., Mori, T., 1986. Studies on liposome-encapsulated heparin. *Thromb. Res.*, **43**, 603-612.

Kitamura, N., Sagawa, K., Takehara, M., 1987. Cosmetics containing alpha-amino fatty acids. *Chem. Abstr.*, **106**, 182464s.

Knipp, G. T., Ho, N. F., Barsuhn, C. L., Borchardt, R. T., 1997. Paracellular diffusion in Caco-2 cell monolayers: effect of perturbation on the transport of hydrophilic compounds that vary in charge and size. *J. Pharm. Sci.*, **86**, 1105-1110.

Knorr, R., Trzeciak, A., Bannwarth, W., Gillesson, D., 1989. New coupling reagents in peptide chemistry. *Tetrahedron lett.*, **30**, 1927-1930.

Kolhe, P., Misra, E., Kannan, R. M., Kannan, S., Lieh-Lai, M., 2003. Drug complexation, in vitro release and cellular entry of dendrimers and hyperbranched polymers. *Int. J. Pharm.*, **259**, 143-160.

Konig, W., Geiger, R., 1970. Eine neue methode zur synthese von peptiden: aktivierung der carboxylgruppe mit dicyclohexylcarbodiimid unter zusatz von 1-hydroxy-benzotriazolen. *Chem. Ber.*, **103**, 788-798.

Kovacs, J., Kisfaludy, L., Ceprini, M. Q., 1967. On optical purity of peptide active esters prepared by N,N'-dicyclohexylcarbodiimide and complexes of N,N'-dicyclohexylcarbodiimide-pentachlorophenol and N,N'-dicyclohexylcarbodiimide-pentafluorophenol. *J. Am. Chem. Soc.*, **89**, 183.

Krasnici, S., Werner, A., Eichhorn, M. E., Schmitt-Sody, M., Pahernik, S. A., Sauer, B., Schulze, B., Teifel, M., Michaelis, U., Naujoks, K., Dellian, M., 2003. Effect of the surface charge of liposomes on their uptake by angiogenic tumour vessels. *Int. J. Cancer*, **105**, 567.

Krishna, T. R., Jayaraman, N., 2003. Synthesis of poly(propyl ether imine) dendrimers and evaluation of their cytotoxic properties. *J. Org. Chem.*, **68**, 9694-9704.

Kuzdzal, S. A., Monnig, C. A., Newkome, G. R., Moorefield, C. N., 1994. Dendrimer Electrokinetic Capillary Chromatography - Unimolecular Micellar Behaviour of Carboxylic-Acid Terminated Cascade Macromolecules. *J. Chem. Soc. Chem. Comm.*, **18**, 2139-2140.

Larson, C. L., Tucker, S. A., 2001. Intrinsic fluorescence of carboxylate-terminated polyamidoamine dendrimers. *Appl. Spectrosc.*, **55**, 679-683.

Lee, Y.-K., Kim, S. H., Byun, Y., 2000. Oral delivery of new heparin derivatives in rats. *Pharm. Res.*, **17**, 1259-1264.

Leone-Bay, A., Paton, D. R., Variano, B., Leipold, H., Rivera, T., Miura-Fraboni, J., Baughman, R. A., Santiago, N., 1998. Acylated non-á-amino acids as novel agents for the oral delivery of heparin sodium USP. *J. Control. Rel.*, **50**, 41-49.

Liang, J. F., Li, Y. T., Song, H., Park, Y. J., Naik, S. S., Yang, V. C., 2002. ATTEMPTS: a heparin/protamine-based delivery system for enzyme drugs. *J. Control. Release*, **78**, 67-79.

Liang, J. F., Zhen, L., Chang, L. C., Yang, V. C., 2003. A less toxic heparin antagonist--low molecular weight protamine. *Biochemistry (Mosc.)*, **68**, 116-120.

Liu, M., Fréchet, J. M., 1999. Designing dendrimers for drug delivery. *Pharm. Sci. Tech. Today*, **2**, 393-401.

Loup, C., Zanta, M. A., Caminade, A. M., Majoral, J. P., Meunier, B., 1999. Preparation of water-soluble cationic phosphorus-containing dendrimers as DNA transfecting agents. *Chem. Eur. J.*, **5**, 3644-3650.

Malik, N., Wiwattanapatapee, R., Klopsch, R., Lorenz, K., Frey, H., Weener, J. W., Meijer, E. W., Paulus, W., Duncan, R., 2000. Dendrimers: relationship between

structure and biocompatibility in vitro, and preliminary studies on the biodistribution of 125I-labelled polyamidoamine dendrimers in vivo. *J. Control. Release*, **65**, 133-148.

Martin, A. N. Diffusion and dissolution, *Physical Pharmacy: Physical Chemical Principles in the Pharmaceutical Sciences,* Williams and Wilkins, Baltimore, 1993, pp324-361.

Maszewska, M., Leclaire, J., Cieslak, M., Nawrot, B., Okruszek, A., Caminade, A. M., Majoral, J. P., 2003. Water-soluble polycationic dendrimers with a phosphoramidothioate backbone: preliminary studies of cytotoxicity and oligonucleotide/plasmid delivery in human cell culture. *Oligonucleotides.*, **13**, 193-205.

Matsueda, G. R., Stewart, J. M., 1981. A *p*-methylbenzhydralamine resin for improved solid-phase synthesis of peptide amides. *Peptides*, **2**, 45-50.

Matthews, O. A., Shipway, A. N., Stoddart, J. F., 1998. Dendrimers - Branching out from curiosities into new technologies. *Prog. Polym. Sci.*, **23**, 1-56.

Merrifield, R. B., 1962. Peptide synthesis on a solid polymer. *Fed. Proc. Fed. Amer. Soc. Exp. Biol.*, **21**, 412.

Merrifield, R. B., 1963. Solid phase peptide synthesis. 1. The synthesis of a tetrapeptide. *J. Am. Chem. Soc.*, **85**, 2149-2154.

Milhem, O. M., Myles, C., McKeown, N. B., Attwood, D., D'Emanuele, A., 2000. Polyamidoamine Starburst dendrimers as solubility enhancers. *Int. J. Pharm.*, **197**, 239-241.

Minard-Basquin, C., Weil, T., Hohner, A., Radler, J. O., Mullen, K., 2003. A polyphenylene dendrimer-detergent complex as a highly fluorescent probe for bioassays. *J. Am. Chem. Soc.*, **125**, 5832-5838.

Mizutani, H., Torigoe, K., Esumi, K., 2002. Physicochemical properties of quaternized poly(amidoamine) dendrimers with alkyl groups and of their mixtures with sodium dodecyl sulphate. *J. Colloid Interface Sci.*, **248**, 493-498.

Moorefield, C. N., Newkome, G., 2003. Unimolecular micelles: supramolecular use of dendritic constructs to create versatile molecular containers. *C. R. Chemi.*, **6**, 715-724.

Morton, A. K., Edwards, H. E., Allen, J. C., Phillips, G. O., 1981. An evaluation of the oral-administration of commercial and fractionated heparin samples in rats. *Int. J. Pharm.*, **9**, 321-335.

Mosmann, T., 1983. Rapid colorimetric assay for cellular growth and survival: application to proliferation and cytotoxicity assays. *J. Immunol. Methods*, **65**, 55-63.

Naylor, A. M., Goddard, W. A., Kiefer, G. E., Tomalia, D. A., 1989. Starburst dendrimers. 5. molecular shape control. *J. Am. Chem. Soc.*, **111**, 2339-2341.

Nellans, N. H., 1991. Mechanisms of peptide and protein absorption. 1. Paracellular intestinal transport- Modulation of absorption. *Adv. Drug Deliv. Rev.*, **7**, 339-364.

New, R. R. C. Preparation of Liposomes, *Liposomes: a Practical Approach,* Oxford University Press, Oxford, 1989, pp33-104.

Newkome, G. R., Baker, G. R., Arai, S., Saunders, M. J., Russo, P. S., Theriot, K. J., Moorefield, C. N., Rogers, L. E., Miller, J. E., Lieux, T. R., Murray, M. E., Phillips, B., Pascal, L., 1990. Cascade Molecules .6. Synthesis and Characterization of 2-Directional Cascade Molecules and Formation of Aqueous Gels. *J. Am. Chem Soc.*, **112**, 8458-8465.

Newkome, G. R., He, E. F., Moorefield, C. N., 1999. Suprasupermolecules with novel properties: Metallodendrimers. *Chem. Rev.*, **99**, 1689-1746.

Newkome, G. R., Lin, X. F., Yaxiong, C., Escamilla, G. H., 1993. 2-Directional Cascade Polymer Synthesis - Effects of Core Variation. *J. Org. Chem.*, **58**, 3123-3129.

Newkome, G. R., Moorefield, C. N., Baker, G. R., Saunders, M. J., Grossman, S. H., 1991. Unimolecular micelles. *Angew. Chem. Int. Ed.*, **30**, 1178-1180.

Newkome, G. R., Yao, Z. Q., Baker, G. R., Gupta, V. K., 1985. Micelles .1. Cascade Molecules - A New Approach to Micelles - A [27]-Arborol. *J. Org. Chem.*, **50**, 2003-2004.

Nigavekar, S. S., Sung, L. Y., Llanes, M., El-Jawahri, A., Lawrence, T. S., Becker, C. W., Balogh, L., Khan, M. K., 2004. 3H dendrimer nanoparticle organ/tumour distribution. *Pharm. Res.*, **21**, 476-483.

Ohsaki, M., Okuda, T., Wada, A., Hirayama, T., Niidome, T., Aoyagi, H., 2002. In vitro gene transfection using dendritic poly(L-lysine). *Bioconjugate Chem*, **13**, 510-517.

Pantzar, N., Lundin, S., Wester, L., Westrom, B. R., 1994. Bidirectional small-intestinal permeability in the rat to some common marker molecules in vitro. *Scand. J. Gastroenterol.*, **29**, 703-709.

Papahadjopoulos, D., Jacobson, K., Nir, S., Isac, T., 1973. Phase transitions in phospholipid vesicles:fluorescence polarization and permeability measurements concerning the effect of temperature and cholesterol. *Biochim. Biophys. Acta*, **311**, 330-334.

Partearroyo, M. A., Urbaneja, M. A., Goni, F. M., 1992. Effective detergent/lipid ratios in the solubilisation of phosphatidylcholine vesicles by Triton X-100. *FEBS Lett.*, **302**, 138-140.

Passirani, C., Barratt, G., Devissaguet, J. P., Labarre, D., 1998. Long-circulating nanoparticles bearing heparin or dextran covalently bound to poly(methyl methacrylate). *Pharm. Res.*, **15**, 1046-1050.

Percec, V., Cho, W.-D., Ungar, G., Yeardley, D. J. P. J., 2001. Synthesis and structural analysis of two constitutional isomeric libraries of AB(2)-based monodendrons and supramolecular dendrimers. *J. Am. Chem. Soc.*, **123**, 1302-1315.

Percec, V., Chu, P. W., Ungar, G., Zhou, J. P., 1995. Rational design of the first nonspherical dendrimer which displays calamitic nematic and smectic thermotropic liquid-crystalline phases. *J. Am. Chem. Soc.*, **117**, 11441-11454.

Percec, V., Glodde, M., Bera, T. K., Miura, Y., Shiyanovskaya, I., Singer, K. D., Balagurusamy, V. S., Heiney, P. A., Schnell, I., Rapp, A., Spiess, H. W., Hudson, S. D., Duan, H., 2002. Self-organization of supramolecular helical dendrimers into complex electronic materials. *Nature*, **419**, 384-387.

Percec, V., Tomazos, D., Heck, J., Blackwell, H., Ungar, G., 1994. Self-assembly of taper-shaped monoesters of oligo(ethylene oxide) with 3,4,5-tris(N-dodecan-1-yloxy)benzoic acid and of their polymethacrylates into tubular supramolecular architectures displaying a columnar hexagonal mesophase. *J. Chem. Soc. , Perkin Trans. 2*, **1**, 31-44.

Peterson, M. W., Gruenhaupt, D., 1990. Protamine increases the permeability of cultured epithelial monolayers. *J. Appl. Physiol*, **68**, 220-227.

Piotti, M. E., Rivera, F., Bond, R., Hawker, C. J., Fréchet, J. M. J., 1999. Synthesis and catalytic activity of unimolecular dendritic reverse micelles with "internal" functional groups. *J. Am. Chem Soc.*, **121**, 9471-9472.

Pisano, C., Aulicino, C., Vesci, L., Casu, B., Naggi, A., Torri, G., Ribatti, D., Belleri, M., Rusnati, M., Presta, M., 2005. Undersulfated, low-molecular-weight glycol-split heparin as an antiangiogenic VEGF antagonist. *Glycobiology*, **15**, 1C-6C.

Pistolis, G., Malliaris, A., Paleos, C. M., Tsiourvas, D., 1997. Study of poly(amidoamine) starburst dendrimers by fluorescence probing. *Langmuir*, **13**, 5870-5875.

Pistolis, G., Malliaris, A., Tsiourvas, D., Paleos, C. M., 1999. Poly(propyleneimine) dendrimers as pH-sensitive controlled-release systems. *Chemistry-A European Journal*, **5**, 1440-1444.

Purohit, G., Sakthivel, T., Florence, A. T., 2003. The interaction of cationic dendrons with albumin and their diffusion through cellulose membranes. *Int. J. Pharm.*, **254**, 37-41.

Quintanar-Guerrero, D., Allemann, E., Doelker, E., Fessi, H., 1998. Preparation and characterization of nanocapsules from preformed polymers by a new process based on emulsification-diffusion technique. *Pharm. Res.*, **15**, 1056-1062.

Ramaswamy, C., Sakthivel, T., Wilderspin, A. F., Florence, A. T., 2003b. Lipidic cationic peptide dendrons as a DNA delivery system: influence of lipid chain in stability to disruption by polyanion-heparin. *J. Pharm. Pharmacol.*, **55**, -S-14.

Ramaswamy, C., Sakthivel, T., Wilderspin, A. F., Florence, A. T., 2003a. Dendriplexes and their characterisation. *Int. J. Pharm.*, **254**, 17-21.

Richter-Egger, D. L., Landry, J. C., Tesfai, A., Tucker, S. A., 2001a. Spectroscopic investigations of polyamido amine starburst dendrimers using the solvatochromic probe phenol blue. *J. Phys. Chem. A*, **105**, 6826-6833.

Richter-Egger, D. L., Li, H., Tucker, S. A., 2000. Spectroscopic investigations of polyamido amine starburst dendrimers with reichardt's ET-30 dye. *Appl. Spectrosc.*, **54**, 1151-1156.

Richter-Egger, D. L., Tesfai, A., Tucker, S. A., 2001b. Spectroscopic investigations of poly(propyleneimine)dendrimers using the solvatochromic probe phenol blue and comparisons to poly(amidoamine) dendrimers. *Anal. Chem.*, **73**, 5743-5751.

Rivera, T. M., Leone-Bay, A., Paton, D. R., Leipold, H. R., Baughman, R. A., 1997. Oral delivery of heparin in combination with sodium N-[8-(2-hydroxybenzoyl)amino]caprylate: pharmacological considerations. *Pharm. Res.*, **14**, 1830-1834.

Robb, I. D.1981. Anionic Surfactants: Physical Chemistry of Surfactant Actions. E. H. Lucassen-Reynders, Marcel Dekker, New York.

Roberts, J. C., Bhalgat, M. K., Zera, R. T., 1996. Preliminary biological evaluation of polyamidoamine (PAMAM) Starburst dendrimers. *J. Biomed. Mater. Res.*, **30**, 53-65.

Robson, R. J., Dennis, E. A., 1979. Mixed micelles of sphingomyelin and phosphatidylcholine with nonionic surfactants. Effect of temperature and surfactant polydispersity. *Biochim. Biophys. Acta*, **573**, 489-500.

Ruponen, M., Yla-Herttuala, S., Urtti, A., 1999. Interactions of polymeric and liposomal gene delivery systems with extracellular glycosaminoglycans: physicochemical and transfection studies. *Biochim. Biophys. Acta*, **1415**, 331-341.

Sadler, K., Tam, J. P., 2002. Peptide dendrimers: applications and synthesis. *J. Biotechnol.*, **90**, 195-229.

Sakharov, D. V., Jie, A. F., Bekkers, M. E., Emeis, J. J., Rijken, D. C., 2001. Polylysine as a vehicle for extracellular matrix-targeted local drug delivery, providing high accumulation and long-term retention within the vascular wall. *Arterioscler. Thromb. Vasc. Biol.*, **21**, 943-948.

Sakthivel, T., Florence, A. T., 2003. Adsorption of amphipathic dendrons on polystyrene nanoparticles. *Int. J. Pharm.*, **254**, 23-26.

Sakthivel, T., Toth, I., Florence, A. T., 1998. Synthesis and physicochemical properties of lipidic polyamide dendrimers. *Pharm. Res.*, **15**, 776-785.

Sakthivel, T., Toth, I., Florence, A. T., 1999. Distribution of a lipidic 2.5 nm diameter dendrimer carrier after oral administration. *Int. J. Pharm.*, **183**, 51-55.

SayedSweet, Y., Hedstrand, D. M., Spinder, R., Tomalia, D. A., 1997. Hydrophobically modified poly(amidoamine) (PAMAM) dendrimers: Their properties at the air-water interface and use as nanoscopic container molecules. *Journal of Materials Chemistry*, **7**, 1199-1205.

Schenning, A. P. H. J., Elissen-Roman, C., Weener, J. W., Baars, M. W. P. L., van der Gaast, S. J., Meijer, E. W., 1998. Amphiphilic dendrimers as building blocks in supramolecular assemblies. *J. Am. Chem. Soc.*, **120**, 8199-8208.

Schick, B. P., Gradowski, J. F., San Antonio, J. D., Martinez, J., 2001. Novel design of peptides to reverse the anticoagulant activities of heparin and other glycosaminoglycans. *Thromb. Haemost.*, **85**, 482-487.

Shah, D. S., Sakthivel, T., Toth, I., Florence, A. T., Wilderspin, A. F., 2000. DNA transfection and transfected cell viability using amphipathic asymmetric dendrimers. *Int. J. Pharm.*, **208**, 41-48.

Shaunak, S., Thomas, S., Gianasi, E., Godwin, A., Jones, E., Teo, I., Mireskandari, K., Luthert, P., Duncan, R., Patterson, S., Khaw, P., Brocchini, S., 2004. Polyvalent dendrimer glucosamine conjugates prevent scar tissue formation. *Nat. Biotechnol.*, **22**, 977-984.

Sheehan, J. C., Hess, G. P., 1955. A new method of forming peptide bonds. *J. Am. Chem. Soc.*, **77**, 1067-1068.

Shen, W. C., Ryser, H. J., 1978. Conjugation of poly-L-lysine to albumin and horseradish peroxidase: a novel method of enhancing the cellular uptake of proteins. *Proc. Natl. Acad. Sci. U. S. A*, **75**, 1872-1876.

Shen, W. C., Ryser, H. J., 1981. Poly(L-lysine) has different membrane transport and drug-carrier properties when complexed with heparin. *Proc. Natl. Acad. Sci. U. S. A*, **78**, 7589-7593.

Shultz, L. G., Zimmerman, S. C., 1999. Dendrimers: potential drugs and drug delivery agents. *Pharm. News*, **6**, 25-29.

Sideratou, Z., Tsiourvas, D., Paleos, C. M., 2000. Quaternized poly(propylene imine) dendrimers as novel pH- sensitive controlled-release systems. *Langmuir*, **16**, 1766-1769.

Solassol, J., Crozet, C., Perrier, V., Leclaire, J., Beranger, F., Caminade, A. M., Meunier, B., Dormont, D., Majoral, J. P., Lehmann, S., 2004. Cationic phosphorus-containing dendrimers reduce prion replication both in cell culture and in mice infected with scrapie. *J. Gen. Virol.*, **85**, 1791-1799.

Srinivasan, M., Harris, A. L., 2002. Drug inhibition of angiogenesis. *Curr. Opin. Pharm.*, **2**, 403-414.

Stevelmans, S., vanHest, J. C. M., Jansen, J. F. G. A., vanBoxtel, D. A. F. J., vandenBerg, E. M. M. D., Meijer, E. W., 1996. Synthesis, characterization, and guest-host properties of inverted unimolecular dendritic micelles. *J. Am. Chem Soc.*, **118**, 7398-7399.

Tajarobi, F., El-Sayed, M., Rege, B. D., Polli, J. E., Ghandehari, H., 2001. Transport of poly amidoamine dendrimers across Madin-Darby canine kidney cells. *Int. J. Pharm.*, **215**, 263-267.

Takino, H., Sagawa, K., Kitamura, N., Kilahara, M., 1987. Lubricants containing alpha-amino fatty acids. *Chem. Abstr.*, **107**, 220318c.

Tam, J. P., Heath, W. F., Merrifield, R. B., 1983. S_N2 deprotection of synthetic peptides with low concentration of HF in dimethyl sulfide: evidence and application in peptide synthesis. *J. Am. Chem. Soc.*, **105**, 6442-6455.

Taylor, S., Folkman, J., 1982. Protamine is an inhibitor of angiogenesis. *Nature*, **297**, 307-312.

Thanou, M., Florea, B. I., Langemeyer, M. W., Verhoef, J. C., Junginger, H. E., 2000. N-trimethylated chitosan chloride (TMC) improves the intestinal permeation of the peptide drug buserelin in vitro (Caco-2 cells) and in vivo (rats). *Pharm. Res.*, **17**, 27-31.

Thanou, M., Nihot, M. T., Jansen, M., Verhoef, J. C., Junginger, H. E., 2001a. Mono-N-carboxymethyl chitosan (MCC), a polyampholytic chitosan derivative, enhances the intestinal absorption of low molecular weight heparin across intestinal epithelia in vitro and in vivo. *J. Pharm. Sci.*, **90**, 38-46.

Thanou, M., Verhoef, J. C., Nihot, M. T., Verheijden, J. H., Junginger, H. E., 2001b. Enhancement of the intestinal absorption of low molecular weight heparin (LMWH) in rats and pigs using Carbopol 934P. *Pharm. Res.*, **18**, 1638-1641.

Tomalia, D. A., Baker, H., Dewald, J., Hall, M., Kallos, G., Martin, S., Roeck, J., Ryder, J., Smith, P., 1985. A New class of polymers - starburst-dendritic macromolecules. *Polymer Journal*, **17**, 117-132.

Tomalia, D. A., Naylor, A. M., Goddard, W. A., 1990. Starburst dendrimers: molecular-level control of size, shape, surface chemistry, topology, and flexibility from atoms to macroscopic matter. *Angew. Chem. Int. Ed.*, **29**, 138-175.

Tomioka, N., Takasu, D., Takahashi, T., Aida, T., 1998. Electrostatic assembly of dendrimer electrolytes: Negatively and positively charged dendrimer porphyrins. *Angew. Chem. Int. Ed.*, **37**, 1531-1534.

Toth, I., 1994. A novel chemical approach to drug delivery: lipidic amino acid conjugate. *J. Drug Targeting*, **2**, 217-239.

Toth, I., Sakthivel, T., Wilderspin, A. F., Bayele, H., Donnell, M. O., Perry, D., Pasi, K., Lee, C., Florence, A. T., 1999. Novel cationic lipidic peptide dendrimer vectors: in vitro gene delivery. *STP Pharma. Sci.*, **9**, 88-93.

Twyman, L. J., Beezer, A. E., Esfand, R., Hardy, M. J., Mitchell, J. C., 1999. The synthesis of water soluble dendrimers, and their application as possible drug delivery systems. *Tetrahedron Lett.*, **40**, 1743-1746.

Ueno, M., Nakasaki, T., Horikoshi, I., Sakuragawa, N., 1982. Oral administration of liposomally-entrapped heparin to beagle dogs. *Chem Pharm. Bull. (Tokyo)*, **30**, 2245-2247.

Uhrich, K. E., Boegeman, S., Fréchet, J. M. J., Turner, S. R., 1991. The solid-phase synthesis of dendritic polyamides. *Polymer Bull.*, **25**, 551-558.

Ungar, G., Liu, Y., Zeng, X., Percec, V., Cho, W. D., 2003. Giant supramolecular liquid crystal lattice. *Science*, **299**, 1208-1211.

Ungar, G., Percec, V., V, Holerca, M. N., Johansson, G., Heck, J. A., 2000. Heat-shrinking spherical and columnar supramolecular dendrimers: their interconversion and dependence of their shape on molecular taper angle. *Chemistry*, **6**, 1258-1266.

Vanhest, J. C. M., Delnoye, D. A. P., Baars, M. W. P. L., Vangenderen, M. H. P., Meijer, E. W., 1995. Polystyrene-dendrimer amphiphilic block-copolymers with a generation-dependent aggregation. *Science*, **268**, 1592-1595.

Varnavski, O., Ispasoiu, R. G., Balogh, L., Tomalia, D., Goodson III, 2001. Ultrafast time-resolved photoluminescence from novel metal-dendrimer nanocomposites. *J. Chem. Phys.*, **114**, 1962-1965.

Vincent, L., Varet, J., Pille, J. Y., Bompais, H., Opolon, P., Maksimenko, A., Malvy, C., Mirshahi, M., Lu, H., Vannier, J. P., Soria, C., Li, H., 2003. Efficacy of dendrimer-mediated angiostatin and TIMP-2 gene delivery on inhibition of tumour growth and angiogenesis: in vitro and in vivo studies. *Int. J. Cancer*, **105**, 419-429.

Wade, D. A., Torres, P. A., Tucker, S. A., 1999. Spectrochemical investigation in dendritic media: evaluation of nitromethane as a selective fluorescence quenching agent in aqueous carboxylate-terminated polyamido amine (PAMAM) dendrimers. *Anal. Chim. Acta.*, **397**, 17-31.

Wang, H., Lin, T., Bai, F. L., and Kaynak, A. Fluorescence quenching behaviour of hyperbranched polymer to the nitro compounds, in: Guceri, S. I., Gogotsi, Y., and Kuzentsov, V., *Nanoengineered nanofibrous materials,* Kluwer academic book publishers, Dordrecht, 2004, pp457-466.

Wang, J. F., Jia, X. R., Li, Y., Zhong, H., Chen, J. Y., Luo, G. B., Li, M. Q., Wei, Y., 2001. Self-assembly ultrathin films based on dendrimers. *Chemical Journal of Chinese Universities-Chinese*, **22**, 1773-1775.

Watkins, D. M., SayedSweet, Y., Klimash, J. W., Turro, N. J., Tomalia, D. A., 1997. Dendrimers with hydrophobic cores and the formation of supramolecular dendrimer-surfactant assemblies. *Langmuir*, **13**, 3136-3141.

Welch, P., Muthukumar, M., 1998. Tuning the density profile of dendritic polyelectrolytes. *Macromolecules*, **31**, 5892-5897.

Wiechelman, K. J., Braun, R. D., Fitzpatrick, J. D., 1988. Investigation of the bicinchoninic acid protein assay: identification of the groups responsible for color formation. *Anal. Biochem.*, **175**, 231-237.

Wiwattanapatapee, R., Carreno-Gomez, B., Malik, N., Duncan, R., 2000. Anionic PAMAM dendrimers rapidly cross adult rat intestine in vitro: a potential oral delivery system? *Pharm. Res.*, **17**, 991-998.

Wiwattanapatapee, R., Jee, R. D., Duncan, R., 1999. PAMAM dendrimers as potential oral drug delivery systems: Dendrimer complexes with Piroxicam. *Proc. Int. Symp. Control. Rel. Bioact. Mater.*, **26**, 241.

Xu, X., London, E., 2000. The effect of sterol structure on membrane lipid domains reveals how cholesterol can induce lipid domain formation. *Biochemistry*, **39**, 844-849.

Yanai, S., Sakthivel, T., Florence, A. T., 2001. Interfacial behaviour and micelle formation of novel amphiphilic sequential lipid-lysine oligomers. *Int. J. Pharm.*, **214**, 49-53.

Yee, S., 1997. In vitro permeability across Caco-2 cells (colonic) can predict in vivo (small intestinal) absorption in man--fact or myth. *Pharm. Res.*, **14**, 763-766.

Yoshimura, T., Fukai, J., Mizutani, H., Esumi, K., 2002. Physicochemical properties of quaternized poly(amidoamine) dendrimers with four octyl chains. *J. Colloid Interface Sci.*, **255**, 428-431.

Zhang, G. D., Nishiyama, N., Harada, A., Jiang, D. L., Aida, T., Kataoka, K., 2003. PH-sensitive assembly of light-harvesting dendrimer zinc porphyrin bearing

peripheral groups of primary amine with poly(ethylene glycol)-b-poly(aspartic acid) in aqueous solution. *Macromolecules*, **36**, 1304-1309.

Zhu, L. Y., He, Y., Zhu, G. L., Li, M. Z., Wang, E. J., Zhu, R. P., Qi, X., 2001a. Synthesis and self-assembly of asymmetric block copolymer of dendritic polyether and poly (N-isopropylacrylamide). *Acta Chim. Sinica*, **59**, 1484-1489.

Zhu, L. Y., Li, M. Z., Wang, E. J., 2001b. Self-assembly of dendritic polyether-poly(acrylic acid) block copolymer in aqueous solution. *Acta Chim. Sinica*, **59**, 291-296.

Zhu, L. Y., Zhu, G. L., Li, M. Z., Wang, E. J., Zhu, R. P., Qi, X., 2002. Thermosensitive aggregates self-assembled by an asymmetric block copolymer of dendritic polyether and poly(N-isopropylacrylamide). *Eur. Polym. J.*, **38**, 2503-2506.

Zimmerman, S. C., Zeng, F., Reichert, D. E., Kolotuchin, S. V., 1996. Self-assembling dendrimers. *Science*, **271**, 1095-1098.

Ziv, E., Eldor, A., Kleinman, Y., Bar-On, H., Kidron, M., 1983. Bile salts facilitate the absorption of heparin from the intestine. *Biochem. Pharmacol.*, **32**, 773-776.

Zloh, M., Ramaswamy, C., Sakthivel, T., Wilderspin, A., Florence, A. T., 2005. Investigation of the association and flexibility of cationic lipidic peptide dendrons by NMR spectroscopy. *Magn Reson. Chem*, **43**, 47-52.

LIST OF PUBLICATIONS

Papers:

1. Al-Jamal, K. T., Sakthivel, T., Florence, A. T., 2003. Dendrisomes: cationic lipidic dendron vesicular assemblies. *Int. J. Pharm.*, 254, 33-36.

2. Al-Jamal, K. T., Sakthivel, T., Florence, A. T., 2004. Dendrisomes: Vesicular structures derived from a cationic lipidic dendron. *J. Pharm. Sci.*, 94, 102-113.

3. Al-Jamal, K. T., Ramaswamy, C., Singh, B., Florence, A. T., Structures from dendrons and dendrimers: monolayers, dendriplexes, nanoparticles and micellar aggregates. *Journal of Drug Delivery Science and Technology*, In press.

4. Al-Jamal, K. T., Sakthivel, T., Florence, A. T., Solubilisation and transformation of amphipathic lipidic dendron vesicles (DENDRISOMES) into mixed micelles. Submitted to *Colloids Surf. A.*

5. Al-Jamal, K. T., Florence, A. T., Amino terminated polyamide polylysine dendrimers: intrinsic fluorescence and interaction with carboxy fluorescein. In preparation.

Abstracts and Proceedings:

1. Al-Jamal, K. T., Sakthivel, T., Florence, A. T. Self-assembly and vesicle formation of lipidic partial dendrimers. *Proceedings of the 5th ULLA Summer School*, UK, London, August 2001.

2. Florence, A. T., Sakthivel, T., Purohit, G., Al-Jamal, K., Chandrasekaran, R., Hussain, N. Dendrimers and partial dendrimers in drug and gene delivery. *The 13th International Symposium on Microencapsulation,* Angers, France, September 5-7, 2001.

3. Al-Jamal, K. T., Sakthivel, T., Florence, A. T. Dendrisomes: dendron-cholesterol vesicles. *Proceedings of the 4th European Workshop on Particulate Systems*, Copenhagen, Denmark, May 2002.

4. Al-Jamal, K. T., Sakthivel, T., Florence, A. T. Interaction between an amphipathic partial dendrimer and a non-ionic surfactant. *Proceedings of the 29th International Symposium on Controlled Release of Bioactive Materials,* Seoul, Korea, July 2002.

5. Al-Jamal, K. T., Sakthivel, T., Florence, A. T. Supramolecular aggregates of cationic lipidic dendrons. *Winter Symposium and 11th International Symposium on Recent Advances in Drug Delivery Systems,* Salt Lake City, Utah, U.S.A, March 2003.

6. Al-Jamal, K. T., Sakthivel, T., Florence, A. T. Effect of a cationic polylysine dendrimer on transepithelial permeability of Caco-2 cells. *Proceedings of the 30th*

International Symposium on Controlled Release of Bioactive Materials, Glasgow, UK, July 2003.

7. Al-Jamal, K. T., Sakthivel, T., Florence, A. T. Dendrimer-heparin complexation. *British Pharmaceutical Conference,* Harrogate, UK, September 2003.

8. Al-Jamal, K. T., Sakthivel, T., Florence, A. T. Dendrimer-Heparin Interaction Study. *3rd International Dendrimer Symposium,* Berlin, Germany, September 2003.